Methods in
Molecular Biology 1461

Springer Protocols

Sung-Bae Kim *Editor*

Bio-
luminescence

Methods and Protocols

Third Edition

Humana Press

METHODS IN MOLECULAR BIOLOGY

Series Editor
John M. Walker
School of Life and Medical Sciences
University of Hertfordshire
Hatfield, Hertfordshire, AL10 9AB, UK

For further volumes:
http://www.springer.com/series/7651

Bioluminescence

Methods and Protocols

Third Edition

Edited by

Sung-Bae Kim

Research Institute for Environmental Management Technology,
National Institute of Advanced Industrial Science and Technology (AIST), Tsukuba, Japan

Humana Press

Editor
Sung-Bae Kim
Research Institute for Environmental Management Technology
National Institute of Advanced Industrial Science and Technology (AIST)
Tsukuba, Japan

ISSN 1064-3745 ISSN 1940-6029 (electronic)
Methods in Molecular Biology
ISBN 978-1-4939-3811-7 ISBN 978-1-4939-3813-1 (eBook)
DOI 10.1007/978-1-4939-3813-1

Library of Congress Control Number: 2016943547

© Springer Science+Business Media New York 2016
This work is subject to copyright. All rights are reserved by the Publisher, whether the whole or part of the material is concerned, specifically the rights of translation, reprinting, reuse of illustrations, recitation, broadcasting, reproduction on microfilms or in any other physical way, and transmission or information storage and retrieval, electronic adaptation, computer software, or by similar or dissimilar methodology now known or hereafter developed.
The use of general descriptive names, registered names, trademarks, service marks, etc. in this publication does not imply, even in the absence of a specific statement, that such names are exempt from the relevant protective laws and regulations and therefore free for general use.
The publisher, the authors and the editors are safe to assume that the advice and information in this book are believed to be true and accurate at the date of publication. Neither the publisher nor the authors or the editors give a warranty, express or implied, with respect to the material contained herein or for any errors or omissions that may have been made.

Printed on acid-free paper

This Humana Press imprint is published by Springer Nature
The registered company is Springer Science+Business Media LLC New York

Preface

Luciferases catalyzing oxidation of luciferins are a nearly ideal reporter for bioanalysis and molecular imaging of intracellular molecular events. Bioluminescent probes fabricated from luciferases generally allow low backgrounds, high signal-to-noise (S/N) ratios, wider dynamic ranges of signals, versatility in the molecular design, and suitability in the imaging of small model animals. Recent studies on bioluminescence-based technologies may be categorized into three major routes: (i) establishment of new luciferases and synthesis of novel luciferins; (ii) fabrication of bioluminescent probes with the luciferases and luciferins; and (iii) practical application of the probes to animal imaging and instrumentations. These three categories are closely correlated in the technical progression: e.g., if we establish de novo luciferases with excellent optical properties, it allows fabrication of new optical probes with a novel strategy. The novel bioluminescent probes should facilitate better optical performance in visualization of molecular events of interest in living subjects. This book represents detailed laboratory protocols regarding the three major route technologies from the establishment of new luciferases, efficient optical probes, to their applications to visualizing molecular events in living subjects.

I am greatly honored to work with the authors who contributed to this book. They are all talented in their research subjects in bioluminescence and generously accepted one or two chapters in this book. I am deeply thankful for Professor John Walker and Dr. Fujii for their timely advices and encouragement. Finally, I owe a special thank you to Young-Eun, my wife, and Tae-Yun and Tae-Hun, my children, for their endless support.

I hope that this book will provide a comprehensive guidance to researchers and technicians on how to establish luciferases and to fabricate bioluminescent probes for molecular imaging.

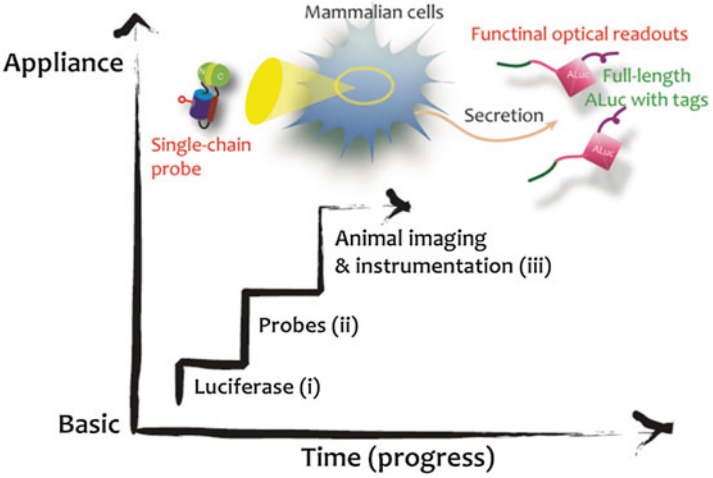

Tsukuba, Japan *Sung-Bae Kim*

Contents

Preface . . . . *v*

Contributors . . . . *xi*

PART I INGREDIENTS OF BIOLUMINESCENT PROBES

1 Label-Free Cell Phenotypic Identification of D-Luciferin as an Agonist for GPR35 3
Heidi Hu, Huayun Deng, and Ye Fang

2 Synthetic Bioluminescent Coelenterazine Derivatives. 19
Ryo Nishihara, Daniel Citterio, and Koji Suzuki

3 Molecular Cloning of Secreted Luciferases from Marine Planktonic Copepods 33
Yasuhiro Takenaka, Kazuho Ikeo, and Yasushi Shigeri

4 How to Fabricate Functional Artificial Luciferases for Bioassays. 43
Sung-Bae Kim and Rika Fujii

5 Quantum Yield Determination Based on Photon Number Measurement, Protocols for Firefly Bioluminescence Reactions 55
Kazuki Niwa

PART II FABRICATION OF BIOLUMINESCENT PROBES

6 Bioluminescent Ligand–Receptor Binding Assays for Protein or Peptide Hormones 65
Ya-Li Liu and Zhan-Yun Guo

7 Bioluminogenic Imaging of Aminopeptidase N In Vitro and In Vivo. 91
Wenxiao Wu, Laizhong Chen, Jing Li, Lupei Du, and Minyong Li

8 Firefly Luciferase-Based Sequential Bioluminescence Resonance Energy Transfer (BRET)-Fluorescence Resonance Energy Transfer (FRET) Protease Assays 101
Bruce Branchini

9 Monitoring Intracellular pH Change with a Genetically Encoded and Ratiometric Luminescence Sensor in Yeast and Mammalian Cells 117
Yunfei Zhang, J. Brian Robertson, Qiguang Xie, and Carl Hirschie Johnson

10 A Protein–Protein Interaction Assay FlimPIA Based on the Functional Complementation of Mutant Firefly Luciferases 131
Yuki Ohmuro-Matsuyama and Hiroshi Ueda

11 Single-Chain Probes for Illuminating Androgenicity of Chemicals 143
Sung-Bae Kim and Hiroaki Tao

12 Multicolor Imaging of Bifacial Activities of Estrogens 153
Sung-Bae Kim and Yoshio Umezawa

13 Circular Permutation Probes for Illuminating Phosphorylation of Estrogen Receptor 165
Sung-Bae Kim and Hiroaki Tao

14 Fabrication of Molecular Strain Probes for Illuminating Protein–Protein Interactions 175
Sung-Bae Kim and Rika Fujii

15 An ALuc-Based Molecular Tension Probe for Sensing Intramolecular Protein–Protein Interactions 183
Sung-Bae Kim, Ryo Nishihara, and Koji Suzuki

16 Live Cell Bioluminescence Imaging in Temporal Reaction of G Protein-Coupled Receptor for High-Throughput Screening and Analysis 195
Mitsuru Hattori and Takeaki Ozawa

17 Imaging Histone Methylations in Living Animals 203
Thillai V. Sekar and Ramasamy Paulmurugan

18 Preparation and Assay of Simple *Light Off* Biosensor Based on Immobilized Bioluminescent Bacteria for General Toxicity Assays. 217
G.V.M. Gabriel and V.R. Viviani

Part III Applications to Living Subjects and Instrumentations

19 In Vivo Bioluminescent Imaging of ATP-Binding Cassette Transporter-Mediated Efflux at the Blood–Brain Barrier 227
Joshua Bakhsheshian, Bih-Rong Wei, Matthew D. Hall, R. Mark Simpson, and Michael M. Gottesman

20 Theranostic Imaging of Cancer Gene Therapy. 241
Thillai V. Sekar and Ramasamy Paulmurugan

21 Development of a Multicolor Bioluminescence Imaging Platform to Simultaneously Investigate Transcription Factor NF-κB Signaling and Apoptosis 255
Vicky T. Knol-Blankevoort, Laura Mezzanotte, Martijn J.W.E. Rabelink, Clemens W.G.M. Lowik, and Eric L. Kaijzel

22 A Multichannel Bioluminescence Determination Platform for Bioassays. 271
Sung-Bae Kim and Ryuichi Naganawa

23 A Bioluminescence Assay System for Imaging Metal Cationic Activities in Urban Aerosols 279
Sung-Bae Kim, Ryuichi Naganawa, Shingo Murata, Takayoshi Nakayama, Simon Miller, and Toshiya Senda

24 Luminescence Imaging: (a) Multicolor Visualization of Ca^{2+} Dynamics in Different Cellular Compartments and (b) Video-Rate Tumor Detection in a Freely Moving Mouse. 289
Kenta Saito, Masahiro Nakano, and Takeharu Nagai

25 Photon Counting System for High-Sensitivity Detection of Bioluminescence at Optical Fiber End 299
Masataka Iinuma, Yutaka Kadoya, and Akio Kuroda

Index 311

Contributors

Bruce Branchini • *Department of Chemistry, Connecticut College, New London, CT, USA*

Joshua Bakhsheshian • *Laboratory of Cell Biology, Center for Cancer Research, National Cancer Institute, National Institutes of Health, Bethesda, MD, USA*

Daniel Citterio • *Department of Applied Chemistry, Faculty of Science and Technology, Keio University, Yokohama, Kanagawa, Japan*

Laizhong Chen • *Department of Medicinal Chemistry, Key Laboratory of Chemical Biology of Natural Products (MOE), School of Pharmacy,, Shandong University, Jinan, Shandong, China*

Huayun Deng • *Biochemical Technologies, Science and Technology Division, Corning Incorporated, Corning, NY, USA*

Lupei Du • *Department of Medicinal Chemistry, Key Laboratory of Chemical Biology of Natural Products (MOE), School of Pharmacy, Shandong University, Jinan, Shandong, China*

Ye Fang • *Biochemical Technologies, Science and Technology Division, Corning Incorporated, Corning, NY, USA*

Rika Fujii • *Research Institute for Environmental Management Technology, National Institute of Advanced Industrial Science and Technology (AIST), Tsukuba, Ibaraki, Japan*

G.V.M. Gabriel • *Laboratory of Biochemistry and Biotechnology of Bioluminescence, Department of Physics, Chemistry and Mathematics, Federal University of São Carlos (UFSCar), Sorocaba, SP, Brazil; Graduate School of Biotechnology and Environmental Monitoring, Federal University of São Carlos (UFSCar), Sorocaba, SP, Brazil; Graduate School of Evolutive Genetics and Molecular Biology, Federal University of São Carlos (UFSCar), São Carlos, SP, Brazil*

Michael M. Gottesman • *Laboratory of Cell Biology, Center for Cancer Research, National Cancer Institute, National Institutes of Health, Bethesda, MD, USA*

Zhan-Yun Guo • *Research Center for Translational Medicine at East Hospital, College of Life Sciences and Technology, Tongji University, Shanghai, China*

Matthew D. Hall • *Laboratory of Cell Biology, Center for Cancer Research, National Cancer Institute, National Institutes of Health, Bethesda, MD, USA*

Mitsuru Hattori • *Department of Chemistry, School of Science, The University of Tokyo, Tokyo, Japan*

Heidi Hu • *Medical Laboratory Science, Jefferson College of Health Science/Carilion Roanoke Memorial Hospital, Quest Diagnostic Lab, Carilion Clinic Health System, Roanoke, VA, USA*

Masataka Iinuma • *Graduate school of Advanced Sciences of Matter, Hiroshima University, Higashi-Hiroshima, Hiroshima, Japan*

Kazuho Ikeo • *Center for Information Biology, National Institute of Genetics, Shizuoka, Japan*

Carl Hirschie Johnson • *Department of Biological Sciences, Vanderbilt University, Nashville, TN, USA*

YUTAKA KADOYA • *Graduate school of Advanced Sciences of Matter, Hiroshima University, Higashi-Hiroshima, Hiroshima, Japan*

ERIC L. KAIJZEL • *Department of Radiology, Leiden University Medical Center, Leiden, The Netherlands*

SUNG-BAE KIM • *Research Institute for Environmental Management Technology, National Institute of Advanced Industrial Science and Technology (AIST), Tsukuba, Ibaraki, Japan*

VICKY KNOL-BLANKEVOORT • *Department of Radiology, Leiden University Medical Center, Leiden, The Netherlands*

AKIO KURODA • *Graduate school of Advanced Sciences of Matter, Hiroshima University, Higashi-Hiroshima, Hiroshima, Japan*

JING LI • *Department of Medicinal Chemistry, Key Laboratory of Chemical Biology of Natural Products (MOE), School of Pharmacy, Shandong University, Jinan, Shandong, China*

MINYONG LI • *Department of Medicinal Chemistry, Key Laboratory of Chemical Biology of Natural Products (MOE), School of Pharmacy, Shandong University, Jinan, Shandong, China*

YA-LI LIU • *Research Center for Translational Medicine at East Hospital, College of Life Sciences and Technology, Tongji University, Shanghai, China*

CLEMENS W.G.M. LÖWIK • *Department of Radiology, Leiden University Medical Center, Leiden, The Netherlands*

LAURA MEZZANOTTE • *Department of Radiology, Leiden University Medical Center, Leiden, The Netherlands*

SIMON MILLER • *Structural Biology Research Center, Photon Factory, Institute of Materials Structure Science, High Energy Accelerator Research Organization (KEK), Tsukuba, Ibaraki, Japan*

SINGO MURATA • *Nishihara Electronics co. ltd, Kashiwa, Chiba, Japan*

TAKEHARU NAGAI • *The Institute of Scientific and Industrial Research, Osaka University, Osaka, Japan*

RYUICHI NAGANAWA • *Research Institute for Environmental Management Technology, National Institute of Advanced Industrial Science and Technology (AIST), Tsukuba, Ibaraki, Japan*

MASAHIRO NAKANO • *The Institute of Scientific and Industrial Research, Osaka University, Osaka, Japan*

TAKAYOSHI NAKAYAMA • *Nishihara Electronics co. ltd., Kashiwa, Chiba, Japan*

RYO NISHIHARA • *Department of Applied Chemistry, Faculty of Science and Technology, Keio University, Yokohama, Kanagawa, Japan*

KAZUKI NIWA • *Quantum Optical Measurement Group, National Metrology Institute of Japan, National Institute of Advanced Industrial Science and Technology, Tsukuba, Ibaraki, Japan*

YUKI OHMURO-MATSUYAMA • *Department of Chemical Science and Engineering, Graduate School of Engineering, Kobe University, Kobe, Hyogo, Japan*

TAKEAKI OZAWA • *Department of Chemistry, School of Science, The University of Tokyo, Tokyo, Japan*

RAMASAMY PAULMURUGAN • *Molecular Imaging Program at Stanford, Bio-X Program, Stanford University School of Medicine, Stanford, CA, USA; Department of Radiology, Stanford University School of Medicine, CA, USA*

MARTIJN J.W.E. RABELINK • *Department of Molecular Cell Biology, Leiden University Medical Center, Leiden, The Netherlands*

J. BRIAN ROBERTSON • *Department of Biological Sciences, Vanderbilt University, Nashville, TN, USA; Department of Biology, Middle Tennessee State University, Murfreesboro, TN, USA*

KENTA SAITO • *The Center for Brain Integration Research, Tokyo Medical and Dental University, Tokyo, Japan*

THILLAI V. SEKAR • *Molecular Imaging Program at Stanford, Bio-X Program, Stanford University School of Medicine, Stanford, CA, USA*

TOSHIYA SENDA • *Structural Biology Research Center, Photon Factory, Institute of Materials Structure Science, High Energy Accelerator Research Organization (KEK), Tsukuba, Ibaraki, Japan*

YASUSHI SHIGERI • *Health Research Institute, National Institute of Advanced Industrial Science and Technology (AIST), Ikeda, Osaka, Japan*

R. MARK SIMPSON • *Laboratory of Cancer Biology and Genetics, Center for Cancer Research, National Cancer Institute, National Institutes of Health, Bethesda, MD, USA*

KOJI SUZUKI • *Department of Applied Chemistry, Faculty of Science and Technology, Keio University, Yokohama, Kanagawa, Japan*

YASUHIRO TAKENAKA • *Department of Diabetes and Endocrinology, Saitama Medical University, Moroyama, Saitama, Japan*

HIROAKI TAO • *AIST Shikoku center, National Institute of Advanced Industrial Science and Technology (AIST), Takamatsu, Kagawa, Japan*

HIROSHI UEDA • *Laboratory for Chemistry and Life Science, Tokyo Institute of Technology, Yokohama, Japan*

YOSHIO UMEZAWA • *Department of Chemistry, School of Science, The University of Tokyo, Tokyo, Japan*

V.R. VIVIANI • *Laboratory of Biochemistry and Biotechnology of Bioluminescence, Department of Physics, Chemistry and Mathematics, Federal University of São Carlos (UFSCar), Sorocaba, SP, Brazil; Graduate School of Biotechnology and Environmental Monitoring, Federal University of São Carlos (UFSCar), Sorocaba, SP, Brazil; Graduate School of Evolutive Genetics and Molecular Biology, Federal University of São Carlos (UFSCar), São Carlos, SP, Brazil*

BIH-RONG WEI • *Laboratory of Cancer Biology and Genetics, Center for Cancer Research, National Cancer Institute, National Institutes of Health, Bethesda, MD, USA*

WENXIAO WU • *Department of Medicinal Chemistry, Key Laboratory of Chemical Biology of Natural Products (MOE), School of Pharmacy, Shandong University, Jinan, Shandong, China*

QIGUANG XIE • *Department of Biological Sciences, Vanderbilt University, Nashville, TN, USA; Laboratory of Molecular and Cellular Biology, College of Life Sciences, Hebei Normal University, Hebei, China*

YUNFEI ZHANG • *Department of Biological Sciences, Vanderbilt University, Nashville, TN, USA; Institute of Health Sciences, Anhui University, Anhui, China*

Part I

Ingredients of Bioluminescent Probes

Chapter 1

Label-Free Cell Phenotypic Identification of D-Luciferin as an Agonist for GPR35

Heidi Hu, Huayun Deng, and Ye Fang

Abstract

D-Luciferin (also known as beetle or firefly luciferin) is one of the most widely used bioluminescent reporters for monitoring in vitro or in vivo luciferase activity. The identification of several natural phenols and thieno[3,2-b]thiophene-2-carboxylic acid derivatives as agonists for GPR35, an orphan G protein-coupled receptor, had motivated us to examine the pharmacological activity of D-Luciferin, given that it also contains phenol and carboxylic acid moieties. Here, we describe label-free cell phenotypic assays that ascertain D-Luciferin as a partial agonist for GPR35. The agonistic activity of D-Luciferin at the GPR35 shall evoke careful interpretation of biological data when D-Luciferin or its analogues are used as probes.

Key words Bioluminescence, Dynamic mass redistribution, G protein-coupled receptor, GPR35, D-Luciferin, Resonant waveguide grating biosensor

1 Introduction

Luciferase genes from firefly and other beetles are commonly used as reporter genes to study transcription regulation, and to localize, track, and quantify a myriad of biological events or functions in living cells and animals [1–4]. As they produce the brightest form of bioluminescence, luciferase genes can be used to transfect tumor cells, stem cells, or infectious species, which are then inoculated into research animals such as rats or mice. As a natural substrate for the beetle luciferase reporter systems, D-Luciferin ((S)-2-(6′-hydroxy-2′-benzothiazolyl)thiazoline-4-carboxylic acid, *see* Fig. 1) is injected into animals so real-time, noninvasive monitoring of disease progression and/or drug efficacy in animal model systems using bioluminescence imaging is possible. D-Luciferin is also commonly used for in vitro luciferase and ATP, gene reporter, high-throughput screening, and various contamination assays [5, 6]. Luciferase catalyzes a bioluminescence reaction that uses luciferin, Mg-ATP, and molecular oxygen to produce a characteristic

Sung-Bae Kim (ed.), *Bioluminescence: Methods and Protocols*, Methods in Molecular Biology, vol. 1461, DOI 10.1007/978-1-4939-3813-1_1, © Springer Science+Business Media New York 2016

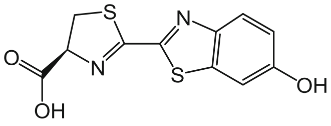

Fig. 1 Chemical structure of D-Luciferin

yellow-green emission, which shifts to red light in vivo at 37 °C [7–10]. However, little is known about the biological activity of D-Luciferin.

Using label-free resonant waveguide grating (RWG) biosensor enabled dynamic mass redistribution (DMR) assays [11–16], we had previously discovered several thieno[3,2-b]thiophene-2-carboxylic acid derivatives [17] and natural phenols [18] as agonists for G protein-coupled receptor 35 (GPR35). These findings had motivated us to search for common fluorescent and bioluminescent probe molecules that contain phenol and/or carboxylic acid moieties, two of which are important for the activation of GPR35 [17, 18]. GPR35 is an orphan G protein-coupled receptor (GPCR) whose natural agonist(s) are still controversial [19–22]. Label-free DMR pharmacological profiling of D-Luciferin in HT-29, a colon cancer cell line endogenously expressing GPR35, showed that D-Luciferin is a partial agonist for this receptor with an EC_{50} of 12.9 μM [23]. Thimm et al. later confirmed using a radioligand binding assay that D-Luciferin binds to GPR35 with a K_i of 9.86 μM [24].

This chapter describes protocols as to how to determine the pharmacological activity of D-Luciferin acting at the GPR35 using multiple types of DMR assays. These assays include (1) one-step agonism assay to detect its agonistic activity, (2) one-step co-stimulation assay to determine its partial agonistic activity, (3) two-step antagonism assay to determine its specificity to activate GPR35, (4) two-step desensitization assay to determine the competitive agonism against known GPR35 agonists.

2 Materials

2.1 Tissue Culture Medium and Cell Line

1. Human colorectal adenocarcinoma HT-29 cell line (ATCC® HTB-38™, American Type Cell Culture, Manassas, VA, USA).
2. Tango™ U2OS-GPR35-*bla* cell line (Invitrogen, Grand Island, NY). This cell line stably expresses human GPR35 linked to a TEV protease site and a Gal4-VP16 transcription factor, as well as a β-arrestin/TEV protease fusion protein and the β-lactamase reporter gene under the control of a UAS response element.
3. McCoy's 5A Medium Modified (Invitrogen).

4. Dulbecco's Modified Eagle's medium (DMEM) (Invitrogen).
5. Antibiotic solution 100×: 10,000 U penicillin/mL, 10,000 μg streptomycin/mL.
6. Complete medium for HT-29 cells: McCoy's 5A Medium Modified supplemented with 10 % fetal bovine serum (FBS), 4.5 g/L glucose, 2 mM glutamine, 50 U/mL penicillin, and 50 μg/mL streptomycin.
7. Complete medium for U2OS-GPR35-*bla* cells: DMEM medium supplemented with 10 % dialyzed FBS, 0.1 μM NEAA, 25 μM Hepes (pH 7.3), 1 mM sodium pyruvate, 100 U/mL penicillin, 100 μg/mL streptomycin, 200 μg/mL zeocin, 50 μg/mL hygromycin, and 100 μg/mL geneticin.
8. Trypsin/ethylenediaminetetraacetic acid (EDTA) solution 10×: 2.5 % Trypsin, 0.2 % 4Na$^+$-EDTA.

2.2 Microplates and Instruments

1. Corning 75 cm^2 tissue culture-treated polystyrene flask with vented cap (T-75) (Corning Incorporated, Corning, NY, USA).
2. Corning 384-well polypropylene compound storage plate.
3. Corning Epic® 384-well microplate tissue culture-treated.
4. 384-well, black-wall, clear bottom assay plates with low fluorescence background (Corning).
5. 8-well chamber slide (Nalge Nunc International, Rochester, NY, USA).
6. Matrix 16-channel electronic pipettor (Thermo Fisher Scientific, Hudson, NH).
7. Epic® system (Corning). This reader is a wavelength interrogation reader system tailored for RWG in microplate (384- and 1536-well). This system consists of a temperature-control unit (26 °C), an optical detection unit, and an on-board liquid handling unit with robotics. The detection unit is centered on integrated fiber optics, and enables kinetic measures of cellular responses with a time interval of ~15 s.
8. Epic® BT system (Corning). This reader is a small-footprint, swept wavelength interrogation-based imaging system [25]. This system has a spatial resolution of 90 μm and a temporal resolution of 3 s.
9. BioTek cell plate washer ELx405 (BioTek Instruments Inc., Winooski, VT, USA).
10. 1.5 mm thick glass cover-slip (Corning).
11. Zeiss confocal microscope Axiovert 40 (Carl Zeiss Microscopy GmbH, Jena, Germany).
12. Tecan Safire II microplate reader (Tecan, Männedorf, Switzerland).

2.3 Reagents and DMR Assays

1. Pamoic acid and D-Luciferin (Sigma Chemical Co., St. Louis, MO, USA).
2. Zaprinast (Enzo Life Sciences, Farmingdale, NY, USA).
3. YE210 (6-bromo-3-methylthieno[3,2-b]thiophene-2-carboxylic acid) (Corning).
4. SP05140, SPB05142 (CID2745687; methyl-5-[(tert-butylcarbamothioyl-hydrazinylidene)-methyl]-1-(2,4-difluorophenyl)-pyrazole-4-carboxylate), and SPB05143 (Ryan Scientific, Inc., Mt. Pleasant, SC).
5. Hank's Balanced Salt Solution (HBSS): 1× with calcium and magnesium, but no phenol red.
6. HEPES buffer: 1 M HEPES, pH 7.1.
7. Assay buffered vehicle solution: 1× HBSS, 10 mM HEPES, pH 7.1.
8. Anti-GPR35 antibody (T-14, intracellular domain) (Santa Cruz biotechnology, Santa Cruz, CA, USA).
9. Alexa Fluor® 594-labeled donkey anti-goat IgG (H+L) (Invitrogen).

2.4 Data Analysis Software

1. Microsoft Excel (Microsoft Inc., Seattle, WA, USA).
2. Epic® Offline Viewer (Corning).
3. GraphPad Prism 5 Software (Graph Pad Software Inc., La Jolla, CA, USA).
4. NIH ImageJ (http://imagej.nih.gov/ij/).

3 Methods

3.1 Cell Culture

This section describes protocols to culture HT-29 cells in biosensor microplates for DMR assays, to culture U2OS-GPR35-*bla* cells in cell assay microplates for Tango β-arrestin translocation gene reporter assay, and to culture HT-29 in 8-well chamber slide for receptor internalization assay.

3.1.1 HT-29 Cell Culture in Biosensor Microplate

1. Passage HT-29 cells in T-75 flasks using 1× trypsin/EDTA. Generally, cells are split every 5 days, and a 1:10 split is used to provide maintenance culture. The confluent cells obtained in one T-75 flask are sufficient for experimental culture in at least one biosensor microplate. The cells between 3 and 15 passages are preferred for DMR assays (*see* **Note 1**).
2. Harvest confluent cells using 1× trypsin-EDTA solution. Centrifuge the cells down, remove the supernatant, and re-suspend the cell pellet in freshly prepared complete medium for HT-29.

3. Seed 3.2×10^4 cells freshly suspended in 50 μL of the complete medium into each well of an Epic® 384-well biosensor microplate using a 16-channel electronic pipettor (*see* **Note 2**).
4. Incubate cells in the laminar flow hood for ~20 min at room temperature to minimize the commonly occurring edge effect.
5. Place the microplate inside an incubator and culture cells for ~24 h at 37 °C under air/5 % CO_2. After overnight culturing the cells usually reach ~95 % confluency and are ready for DMR assays.

3.1.2 U2OS-GPR35-bla Cell Culture in Microplate

1. Passage U2OS-GPR35-*bla* cells in T-75 flasks. The cells between 3 and 15 passages are used for Tango assay (see below).
2. Harvest confluent cells using 1× trypsin-EDTA solution. Centrifuge the cells down, remove the supernatant, and re-suspend the cell pellet in the complete medium for this cell line.
3. Seed 10,000 cells in 50 μL of the complete medium/well in 384-well, black-wall, clear bottom assay plates with low fluorescence background using a 16-channel electronic pipettor.
4. Incubate cells in the laminar flow hood for ~20 min at room temperature.
5. Place the microplate inside an incubator and culture cells for ~24 h at 37 °C under air/5 % CO_2.

3.1.3 HT-29 Cell Culture in 8-Well Chamber Slide

1. Seed 10,000 cells in 100 μL of the complete medium/well into each well of an 8-well chamber slide using an electronic pipettor.
2. Place the slide inside an incubator and culture cells for ~24 h at 37 °C under air/5 % CO_2 for overnight.

3.2 DMR Agonist Assay

This section describes the one-step protocol to detect potential agonistic activity of ligands in a given cell line. Since the DMR signal of a ligand is obtained after the cells reach confluency, it primarily reflects the effect of the ligand on the cells. The confluent cells typically give rise to a steady baseline during the assay duration (~hours). A ligand that triggers a detectable DMR is considered to have an agonistic activity in the cells. Since the DMR signal is an integrated whole cell response, the similarity in DMR signature is often useful to hypothesize that two ligands that trigger similar DMR in a cell line may activate the same pathway, sometime via the same target [26–29].

Figure 2 compares the dose responses of D-Luciferin with three known GPR35 agonists, pamoic acid [30], zaprinast [31], and YE210 [17]. All compounds triggered a dose-dependent DMR signal that shares similar characteristics; that is, all are biphasic, consisting of an early positive DMR (P-DMR) event and a late negative-DMR (N-DMR) event. Based on their P-DMR

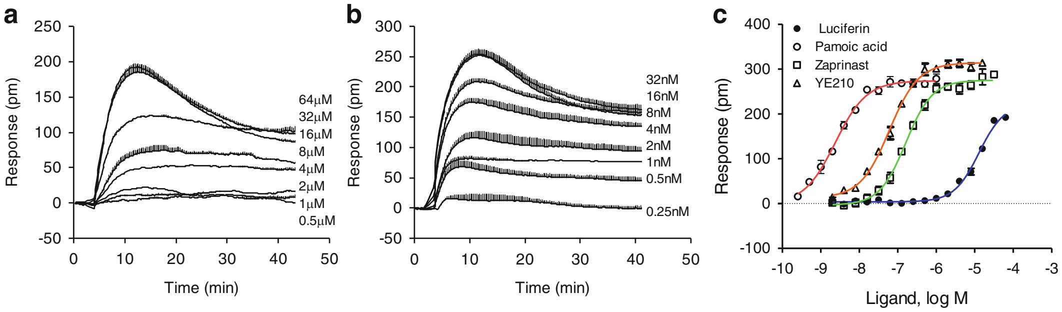

Fig. 2 The DMR characteristics of ligands in HT-29 cells. (**a**) The dose-dependent kinetic DMR signals of D-Luciferin; (**b**) the dose-dependent kinetic DMR signals of pamoic acid; and (**c**) the P-DMR amplitudes of four ligands as a function of ligand dose. All data represent mean ± s.d. (*n* = 4, except for *n* = 8 for zaprinast). This figure is reproduced from ref. 23 through the Creative Commons Attribution License

amplitudes, the DMR dose-responses of all compounds fitted well with a monophasic sigmoidal curve, leading to an EC_{50} of 0.0024, 0.064, 0.16, and 12.9 μM for pamoic acid, YE210, zaprinast, and D-Luciferin, respectively.

1. Prepare 4× compound solutions, each with 14 point 2× dilution series, by diluting the stored concentrated solutions with the assay buffered solution (1× HBSS). Prepare 2× dilution series of buffer solutions containing equal amount of dimethyl sulfoxide (DMSO) as intra-plate negative controls (*see* **Note 3**). Transfer all solutions into a 384-well polypropylene compound storage plate using a pipettor to prepare a compound source plate.
2. After culture, wash the confluent cells in the biosensor microplate twice with the HBSS using the BioTek washer, and maintain in 30 μL HBSS to prepare a cell assay plate (*see* **Note 4**).
3. Place the cell assay plate and the compound source plate inside the hotel of the Epic® system for about 1 h (*see* **Note 5**).
4. Record the baseline wavelengths of all biosensors in the cell assay microplate, normalize to zero, and record a 2–5 min baseline (*see* **Note 6**).
5. Pause the reader, and transfer 10 μL 4× of compound solutions from the compound source plate to the cell assay plate using the on-board liquid handler.
6. Run the reader immediately after compound addition (*see* **Note 7**), and record the DMR for about 1 h (*see* **Note 8**).
7. Background-correct all DMR signals (*see* **Note 9**).
8. Plot the maximal DMR response, or the DMR amplitude at specific time point post stimulation as a function of compounds, or compound doses (*see* **Note 10**).
9. Calculate the EC_{50} values of different agonists using nonlinear activation function of the Prism software.

3.3 DMR Co-stimulation Assay

This section describes the one-step protocol to determine the partial agonism of D-Luciferin using co-stimulation assay. Here, concentration-response curves to pamoic acid are performed in the presence of D-Luciferin at different fixed doses; vice versa, the concentration-response curves to luciferin are done in the presence of pamoic acid at different fixed doses. Pamoic acid behaves as a full agonist in DMR assays using HT-29 cells [23]. Results showed that the presence of D-Luciferin did not alter the potency of pamoic acid, but increased the starting signal in a dose-dependent manner (*see* Fig. 3a). Conversely, for low doses of pamoic acid (2 and 20 nM), D-Luciferin dose-dependently led to an increased DMR signal; however, for pamoic acid at 200 nM (a saturating concentration), D-Luciferin at high doses reduced the DMR in a dose-dependent manner (*see* Fig. 3b). These results suggest that the two compounds interact at an overlapping binding site, and D-Luciferin is less efficacious agonist of GPR35 than pamoic acid.

1. Prepare a series of mixtures consisting of D-Luciferin at a fixed dose and pamoic acid at 2× dilution dose series by diluting the stored concentrated solutions of pamoic acid with the D-Luciferin solution. D-Luciferin is fixed to 0, 4, 40, or 200 μM in 1× HBSS.
2. Prepare a series of mixtures consisting of pamoic acid at a fixed dose and D-Luciferin at 2× dilution dose series by diluting the stored concentrated solutions of D-Luciferin with the pamoic acid solution. Pamoic acid is fixed at 0, 8, 80, or 800 nM in 1× HBSS.

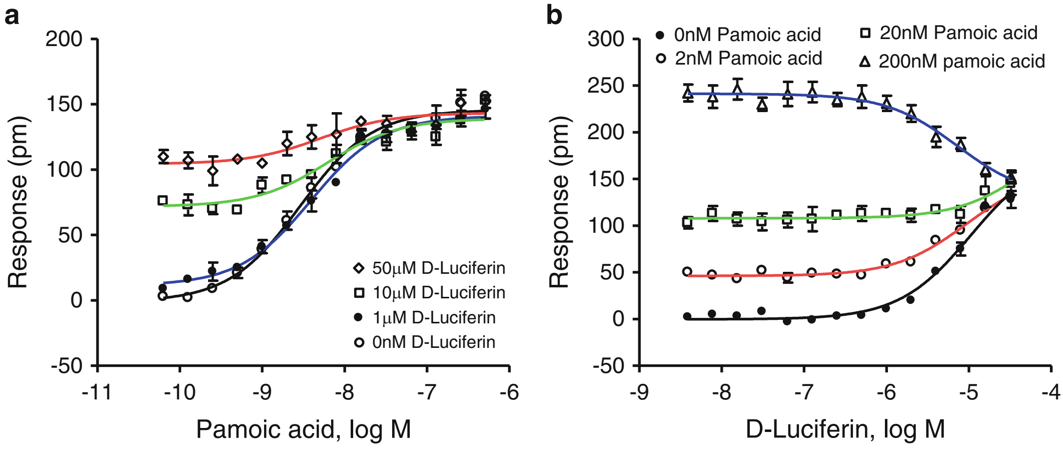

Fig. 3 The DMR arising from co-stimulation with two agonists. (**a**) The dose-dependent responses of pamoic acid in the absence and presence of D-Luciferin at three different fixed doses; the cell seeding density was 25,000 cells/well; and (**b**) the dose-dependent response of D-Luciferin in the absence and presence of pamoic acid at three fixed doses, the cell seeding density was 32,000 cells/well. The ligand P-DMR amplitudes were plotted in mean ± s.d. ($n = 4$). This figure is reproduced from ref. 23 through the Creative Commons Attribution License

3. Transfer all solutions into a 384-well polypropylene compound storage plate using a pipettor to prepare a 4× compound source plate.
4. Repeat the **steps 2**–**7** in Subheading 3.2 to obtain the DMR arising from pamoic acid in the absence or presence of D-Luciferin at three different fixed doses, or from D-Luciferin in the absence or presence of pamoic acid at three different fixed doses.
5. Calculate the P-DMR amplitudes using the Epic® offline viewer. Fit the dose responses with nonlinear regression activation model using the Prism software to generate EC_{50} values.

3.4 DMR Antagonist Assay

This section describes the two-step protocol to determine the competitive nature of D-Luciferin against three GPR35 antagonists, SP05140, SP05142, and SP05143. Here, the cells are pretreated with a known GPR35 antagonist at different doses for 5 min, followed by stimulation with D-Luciferin at a fixed dose (typically at its EC_{80}, or EC_{100}). SPB05142 is a known GPR35 antagonist [30], but the antagonistic activity of its analogues, SPB05140 and SPB05143, is unknown. Figure 4 shows the ability of three antagonists to block the DMR of 32 μM D-Luciferin. All three antagonists did not result in any detectable DMR in HT-29 cells, but almost completely blocked the DMR of D-Luciferin (*see* Fig. 4a), resulting in an apparent IC_{50} value of 5.0 ± 0.9 μM, 1.5 ± 0.2 μM, and 2.6 ± 0.3 μM ($n = 4$) for SPB05140, SPB05142, and SPB05143, respectively (*see* Fig. 4b), suggesting that D-Luciferin is a GPR35 agonist.

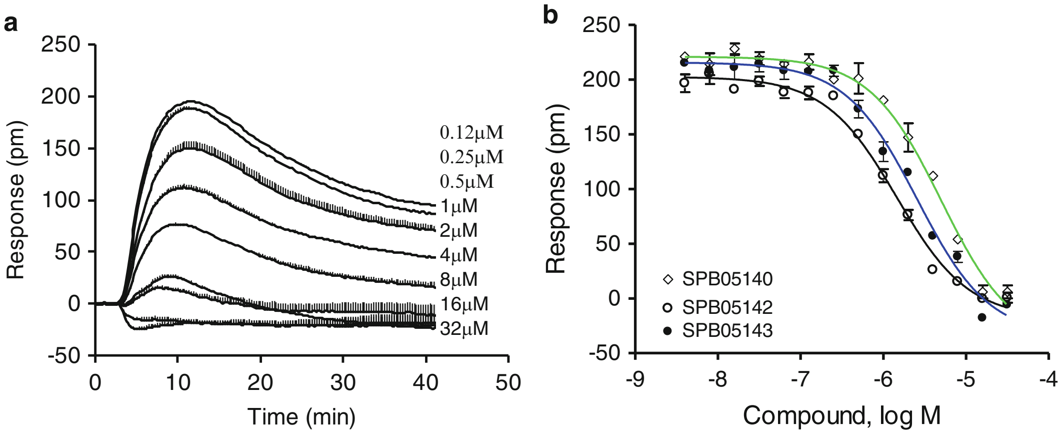

Fig. 4 The inhibition of the DMR of 32 μM D-Luciferin by three GPR35 antagonists in HT-29 cells. (**a**) The real-time kinetic response of D-Luciferin after pretreated with SPB05142 at different doses; and (**b**) the D-Luciferin P-DMR amplitudes as a function of three antagonist doses. The three GPR35 antagonists were SPB05140, SPB05142, and SPB05143 ($n = 4$). This figure is reproduced from ref. 23 through the Creative Commons Attribution License

1. After both cell and compound plates reach equilibrium inside the reader, pretreat the cells with antagonists at different doses for 5 min.
2. Establish a 2 min baseline.
3. Stimulate the cells with D-Luciferin at 32 μM.
4. Record DMR for about 1 h.
5. Background-correct all DMR signals using intra-plate negative controls.
6. Plot the P-DMR amplitudes of 32 μM D-Luciferin as a function of antagonist doses to determine their IC_{50} values using nonlinear regression.

3.5 DMR Desensitization Assay

This section describes the two-step protocol to detect the ability of D-Luciferin to desensitize the cells responding to the repeated stimulation with known GPR35 agonists. This assay is similar to the antagonist assay, except that the two steps are often separated by 1 h. Results showed that D-Luciferin dose-dependently caused HT-29 cells desensitized to the repeated stimulation with 250 nM zaprinast, leading to an apparent IC_{50} of 6.8 μM (*see* Fig. 5), which was close to the EC_{50} of D-Luciferin (12.9 μM). This result suggests that both D-Luciferin and zaprinast activate the same receptor, GPR35.

1. Prepare cell assay and compound source plates similar to the **steps 1** and **2** in Subheading 3.2.
2. Incubate cell and compound plates inside the reader for about 1 h.

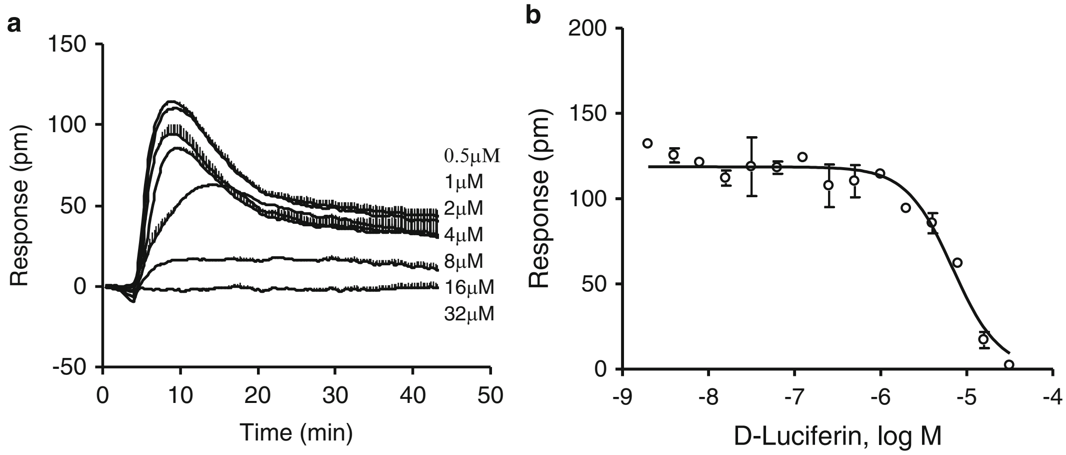

Fig. 5 The desensitization of HT-29 to 250 nM zaprinast after 1 h pretreatment with D-Luciferin at different doses. Only the zaprinast-induced DMR signals were shown: (**a**) the real-time kinetic response of zaprinast; and (**b**) the zaprinast P-DMR amplitudes as a function of D-Luciferin concentration ($n = 4$). This figure is reproduced from ref. 23 through the Creative Commons Attribution License

3. Establish a 2 min baseline.
4. Pause the reader, and add D-Luciferin dose series solutions.
5. Run the reader immediately, and record the DMR of D-Luciferin for about 1 h.
6. Stop the reader, and reestablish a second 2 min baseline.
7. Pause the reader, and add solutions of 250 nM zaprinast.
8. Run the reader immediately, and record the DMR of zaprinast for about 1 h.
9. Background-correct all DMR signals using intra-plate negative controls.
10. Plot the P-DMR amplitudes of 250 nM zaprinast as a function of D-Luciferin dose to determine its IC_{50} to desensitize the cells responding to zaprinast using nonlinear regression.

3.6 Receptor Internalization Assay

This section describes the protocol to stain GPR35 to visualize the location of GPR35 before and after stimulation with zaprinast or D-Luciferin. Results showed that similar to zaprinast, D-Luciferin resulted in remarked internalization of endogenous GPR35 in HT-29 cells (*see* Fig. 6).

1. After overnight culture, add agonist solutions to the cells and incubate at 37 °C for 1 h. Equal amount of DMSO solution is used as the negative control.
2. Fix the cells with 4% formaldehyde in 1× PBS for 15 min.
3. Permeabilize the cells with a buffer containing 4% goat serum, 0.1% bovine serum albumin (BSA), 0.1% Triton X100 in 1× PBS for 2 h. The use of serum and BSA is to block nonspecific binding of antibody.

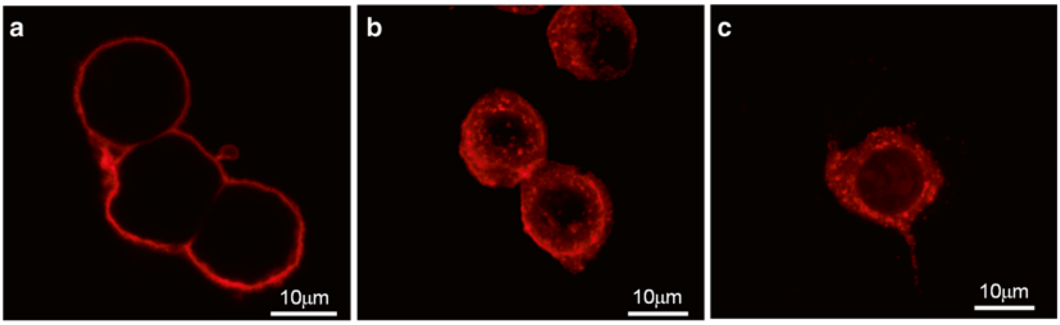

Fig. 6 Confocal fluorescence images of HT-29 after different treatments. (**a**) the assay vehicle containing 0.1% DMSO; (**b**) 32 μM D-Luciferin; (**c**) 10 μM zaprinast. The images were obtained after compound treatment for 1 h, permeabilized, stained with anti-GPR35, followed by fluorescent secondary antibody. *Red*: GPR35 stains. Representative images obtained from two independent measurements were used. This figure is reproduced from ref. 23 through the Creative Commons Attribution License

4. Wash the cells with PBS for 5 min, and incubate with the anti-GPR35 (1:500) in 3% BSA/PBS buffer for 24 h (*see* **Note 11**).
5. Incubate with the secondary antibody Alexa Fluor® 594 donkey anti-goat IgG (H+L) (1:500) in 3% BSA/PBS for 1 h at room temperature.
6. Wash the cells once with PBS, and seal the cells with 1.5 mm thick glass cover-slip.
7. Store the dried slide at 4 °C until imaging.
8. Perform confocal imaging with Zeiss confocal microscope Axiovert 40.
9. Analyze the images using NIH Image J software.

3.7 Tango β-Arrestin Translocation Assay

This section describes the protocol to perform Tango β-arrestin translocation assay using U2OS-GPR35-*bla* cells. This assay measures gene reporter activity arising from GPR35 activation. Agonist binding to GPR35 causes recruitment of protease tagged β-arrestin to GPR35 at the cell plasma surface. The protease then cleaves a protease cleavage site that links a transcription factor with the receptor C-terminus, thus releasing the transcription factor, which then translocates to the nucleus and activates the expression of β-lactamase. Results showed that zaprinast, pamoic acid, and D-Luciferin all led to a dose-dependent response in U2OS-GPR35-*bla* cells, yielding an EC_{50} of 5.0 μM, 9.4 μM, and 277 μM, respectively (*see* Fig. 7). Interestingly, in this assay zaprinast acted as a full agonist, pamoic acid a strong partial agonist, D-Luciferin a weak partial agonist.

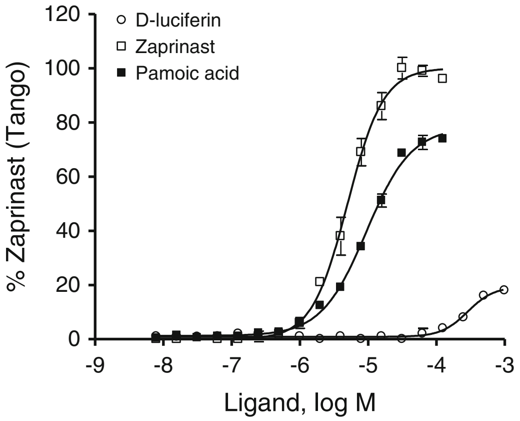

Fig. 7 D-Luciferin caused β-arrestin translocation via GPR35. The dose-dependent responses of three ligands as measured using Tango™ β-arrestin translocation gene reporter assays. The data represents mean ± s.d. from two independent measurements, each in duplicate ($n=4$). This figure is reproduced from ref. 23 through the Creative Commons Attribution License

1. After overnight culture in 384-well, black-wall, clear bottom assay plate with low fluorescence background, treat the cells with ligands for 5 h in a humidified 37 °C/5 % CO_2.
2. Add the cell permeable LiveBLAzer™ FRET B/G substrate to the cells.
3. Incubate for 2 h, and measure the coumarin:fluorescein ratio using Tecan Safire II microplate reader.
4. Background-correct all responses using intra-plate negative controls.
5. Normalize all coumarin:fluorescein ratios to the zaprinast maximal responses using an intra-plate referencing protocol; that is, a dose response of zaprinast is obtained within the same plate, and a compound response is then normalized to the maximal response of zaprinast which is set to be 100 %.
6. Determine the potency and efficacy of D-Luciferin.

4 Notes

1. Cells can undergo genetic drifting during passaging. Given the high sensitivity of DMR assays, the DMR of a ligand may be sensitive to passages of cells under culture.
2. The biosensor microplate is tissue culture treated and ready to use. However, aged biosensor microplate may become hydrophobic, resulting in air bubbles during cell seeding and possible cell death. Pre-incubation with the complete medium followed by one-time rinse often solves this problem. When air bubble is formed and trapped in the bottoms of the wells, one can use the pipettor to manually remove air bubble(s) after seeding.
3. Many compounds are stored in DMSO. DMSO is a solvent with dual effects on biosensor cell assays; namely, bulk index effect due to its high refractive index, and nonspecific effect on cells due to its biological activity. Thus, it is important to minimize the DMSO concentration in the final compound solution (typically <0.1 v/v%).
4. Many cell types are sensitive to mechanical disturbance during the wash. Receptor signaling is also often sensitive to buffer conditions (e.g., salts, growth factors in medium, pH, etc.). Thus, it is important to optimize the wash protocol so gentle and thorough wash is warranted to obtain optimal assays.
5. RWG biosensor measures changes in local refractive index in living cells upon stimulation. Given that refractive index is sensitive to temperature, any temperature mismatch between the two solutions could cause noticeable interference. A pre-equilibrium step is important to minimize the thermal mismatch effect.

6. Confluent cells generally give rise to a steady baseline. However, washing and thermal equilibrium steps may cause baseline drifting. So, baseline monitoring for a short period of time is essential to high quality data acquisition. Typically, the drifting that is <10 picometer (pm in wavelength shift) within 5 min is considered to be steady and acceptable.
7. The activation of certain receptors may lead to rapid on-set response. Thus, it is important to minimize the blackout period between the baseline and the first recording after compound addition. The blackout period is ideally <1 min.
8. The DMR recording duration is dependent on applications. For drug pharmacology profiling and receptor biology study, it is typically about 1 h. For long-term effect of drugs, it can be long as several days. The temporal resolution of DMR recording can also be variable and adjustable (typically in the range of 3 s to 1 min).
9. Background could be aroused from multiple sources, such as temperature mismatch, plate movement, mechanical disturbance during compound addition, and buffer composition mismatch. Most of background signals can be corrected by using intra-plate negative controls, which contain equal amount of DMSO used for compound solutions; or DMSO dose series equal to the compound dose series. Alternative solvents such as ethanol or water can be used if necessary.
10. DMR is a real-time kinetic response, thus enabling the extraction of multiple kinetic parameters for analyzing drug pharmacology [32–36]. These parameters include the transition time from one to another event, and the amplitudes, duration, and kinetics of each event. For a panel of agonists for the same receptor, multiparameter analysis is useful to examine biased agonism.
11. The specificity of anti-GPR35 was confirmed by the control peptide from the supplier. Staining showed that the control peptide completely blocked the staining of HT-29 cells with the anti-GPR35 antibody.

References

1. Contag CH, Bachmann MH (2002) Advances in in vivo bioluminescence imaging of gene expression. Annu Rev Biomed Eng 4: 235–260
2. Negrin RS, Contag CH (2006) In vivo imaging using bioluminescence: a tool for probing graft-versus-host disease. Nat Rev Immunol 6:484–490
3. Luker GD, Luker KE (2008) Optical imaging: current applications and future directions. J Nucl Med 49:1–4
4. Keyaerts M, Caveliers V, Lahoutte T (2012) Bioluminescence imaging: looking beyond the light. Trends Mol Med 18:164–172
5. Greer LF III, Szalay AA (2002) Imaging of light emission from the expression of luciferases in living cells and organisms. Luminescence 17:43–74
6. Shinde R, Perkins J, Contag CH (2006) Luciferin derivatives for enhanced in vitro and in vivo bioluminescence assays. Biochemistry 45:11103–11112

7. White EH, Rapaport E, Hopkins TA, Seliger HH (1969) Chemi- and bioluminescence of firefly luciferin. J Am Chem Soc 91:2178–2180
8. Ando Y, Niwa K, Yamada N, Enomoto T, Irie T, Kubota H, Ohmiya Y, Akiyama H (2008) Firefly bioluminescence quantum yield and colour change by pH-sensitive green emission. Nat Photonics 2:44–47
9. Nakatsu T, Ichiyama S, Hiratake J, Saldanha A, Kobashi N, Sakata K, Kato H (2006) Structural basis for the spectral difference in luciferase bioluminescence. Nature 440:372–376
10. Jathoul AP, Grounds H, Anderson JC, Pule MA (2014) A dual-color far-red to near-infrared firefly luciferin analogue designed for multiparametric bioluminescence imaging. Angew Chem Int Ed Engl 53:13059–13063
11. Fang Y, Ferrie AM, Fontaine NH, Yuen PK (2005) Characteristics of dynamic mass redistribution of EGF receptor signaling in living cells measured with label free optical biosensors. Anal Chem 77:5720–5725
12. Fang Y, Ferrie AM, Fontaine NH, Mauro J, Balakrishnan J (2006) Resonant waveguide grating biosensor for living cell sensing. Biophys J 91:1925–1940
13. Schröder R, Janssen N, Schmid J, Kebig A, Merten N, Hennen S, Müller A, Blättermann S, Mohr-Andrä M, Zahn S, Wenzel J, Smith NJ, Gomeza J, Drewke C, Milligan G, Mohr K, Kostenis E (2010) Deconvolution of complex G protein-coupled receptor signaling in live cells using dynamic mass redistribution measurements. Nat Biotechnol 28:943–949
14. Verrier F, An S, Ferrie AM, Sun H, Kyoung M, Fang Y, Benkovic SJ (2011) GPCRs regulate the assembly of a multienzyme complex for purine biosynthesis. Nat Chem Biol 7:909–915
15. Fang Y (2014) Label-free drug discovery. Front Pharmacol 5:52
16. Fang Y (2015) Combining label-free cell phenotypic profiling with computational approaches for novel drug discovery. Expert Opin Drug Discov 10:331–343
17. Deng H, Hu H, He M, Hu J, Niu W, Ferrie AM, Fang Y (2011) Discovery of 2-(4-methylfuran-2(5H)-ylidene)malononitrile and thieno[3,2-b]thiophene-2-carboxylic acid derivatives as G protein-coupled receptor 35 (GPR35) agonists. J Med Chem 54: 7385–7396
18. Deng H, Hu H, Ling S, Ferrie AM, Fang Y (2012) Discovery of natural phenols as G protein-coupled receptor-35 (GPR35) agonists. ACS Med Chem Lett 3:165–169
19. MacKenzie AE, Lappin JE, Taylor DL, Nicklin SA, Milligan G (2011) GPR35 as a novel therapeutic target. Front Endocrinol 2:68
20. Deng H, Hu H, Fang Y (2012) Multiple tyrosine metabolites are GPR35 agonists. Sci Rep 2:373
21. Divorty N, Mackenzie AE, Nicklin SA, Milligan G (2015) G protein-coupled receptor 35: an emerging target in inflammatory and cardiovascular disease. Front Pharmacol 6:41
22. Shore DM, Reggio PH (2015) The therapeutic potential of orphan GPCRs, GPR35 and GPR55. Front Pharmacol 6:69
23. Hu H, Deng H, Fang Y (2012) Label-free phenotypic profiling identified D-luciferin as a GPR35 agonist. PLoS One 7:e34934
24. Thimm D, Funke M, Meyer A, Müller CE (2013) 6-Bromo-8-(4-[3H]methoxybenzamido)-4-oxo-4H-chromene-2-carboxylic acid: a powerful tool for studying orphan G protein-coupled receptor GPR35. J Med Chem 56:7084–7099
25. Ferrie AM, Wu Q, Fang Y (2010) Resonant waveguide grating imager for live cell sensing. Appl Phys Lett 97:223704
26. Fang Y (2013) Troubleshooting and deconvoluting label-free cell phenotypic assays in drug discovery. J Pharmacol Toxicol Methods 67:69–81
27. Ferrie AM, Sun H, Zaytseva N, Fang Y (2014) Divergent label-free cell phenotypic pharmacology of ligands at the overexpressed β_2-adrenergic receptors. Sci Rep 4:3828
28. Zhang X, Deng H, Xiao Y, Xue X, Ferrie AM, Tran E, Liang X, Fang Y (2014) Label-free cell phenotypic profiling identifies pharmacologically active compounds in two Traditional Chinese Medicinal plants. RSC Adv 4:26368–26377
29. Fang Y (2014) Label-free cell phenotypic drug discovery. Comb Chem High Throughput Screen 17:566–578
30. Zhao P, Sharir H, Kapur A, Cowan A, Geller EB, Adler MW, Seltzman HH, Reggio PH, Heynen-Genel S, Sauer M, Chung TD, Bai Y, Chen W, Caron MG, Barak LS, Abood ME (2010) Targeting of the orphan receptor GPR35 by pamoic acid: a potent activator of ERK and β-arrestin2, with antinociceptive activity. Mol Pharmacol 78:560–568
31. Taniguchi Y, Tonai-Kachi H, Shinjo K (2006) Zaprinast, a well-known cyclic guanosine monophosphate-specific phosphodiesterase inhibitor, is an agonist for GPR35. FEBS Lett 580:5003–5008
32. Fang Y, Ferrie AM (2008) Label-free optical biosensor for ligand-directed functional selectivity acting on β_2-adrenoceptor in living cells. FEBS Lett 582:558–564

33. Fang Y, Ferrie AM, Tran E (2009) Resonant waveguide grating biosensor for whole cell GPCR assays. Methods Mol Biol 552: 239–252
34. Deng H, Wang C, Su M, Fang Y (2012) Probing biochemical mechanisms of action of muscarinic M_3 receptor antagonists with label-free whole-cell assays. Anal Chem 84:8232–8239
35. Deng H, Sun H, Fang Y (2013) Label-free cell phenotypic assessment of the biased agonism and efficacy of agonists at the endogenous muscarinic M_3 receptors. J Pharmacol Toxicol Methods 68:323–333
36. Fang Y (ed) (2015) Label-free biosensor methods in drug discovery, Methods in pharmacology and toxicity. Springer, New York

Chapter 2

Synthetic Bioluminescent Coelenterazine Derivatives

Ryo Nishihara, Daniel Citterio, and Koji Suzuki

Abstract

The development of coelenterazine (CTZ) derivatives resulting in superior optical characteristics is an efficient method to extend the range of its possible applications. Here, we describe the synthesis of three C-6 substituted CTZ derivatives retaining the recognition by *Renilla* luciferase (RLuc) and its derivatives. The novel derivatives are useful as bright blue-shifted CTZ derivatives, which can be used as an alternative to hitherto reported compound DeepBlueC™.

Key words Bioluminescence, Coelenterazine (CTZ), *Renilla* Luciferase (RLuc), DeepBlueC, Luciferin, Luciferase, Chemiluminescence

1 Introduction

Bioluminescence is emitted by an enzymatic oxidation reaction involving a bioluminescent substrate (luciferin) and an enzyme (luciferase). Firefly luciferin, which emits light at a relatively long wavelength ($\lambda_{max} = 560$ nm) in the presence of Mg^{2+} and ATP as cofactors, is widely used in bioassays. However, the cofactors potentially lead to complex assay protocols in bioanalysis [1]. In contrast, marine luciferases such as *Renilla* luciferase (RLuc) generate cofactor-free bioluminescence with native coelenterazine (nCTZ). There is a lot of interest in developing new CTZ derivatives [2–7]. However, the design of novel CTZ derivatives resulting in enhanced optical intensity with prolonged bioluminescence is challenging, because the detailed enzymatic recognition mechanism of the RLuc/CTZ reaction is still mostly unknown [8–10]. In fact, most of the reported CTZ analogs fail to emit bioluminescence, since their structural modifications prevent their enzymatic recognition.

As the bioluminescence capacity of CTZ is due to its imidazopyrazinone backbone, precedent studies have focused on the effect of substitution at the C-2, C-5, C-6, and C-8 positions of the backbone [2, 3, 7, 11, 12]. Although the substitution effect at

Sung-Bae Kim (ed.), *Bioluminescence: Methods and Protocols*, Methods in Molecular Biology, vol. 1461,
DOI 10.1007/978-1-4939-3813-1_2, © Springer Science+Business Media New York 2016

the C-2 position on enzymatic recognition is relatively low, most of the CTZ analogs substituted at C-2 position cannot show bioluminescence properties superior to those of native CTZ. In contrast to the C-2 position, the substitution at the C-8 position resulted in negligibly low bioluminescence in combination with RLuc [2, 13]. Formation of a bridge between C-5 and C-6 positions leads to more planar and rigid molecular structures and sacrifices chemical stability [14]. Although the C-6 position is an alternative site for substitution, most of the studies have focused on the chemiluminescence properties [5, 6, 15, 16].

In this protocol, we introduce the creation of efficient CTZ derivatives optimized for RLuc and its derivatives, which is the most widely used marine luciferase [17].

2 Materials

2.1 Components for Synthesis of CTZ

All solvents and routine reagents for organic synthesis can be purchased from commercial suppliers.

1. 2-Amino-3,5-dibromopyrazine (starting material; store at 5 °C).
2. Benzylmagnesium chloride solution 2.0 M in THF (Grignard reagent).
3. Zinc chloride.
4. Tetrakis(triphenylphosphine)palladium(0) (store at −30 °C).
5. Trans-2-phenylvinylboronic acid.
6. Trans-2-(4-methoxyphenyl)vinylboronic acid (Aldrich Chemical).
7. Trans-(2-([1,1′-biphenyl]-4-yl)vinyl)boronic acid (Aldrich Chemical).
8. 1.0 M Boron tribromide dichloromethane solution (Lewis acid).
9. 4-Hydroxybenzaldehyde (starting material).
10. *tert*-Butyldimethylchlorosilane.
11. Triethylamine.
12. Sodium tetrahydridoborate (reducing reagent).
13. Methanesulfonyl chloride.
14. Magnesium turnings.
15. Ethyl diethoxyacetate.

2.2 Components for Chemiluminescence Assay

All solvents for spectrometry can be purchased from commercial suppliers.

1. Native CTZ (nCTZ, Biotium) (store at −30 °C) (*see* **Note 1**).
2. DeepBlueC™ (Biotium) (store at −30 °C).

2.3 Components for Bioluminescence Assay

1. pcDNA3.1(+) (Invitrogen) encoding wild-type Renilla luciferase (pGL4.75) (Promega, Madison, WI, USA).
2. pcDNA3.1(+) (Invitrogen) encoding RLuc variants (RLuc8 and RLuc8.6-535) (Gambhir lab., Stanford Univ.).
3. Native CTZ (nCTZ, NanoLight Technologies, Pinetop, AZ, USA).
4. TransIT-LT1 transfection reagent (Takara, Osaka, Japan).
5. Lysis buffer (E291A) (Promega, Madison, WI, USA).
6. Hanks' balanced salt solution (HBSS).

3 Methods

3.1 General Procedure for Synthesis

1. Carry out all moisture-sensitive reactions under an atmosphere of argon.
2. The composition of mixed solvents is given by the volume ratio (v/v).
3. Record ^{1}H-NMR and ^{13}C-NMR spectra on an ECA-500 (JEOL Ltd.) or ECA-600 (JEOL Ltd.) spectrometer at room temperature.
4. The measurement for ^{1}H-NMR is performed at 500 MHz.
5. The measurement of ^{13}C-NMR is performed at 125 MHz or 150 MHz.
6. All chemical shifts are relative to an internal standard of tetramethylsilane ($\delta = 0.0$ ppm) or solvent residual peaks ($CDCl_3$: $\delta = 7.26$ ppm, CD_3OD: $\delta = 3.31$ ppm, DMSO-d_6: $\delta = 2.50$ ppm for ^{1}H; $CDCl_3$: $\delta = 77.16$ ppm, CD_3OD: $\delta = 49.00$ ppm, DMSO-*d6*: $\delta = 39.52$ ppm for ^{13}C), and coupling constants are given in Hz.
7. Conduct flash chromatography separation using a YFLC-Al-560 chromatograph (Yamazen Co. Ltd.).
8. Perform HPLC purification on a reversed-phase column, Inertsil ODS-3 (30 × 50 mm) (GL Sciences Inc.), fitted on an LC-918 recycling preparative HPLC system (Japan Analytical Industry Co. Ltd.).
9. Record high-resolution MS spectra (HR-MS) on a Waters LCT premier XE with MeOH as the eluent.

3.1.1 Synthesis of 3-Benzyl-5-bromopyrazin-2-amine (See Fig. 1 Compound (2))

1. Dissolve zinc chloride (1.62 g, 11.9 mmol, 3.0 eq.) in Et_2O (12 mL) and THF (27 mL) (*see* **Note 2**).
2. Add 2.0 M benzylmagnesium chloride solution (4.4 mL, 8.94 mmol, 2.2 eq.) slowly into the solution at room temperature under argon (*see* **Note 3**).
3. Add 3,5-dibromopyrazin-2-amine (1.0 g, 3.96 mmol, 1 eq.) dissolved in THF (5 mL) into the solution (*see* **Note 4**).

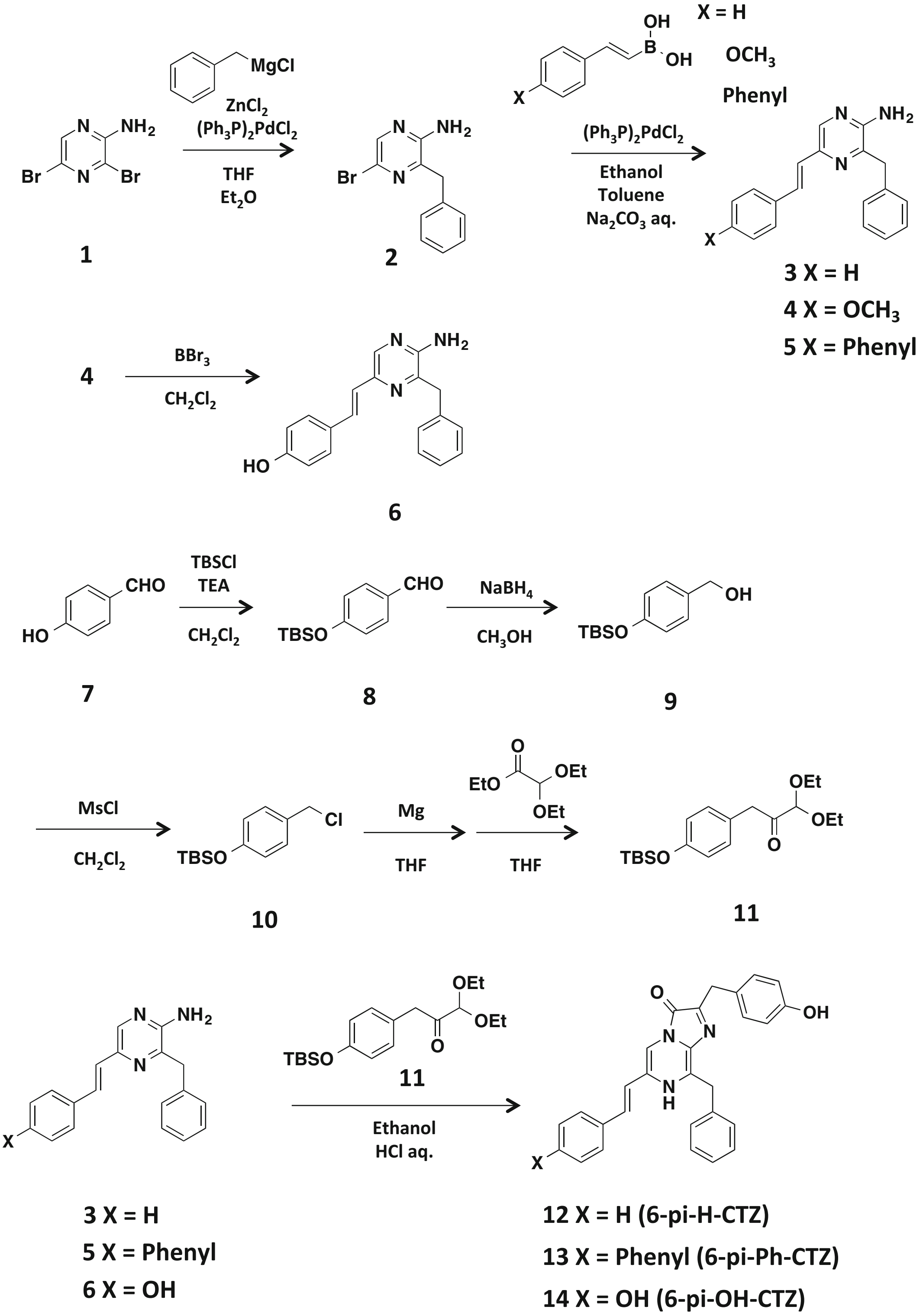
MgCl
ZnCl$_2$
(Ph$_3$P)$_2$PdCl$_2$
THF
Et$_2$O
Br
NH$_2$
N
1
2
X = H
OCH$_3$
Phenyl
OH
B
(Ph$_3$P)$_2$PdCl$_2$
Ethanol
Toluene
Na$_2$CO$_3$ aq.
X
3 X = H
4 X = OCH$_3$
5 X = Phenyl
4
BBr$_3$
CH$_2$Cl$_2$
HO
6
CHO
TBSCl
TEA
CH$_2$Cl$_2$
TBSO
NaBH$_4$
CH$_3$OH
OH
7
8
9
MsCl
CH$_2$Cl$_2$
Cl
Mg
THF
EtO
O
OEt
THF
10
11
Ethanol
HCl aq.
H
3 X = H
5 X = Phenyl
6 X = OH
12 X = H (6-pi-H-CTZ)
13 X = Phenyl (6-pi-Ph-CTZ)
14 X = OH (6-pi-OH-CTZ)

Fig. 1 Synthesis scheme for 6-pi-H-CTZ, 6-pi-Ph-CTZ, and 6-pi-OH-CTZ Compound (**2**), (**3**), (**8**), (**9**), (**10**), and (**11**) were synthesized according to reported procedure [18–20]

4. After vacuum deaeration, add a catalytic amount of tetrakis(triphenylphosphine)palladium(0) into the solution, deaerate the mixture again and stir for 23 h at room temperature (*see* **Note 5**).
5. Filter the solution through a Celite pad to remove the palladium catalyst, and evaporate to remove most of solvent.
6. Extract the residue with ethyl acetate, and wash the yellow organic phase with water and brine, dry over Na_2SO_4, and evaporate.
7. Purify the resulting residue by flash chromatography (silica gel, eluent composition: n-hexane/ethyl acetate = 80/20 to 70/30), affording 3-benzyl-5-bromopyrazin-2-amine (**2**) as yellow liquid (0.73 g, 69%).

^{1}H-NMR (500 MHz, $CDCl_3$): δ (ppm) = 8.04 (s, 1H), 7.21–7.38 (m, 5H), 4.37 (s, 2H), 4.08 (s, 2H).

3.1.2 General Procedure for Preparations of Compounds (3) to (5)

1. Dissolve 3-benzyl-5-bromopyrazine-2-amine (**2**) (200 mg, 0.76 mmol, 1 eq.) and (*E*)-styrylboronic acid derivatives (1.22 mmol, 1.6 eq.) in toluene (16 mL) and stir at room temperature.
2. Add ethanol (2.4 mL) and 1 M Na_2CO_3 aq. (6 mL) into the reaction mixture.
3. After vacuum deaeration, add a catalytic amount of tetrakis(triphenylphosphine)palladium(0) into the solution, deaerate the mixture again, and stir for 12 h at 100 °C.
4. After cooling to room temperature, filter the solution through a Celite pad to remove the palladium catalyst.
5. Extract the solution with ethyl acetate, and wash the brown organic phase with water and brine, dry over Na_2SO_4, and evaporate.
6. Purify the resulting residue by flash chromatography (silica gel, eluent: *n*-hexane/ethyl acetate).

3.1.3 Synthesis of (E)-3-Benzyl-5-styrylpyrazin-2-amine (See Fig. 1 Compound (3))

Yield 67% (yellow solid compound). Eluent composition: n-hexane/ethyl acetate = 67/33 to 50/50. ^{1}H-NMR (500 MHz, $CDCl_3$): δ (ppm) = 7.94 (s, 1H), 7.53 (d, *J* = 7.7 Hz, 2H), 7.47 (d, *J* = 16.0 Hz, 1H), 7.23–7.36 (m, 8H), 7.06 (d, *J* = 16.0 Hz, 1H), 4.49 (s, 2H), 4.12 (s, 2H). ^{13}C-NMR (125 MHz, $CDCl_3$): δ (ppm) = 41.5, 124.9, 126.8, 127.2, 127.9, 128.6, 128.7, 129.1, 136.7, 137.2, 139.6, 141.1, 141.3, 151.8. HR-MS: m/z calcd for $C_{19}H_{17}N_3$: 287.1422, found: 288.1501 $[M+H]^+$.

3.1.4 Synthesis of (E)-3-Benzyl-5-(4-methoxystyryl)pyrazin-2-amine (See Fig. 1 Compound (4))

Yield 50% (yellow solid compound). Eluent composition: n-hexane/ethyl acetate = 80/20 to 50/50. ^{1}H-NMR (500 MHz, $CDCl_3$): δ (ppm) = 7.99 (s, 1H), 7.47 (dd, *J* = 8.6 Hz, 16.0 Hz, 2H), 7.24–7.33 (m, 5H), 6.96 (d, *J* = 16.0 Hz, 1H), 6.90 (d, *J* = 14.6 Hz, 2H), 4.42 (s, 2H), 4.15 (s, 2H), 3.82 (s, 3H). ^{13}C-

NMR (125 MHz, $CDCl_3$): δ (ppm) = 41.4, 55.4, 114.2, 122.8, 127.1, 128.1, 128.6, 129.1, 129.3, 130.0, 136.8, 139.2, 141.0, 141.7, 151.6, 159.5. HR-MS: m/z calcd for $C_{20}H_{19}N_3O$: 317.1528, found: 318.1606 $[M+H]^+$.

3.1.5 Synthesis of (E)-5-(2-([1,1′-Biphenyl]-4-yl)vinyl)-3-benzylpyrazin-2-amine (See Fig. 1 Compound (5))

Yield 24% (yellow solid compound). Eluent composition: n-hexane/ethyl acetate = 80/20 to 50/50. ^{1}H-NMR (500 MHz, $CDCl_3$): δ (ppm) = 8.03 (s, 1H), 7.63–7.59 (m, 7H), 7.54 (d, J = 16.0 Hz, 1H), 7.43 (t, J = 15.5, 2H), 7.34–7.31 (m, 3H), 7.27–7.24 (m, 3H), 7.14 (d, J = 16.0 Hz, 1H), 4.45 (s, 2H), 4.16 (s, 2H). ^{13}C-NMR (125 MHz, $CDCl_3$): δ (ppm) = 41.4, 124.8, 127.0, 127.2, 127.3, 127.4, 128.6, 128.9, 129.1, 136.3, 136.6, 139.6, 140.5, 140.7, 141.1, 141.3, 151.8. HR-MS: m/z calcd for $C_{25}H_{21}N_3$: 363.1735, found: 364.1814 $[M+H]^+$.

3.1.6 Synthesis of (E)-4-(2-(5-Amino-6-benzylpyrazin-2-yl)vinyl)phenol (See Fig. 1 Compound (6))

1. Dissolve (*E*)-3-benzyl-5-(4-methoxystyryl)pyrazin-2-amine (**4**) (202 mg, 0.64 mmol, 1 eq.) in dichloromethane (12 mL) (*see* **Note 6**).
2. Add 1.0 M boron tribromide dichloromethane solution (12 mL) slowly into the solution at 0 °C, followed by stirring for 13 h at 40 °C (*see* **Note 7**).
3. After cooling to room temperature, add saturated $NaHCO_3$ aq. into the reaction mixture to neutralize, and evaporate to remove most of the solvent.
4. Extract the residue with ethyl acetate, and wash the yellow organic phase with water and brine, dry over Na_2SO_4, and evaporate.
5. Purify the resulting residue by flash chromatography (silica gel, eluent composition: n-hexane/ethyl acetate = 50/50), affording (*E*)-4-(2-(5-amino-6-benzylpyrazin-2-yl)vinyl)phenol (**6**) as a yellow solid (42.7 mg, 22%).

^{1}H-NMR (500 MHz, CD_3OD): δ (ppm) = 7.93 (s, 1H), 7.37 (d, J = 8.6 Hz, 2H), 7.38–7.21 (m, 6H), 6.93 (d, J = 16.0 Hz, 1H), 6.77 (d, J = 8.6 Hz, 2H), 4.11 (s, 2H). ^{13}C-NMR (125 MHz, DMSO-*d6*): δ (ppm) = 39.2, 116.1, 122.6, 126.7, 127.7, 128.3, 128.7, 128.8, 129.3, 138.7, 139.3, 139.5, 141.1, 152.9, 157.7 HR-MS: m/z calcd for $C_{19}H_{17}N_3O$: 303.1372, found: 304.1450 $[M+H]^+$.

3.1.7 Synthesis of 4-((tert-Butyldimethylsilyl)oxy)benzaldehyde (See Fig. 1 Compound (8))

1. Dissolve 4-hydroxybenzaldehyde (**7**) (10.0 g, 82.3 mmol, 1 eq.) and *tert*-butyldimethylsilyl chloride (13.6 g, 90.8 mmol, 1.1 eq.) in dichloromethane (400 mL).
2. Add triethylamine (15 mL) into the solution at 0 °C, followed by stirring for 18 h at room temperature.
3. Evaporate to remove a part of the solvent and wash the transparent organic phase with water and brine, dry over Na_2SO_4, and evaporate.

4. Purify the resulting residue by flash chromatography (silica gel, eluent composition: n-hexane/ethyl acetate = 90/10), affording 4-((*tert*-butyldimethylsilyl)oxy)benzaldehyde (**8**) as a water-clear viscous oil (18.5 g, 95 %).

^{1}H-NMR (500 MHz, $CDCl_3$): δ (ppm) = 9.89 (s, 1H), 7.99 (d, *J* = 8.7 Hz, 2H), 6.95 (d, *J* = 8.7 Hz, 2H), 1.00 (s, 9H), 0.25 (s, 6H).

3.1.8 Synthesis of (4-((tert-Butyldimethylsilyl)oxy)phenyl)methanol (See Fig. 1 Compound (9))

1. Dissolve 4-((*tert*-butyldimethylsilyl)oxy)benzaldehyde (**8**) (18.9 g, 79.9 mmol, 1 eq.) in methanol (300 mL).
2. Add sodium borohydride (3.7 g, 97.5 mmol, 1.2 eq.) into the solution, followed by stirring for 30 min at room temperature.
3. Evaporate to remove most of the solvent.
4. Extract the residue with dichloromethane, and wash the transparent organic phase with water and brine, dry over Na_2SO_4, and evaporate, affording (4-((*tert*-butyldimethylsilyl)oxy)phenyl)methanol (**9**) as a water-clear viscous oil (21.1 g, 99 %).

^{1}H-NMR (500 MHz, $CDCl_3$): δ (ppm) = 7.24 (d, *J* = 8.4 Hz, 2H), 6.83 (d, *J* = 8.4 Hz, 2H), 4.61 (s, 2H), 0.95 (s, 9H), 0.20 (s, 6H).

3.1.9 Synthesis of tert-Butyl(4-(chloromethyl)phenoxy)dimethylsilane (See Fig. 1 Compound (10)) (see Note 8)

1. Dissolve (4-((*tert*-butyldimethylsilyl)oxy)phenyl)methanol (**9**) (7.0 g, 29.3 mmol, 1.0 eq.) and triethylamine (8.0 mL, 58.6 mmol, 2.0 eq.) in dichloromethane (150 mL).
2. Add methylsulfonyl chloride (3.4 g, 44.6 mmol, 1.5 eq.) dissolved in dichloromethane (50 mL) into the solution at 0 °C, followed by stirring for 3 h at room temperature.
3. Evaporate to remove a part of the solvent and wash the transparent organic phase with water and brine, dry over Na_2SO_4, and evaporate.
4. Purify the resulting residue by flash chromatography (silica gel, eluent composition: n-hexane/ethyl acetate = 95/5), affording *tert*-butyl(4-(chloromethyl)phenoxy)dimethylsilane (**10**) as a water-clear viscous oil (5.09 g, 68 %).

^{1}H-NMR (500 MHz, $CDCl_3$): δ (ppm) = 7.24 (d, *J* = 8.6 Hz, 2H), 6.81 (d, *J* = 8.6 Hz, 2H), 4.55 (s, 2H), 0.98 (s, 9H), 0.20 (s, 6H).

3.1.10 Synthesis of 3-(4-((tert-Butyldimethylsilyl)oxy)phenyl)-1,1-diethoxypropane-2-one (See Fig. 1 Compound (11))

1. Add magnesium turnings (774.5 mg, 31.9 mmol, 2 eq.) into THF (10 mL), followed by additional THF (10 mL) and a catalytic amount of 1,2-dibromoethane (0.4 mL, 0.004 mmol) under argon to activate magnesium turnings.
2. Add *tert*-butyl(4-(chloromethyl)phenoxy)dimethylsilane (**10**) (4.0 g, 15.6 mmol, 1.0 eq.) dissolved in THF (40 mL) slowly into the solution, followed by stirring for 1 h at 50 °C (*see* **Note 9**).

3. After cooling to room temperature, the Grignard reagent is obtained as dark gray solution.
5. Add ethyl diethoxyacetate (3.2 mL, 17.9 mmol, 0.9 eq.) and THF (30 mL) into a separate reaction flask, followed by stirring at −78 °C (acetone / dry ice).
4. Add the Grignard reagent slowly into the solution under argon, followed by stirring for 2 h at −78 °C.
5. Add water into the solution to quench, followed by warming to room temperature and evaporating to remove most of the solvent.
6. Extract the residue with ethyl acetate, and wash the transparent organic phase with water and brine, dry over Na_2SO_4, and evaporate.
7. Purify the resulting residue by silica gel chromatography (eluent composition: n-hexane/ethyl acetate = 95/5 to 90/10), affording 3-(4-((*tert*-butyldimethylsilyl)oxy)phenyl)-1,1-diethoxypropane-2-one (**11**) as a water-clear viscous oil (2.5 g, 47%).

^{1}H-NMR (500 MHz, $CDCl_3$): δ (ppm) = 7.08–7.06 (m, 2H), 6.79–6.76 (m, 2H), 4.62 (s, 1H), 3.80 (s, 2H), 3.73–3.63 (m, 2H), 3.58–3.48 (m, 2H), 1.24 (t, *J* = 7.1 Hz, 6H), 0.97 (s, 9H), 0.18 (s, 6H).

3.1.11 General Procedure for Preparation of Compounds (12) to (14)

1. Dissolve corresponding coelenteramines (compounds (**3**), (**5**), or (**6**)) (0.10 mmol, 1 eq.) and ketoacetal (**11**) (76.62 mg, 0.21 mmol, 2 eq.) in ethanol (2.0 mL) and H_2O (0.2 mL) and stir at room temperature (*see* **Note 10**).
2. Cool the solution to 0 °C and add HCl (0.1 mL) under nitrogen flow.
3. Once the solution reached room temperature, heat it and stir for 10 h at 70 °C.
4. Evaporate the solvent under vacuum and purify the crude compound by semi-preparative reversed-phase HPLC.

3.1.12 Synthesis of (E)-8-Benzyl-2-(4-hydroxybenzyl)-6-styrylimidazo[1,2-a]pyrazin-3(7H)-one (See Fig. 1 Compound (12)) (6-pi-H-CTZ)

Yield 22% (yellow solid compound). Eluent composition: MeCN/H_2O = 50/50 with 0.1% formic acid.

^{1}H-NMR (500 MHz, CD_3OD, $CDCl_3$): δ (ppm) = 7.59 (s, 1H), 7.37–7.21 (m, 10H), 7.15 (d, *J* = 8.6 Hz, 2H), 6.96 (t, *J* = 16.3 Hz, 1H), 6.69 (d, *J* = 8.6 Hz, 2H), 4.40 (s, 2H), 4.04 (s, 2H). ^{13}C-NMR (150 MHz, CD_3OD, $CDCl_3$): δ (ppm) = 33.8, 115.9, 127.4, 127.9, 129.3, 129.3, 129.4, 129.5, 130.5, 156.3. HR-MS: m/z calcd for $C_{28}H_{23}N_3O_2$: 433.1790, found: 432.1712 $[M-H]^-$.

3.1.13 Synthesis of (E)-6-(2-([1,1′-Biphenyl]-4-yl)vinyl)-8-benzyl-2-(4-hydroxybenzyl) imidazo [1,2-a]pyrazin-3(7H)-one (See Fig. 1 Compound (13)) (6-pi-Ph-CTZ)

Yield 5 % (yellow solid compound). Eluent composition; $CH_3OH/H_2O = 20/1$ with 0.1 % formic acid.

^{1}H-NMR (500 MHz, CD_3OD): δ (ppm) = 7.62–7.57 (m, 7H), 7.43–7.22 (m, 9H), 7.15 (d, J = 8.59 Hz, 2H), 7.05 (d, J = 15.4 Hz, 1H), 6.69 (d, J = 8.59 Hz, 2H), 4.39 (s, 2H), 4.03 (s, 2H). ^{13}C-NMR (150 MHz, CD_3OD, $CDCl_3$): δ (ppm) = 21.4, 116.2, 127.8, 128.3, 128.5, 129.7, 129.9, 130.7, 130.8, 131.3, 136.6, 138.2, 141.7, 142.4, 156.9. HR-MS: m/z calcd for $C_{34}H_{27}N_3O_2$: 509.2103, found: 509.2025 $[M\text{-}H]^-$.

3.1.14 Synthesis of (E)-8-Benzyl-2-(4-hydroxybenzyl)-6-(4-hydroxystyryl) imidazo[1,2-a]pyrazin-3(7H)-one (See Fig. 1 Compound (14)) (6-pi-OH-CTZ)

Yield 23 % (yellow solid compound). Eluent composition: $MeCN/H_2O = 33/67$ with 0.1 % formic acid.

^{1}H-NMR (500 MHz, CD_3OD, $CDCl_3$): δ (ppm) = 7.52 (s, 1H), 7.41–7.21 (m, 10H), 6.82 (d, J = 8.6 Hz, 2H), 6.82 (d, J = 8.6 Hz, 2H), 6.75 (d, J = 8.6 Hz, 2H), 6.62 (d, J = 16.9 Hz, 1H), 4.37 (s, 2H), 4.09 (s, 2H). ^{13}C-NMR (150 MHz, CD_3OD, $CDCl_3$): δ (ppm) = 33.6, 33.8, 108.6, 115.9, 116.4, 127.9, 128.9, 129.3, 129.4, 130.5, 137.3, 149.9, 153.7, 156.2, 158.8. HR-MS: m/z calcd for $C_{28}H_{23}N_3O_3$: 449.1739, found: 448.1661 $[M\text{-}H]^-$.

3.2 Chemiluminescence Assay of CTZ Derivatives

1. Add a CH_3OH solution of the respective CTZ derivative (1 mM, 200 μL) to a quartz cell and set in a SREX Fluorolog-3 fluorescence spectrophotometer (Model FL-3-11, Horiba Jobin Yvon, Kyoto, Japan).
2. Measure the chemiluminescence spectra at a scan rate of 1200 nm/min after injecting 2 mL of DMSO (*see* **Note 11**). Figure 1 shows the chemiluminescence spectra of native CTZ and the CTZ derivatives (*see* Fig. 2).

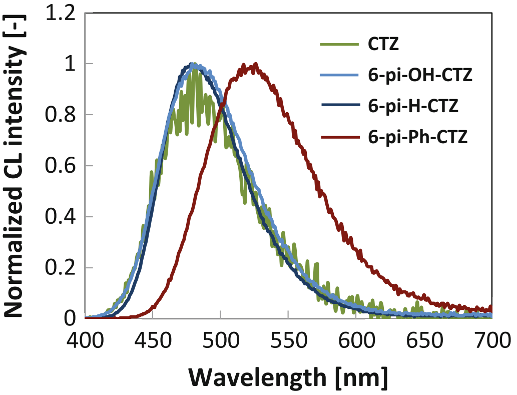

Fig. 2 Chemiluminescence spectra. The chemiluminescence reaction is triggered by addition of DMSO to stock solution of MeOH. The spectra are normalized to 1 at the peak emission

3.3 Bioluminescence Assay of CTZ Derivatives

3.3.1 General Procedure for Bioluminescence Assay

1. To determine the bioluminescence properties of the novel CTZ derivatives, transfect plasmids encoding wild-type Renilla luciferase (RLuc), and variants RLuc8 and RLuc8.6 separately into COS-7 cells cultured in a 24-well plate using a TransIT-LT1 transfection reagent (Takara, Osaka, Japan).
2. Incubate the cells for 48 h and treat with a lysis buffer (E291A) (Promega, Madison, WI, USA) according to the manufacturer's protocol.

3.3.2 Bioluminescence Intensities

1. To measure bioluminescence intensities, mix an aliquot of the cell lysate (1 μL) with Hanks' balanced salt solution (HBSS) (50 μL) containing 2 μM native CTZ or the respective CTZ derivative in Röhren polystyrene tubes (Sarstedt, Nümbrecht, Germany).
2. Measure the bioluminescence intensities of native CTZ and the derivatives immediately for the first 1 s with a Lumat LB 9507 luminometer (Berthold Technologies, Bad Wildbad, Germany) (*see* Fig. 3).

3.3.3 Kinetic Profiles of Bioluminescence

1. To measure the kinetic profiles of bioluminescence, continue signal monitoring for 600 s after mixing.
2. The reaction conditions are identical to those described in the previous section (*see* Table 1).

3.3.4 Bioluminescence Spectra

1. For the recording of bioluminescence spectra, mix an aliquot of the lysate (100 μL) with HBSS (400 μL) containing 20 μM native CTZ or CTZ derivative in a quartz cell, and measure the mixture with a F-7000 spectrophotometer (Hitachi, Tokyo, Japan) at a scan rate of 2400 nm/min.

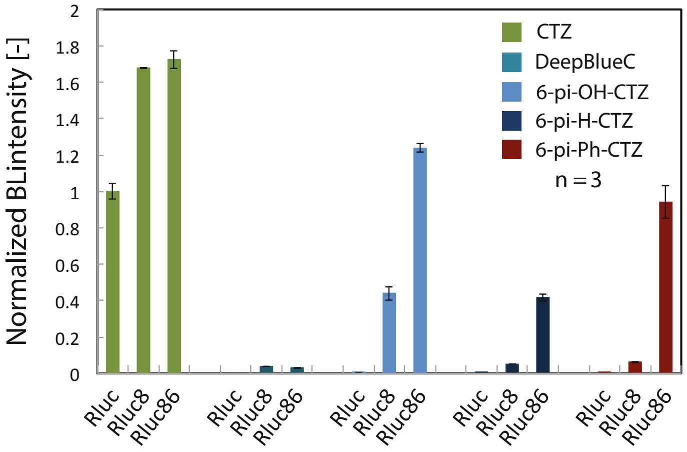

Fig. 3 Bioluminescence intensity. The intensities are normalized to intensity of native CTZ in combination with RLuc. C-6 substituted CTZ derivatives show drastically robust bioluminescence compared to that of DeepBlueC™ in combination with RLuc8. DeepBlueC™/RLuc8 pair is applied as bioluminescence resonance energy transfer (BRET) research

Table 1 Kinetic profile of native CTZ, CTZ derivatives (6-pi-X-CTZ: X = OH, H, Phenyl) and DeepBlueC™

	Native CTZ	OH	H	Phenyl	DeepBlueC™
BL half-life time (RLuc8) [s]	433	544	>600	213	342
BL half-life time (RLuc8.6) [s]	313	463	325	182	59

The kinetic profiles are obtained in 1 s intervals for 600 s

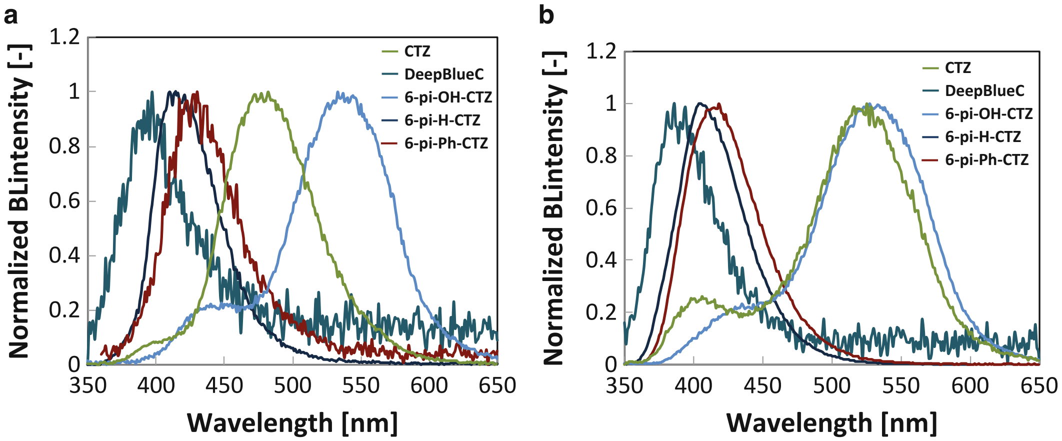

Fig. 4 Bioluminescence spectra obtained with (**a**) RLuc8 and (**b**) RLuc8.6. The spectra are normalized to 1 at the peak. All CTZ derivatives except for 6-pi-OH-CTZ show an approximately 40 nm blue-shifted emission compared to native CTZ/RLuc pair (480 nm). These blue-shifted spectra are in a wavelength range similar to that of DeepBlueC™

2. Determine the wavelengths of maximal bioluminescence intensities (λ_{max}) using the instrument software (FL Solutions ver. 2.1) (*see* Fig. 4).

4 Notes

1. CTZ should be stored at −30 °C and protected from light. In addition, it should be stored in the solid state, because this is more stable than the liquid state. If CTZ is stored as ethanol or methanol stock solution, the stability is enhanced by addition of a trace of HCl [21].
2. To efficiently prepare the organozinc reagent, zinc chloride needs to be sufficiently dried before addition of benzylmagnesium chloride.
3. Benzylmagnesium chloride should be used and stored under inert gas. We find that it is best to prepare this fresh.
4. 3,5-Dibromopyrazin-2-amine (**1**) needs to be dried enough before adding.

5. Tetrakis(triphenylphosphine)palladium(0) is unstable under aerobic conditions. The reaction mixture needs to be deaerated before and after adding of palladium catalyst.
6. (*E*)-3-Benzyl-5-(4-methoxystyryl)pyrazin-2-amine (**4**) needs to be sufficiently dried before adding.
7. Boron tribromide is decomposed by water. The reaction system needs to be sufficiently dried before adding of boron tribromide.
8. 3-(4-((*tert*-Butyldimethylsilyl)oxy)phenyl)-1,1-iethoxypropane-2-one (**11**) can be synthesized from *tert*-butyl[4-(bromomethyl) phenoxy]dimethylsilane, which is the bromo compound corresponding to compound (**10**). However, the stability of *tert*-butyl[4-(bromomethyl)phenoxy]dimethylsilane is lower than compound (**10)** [19].
9. *tert*-Butyl(4-(chloromethyl)phenoxy)dimethylsilane (**10**) is delivered dropwise into the reaction mixture immediately after magnesium turnings start to activate.
10. CTZ is very unstable under aerobic conditions. Therefore, after dissolving the coelenteramine and the ketoacetal in solvents, the solution should be deaerated.
11. In DMSO, CTZ is decomposed while showing chemiluminescence emission. After injection of DMSO, the measurement was started immediately.

Acknowledgement

This work was supported by JSPS KAKENHI Grant Number 24225001.

References

1. Thorne N, Inglese J, Auld DS (2010) Illuminating insights into firefly luciferase and other bioluminescent reporters used in chemical biology. Chem Biol 17:646–657
2. Goto T (1968) Chemistry of bioluminescence. Pure Appl Chem 17:421–442
3. Teranishi K, Hisamatsu M, Yamada T (1999) Chemiluminescence of 2-methyl-6-arylimidazo-[1,2-a]pyrazin-3(7H)-one in protic solvents: electron-donating substituent effect on the formation of the neutral singlet excited-state molecule. Luminescence 14:297–302
4. Nakamura H, Wu C, Murai A, Inouye S, Shimomura O (1997) Efficient bioluminescence of bisdeoxycoelenterazine with the luciferase of a deep-sea shrimp oplophorus. Tetrahedron Lett 38:6405–6406
5. Saito R, Hirano T, Maki S, Niwa H, Ohashi M (2011) Influence of electron-donating and electron-withdrawing substituents on the chemiluminescence behavior of coelenterazine analogs. Bull Chem Soc Jap 84:90–99
6. Saito R, Hirano T, Niwa H, Ohashi M (1998) Substituent effects on the chemiluminescent properties of coelenterazine analogues. Chem Lett 27:95–96
7. Inouye S, Shimomura O (1997) The use of *Renilla* Luciferase, Oplophorus Luciferase, and Apoaequorin as bioluminescent reporter protein in the presence of coelenterazine analogues as substrate. Biochem Biophys Res Commun 233:349–353
8. Loening AM, Wu AM, Gambhir SS (2007) Red-shifted *Renilla reniformis* luciferase variants for

imaging in living subjects. Nat Methods 4:641–643

9. Woo J, Howell MH, von Arnim AG (2008) Structure–function studies on the active site of the coelenterazine-dependent luciferase from *Renilla*. Protein Sci 17:725–735
10. Loening AM, Fenn TD, Gambhir SS (2007) Crystal structures of the luciferase and green fluorescent protein from *Renilla reniformis*. J Mol Biol 374:1017–1028
11. Qi CF, Gomi Y, Hirano T, Ohashi M, Ohymiya Y, Tsuji FI (1992) Chemi- and bioluminescence of coelenterazine analogues with phenyl homologues at the C-2 position. J Chem Soc Perkin Trans 1:1607–1611
12. De A, Gambhir SS (2005) Noninvasive imaging of protein–protein interactions from live cells and living subjects using bioluminescence resonance energy transfer. FASEB J 19:2017–2019
13. Wu C, Nakamura H, Murai A, Shimomura O (2001) Chemi- and bioluminescence of coelenterazine analogues with a conjugated group at the C-8 position. Tetrahedron Lett 42:2997–3000
14. Stepanyuk GA, Unch J, Malikova NP, Markova SV, Lee J, Vysotski ES (2010) Coelenterazine-*v* ligated to Ca-triggered coelenterazine-binding protein is a stable and efficient substrate of the red-shifted mutant of *Renilla muelleri* luciferase. Anal Bioanal Chem 398:1809–1817
15. Imai Y, Shibata T, Maki S, Niwa H, Ohashi M, Hirano T (2001) Fluorescence properties of phenolate anions of coelenteramide analogues: the light-emitter structure in aequorin bioluminescence. J Photochem Photobiol A Chem 146:95–107
16. Shimomura O, Teranishi K (2000) Light-emitters involved in the luminescence of coelenterazine. Luminescence 15:51–58
17. Nishihara R, Suzuki H, Hoshino E, Suganuma S, Sato M, Saitoh T, Nishiyama S, Iwasawa N, Citterio D, Suzuki K (2015) Bioluminescent coelenterazine derivatives with imidazopyrazinone C-6 extended substitution. Chem Commun 51:391–394
18. Adamczyk M, Akireddy SR, Johnson DD, Mattingly PG, Pan Y, Reddy RE (2003) Synthesis of 3,7-dihydroimidazo[1,2a]pyrazine-3-ones and their chemiluminescent properties. Tetrahedron 59:8129–8142
19. Adamczyk M, Johnson DD, Mattingly PG, Pan Y, Reddy RE (2001) Synthesis of coelenterazine. Org Prep Proc Int 33:477–485
20. Phakhodee W, Toyoda M, Chou CM, Khunnawutmanotham N, Isobe M (2011) Suzuki–Miyaura coupling for general synthesis of dehydrocoelenterazine applicable for 6-position analogs directing toward bioluminescence studies. Tetrahedron 67:1150–1157
21. Shimomura O (2012) Bioluminescence chemical principles and methods revised edition. World Scientific Publishing, Singapore

Chapter 3

Molecular Cloning of Secreted Luciferases from Marine Planktonic Copepods

Yasuhiro Takenaka, Kazuho Ikeo, and Yasushi Shigeri

Abstract

Secreted luciferases isolated from copepod crustaceans are frequently used for nondisruptive reporter-gene assays, such as the continuous, automated and/or high-throughput monitoring of gene expression in living cells. All known copepod luciferases share highly conserved amino acid residues in two similar, repeated domains in the sequence. The similarity in the domains are ideal nature for designing PCR primers to amplify cDNA fragments of unidentified copepod luciferases from bioluminescent copepod crustaceans. Here, we introduce how to establish a cDNA encoding novel copepod luciferases from a copepod specimen by PCR with degenerated primers.

Key words Copepod, GLuc, Luciferase, MLuc, MpLuc, Plankton

1 Introduction

Copepods are the most numerous taxa in zooplankton communities in the ocean worldwide. Certain species of copepods are known to have secreted bioluminescent abilities. Over the past decade, several studies have been made on the molecular identification and functional analyses of copepod luciferases [1–3]. These luciferases have been used for nondisruptive reporter-gene assays, such as the continuous, automated and/or high-throughput monitoring of gene expression in living cells and in vivo [4, 5]. Copepod luciferases have the following characters: (a) they are efficiently secreted into culture medium, even when expressed in mammalian cells; (b) light emission simply depends on the presence of the substrate, coelenterazine, and no other cofactors are required; and (c) they are relatively small in size proteins (20–30 kDa). Secreted luciferase from the copepod, *Gaussia princeps* was first cloned in 2002 [1], followed by *Metridia longa* luciferase next in 2004 [2]. Both genes have been isolated by screening cDNA expression libraries using *Escherichia coli* (*E. coli*). After the initial reports of the two luciferases, we went on to cloned more than 20 other copepod

Sung-Bae Kim (ed.), *Bioluminescence: Methods and Protocols*, Methods in Molecular Biology, vol. 1461,
DOI 10.1007/978-1-4939-3813-1_3, © Springer Science+Business Media New York 2016

luciferases using a PCR-based cloning method [3, 6, 7]. All known copepod luciferases share highly conserved amino acid residues in two similar, repeated domains in the sequence [6]. Typical nucleotide sequence in the conserved domains enables us to design PCR primers to amplify new cDNA fragments of unidentified copepod luciferases from bioluminescent copepod specimens.

Here, we describe the preparation of cDNAs from copepod specimens and the method to obtain the partial and full-length cDNAs encoding copepod luciferase using PCR with degenerated primers.

2 Materials

2.1 RNA Purification

When one tackles copepod mRNA, always use RNase-free disposable plastic tubes, tips, and pipettes. Further, it is recommended to wear suitable disposable gloves while handling the RNA samples.

1. RNA*later* RNA Stabilization reagent (Qiagen).
2. All glass, tapered tissue homogenizer that has grinding surfaces on a pestle and tube (*see* Fig. 1). Rinse a pestle and tube with RNase AWAY, a decontamination reagent (Thermo Scientific) immediately before its use.
3. RNeasy Micro kit (Qiagen).

2.2 cDNA Synthesis and PCR with Degenerated Primers

1. SMART RACE cDNA Synthesis Kit (Takara Bio).
2. Sensiscript RT (Qiagen).
3. Advantage 2 DNA polymerase (Takara Bio).

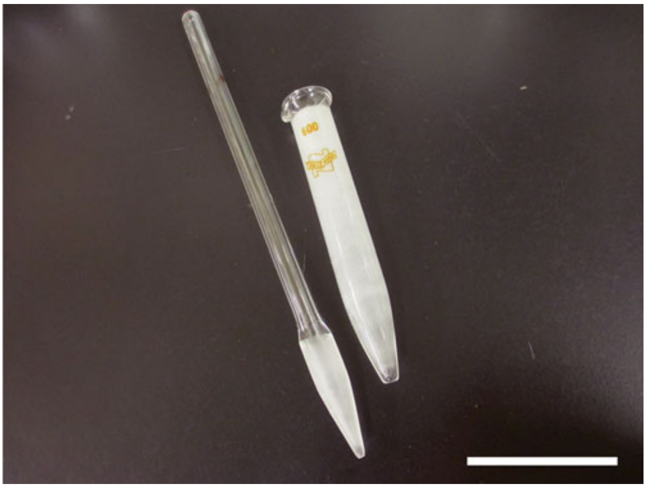

Fig. 1 All glass, tapered tissue homogenizer used for homogenization of copepod specimen in tissue lysis buffer. Outer length: 15 × 110 mm. *Horizontal line* = 5.0 cm

4. RNase inhibitor (Toyobo).
5. TOPO TA Cloning Kit (Life Technologies).
6. 1/10× Tris-EDTA buffer: 1 mM Tris–HCl, pH 8.0, 0.1 mM EDTA.
7. Degenerated primers designed for amplification of calanoid luciferases (*see* Fig. 2).

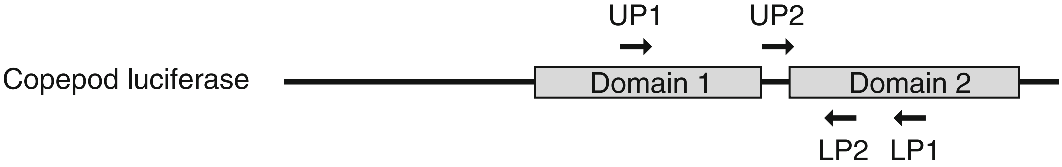

Upper primer

White luc UP1

M. pacifica (MpLuc1)	Nucleotide	aaa	gct	ggc	tgc	acc	agg	gga	tgt	ctc	atc	tgt	ctt	tca
	Amino acid	K	A	G	C	T	R	G	C	L	I	C	L	S
G. princeps	Nucleotide	aaa	gct	ggc	tgc	act	agg	gga	tgt	ctg	ata	tgc	ctg	tca
	Amino acid	K	A	G	C	T	R	G	C	L	I	C	L	S
M. longa	Nucleotide	aaa	gct	ggc	tgc	acc	agg	gga	tgc	ctt	atc	tgt	ctt	tca
	Amino acid	K	A	G	C	T	R	G	C	L	I	C	L	S
Degenerated sequence				GGC	TGC	ACY	AGG	GGA	TGY	CTK	ATM	TG	→	
Degeneracy				1	1	2	1	1	2	2	2	1		

26 mer
16 degeneracy

White luc UP2

M. pacifica (MpLuc1)	Nucleotide	gcc	att	gtt	gac	att	ccc	gaa	att
	Amino acid	A	I	V	D	I	P	E	I
G. princeps	Nucleotide	gct	att	gtt	gac	att	cct	gaa	att
	Amino acid	A	I	V	D	I	P	E	I
M. longa	Nucleotide	gca	att	gtt	gac	att	ccc	gaa	atc
	Amino acid	A	I	V	D	I	P	E	I
Degenerated sequence		GCT	ATT	GTT	GAY	ATY	CCY	GAR	AT →
Degeneracy		1	1	1	2	2	2	2	1

23 mer
16 degeneracy

Lower primer

White luc LP1

M. pacifica (MpLuc1)	Nucleotide	tgc	aca	act	ggc	tgc	ctc	aaa	ggt	ctt	gcc	aat	gtc
	Amino acid	C	T	T	G	C	L	K	G	L	A	N	V
G. princeps	Nucleotide	tgc	aca	act	gga	tgc	ctc	aaa	ggt	ctt	gcc	aat	gtg
	Amino acid	C	T	T	G	C	L	K	G	L	A	N	V
M. longa	Nucleotide	tgc	act	act	gga	tgt	ctc	aaa	ggt	ctt	gcc	aat	gtt
	Amino acid	C	T	T	G	C	L	K	G	L	A	N	V
Degenerated sequence						TGY	CTB	AAR	GGT	CTT	GCC	AAT	GT
Degeneracy						2	3	2	1	1	1	1	1
					←	ACR	GAV	TTY	CCA	GAA	CGG	TTA	CA

23 mer
12 degeneracy

White luc LP2

M. pacifica (MpLuc1)	Nucleotide	ccc	atg	gag	cag	ttt	att	gct	caa	gtt	gat
	Amino acid	P	M	E	Q	F	I	A	Q	V	D
G. princeps	Nucleotide	ccc	atg	gaa	caa	ttc	att	gca	caa	gtt	gac
	Amino acid	P	M	E	Q	F	I	A	Q	V	D
M. longa	Nucleotide	ccc	atg	gaa	cag	ttc	att	gct	caa	gtt	gat
	Amino acid	P	M	E	Q	F	I	A	Q	V	D
Degenerated sequence			ATG	GAR	CAR	TTY	ATT	GAW	CAA	GTT	GA
Degeneracy			1	2	2	2	1	2	1	1	1
	←		TAC	CTY	GTY	AAR	TAA	CTW	GTT	CAA	CT

26 mer
16 degeneracy

Fig. 2 Positions and sequences of four degenerate primers for amplification of partial luciferase cDNA. UP and LP indicate "upper primer" and "lower primer," respectively. Conserved amino acid residues in domain 1 and 2 contained in *M. pacifica*, *M. longa*, and *G. princeps* luciferases are presented with their nucleotide sequences

3 Methods

3.1 Sample Homogenization and RNA Purification

1. Transfer the isolated live zooplankton specimens (*see* Fig. 3) into chilled sea water immediately.
2. Examine live specimens under a stereomicroscope to sort out individual copepod species.
3. Immerse 1–20 live copepods (*see* **Note 1**) into 1 mL RNAlater reagent in a screw-capped microtube, keep them at 4 °C for 1 day and then store in a −30 °C freezer.
4. Thaw the specimens in the RNA*later* reagent at room temperature. Transfer each specimen into all grass, tapered tissue homogenizer containing 350 μL of Buffer RLT, a lysis buffer (*see* **Note 2**) by a tweezer.
5. Homogenize the specimen in Buffer RLT with more than 20 up-and-down strokes (*see* **Note 3**).
6. Transfer the lysate into a fresh 1.5 mL microtube and centrifuge it for 5 min at a maximal speed at 4 °C.
7. Transfer the supernatant into a fresh 1.5 mL microtube.
8. Add an equivalent volume of 70 % ethanol with the supernatant to the lysate. Mix the sample well by pipetting and transfer it to an RNeasy MinElute spin column set in 2 mL collection tube.
9. Centrifuge the spin column for 15 s at 10,000 × *g*, and discard the flow-through.
10. Add 700 μL of Buffer RW1 (*see* **Note 2**) to the column and centrifuge it for 15 s at 10,000 × *g*, and discard the flow-through and collection tube.

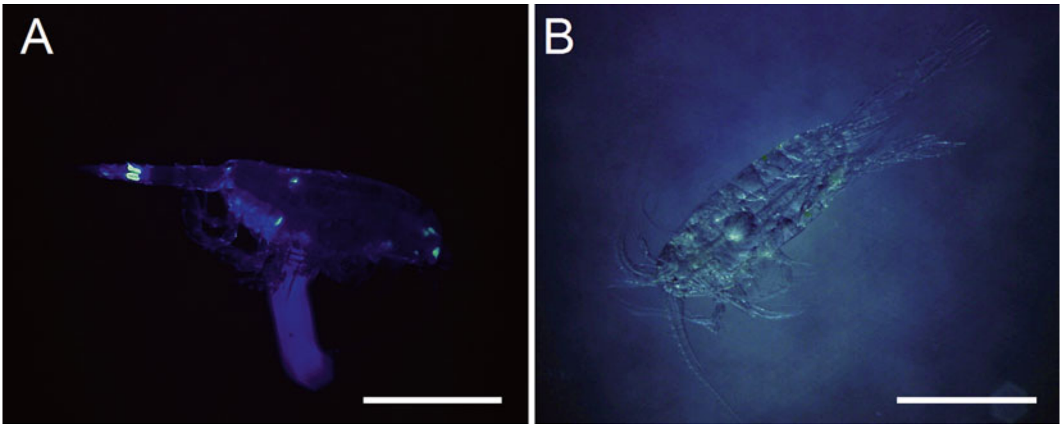

Fig. 3 Fluorescent (**a**) and bright-field (**b**) images of live calanoid copepod *Metridia pacifica*. A specimen in (**a**) was illuminated with ultraviolet. *Horizontal line* in each frame = 1.0 mm

11. Set the spin column in a fresh 2 mL collection tube, add 500 μL of Buffer RPE (*see* **Note 2**) to the column, and centrifuge it for 15 s at 10,000 × *g*, discard the flow-through.
12. Add 500 μL of 80% ethanol to the column, and centrifuge it for 2 min at 10,000 × *g*. Discard the flow-through and collection tube.
13. Place the spin column in a fresh 2 mL collection tube, and centrifuge it for 5 min at maximal speed. Discard the flow-through and collection tube.
14. Place the spin column in a fresh 1.5 mL microtube, and add 14 μL of RNase-free water to the column. Centrifuge the column for 1 min at maximal speed to collect the RNA.

3.2 Reverse Transcription

1. Make the following cocktail to prepare 5′- and 3′-Ready SMART cDNAs. Add the upper-prepared template RNA at last.

For 5′-Ready SMART cDNA

Reagents	Volume (μL)
RNase-free water	0.37
10× Buffer RT	1.0
5 mM dNTP	1.0
RNase inhibitor	0.13
10 μM SMART II oligo (*see* **Note 4**)	1.0
10 μM 5′-CDS primer (*see* Table 1)	1.0
Sensiscript RT	0.5
Template RNA (from **step 14** in Subheading 3.1)	5
Total volume	10

For 3′-Ready SMART cDNA

Reagents	Volume
RNase-free water	1.37
10× Buffer RT	1.0
5 mM dNTP	1.0
RNase inhibitor	0.13
10 μM 3′-CDS primer (*see* Table 1)	1.0
Sensiscript RT	0.5
Template RNA (from **step 14** in Subheading 3.1)	5
Total volume	10

2. Incubate the reaction mixtures above for 60 min at 37 °C.
3. Inactivate the Sensiscript RT by heating the reaction mixture for 3 min at 95 °C.
4. Add a 90 μL of 1/10× Tris-EDTA into the reaction mixture to prepare 1:10 diluted cDNA template.
5. Store the diluted reaction mixture in the freezer at −30 °C unless it is immediately used for a PCR reaction.

3.3 PCR with Degenerated Primers, 5′ and 3′ RACE

1. Prepare the following reagent cocktail in a 0.2 mL PCR tube to amplify the partial cDNA fragment of a copepod luciferase carrying two conserved domains. Add 1:10 diluted 3′-Ready SMART cDNA at last.

Reagents	Volume
PCR-grade water	12.4 μL
10 × Advantage 2 PCR Buffer	2 μL
2 mM dNTP	2 μL
10 μM Forward primer (*see* Table 1 and Fig. 2)	0.6 μL
10 μM Reverse primer (*see* Table 1 and Fig. 2)	0.6 μL
50× Advantage 2 Polymerase Mix	0.4 μM
1:10 diluted 3′-Ready SMART cDNA	2 μL
Total volume	20 μL

2. Shortly spin the rigidly capped PCR tubes, and then start a PCR reaction (Bio-Rad S1000™ Thermal Cycler) using the following program:

   96 °C for 1 min to denature template cDNAs.

   35 cycles with

      96 °C for 5 s for the denaturing.

      55 °C for 10 s for the annealing.

      68 °C for 30 s for the extension.

      1 cycle for the last extention step.

      68 °C for 30 s.

3. Apply 3 μL out of 20 μL PCR reaction on 1.6% TAE-agarose gel with suitable DNA size marker to analyze PCR products.
4. If a single discrete band around 100–300 bp is observed, cut the band from the gel and gel-purify the product using the gel purification kit (*see* **Note 5**).

5. Mix 1–2 μL of the purified PCR product and 0.5 μL pCR2.1-TOPO vector (Life Technologies), then incubate for 5–15 min at room temperature, and transform into the competent cells, such as TOP10 or DH5α (Life Technologies). Spread appropriate volume of each transformation on LB agar plates with carbenicillin (50 μg/mL).
6. Analyze 4–8 colonies by colony direct PCR or by digesting isolated plasmid DNA with appropriate restriction enzymes.
7. Purify the plasmid DNA containing the PCR insert using plasmid miniprep kit.
8. Check nucleotide sequence of the insert, translate it to deduced amino acid sequences, and then analyze its sequence similarity to amino acid sequences of other known copepod luciferases using ClustalW or BLAST search.
9. Amplify the 5′- and 3′-ends of copepod luciferase cDNAs using the gene-specific primers, Universal Primer Mix (*see* Table 1), and 5′- or 3′-Ready SMART cDNA following the manufacturer's instructions. After sequencing the 5′- and 3′-RACE products, amplify the full-length cDNA using additional gene-specific primers.

Table 1
The nucleotide sequences of primers used in this protocol

Primer name	Sequence	Usage
5′-CDS primer	5′-$(T)_{25}$VN-3′	Oligo dT primer
3′-CDS primer	5′-AAGCAGTGGTAACAACGCAGAGTAC$(T)_{30}$VN-3′	Oligo dT primer
Universal Primer Mix	Mixture of 0.2 μM long oligo, 5′-CTAATACGACTCACTATAGGG CAAGCAGTGGTAACAACGCAGAGT-3′ and 1 μM short oligo, 5′-CTAATACGACTCACTATAGGGC-3′	Universal primer for 5′ and 3′ RACE
White_luc UP1[a]	5′-GGCTGCACYAGGGGATGYCTKATMTG-3′	Forward primer
White_luc UP2[a]	5′-GCTATTGTTGAYATYCCYGARAT-3′	Forward primer
White_luc LP1[a]	5′-ACATTGGCAAGACCYTTVAGRCA-3′	Reverse primer
White_luc LP2[a]	5′-TCAACTTGWTCAATRAAYTGYTCCAT-3′,	Reverse primer

[a] These primers were designed based on the conserved region of MLuc (AAR17541, *M. longa*), GLuc (AAG54095, *G. princeps*), MpLuc1, and MpLuc2 (AB195233 and AB195234, respectively, *M. pacifica*) luciferases (*see* Fig. 2). If combination of White_luc UP1 and White_luc LP1, or White_luc UP2, and White_luc LP2 produces no significant PCR bands, try other combination, such as White_luc UP1 and White_luc LP2

4 Notes

1. Number of specimen varies with body size of copepods. Submerge specimens completely in at least 10 volumes of RNA*later* reagent. For more information, refer to an instruction manual for the reagent.
2. Buffers RLT, RW1, and RPE are components of RNeasy Micro Kit. Add 10 μL of β-mercaptoethanol per 1 mL of Buffer RLT immediately before use.
3. Complete homogenization is essential for higher RNA yields. Insert and rotate a pestle at least 20 times. Monitor sample lysis carefully, and perfom the homogenization with enough up-and-down strokes. The stroking times depend on the hardness of zooplankton.
4. SMART II Oligo is a component of SMART RACE cDNA Synthesis Kit, and its nucleotide sequence is as follows,

   5′-AAGCAGTGGTAACAACGCAGAGTACGC-r(GGG)-3′

   r(GGG) indicates triple guanosine so that SMART II Oligo is DNA-RNA hybrid oligonucleotide [8].
5. We use a QIAquick Gel Extraction kit (QIAGEN) for extraction and purification of the PCR product from the excised agarose gel.

Acknowledgement

We are grateful to Prof. Gary Wayman (Washington State University, Pullman) for his careful reading of our manuscript. This work was supported by an AIST research grant and the NIG Cooperative Research Program (Y. Shigeri and K. Ikeo, 2014-A63, 2015-A47).

References

1. Verhaegen M, Christopoulos T (2002) Recombinant *Gaussia* luciferase. Overexpression, purification, and analytical application of a bioluminescent reporter for DNA hybridization. Anal Chem 74:4378–4385
2. Markova SV, Golz S, Frank LA, Kalthof B, Vysotski ES (2004) Cloning and expression of cDNA for a luciferase from the marine copepod *Metridia longa*. A novel secreted bioluminescent reporter enzyme. J Biol Chem 279:3212–3217
3. Takenaka Y, Masuda H, Yamaguchi A, Nishikawa S, Shigeri Y, Yoshida Y, Mizuno H (2008) Two forms of secreted and thermostable luciferases from the marine copepod crustacean, *Metridia pacifica*. Gene 425:28–35
4. Maguire CA, Deliolanis NC, Pike L, Niers JM, Tjon-Kon-Fat LA, Sena-Esteves M, Tannous BA (2009) *Gaussia* luciferase variant for high-throughput functional screening application. Anal Chem 81:7102–7106

5. Tannous BA (2009) *Gaussia* luciferase reporter assay for monitoring biological processes in culture and in vivo. Nat Protoc 4:582–591
6. Takenaka Y, Yamaguchi A, Tsuruoka N, Torimura M, Gojobori T, Shigeri Y (2012) Evolution of bioluminescence in marine planktonic copepods. Mol Biol Evol 29:1669–1681
7. Takenaka Y, Noda-Ogura A, Imanishi T, Yamaguchi A, Gojobori T, Shigeri Y (2013) Computational analysis and functional expression of ancestral copepod luciferase. Gene 528:201–205
8. Zhu YY, Machleder EM, Chenchik A, Li R, Siebert PD (2001) Reverse transcriptase template switching: a SMART approach for full-length cDNA library construction. Biotechniques 30:892–897

Chapter 4

How to Fabricate Functional Artificial Luciferases for Bioassays

Sung-Bae Kim and Rika Fujii

Abstract

The present protocol introduces fabrication of artificial luciferases (ALuc®) by extracting the consensus amino acids from the alignment of copepod luciferase sequences. The made ALucs have unique sequential identities that are phylogenetically distinctive from those of any existing copepod luciferase. Some ALucs exhibited heat stability, and strong and greatly prolonged optical intensities. The made ALucs are applicable to various bioassays as an optical readout, including live cell imaging, single-chain probes, and bioluminescent tags of antibodies. The present protocol guides on how to fabricate a unique artificial luciferase with designed optical properties and functionalities.

Key words Artificial luciferase, Consensus amino acids, Bioluminescence, Bioluminescent capsules, Optical readout

1 Introduction

Luciferases are a family of light-generating proteins that can be isolated from a large variety of insects, marine organisms, and prokaryotes [1, 2]. Although our knowledge on luciferases is rapidly emerging, the practical strategy to engineer luciferases has been confined to mutagenesis. Either point or random mutagenetic approaches are generally slow and tedious, and they consume great time and labor. Crystallographic information on luciferases is also rarely available [3].

An alignment of many relative protein sequences in public databases facilitates new insights on the phylogenetic history, putative structural information, and consensus amino acids. For example, the "*consensus sequence-driven mutagenesis strategy* (CSMS)" uses a sequence alignment, in which consensus amino acids and mutagenesis sites were estimated [4, 5]. This approach is based on the premise that frequently occurring amino acids at a given position have a larger thermostabilizing effect than less frequent amino acids do. Another example called "*statistical coupling analysis*

Sung-Bae Kim (ed.), *Bioluminescence: Methods and Protocols*, Methods in Molecular Biology, vol. 1461,
DOI 10.1007/978-1-4939-3813-1_4, © Springer Science+Business Media New York 2016

(SCA)" was developed to explain the evolutionary constraints of proteins by measuring the relative entropy (D_i) of an amino acid [6]. We had also suggested that a putative core region of marine luciferases may be estimated by a hydrophilicity search and an overlapping approach of the two consecutive domains of copepod luciferases, named "*single-sequence alignment* (SSA)" [3].

The precedent knowledge on aligned luciferase sequences allowed us to fabricate whole-scale consensus amino acid sequences of artificial luciferases (ALuc®) that have never existed before, instead of undertaking heavily labor-consuming mutagenesis of existing luciferases.

The alignment was obtained from many existing luciferases in a public database, i.e., the National Center for Biotechnology Information (NCBI), whose sequences have been accumulated by great devotion of many researchers. The validity of this idea was examined with an alignment of 13 copepod luciferases in the public domain [7], from which frequently occurring amino acids were extracted to reconstitute a prototypical sequence of artificial luciferases. Using the above-mentioned process, very diverse artificial luciferases in the identities from any existing marine luciferases in the database were practically made. The maximal sequence identities of which were below 83% according to the NCBI Blast and less than 76% according to the Swiss Institute of bioinformatics (SIB) Blast, compared with any existing luciferases in the public databases.

The present protocol guides on the detailed procedure on how to create whole sequences of ALucs, instead of identifying several mutation sites in existing luciferases.

2 Materials

Used buffers

1. Phosphate-buffered saline (PBS)
2. Hank's balanced salt solution buffer (HBSS, Gibco)
3. Lysis buffer (E291A; Promega) included in a bioluminescence assay kit (E2820, Promega)
4. *Renilla* luciferase (RLuc) assay buffer (E290B, Promega) included in a bioluminescence assay kit (E2820, Promega)

Cells and protein expression-related reagents

5. pcDNA3.1(+) vector (Invitrogen) for mammalian cell expression
6. pColdIV vector (Takara) for E. coli expression
7. pEHX1.1 vector (Toyobo) for mammalian cell expression
8. *Escherichia coli* (*E. coli*, DH5α)-based competent cell
9. CHO cells derived from Chinese hamster ovary
10. COS-7 cells derived from African green monkey kidney fibroblast cells

11. Dulbecco's minimal essential medium (DMEM) (Gibco)
12. 10% heat-inactivated fetal bovine serum (FBS) (Gibco)
13. 1% penicillin-streptomycin (P/S) (Gibco)
14. TransIT-LT1 (Mirus), a lipofection reagent
15. Protein A-tag, IgG-Sepharose, or Ni-NTA-Agarose affinity columns for protein purification
16. Isopropyl β -D-1-thiogalactopyranoside (IPTG)

Western blot and staining reagent

17. Anti-FLAG®-Tag antibody (MBL, Japan)
18. Anti-His-tag antibody (MBL, Japan)
19. Horseradish peroxidase (HRP)-linked antibody (HRP-ab; GE Healthcare)
20. Coomassie brilliant blue (CBB) reagent for protein staining after SDS-PAGE (i.e., Bradford reagent, BIO-RAD)
21. Precast gel cassette for SDS-polyacrylamide gel electrophoresis (SDS-PAGE)

Assay and light-developing reagents

22. Endoplasmic reticulum (ER) tracker (Invitrogen), a live-cell staining reagent emitting fluorescence
23. *Renilla* luciferase (RLuc) assay system (E2820, Promega), a bioluminescence assay kit
24. Immunostar LD (Warko), a chemiluminescence reagent
25. Native coelenterazine (nCTZ; E2820, Promega)
26. CTZ *n*, a coelenterazine analogue
27. CTZ *i*, a coelenterazine analogue
28. CTZ *f*, a coelenterazine analogue
29. CTZ *h*, a coelenterazine analogue
30. Staurosporine (STS), an apoptosis inducer

3 Methods

3.1 Construction of Artificial Luciferases from Public Databases

The mammalian codon-optimized cDNA sequences encoding ALucs are custom-fabricated according to the following procedure (*see* Fig. 1).

1. Obtain the amino acid sequences of copepod-derived marine luciferases from public databases like the NCBI or the SIB Blast.

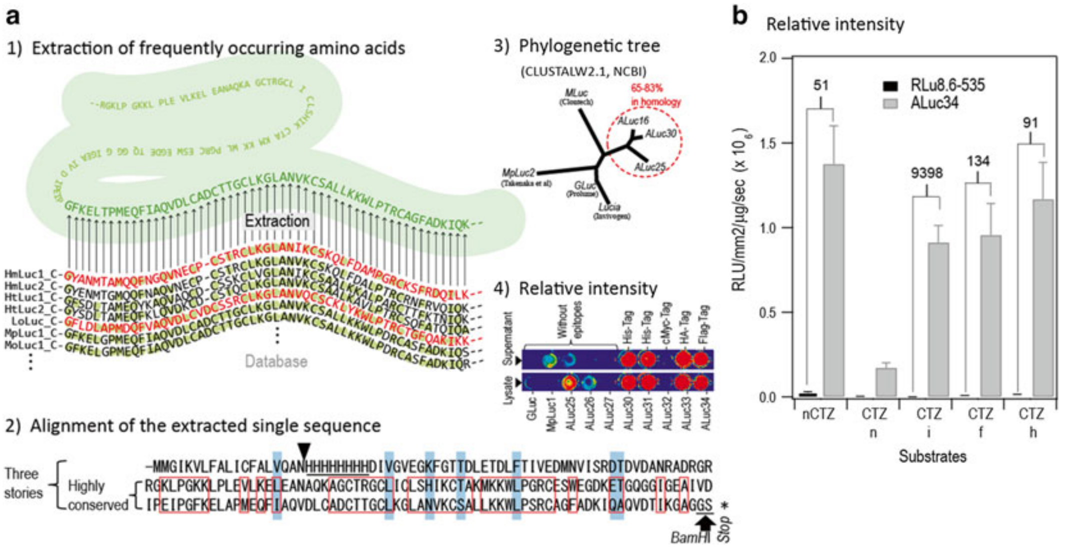
a
1) Extraction of frequently occurring amino acids
Extraction
HmLuc1_C-
HmLuc2_C-
HtLuc1_C-
HtLuc2_C-
LoLuc_C-
MpLuc1_C-
MoLuc1_C-
Database
3) Phylogenetic tree
(CLUSTALW2.1, NCBI)
MLuc
MpLuc2
GLuc
Lucia
ALuc16
ALuc30
ALuc25
65-83% in homology
4) Relative intensity
Supernatant
Lysate
Without epitopes
His-Tag
His-Tag
cMyc-Tag
HA-Tag
Flag-Tag
GLuc
MpLuc1
ALuc25
ALuc26
ALuc27
ALuc30
ALuc31
ALuc32
ALuc33
ALuc34
2) Alignment of the extracted single sequence
Three stories
Highly conserved
-MMGIKVLFALICFALVQANHHHHHHHHDIVGVEGKFGTTDLETDLFTIVEDMNVISRDTDVDANRADRGR
RGKLPGKKLPLEVLKELEANAQKAGCTRGCLICLSHIKCTAKMKKWLPGRCESWEGDKETGQGGIGEAIVD
IPEIPGFKELAPMEQFIAQVDLCADCTTGCLKGLANVKCSALLKKWLPSRCAGFADKIQAQVDTIKGAGGS *
BamHI
Stop
b
Relative intensity
RLU/mm2/μg/sec (x 10_6)
2.0
1.5
1.0
0.5
0.0
RLu8.6-535
ALuc34
51
9398
134
91
nCTZ
CTZ n
CTZ i
CTZ f
CTZ h
Substrates

Fig. 1 (**a**) Experimental procedure for the fabrication of artificial luciferases (ALucs). In the *step 1)*, frequently occurring amino acids are extracted from the alignment. In the *step 2)*, the extracted prototype sequence folded up in three stories, whose homology is increased by adjusting the corresponding amino acids If necessary, an epitope sequence like His-tag may be included at the amino acid position 20. In the *step 3)*, the phylogenetic tree is drawn to show the relative sequential homology between ALucs and conventional luciferases. The *red circle* indicates the relative position of **A16**, **A25**, and **A30** in the tree. The percentages demonstrate the homology range of ALucs from NCBI Blast and SIB Blast. In the *step 4)*, the relative optical intensities are determined after the expression in mammalian COS-7 cells. The picture shows the pseudocolor image of the bioluminescence generated by ALucs, obtained by cooled CCD camera equipped in an image analyzer (LAS-4000, FujiFilm). (**b**) Relative optical intensities of ALuc34 and RLuc8.6-535, according to substrates. The *numbers on the bars* indicate each fold intensity of ALuc34, compared with that of *Renilla* luciferase 8.6-535. Abbreviations: *nCTZ* native coelenterazine, *CTZ n* coelenterazine n, *CTZ i* coelenterazine i, *CTZ f* coelenterazine f, *CTZ h* coelenterazine h. Reproduced in part from Kim et al. with permission from Bioconjugate Chem. (ACS) and Biochem. Biophys. Res. Comm. (Elsevier) [12, 13]

2. Align the obtained sequences to highlight the frequently occurring amino acids with ClustalW or other alignment software (*see* **Note 1**). The software reveals consensus amino acids.
3. Compose several prototype sequences from the consensus amino acids (*see* **Note 2**).
4. Confirm that the prototype sequence consists of three different regions; the initial N-terminal domain is relatively variable, but the other two domains share high homolgy and are mirror-imaged each other.
5. Fold up the prototype sequence into three stories on the basis of homology: i.e., single-sequence alignment (SSA).
6. Further adjust the amino acids to increase the homology between the middle and low stories (*see* **Note 3**).
7. Optionally, the N- or C-terminal ends may be fused with signal peptides according to researcher's preference: e.g., add an

endoplasmic reticulum (ER) retention signal, i.e., KDEL, at the C-terminal end of the prototype sequence for the retention in the ER after expression (*see* **Notes 4** and **5**).

8. Determine the maximal identity and similarity ranking of the prototype sequences without KDEL, compared with existing luciferases (*see* **Notes 6** and 7).
9. Custom-synthesize the cDNA encoding the finally designed prototype sequence (*see* **Note 8**).
10. Subclone the synthesized cDNAs into a mammalian expression vector, e.g., pcDNA3.1(+) (Invitrogen), using the specific restriction sites, e.g., *Hind*III and *Xho*I.
11. Confirm the overall sequence fidelity with a DNA sequence analyzer (Applied Biosystems or Beckman Coulter). The fabricated strain of luciferases may be named Artificial Luciferase (ALuc®). The ALuc® variants, ALuc16 (abbreviated to **A16**), ALuc25 (abbreviated to **A25**) and ALuc30 (abbreviated to **A30**), is used in this protocol.

3.2 Optical Intensities of ALucs Compared with Conventional Luciferases

1. Grow COS-7 cells in a 96-well optical bottom plate (Nunc) with Dulbecco's minimal essential medium (DMEM) (Gibco) supplemented with 10% heat-inactivated fetal bovine serum (FBS) (Gibco) and 1% penicillin/streptomycin (P/S) (Gibco).
2. Transiently transfect the COS-7 cells with the pcDNA3.1(+) vectors encoding each ALuc® (*see* Fig. 1) or existing marine luciferases, i.e., *Gaussia princeps* luciferase (GLuc; GenBank AAG54095.1), *Metridia pacifica* luciferase 1 (MpLuc1; GenBank AB195233), or *Renilla reniformis* luciferase 8.6-535 (RLuc8.6-535) as the internal references using a lipofection reagent, TransIT-LT1 (Mirus).
3. 16 h after the transfection, lyse the cells on each well with 50 μL of a lysis buffer (E291A; Promega).
4. Transfer an aliquot of the lysates (10 μL) into two separated fresh 96-well plates (Nunc) using an 8-channel pipette; one of the plates is used for determining the relative bioluminescence intensities, while the other is for the adjustment of variance of the protein amounts (control).
5. (In case to use an image analyzer) Determine the optical images from the above prepared lysates also with an image analyzer (LAS-4000, FujiFilm) immediately after a simultaneous injection of 40 μL of the RLuc assay buffer carrying nCTZ, CTZ *n*, CTZ *i*, CTZ *f*, or CTZ *h* to each well carrying 10 μL of the lysates using a multichannel pipette (*see* Fig. 1, **step 4** in Subheading 3.2, Fig. 1b).
6. Normalize the optical intensities to the applied protein amounts of the lysates (μg) and light integration time (sec).

7. (In case to use a microplate reader) Determine the relative bioluminescence intensities from the lysates after a programmed, automatic injection of the specific substrate, native coelenterazine (nCTZ; Promega), dissolved in an RLuc assay buffer (E290B, Promega) using a microplate reader equipped with an automatic injector (SH-9000lab, Corona).
8. Normalize the luminescence intensitiesto the applied protein amounts of the lysates (μg) and light integration time (sec).
9. (In case to use a spectrophotometer) Estimate the bioluminescence spectra from the above-prepared lysates with a high-fidelity spectrophotometer (AB-1850, ATTO) equipped with a cooled charge-coupled device (CCD) camera (*see* **Notes 9** and **10**).
10. Normalize the spectra in relative percentages to the maximal intensity (λ_{max}) (*see* Fig. 3 and **Note 11**).

3.3 Application to Bioluminescent Capsules

ALuc® can be linked to a membrane localization signal (MLS). Any protein including a fluorescent protein can be inserted between ALuc and MLS. This type of probes are named "bioluminescent capsule," the fabrication procedure of which is briefly described in the caption of Fig. 2. The basic concept was described in our previous study [8] (*see* Fig. 2).

1. Introduce the *Hind*III and *BamH*I sites at the 5′ and 3′ ends of cDNA encoding ALuc16 by PCR.

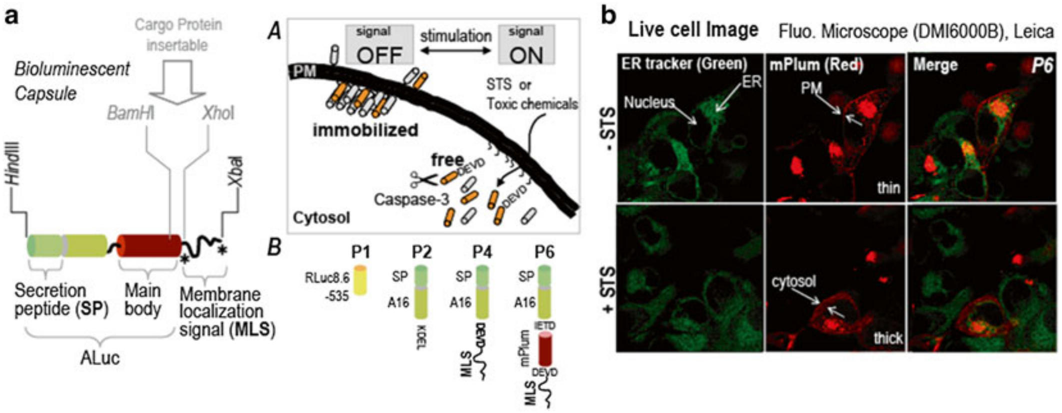
a
Cargo Protein insertable
Bioluminescent Capsule
BamHI
XhoI
HindIII
XbaI
Secretion peptide (SP)
Main body
Membrane localization signal (MLS)
ALuc
A
signal OFF
stimulation
signal ON
PM
STS or Toxic chemicals
immobilized
free
DEVD
Caspase-3
Cytosol
B
P1
P2
P4
P6
RLuc8.6 -535
SP
A16
KDEL
DEVD
MLS
IETD
mPlum
b
Live cell Image
Fluo. Microscope (DMI6000B), Leica
ER tracker (Green)
mPlum (Red)
Merge
P6
ER
Nucleus
PM
thin
- STS
+ STS
cytosol
thick

Fig. 2 Bioluminescent capsules and their applications to live cell imaging. (**a**) Cartoon illustration of the molecular structures of the bioluminescent capsules. *Inset A* shows the working mechanism of a bioluminescent capsule, anchoring in the PM. A capsule is diffused to the cytosol by an apoptosis signal. *Inset B* illustrates the molecular structures of various bioluminescent capsules bearing different cargo proteins. (**b**) Molecular imaging of living mammalian cells with fluorescence. The red fluorescence indicates locating of **P6** in living COS-7 cells before and after stimulation of STS. **P6** is located in the PM or the ER in the basal condition. **P6** releases **A16** and mPlum to the cytosol in the presence of STS. The green fluorescence obtained by an ER Tracker Green (Molecular Probes) shows the regions of the ER and the Golgi apparatus. Abbreviations: *STS* staurosporine, *SP* secretion peptide, *ER* endoplasmic reticulum, *PM* plasma membrane. Reproduced in part from Kim et al. with permission from Bioconjugate Chem. (ACS) [12]

2. Further link a cDNA sequence encoding MLS to the 3′ end of the cDNA via a flexible linker comprising the *BamH*I and *Xho*I sites.
3. Insert the cDNAs encoding a substrate sequence of caspase 3 and 7 (i.e., Asp-Glu-Val-Asp (DEVD)) and mPlum as cargos between the *BamH*I and *Xho*I sites.
4. Subclone the made construct into pcDNA3.1(+) vector to create a plasmid expressing the bioluminescent capsule. The new plasmid may be named pP6.

A signal-dependent release of the cargo, mPlum, from the capsule (**P6**) in living COS-7 cells can be observed with a fluorescent microscope (DMI6000B, Leica) as follow:

5. Grow the COS-7 cells in a 3.5 cm glass-bottom dish (Iwaki) and transiently transfect with pP6.
6. 24 h after the transfection, stain the ER regions of the cells green with an ER tracker (Invitrogen) according to the manufacturer's instruction.
7. Stimulate the cells expressing **P6** with a vehicle (PBS buffer) or 5 μM of staurosporine (STS) for 20 min.
8. Replace the culture media with a Hank's balanced salt solution (HBSS, Gibco) buffer.
9. Image the compartment and localization regions of the ER and the capsules with a fluorescent microscope equipped with a 510–530 nm band-pass filter (green, the ER) and 600 nm long-pass filter (red, mPlum) (*see* Fig. 3c and **Note 12**).

3.4 Fabrication of Bioluminescent Antibodies

ALuc®-fused divalent single-chain variable fragments (di-scFv) are fabricated and the optical intensity is compared with that of a horseradish peroxidase (HRP)-linked antibody as follow (*see* Fig. 3).

1. First, generate three cDNA constructs encoding the fusion protein as shown in Fig. 3a, inset *a* with consecutive PCR and ligation. Further conduct PCR for introducing the oligomers encoding the purification tags at the 5′ and 3′-terminal ends.
2. Subclone the cDNA construct encoding **A16**-**v1** into pColdIV vector (Takara) for *E. coli* expression or fuse the cDNA constructs encoding **A16**-**v2** or -**v3** into pEHX1.1 vector (Toyobo) for CHO cell expression. The corresponding antibodies are named **A16**-**v1**, **A16**-**v2**, and **A16**-**v3**.
3. Transform the pColdIV vector into a competent DH5α *E. coli.* using a heat-shock protocol.
4. Induce the expression of the **A16**-**v1** in *E. coli* with shaking at 15°C after addition of IPTG (final conc.: 0.1–1.0 mM) according to the cold shock protocol of the manufacturer (Takara) for 1 day.
5. Homogenize the cells with a tip sonicator (Qsonica) in ice, centrifuge it, and take the supernatant for an affinity column purification at **step** 7.

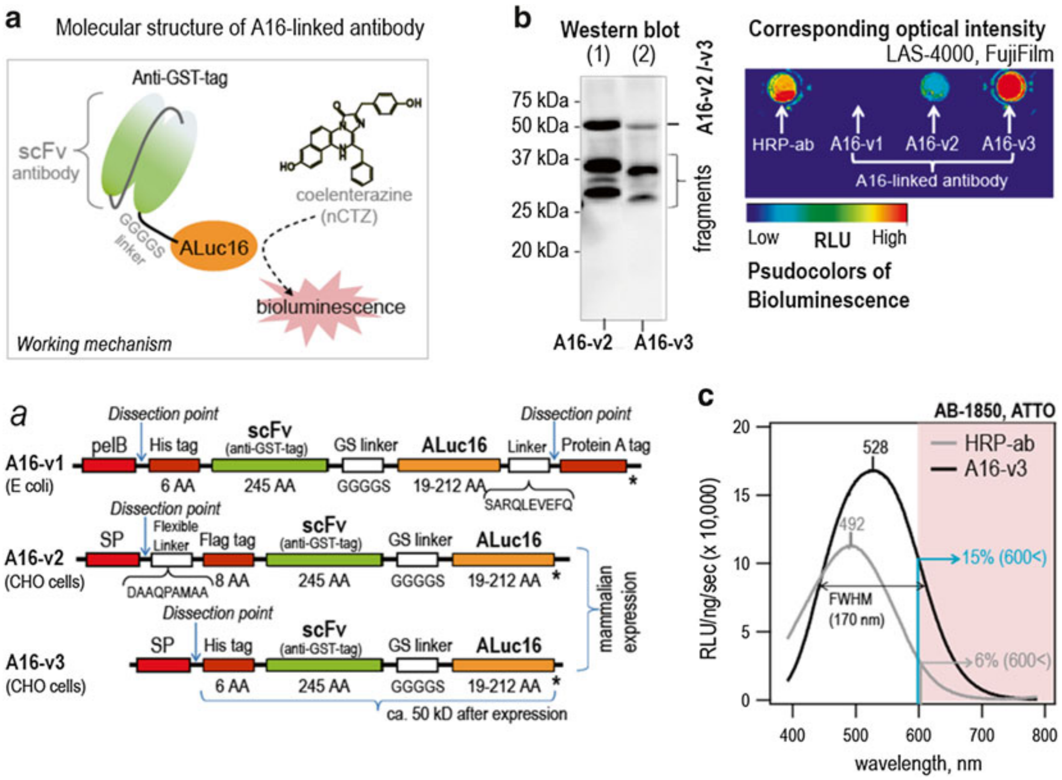
a
Molecular structure of A16-linked antibody
Anti-GST-tag
scFv antibody
GGGGS linker
ALuc16
coelenterazine (nCTZ)
bioluminescence
Working mechanism
b
Western blot
(1) (2)
75 kDa
50 kDa
37 kDa
25 kDa
20 kDa
A16-v2 /-v3
fragments
A16-v2 A16-v3
Corresponding optical intensity
LAS-4000, FujiFilm
HRP-ab A16-v1 A16-v2 A16-v3
A16-linked antibody
Low RLU High
Psudocolors of Bioluminescence
a
Dissection point
A16-v1
(E coli)
pelB
His tag
6 AA
scFv (anti-GST-tag)
245 AA
GS linker
GGGGS
ALuc16
19-212 AA
Linker
SARQLEVEFQ
Protein A tag
A16-v2
(CHO cells)
SP
Flexible Linker
DAAQPAMAA
Flag tag
8 AA
A16-v3
(CHO cells)
mammalian expression
ca. 50 kD after expression
c
AB-1850, ATTO
HRP-ab
A16-v3
528
492
15% (600<)
6% (600<)
FWHM (170 nm)
RLU/ng/sec (x 10,000)
0 5 10 15 20
400 500 600 700 800
wavelength, nm

Fig. 3 Construction of bioluminescent antibodies and their optical properties. (**a**) The light-emitting mechanism of an **A16**-linked antibody (named **A16-v3**). The C-terminal end of an anti-GST-tag antibody was genetically fused to **A16**, which luminesces in the presence of nCTZ. *Inset a* shows the cDNA constructs of ALuc®-linked antibody. (**b**) A western blot analysis and bioluminescence imaging of **A16-v1**, **A16-v2**, and **A16-v3**. The bioluminescence image indicates the relative optical intensities of 1 μg/mL of HRP or **A16**-linked antibodies in pseudocolor. (**c**) The normalized bioluminescence spectra generated by **HRP-ab** and **A16-v3. A16-v3** exerted a stronger red-shifted optical intensity than **HRP-ab** ($n = 2$). The spectra were obtained with a high-precision spectrophotometer (AB1850; ATTO). FWHM means full width at half maximum. Reproduced in part from Kim et al. with permission from Bioconjugate Chem. (ACS) [12]

6. Separately, transfect the pEHX1.1 vector into Chinese hamster ovary (CHO) cells and induce the expression of **A16-v2** and **A16-v3** by overnight incubation in a CO_2 incubator. The **A16-v2** and **A16-v3** are naturally secreted into the extracellular compartment as the expression proceeds.
7. Purify the antibodies in the culture media with the corresponding affinity columns, i.e., protein A-tag, IgG-Sepharose, and/or Ni-NTA-Agarose columns, according to the purification tags.
8. Examine the relative amounts and fragmentation of the purified antibodies with Western blot analysis: i.e., blot **A16-v2** and **A16-v3** bands with an anti-FLAG®-Tag antibody (MBL, Japan) and an anti-His-tag antibody (MBL, Japan), respectively, after PAGE.

9. Examine the relative optical intensities of **A16-v1**, **A16-v2**, and **A16-v3** compared to that of an HRP-linked antibody (named **HRP-ab**; GE Healthcare) with an image analyzer (FujiFilm) (*see* Fig. 3b).
10. Before the comparative evaluation, equalize the antibody amounts (**A16-v1**, **A16-v2**, **A16-v3**, and **HRP-ab**) by diluting them with an HBSS buffer or a PBS buffer (final conc: 1 μg/mL).
11. Transfer an aliquot of the diluted solutions (5 μL) to a 96-well plate (Nunc) and simultaneously mix with 95 μL of the following substrate solutions using a multichannel pipet (Eppendorf): (1) Immunostar LD (Warko) for the **HRP-ab** and (2) a bioluminescence assay kit (E2820, RLuc assay system, Promega) for **A16-v1**, **A16-v2**, and **A16-v3**.
12. Determine the developed bioluminescence intensities with LAS-4000 (FujiFilm) in high-resolution mode with 1 s of the integration time (*see* **Note 13**).
13. Determine the corresponding bioluminescence spectra of **A16-v3** and **HRP-ab** with a spectrophotometer (AB-1850, ATTO) (*see* Fig. 3c). For the measurement, adjust the above diluted solutions to be 0.5 μg/mL. Immediately after mixing 0.5 μL of the enzyme solutions with 15 μL of the assay solutions carrying the respective substrates (Promega and Wako), determine the consequent bioluminescence spectra with the spectrophotometer in an integration time of 5 s (*see* **Note 14**).

4 Notes

1. Frequently occurring amino acids from an alignment can be easily assigned even with the help of web services including Sequence Logos and WebLogo: e.g., http://weblogo.berkeley.edu/info.html.
2. Upon decision of the consensus amino acids, take the highly frequent amino acids in the conserved regions, but decide the remaining amino acids in the variable region on an occasional basis to complete the prototype. The authors recommend that an epitope like Flag® or His-tags is included near the amino acid numbers 20–30 in the upper story, if necessary.
3. It is because the middle and low stories are considered to form two catalytic domains [7, 9], the sequential homology of which enhances optical intensity and stability according to the precedent studies [12, 13].
4. The amino acid sequence, KDEL, is a typical ER retention signal. Because copepod luciferases have a secretion peptide at the N-terminal end, the luciferases are supposed to be secreted to the extracellular compartment after expression. The majority of

the luciferases are retained in the ER if copepod luciferases are tagged with the KDEL signal.

5. Although the C-terminal ends of **ALucs** are fused with an ER retention signal (KDEL), a relatively higher portion of **A16** may be secreted to the extracellular compartment. The KDEL signal does not completely repress the secretory property of ALucs: the secretion ratio of **A16** is 8.8 (±1.2 s.d.) %.
6. The homology ranking can be determined with an alignment search tool provided by NCBI Blast (ver. BLASTP 2.2.27+; http://www.ncbi.nlm.nih.gov/) or SIB Blast (http://web.expasy.org/blast).
7. Their maximal identities to any existing luciferases are less than 83% by NCBI Blast and 76% by SIB Blast, respectively.
8. Many companies provide a cDNA synthesis service for researchers in cheaper price than before. The codons may be optimized for mammalian cell expression.
9. The bioluminescence decays by time. The authors recommend a spectrophotometer which simultaneously captures the entire wavelengths of light for a high-fidelity determination of the spectra.
10. Typically, mix the lysate (5 μL) with 50 μL of the RLuc assay buffer carrying nCTZ (E2820, Promega) and determine the spectra without delay. Accumulate the light emission for 10 s in a precision mode.
11. The λ_{max} of ALucs with nCTZ is in the range of 500–530 nm, and the photon ratio greater than 600 nm (I_{600}) is ca. 5–15%. The λ_{max} values have been frequently discussed with respect to the hydrophilicity at the binding site of luciferases [10] and the protonation environment of the light emitters during the bioluminescence reaction (i.e., pH) [11]. The higher λ_{max} values (i.e., red-shifts) of ALucs than those of other existing marine luciferases suggest that the active site of ALucs provides a relatively hydrophilic environment in the nCTZ-consuming reactions.
12. The bioluminescent capsules are an excellent example of an artificially designed optical reporter to visualize molecular events in the plasma membrane of living mammalian cells under the circumstance of stable supply of the substrate and molecular oxygen (O_2).
13. **A16-v3** is much brighter than **A16-v1**. This result shows that (1) an excellent folding environment for **A16**-linked antibodies are achieved in the ER of mammalian cells (not in *E. coli*) and secreted to the extracellular compartment, and (2) the optical properties of **A16** are robust enough not to be significantly hampered by the antibody linkage.

14. The following factors are considered to have led the success of this approach: (1) as the sequences of many copepod luciferases have been recently accumulated in the public database [7], common features on their two-dimensional structures became more elucidative; (2) the sequences of copepod luciferases are highly conserved, whose nature makes it easy to identify consensus amino acids; and (3) copepod luciferases have two repeated catalytic domains [9], whose N- and C-terminal domains share a high homology each other and thus alignable to easily identify the variable and consensus amino acids, where we actually tried to increase cases of the consensus amino acids between the N- and C-terminal domains. Empirically, we know that the higher homology allows the stronger bioluminescence intensity.

Acknowledgements

This work was supported by grants from Japan Society for the Promotion of Science (JSPS), grant numbers 26288088, 15KK0029, and 16K14051.

References

1. Hastings JW (1996) Chemistries and colors of bioluminescent reactions. Gene 173:5–11
2. Viviani VR, Uchida A, Viviani W, Ohmiya Y (2002) The influence of Ala243 (Gly247), Arg215 and Thr226 (Asn230) on the bioluminescence spectra and pH-sensitivity of railroad worm, click beetle and firefly luciferases. Photochem Photobiol 76:538–544
3. Kim SB (2012) Labor-effective manipulation of marine and beetle luciferases for bioassays. Protein Eng Des Sel 25:261–269
4. Lehmann M, Loch C, Middendorf A, Studer D, Lassen SF, Pasamontes L, van Loon APGM, Wyss M (2002) The consensus concept for thermostability engineering of proteins: further proof of concept. Protein Eng 15:403–411
5. Loening AM, Fenn TD, Wu AM, Gambhir SS (2006) Consensus guided mutagenesis of *Renilla* luciferase yields enhanced stability and light output. Protein Eng Des Sel 19:391–400
6. Russ WP, Lowery DM, Mishra P, Yaffe MB, Ranganathan R (2005) Natural-like function in artificial WW domains. Nature 437:579–583
7. Takenaka Y, Yamaguchi A, Tsuruoka N, Torimura M, Gojobori T, Shigeri Y (2012) Evolution of bioluminescence in marine planktonic copepods. Mol Biol Evol 29:1669–1681
8. Kim SB, Ito Y, Torimura M (2012) Bioluminescent capsules for live-cell imaging. Bioconjug Chem 23:2221–2228
9. Inouye S, Sahara Y (2008) Identification of two catalytic domains in a luciferase secreted by the copepod *Gaussia princeps*. Biochem Biophys Res Commun 365:96–101
10. Shimomura O, Teranishi K (2000) Light-emitters involved in the luminescence of coelenterazine. Luminescence 15:51–58
11. Shimomura O (2006) Bioluminescence. World Scientific Publishing Co. Pte. Ltd., Singapore
12. Kim SB, Torimura M, Tao H (2013) Creation of artificial luciferases for bioassays. Bioconjug Chem 24:2067–2075
13. Kim SB, Izumi H (2014) Functional artificial luciferases as an optical readout for bioassays. Biochem Biophys Res Commun 448: 418–423

Chapter 5

Quantum Yield Determination Based on Photon Number Measurement, Protocols for Firefly Bioluminescence Reactions

Kazuki Niwa

Abstract

Quantum yield (*QY*), which is defined as the probability of photon production by a single bio /chemiluminescence reaction, is an important factor to characterize luminescence light intensity emitted diffusively from the reaction solution mixture. Here, methods to measure number of photons to determine *QY* according to the techniques of national radiometry standards are described. As an example, experiments using firefly bioluminescence reactions are introduced.

Key words Firefly luciferase, Quantum yield, Bioluminescence, Luminometer, National radiometry standard

1 Introduction

Firefly bioluminescence reaction is well known about its high *QY*. In 1959, Seliger and McElroy reported the value of 0.88 [1], which had been frequently referred as an evidence of highly efficient energy conversion to produce light from a chemical reaction in firefly bioluminescence system. Recently Ando et al. and Niwa et al. have reported the value of 0.41 and 0.48, respectively, using independent absolute photon measurement systems [2, 3]. The luciferase used in these three reports was that from *Photinus pyralis* (firefly). However, there are number of curious beetle luciferases with various colors and properties. More recently, the highest *QY*, 0.61, was obtained using *Pyrearinus termitilluminance* luciferase whose peak wave length 539 nm is the shortest among beetle luciferases [4].

In order to determine *QY* value, total photon flux (photons/s) has to be absolutely quantified. Total photon flux here is defined as the spatially and spectrally integrated photon flux emitted diffusively from a luminescence reaction solution in a test tube.

Sung-Bae Kim (ed.), *Bioluminescence: Methods and Protocols*, Methods in Molecular Biology, vol. 1461, DOI 10.1007/978-1-4939-3813-1_5, © Springer Science+Business Media New York 2016

Luminometers are sensitive photon-counting detectors widely employed to observe weak luminescence from reaction solutions. However, they are neither spectrometric nor designed with ideal point-source geometry, with the result that they are not considered to be "absolute" instruments. For the purpose of photon flux measurement using a sensitive luminometer, we have to calibrate its responsivity. Here we define the "responsivity" of the luminometer as the sensitivity (in counts/photon) to the total photon flux emitted from the sample solution. Because the responsivity varies depending on the sample spectrum, it is ideal to calibrate using identical luminescence reaction solution itself as the reference light source with absolute value of total photon flux, which is hereafter referred to as the "reference solution." Total photon flux value of the reference solution was calibrated using an absolute total photon flux measurement system that we have specially designed.

Here we describe our integrating-sphere based absolute total photon flux measurement system and its calibration method according to the national standard of photometry and radiometry. Using this apparatus, methodologies to determine *QY* using *P. pyralis* luciferase (FLuc) is introduced as an example experiment.

2 Materials

2.1 Total Photon Flux Measurement Apparatus

1. An integrating sphere-based total photon flux measurement system (*see* Fig. 1). This system is comprised of a 6 in. integrating sphere (Labsphere, North Sutton, NH, USA) and a multichannel spectrometer equipped with a cooled CCD detector (Roper Technologies, Sarasota, Florida).
2. A luminometer (AB-2200, ATTO, Tokyo, Japan).
3. Standard lamp (500 W spectral irradiance standard lamp, Ushio, Tokyo, Japan). Spectral irradiance value of the lamp is certified by JEMIC (Tokyo, Japan).

2.2 Reagents for Bioluminescence Reaction

1. D-Luciferin sodium salt (HPLC assay 99 % purity, 128-03954, Wako, Osaka, Japan).
2. A chiral column (Chiralcel OD-RH, Daicel Chemistry, Tokyo, Japan).
3. *Photinus pyralis* luciferase (L9506, crystallized chromatographic grade (Sigma-Aldrich, St. Louis, MO)).
4. ATP (adenosin-5-triphosphoric acid disodium salt, Oriental Yeast, Tokyo, Japan).
5. PicaGene® reagent (Wako, Osaka, Japan).
6. 1 M Tris–HCl [pH 8.0] buffer.
7. $MgSO_4 \cdot 7H_2O$, HCl, distilled water, and other generally used chemicals.

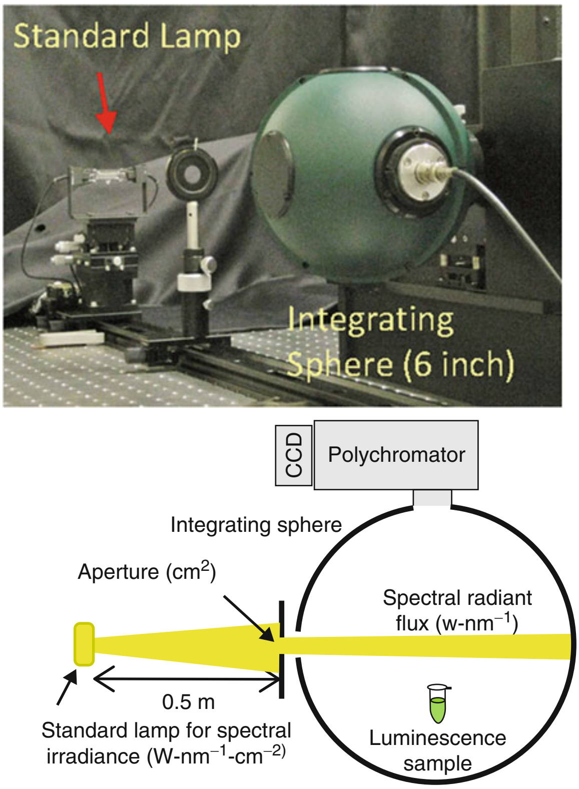
Standard Lamp
Integrating Sphere (6 inch)
CCD
Polychromator
Integrating sphere
Aperture (cm^2)
Spectral radiant flux (w-nm^{-1})
0.5 m
Standard lamp for spectral irradiance (W-nm^{-1}-cm^{-2})
Luminescence sample

Fig. 1 Integrating sphere-based multichannel spectrometer system employed in this study

2.3 Stock Solutions of Bioluminescence Reaction Using FLuc

Stock solutions below can be stored at −30 °C for a several months and should be consumed within a few days after thawing without refreezing.

1. D-Luciferin: 1×10^{-2} M aqueous D-Luciferin from D-Luciferin sodium salt.
2. Luciferase: 1 mg/mL in 0.1 M Tris buffer containing 10% glycerol from FLuc.
3. ATP: 20 mM ATP (neutralized with NaOH) in 0.1 M Tris buffer.

3 Methods

3.1 Absolute Calibration of an Integrating Sphere System

1. Set up the integrating sphere system.
2. Place a spectral irradiance standard lamp as the external light source coupled with an aperture with a known area (cm^2) at the entrance of the sphere, which gives spectral radiant flux with absolute value in W/nm (*see* **Note 1**).

3. Calibrate spectral responsivity (counts/W/nm) of the sphere system against spectral radiant flux (W/nm) using the spectral irradiance standard lamp (*see* **Note 2**).
4. Calculate spectral photon flux responsivity value (counts/photon/s/nm) from the spectral radiant flux value by a single photon energy value (E) according to a formula, $E = ch/\lambda$, here c is velocity of light, h is Planck's constant, and λ is the wavelength of the photon.

3.2 Absolute Calibration of a Luminometer

1. Prepare luciferase dilution series solution from the stock solution with the Tris buffer containing 10% glycerol (*see* **Note 4**).
2. Prepare a reference solution by mixing 5 μL of a diluted luciferase solution with 200 μL of PicaGene® solution (*see* **Note 5**).
3. The reference solution was divided into two test tubes of 100 μL solution which are homogenous to give identical light intensity.
4. Place each test tube into a luminometer and the integrating sphere system.
5. Simultaneously measure the light intensity of the reference solutions using the luminometer and the integrating sphere system.
6. Calculate total spectral photon flux (photons/s/nm) by the result using the integrating sphere system with spectral photon flux responsivity (counts/photon/s/nm) (*see* **Note 6**).
7. Calculate the luminometer responsivity (counts/photon/s) from the simultaneous measurement results, that is, counts value by the luminometer and total photon flux value by the integrating sphere (*see* **Note 7**).
8. Confirm the validity of the responsivity value, by repeating with wide range of concentration of luciferase (*see* **Note 8**).

3.3 Quantum Yield Measurement

1. Characterize the accurate concentration by absorbance with $\log \omega_{327\mathrm{nm}} = 4.27$ [5].
2. Confirm the D-form purity of luciferin in the stock solution using HPLC with the chiral column.
3. Dilute the D-Luciferin solution to 1×10^{-7} M with 0.1 M Tris buffer.
4. Prepare a reaction mixture containing 2 mM ATP and 4 mM $MgSO_4$ in 0.1 M Tris buffer using the ATP stock solution, 1 M Tris buffer and $MgSO_4 \cdot 7H_2O$.
5. In a test tube for the luminometer, place 5 μL of the 1×10^{-6} M D-Luciferin solution, 5 μL of 1 mg/mL luciferase stock solution, and place the test tube into the absolutely calibrated luminometer. Here, applied D-luciferin is 5×10^{-12} mol (3.01×10^{10} molecules).

6. Start luminometer to measure total photon flux in the complete darkness.
7. Initiate the luminescence reaction by applying 90 μL of the reaction mixture of ATP-Mg^{2+} into the test tube.
8. Stop the data recording after all the substrate is consumed.
9. Calculate number of photons by time integration of the total photon flux recorded by the luminometer, which is determined by count value and responsivity value of the luminometer.
10. Divide the number of photons by the number of D-luciferin molecule reacted, which gives *QY* value.

4 Notes

[Absolute calibration of an integrating sphere system]

1. The integrating sphere-based absolute total radiant flux measurement is well established in photometry and radiometry [6]. Spectral responsivity of the sphere system is obtained by using a spectral irradiance standard lamp. Using integrating sphere, liner flux from the standard lamp through the aperture outside the sphere and total flux from the light source placed inside the sphere are able to be measured equally.
2. The level of the photon flux through the aperture should be reduced to the level of luminescence from the reference solution that will be placed inside the sphere.
3. The total spectral photon flux responsivity of the sphere system has to be linear in the intensity range of interest, which can be confirmed by changing the radiant flux through the aperture.

[Absolute calibration of a luminometer]

4. We employed a long-lasting luminescence solution as a reference solution that is the light source optimized for the calibration of a luminometer. This solution consists of the same firefly luciferin-luciferase reaction reagents as the sample solution whose quantum yield was of interest, resulting in excellent spectral matching.
5. In order to obtain ideal reference solution having long-lasting luminescence intensity using FLuc, PicaGene® reagent was employed to prepare bioluminescence reaction solution. This reagent contains coenzyme-A and dithiothreitol as additives to obtain long-lasting luminescence with a half decay time of more than 10 min [7].
6. An absolute luminescence spectrum of the reference solution was obtained by employing thus calibrated integrating sphere

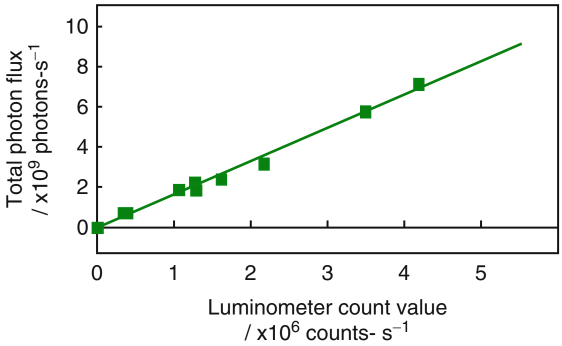

Fig. 2 Calibration plot of the total photon flux responsivity of the luminometer with various intensity levels for FLUC. The line indicates the least square linear fit

system. Total photon flux value is obtained from this spectrum by integrating spectrally.

8. The luminescence intensity of a bioluminescence reaction has poor reproducibility. To avoid this disadvantage, the reference solution was simply duplicated by dividing the homogeneous reaction solution into two test tubes. And then, one of them was put into the integrating sphere system and the other into the luminometer to measure simultaneously the absolute total photon flux of the reference solution and the absolute responsivity of the luminometer, respectively.
9. To confirm the linearity of the total photon flux responsivity of the luminometer, reference solutions with a wide range of luminescence intensities for each luciferase were prepared by controlling the concentration. As a result, the luminometer employed in our study exhibited a good linear response at the usual detection level for bioluminescence measurements, as indicated in Fig. 2. By linear fitting of the plots, the absolute responsivity of 6.05×10^{-4} counts/photon was obtained for the luminometer using FLuc bioluminescence solution.

Acknowledgement

K.N. would like to thank Y. Ichino for helpful discussions about absolute calibrations and Y. Ohmiya for his discussions about bioluminescence reactions. This work was supported by a Grant-in-Aid from the Japan Society for the Promotion of Science.

References

1. Seliger HH, McElroy WD (1959) Quantum yield in the oxidation of firefly luciferin. Biochem Biophys Res Commun 1:21–24
2. Ando Y, Niwa K, Yamada N, Enomoto T, Irie T, Kubota H, Ohmiya Y, Akiyama H (2007) Firefly bioluminescence quantum yield and color change by pH-sensitive green emission. Nat Photon 2:44–47
3. Niwa K, Ichino Y, Ohmiya Y (2010) Quantum yields measurements of firefly bioluminescence reactions using a commercial lumnometer. Chem Lett 39:291–293
4. Niwa K, Ichino Y, Kumata S, Nakajima Y, Hiraishi Y, Kato D, Viviani RV, Ohmiya Y (2010) Quantum yields and kinetics of the firefly bioluminescence reaction of beetle luciferases. Photochem Photobiol 86:1046–1049
5. Seliger HH, McElroy WD, White EH, Field GF (1961) Stereospecificity and firefly bioluminescence, a comparison of natural and synthetic luciferins. Proc Natl Acad Sci U S A 47:1129–1134
6. Zong Y, Miller CC, Lykke KR, Ohno Y (2004) Measurement of total radiant flux of UV LEDs. Proc CIE CIE x026:107–110
7. Wood KV (1995) The chemical mechanism and evolutionary development of beetle bioluminescence. Photochem Photobiol 62:662–673

Part II

Fabrication of Bioluminescent Probes

Chapter 6

Bioluminescent Ligand–Receptor Binding Assays for Protein or Peptide Hormones

Ya-Li Liu and Zhan-Yun Guo

Abstract

Bioluminescence has been widely used in biomedical research due to its high sensitivity, low background, and broad linear range. In recent studies, we applied bioluminescence to ligand–receptor binding assays for some protein or peptide hormones based on a newly developed small monomeric Nanoluciferase (NanoLuc) reporter that has the so far brightest bioluminescence. The conventional ligand–receptor binding assays rely on radioligands that have drawbacks, such as radioactive hazards and short shelf lives. In contrast, the novel bioluminescent binding assays use the NanoLuc-based protein or peptide tracers that are safe, stable, and ultrasensitive. Thus, the novel bioluminescent ligand–receptor binding assay would be applied to more and more protein or peptide hormones for ligand–receptor interaction studies in future. In the present article, we provided detailed protocols for setting up the novel bioluminescent ligand–receptor binding assays using two representative protein hormones as examples.

Key words Bioluminescence, Binding, Ligand, Peptide, Protein, Receptor, Tracer

1 Introduction

Bioluminescence is a kind of light emission produced from enzyme-catalyzed chemical reactions. It occurs widely in marine vertebrates and invertebrates, as well as in some fungi and bacteria. Some enzymes catalyzing bioluminescence reactions have been developed as reporters widely used in biomedical studies, such as firefly luciferase, *Renilla* luciferase, and *Gaussia* luciferase. Bioluminescent reporters have been widely used in reporter gene assays, in vivo imaging and some other quantitative assays due to their high sensitivity, low background, and broad linear range [1–3]. In 2012, Promega developed an engineered small monomeric Nanoluciferase (NanoLuc) reporter (171 amino acids, 19 kDa) that can produce the brightest bioluminescence reported to date (~150-fold higher than the conventional firefly luciferase and *Renilla* luciferase) [4]. NanoLuc emits long half-life glow-type bioluminescence in an ATP-independent manner, has high physical stability and lacks

Sung-Bae Kim (ed.), *Bioluminescence: Methods and Protocols*, Methods in Molecular Biology, vol. 1461,
DOI 10.1007/978-1-4939-3813-1_6, © Springer Science+Business Media New York 2016

posttranslational modifications. Thus, it represents a new generation of bioluminescent reporters for various biomedical studies.

Protein or peptide hormones are a large group of signaling molecules playing critical biological functions mediated by specific cell membrane receptors. To study their interactions with receptors, ligand–receptor binding assay is an important technique that has been widely used for decades. The conventional ligand–receptor binding assays rely on radioligands (hot tracers) labeled by radioisotopes, such as radioactive iodine-125 (^{125}I) for labeling of protein or peptide hormones [5–10, 20]. However, use of radioactive tracers has drawbacks, including the radioactive hazards to operators and environments, short shelf lives and constant specific activity change due to spontaneous decay of the radioisotopes. In recent years, nonradioactive ligand–receptor binding assays have been developed for some protein or peptide hormones based on the sensitive time-resolved fluorescence of lanthanides (typically europium) [11–16]. However, preparation of the lanthanide-labeled tracers is quite difficult and expensive. In recent studies, our laboratory developed bioluminescent ligand–receptor binding assays for some protein or peptide hormones based on the ultrasensitive bioluminescence of the newly developed NanoLuc reporter [17–19]. The novel bioluminescent tracers are safe, stable, and ultrasensitive, thus the novel bioluminescent ligand–receptor binding assays would be applied to more and more protein or peptide hormones for ligand–receptor interaction studies in future.

In the present chapter, we present step-to-step protocols for preparation of the bioluminescent protein or peptide tracers and setting up bioluminescent ligand–receptor binding assays using insulin-like peptide 3 (INSL3) and leukemia inhibitory factor (LIF) as examples.

2 Materials

2.1 *Escherichia coli (E. coli)* Culture

Prepare LB medium using distilled water and other solutions using ultrapure water (18 MΩ cm at 25 °C). Reagents used in these experiments are at least analytical grade.

1. Liquid LB medium: 10 g/L tryptone, 5 g/L yeast extract and 10 g/L NaCl. Weigh 10 g tryptone, 5 g yeast extract and 10 g NaCl to a 2-L beaker, add 1 L water and stir to dissolve. Aliquot the liquid medium to several glass shaking flasks (50 mL per 250-mL flask or 250 mL per 2-L flask), autoclave at 121 °C for 20 min and store at room temperature.
2. Amp stock solution: 50 mg/mL ampicillin sodium salt (Amp). Weigh 500 mg Amp powder to a 15-mL tube, add 10 mL water and vertex to dissolve. Pass the solution through a sterile 0.22-μm filter to several 1.5-mL sterile eppendorf tubes and store at −20 °C.

3. IPTG stock solution: 1.0 M isopropyl β-d-1-thiogalactopyranoside (IPTG). Weigh 2.38 g IPTG to a 15-mL tube, add 10 mL water and vertex to dissolve. Pass the solution through a sterile 0.22-μm filter to several 1.5-mL sterile eppendorf tubes and store at −20 °C.

2.2 Protein Purification

1. 20 mM phosphate buffer (pH 7.5): Weigh 2.99 g $Na_2HPO_4 \cdot 2H_2O$ and 0.50 g $NaH_2PO_4 \cdot 2H_2O$, add water to 1 L and stir to dissolve (*see* **Note 1**). Pass through a 0.22-μm filter and store at room temperature.
2. High salt phosphate buffer: 20 mM phosphate (pH 7.5) plus 0.5 M NaCl. Weigh 29.25 g NaCl into 1 L of 20 mM phosphate buffer (pH 7.5) and stir to dissolve. Pass through a 0.22-μm filter and store at room temperature.
3. 0.5 M imidazole solution: Weigh 3.40 g imidazole into 100 mL of high salt phosphate buffer and stir to dissolve. Pass through a 0.22-μm filter and store at room temperature.
4. 1.0 M DTT stock solution: Weigh 154 mg dithiothreitol (DTT) to a 1.5-mL eppendorf tube, add 1.0 mL water, vertex to dissolve and store at −20 °C.

2.3 Bioluminescence Measurement

1. PBS solution: Weigh 8 g NaCl, 0.2 g KCl, 1.78 g $Na_2HPO_4 \cdot 2H_2O$, and 0.24 g KH_2PO_4, add 900 mL water to dissolve. Adjust pH to 7.4 by adding appropriate amount of 1 M HCl solution monitored using a pH meter. Adjust total volume to 1 L by adding appropriate amount of water, autoclave at 121 °C for 20 min and store at room temperature.
2. Dilution Buffer: PBS plus 1% BSA. Weigh 400 mg lyophilized bovine serum albumin (BSA) into a 50-mL tube, add 40 mL PBS solution, vertex to dissolve and store at −20 °C (*see* **Note 2**).

2.4 Chemical Conjugation of NanoLuc with INSL3

1. INSL3 stock solution: Weigh 2.0 mg purified easily labeled INSL3 powder into a 1.5-mL eppendorf tube, add 100 μL dimethylsulfone (DMSO), vertex to dissolve and store at −20 °C. The resultant INSL3 concentration in the stock is ~3 mM (*see* **Note 3**).
2. SPDP stock solution: Add 534 μL anhydrous *N*,*N*-dimethylformamide (DMF) to a vial (5 mg) of *N*-succinimidyl 3-(2-pyridyldithio)propionate (SPDP) (SigmaAldrich, St. Louis, MO, USA), vertex to dissolve and store at −80 °C (*see* **Note 4**). The resultant SPDP concentration in the stock is 30 mM.
3. Modification Buffer: 150 mM phosphate and 1.5 M guanidine chloride (pH 7.5) (*see* **Note 5**). Weigh 2.34 g $NaH_2PO_4 \cdot 2H_2O$ and 14.33 g guanidine hydrochloride, add 80 mL water and stir to dissolve. Adjust its pH to 7.5 by adding appropriate amount of 1 M NaOH solution monitored using a pH meter.

Adjust total volume to 100 mL by adding appropriate amount of water after pH adjustment and store at room temperature.

4. 50% TFA solution: Mix 50 mL water with 50 mL trifluoroacetic acid (TFA) in a brown glass bottle and store at room temperature.
5. SPDP-modified INSL3 solution: Add a small volume of 1.0 mM aqueous HCl solution (pH 3.0) to the tube containing the lyophilized SPDP-modified INSL3 and vertex to dissolve (*see* **Note 6**). Transfer 10 μL of the stock solution to 90 μL of 1.0 mM HCl solution and measure its absorbance at 280 nm using a 100 μL-cuvette on a photometer. Calculate the accurate concentration of the SPDP-modified INSL3 in the stock solution using an extinction coefficient of $\varepsilon_{280\ \text{nm}} = 12260\ \text{M}^{-1}\ \text{cm}^{-1}$ (*see* **Note 7**).
6. Conjugation Buffer: 300 mM Tris–HCl, 3 mM EDTA, 1.5 M urea, pH 7.5 (*see* **Note 8**). Weigh 1.45 g Tris base and 3.60 g urea to a 50-mL tube, add 240 μL of 0.5 M EDTA stock solution (pH 8.0) and 30 mL water. Adjust its pH to 7.5 by adding appropriate amount 1.0 M HCl solution monitored using a pH meter. Adjust its final volume to 40 mL by adding appropriate amount of water after pH adjustment and store at room temperature.

2.5 Cell Culture and Binding Assays

1. Complete medium: the basic medium (*see* **Note 9**) supplemented with 10% fetal bovine serum, 100 U/mL penicillin and 100 μg/mL streptomycin. To 500 mL of basic medium, add 50 mL of fetal bovine serum and 5 mL of 100× antibiotic stock solution and store at 4 °C. If the basic medium doesn't contain l-glutamine, add glutamine stock solution to the final concentration of 2 mM.
2. Binding Solution: serum-free basic medium plus 1% BSA (*see* **Note 10**). Weigh 400 mg of BSA powder to a 50-mL tube, add 40 mL of basic medium, vertex to dissolve and store at −20 °C.

3 Methods

3.1 Overexpression and Purification of an Engineered NanoLuc for Conjugation

NanoLuc can be efficiently overexpressed in *E. coli* with full enzymatic activity [17]. It contains a single buried cysteine residue at the C-terminus. For chemical conjugation with protein or peptide hormones, we designed an engineered 6×His-Cys-NanoLuc that carries a unique exposed cysteine residue at the N-terminus [17] (*see* **Note 11**). The engineered NanoLuc is fully active, can be efficiently overexpressed in *E. coli* and be conveniently purified to homogeneity.

1. Take out a tube (100 μL) of competent cells of *E. coli* strain BL21(DE3) from −80 °C refrigerator (*see* **Note 12**) and thaw it on ice. Add 1–2 μL (50–200 ng plasmid) of the expression construct pET/6×His-Cys-NanoLuc [17] to the competent

cells, gently mix and incubate on ice for 30 min. Thereafter, put the tube into a 42 °C water-bath for 60 s and then put it on ice for 2–5 min. Add 0.5 mL of liquid LB medium and put the tube into a 37 °C shaker for 30–45 min with gentle shaking (150 rpm). Finally, transfer 100–200 μL of the transformed cells to a 250-mL shaking flask containing 50 mL liquid LB medium, add 100 μL of Amp stock solution and put the flask into a 37 °C shaker overnight with vigorous shaking (250 rpm) (*see* **Note 13**).

2. Next day, transfer 2.5 mL of the overnight culture broth to each 2-L shaking flask containing 250 mL liquid LB medium. Typically, use four 2-L flasks for each large-scale overexpression (*see* **Note 14**). Add 0.5 mL of Amp stock solution to each flask and put them into a 37 °C shaker with vigorous shaking (250 rpm).
3. Monitor growth of the *E. coli* cells by measuring the optical density ($OD_{600\ nm}$) of the culture broth using a photometer. At an interval of ~0.5 h, take 0.5 mL of the culture broth from the shaking flask and measure its $OD_{600\ nm}$ using LB medium as a blank. Once $OD_{600\ nm}$ reached ~1.0, turn down the temperature of the shaker to 25 °C.
4. After temperature of the shaker reached 25 °C, add 250 μL IPTG stock solution to each flask and continuously culture the cells in the shaker for 6–8 h or overnight with gentle shaking (150 rpm) (*see* **Note 15**).
5. After induction, transfer the culture broth to centrifuge tubes (250 mL each) and centrifuge at 5000 ×*g* for 10 min. After centrifugation, discard the supernatant and resuspend the cell pellet in cold high salt phosphate buffer (*see* **Note 16**). Typically, use 30 mL of high salt phosphate buffer for the cell pellet from 1 L of culture broth.
6. Lyse the *E. coli* cells in the suspension by sonication or French press according to the user's manual of the apparatus.
7. Transfer the cell lysate to centrifuge tubes (50 mL each) and centrifuge at 8000 ×*g* for 20 min at 4 °C. After centrifugation, carefully transfer the supernatant to another tube and discard the pellet.
8. Load the supernatant to a home-made or a pre-packed Ni^{2+} column pre-equilibrated with the high salt phosphate buffer (*see* **Note 17**). After loading, wash the column thoroughly with the high salt phosphate buffer and 30 mM imidazole solution (in the high salt phosphate buffer), then elute the bound 6×His-Cys-NanoLuc by 250 mM imidazole (in the high salt phosphate buffer). Alternatively, elute the bound 6×His-Cys-NanoLuc using a linear imidazole gradient by mixing solution A (the high salt phosphate buffer) and solution B

(0.5 M imidazole in the high salt phosphate buffer). Collect the eluted 6×His-Cys-NanoLuc fraction manually or by an automated fractioner (*see* **Note 18**).

9. Transfer 6×His-Cys-NanoLuc fraction (~10 mL) to a dialysis tube (cutoff molecular weight of 3 kDa) and dialyze against cold 20 mM phosphate buffer (pH 7.5) at 4 °C (*see* **Note 19**).
10. Transfer the dialyzed 6×His-Cys-NanoLuc fraction to a 15-mL tube, add DTT stock solution to the final concentration of 10–20 mM and incubate at room temperature for 20 min (*see* **Note 20**).
11. Load the DTT-treated 6×His-Cys-NanoLuc fraction to an ion-exchange column (TSKgel DEAE-5PW, 7.5 mm × 75 mm, from Sigma Aldrich, St. Louis, MO, USA) that is connected to an Agilent HPLC1100 apparatus (*see* **Note 21**). Elute 6×His-Cys-NanoLuc from the column using a linear sodium chloride gradient by mixing buffer A (20 mM phosphate buffer, pH 7.5) and buffer B (the high salt phosphate buffer). Collect 6×His-Cys-NanoLuc fraction manually and analyze it by SDS-PAGE (*see* **Note 22**).
12. Quantify concentration of the purified 6×His-Cys-NanoLuc by bicinchoninic acid (BCA) method using BSA as a standard (*see* **Note 23**). Aliquot the purified 6×His-Cys-NanoLuc fraction into several 1.5-mL eppendorf tubes and store at −80 °C.

3.2 Bioluminescence Measurement

Bioluminescence of NanoLuc and various NanoLuc-based tracers can be conveniently measured using a plate reader with luminescence mode, such as a SpectraMax M5 plate reader (Molecular Devices, Sunnyvale, CA, USA) (*see* **Note 24**). For bioluminescence measurement, insure all solutions are equilibrated at room temperature for enough time, because temperature has effects on NanoLuc activity.

1. Appropriately dilute NanoLuc or NanoLuc-based tracers using Dilution Buffer (PBS plus 1% BSA) (*see* **Note 25**). Take several eppendorf tubes and label them as 1, 2, 3, etc. Add 90 μL Dilution Buffer to each tube. Transfer 10 μL stock solution of NanoLuc or NanoLuc-based tracer to tube 1 and mix thoroughly. Then, transfer 10 μL mixed solution from tube 1 to tube 2 and mix thoroughly, so on until the last tube.
2. Transfer 10 μL diluted enzyme, in a triplicate, from the diluted tubes to a white opaque 96-well plate (*see* **Note 26**).
3. Add 50 μL Lysis Buffer (Promega, Madison, WI, USA) to each assay well and mix thoroughly (*see* **Note 27**).
4. 20-fold dilute the stock solution of substrate furimazine (Promega) using PBS (*see* **Note 28**). Add 40 μL diluted substrate to each well, mix, and immediately measure on a SpectraMax M5 plate reader using luminescence mode (*see* **Note 29**).

5. Plot the measured bioluminescence data (in logarithmic scale, *Y*-axis) against the NanoLuc amount (fmol, in logarithmic scale, *X*-axis), a linear curve will be obtained at appropriate range and specific activity (counts/fmol) will be calculated from the linear range.
6. Based on the measured specific activity, NanoLuc and various NanoLuc-based tracers can be quickly and accurately quantified through bioluminescence measurement.

3.3 Chemical Conjugation of NanoLuc with INSL3

INSL3 is a protein hormone belonging to the insulin/relaxin superfamily. It involves in regulation of reproduction by binding and activating a G protein-coupled receptor RXFP2. To develop a novel bioluminescent receptor-binding assay for INSL3, we prepared a NanoLuc-based INSL3 tracer through a chemical conjugation approach [17] as shown in Fig. 1. First, an active disulfide bond (pyridyldithiol moiety) was introduced to the A-chain N-terminus of an easily labeled INSL3 (*see* **Note 30**) by reaction with a bifunctional reagent SPDP that carries a pyridyldithiol moiety and a primary amine-specific N-hydroxysuccinimidyl (NHS) ester moiety (*see* **Note 31**). Second, 6×His-Cys-NanoLuc was covalently crosslinked with INSL3 via a reversible disulfide linkage by reaction of the unique exposed Cys of 6×His-Cys-NanoLuc with the active disulfide bond of the SPDP-modified INSL3 (*see* **Note 32**).

1. Prepare easily labeled INSL3 through overexpression of a single-chain precursor in *E. coli* and subsequent purification, in vitro refolding and enzymatic maturation according to our previous procedure [14].
2. For SPDP-modification reaction, sequentially add 30 μL Modification Buffer, 30 μL INSL3 stock solution (~600 μg INSL3) and 30 μL SPDP stock solution to a 1.5-mL eppendorf tube, mix thoroughly, and incubate at 30 °C for 2 h (*see* **Note 33**).
3. After incubation, add 800 μL water to the reaction tube and adjusted its pH to 3–4 by adding appropriate amount of 50 % TFA solution monitored by pH paper.
4. Load the diluted reaction mixture to a C18 reverse-phase column (Zorbax 300SB-C18, 4.6 mm × 250 mm, from Agilent) that is connected to an Agilent HPLC1100 apparatus. Elute the column by a linear acetonitrile gradient composed of solvent A (0.1 % aqueous TFA) and solvent B (acetonitrile containing 0.1 % TFA), and manually collect all peaks into 1.5-mL eppendorf tubes (*see* **Note 34**).
5. After lyophilization, the tube with white powder probably contains the modified INSL3. Take an aliquot for mass spectrometry analysis to confirm its identity.
6. For NanoLuc-conjugation reaction, add 100 μL Conjugation Buffer, 100 μL 6×His-Cys-NanoLuc (eluted from the ion-exchange

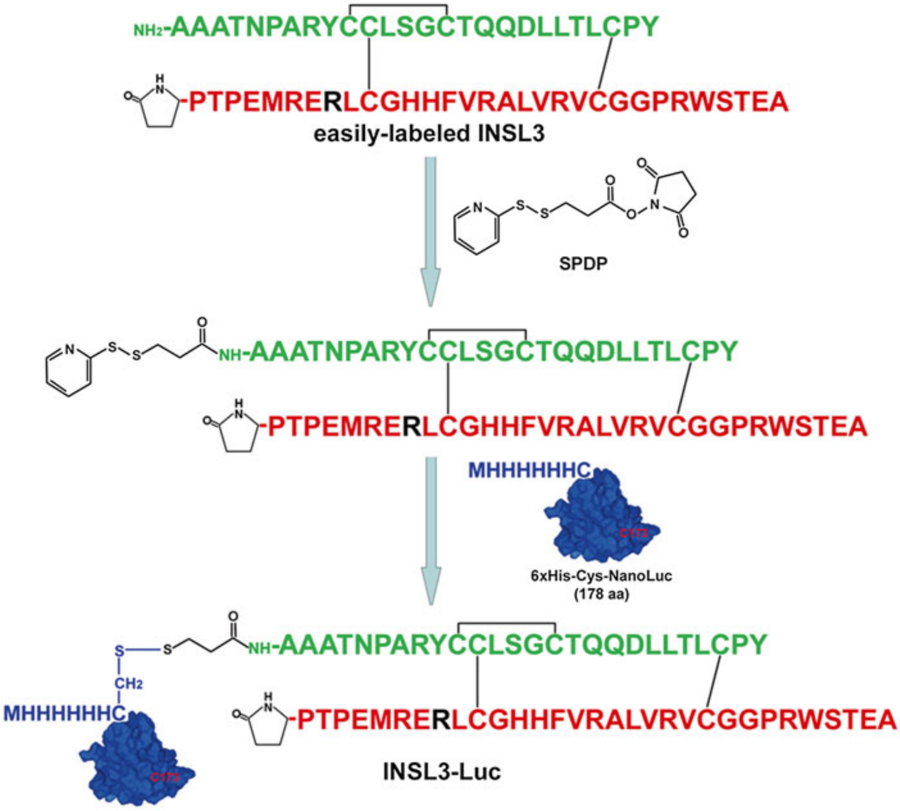
NH2-AAATNPARYCCLSGCTQQDLLTLCPY
-PTPEMRERLCGHHFVRALVRVCGGPRWSTEA
easily-labeled INSL3
SPDP
NH-AAATNPARYCCLSGCTQQDLLTLCPY
-PTPEMRERLCGHHFVRALVRVCGGPRWSTEA
MHHHHHHC
C173
6xHis-Cys-NanoLuc
(178 aa)
S
S
CH2
MHHHHHHC
NH-AAATNPARYCCLSGCTQQDLLTLCPY
-PTPEMRERLCGHHFVRALVRVCGGPRWSTEA
C173
INSL3-Luc

Fig. 1 The strategy for chemical conjugation of NanoLuc with INSL3 for novel bioluminescent ligand–receptor binding assays (Reproduced from ref. 17 with permission from Elsevier)

column in Subheading 3.1) (*see* **Note 35**), and appropriate amount of SPDP-modified INSL3 to a 1.5-mL eppendorf tube. Insure the molar ratio of INSL3 to NanoLuc is 3:1 (*see* **Note 36**). Incubate the tube at 30 °C for 30 min.

7. After conjugation, two-fold dilute the reaction mixture with water and load it onto an ion-exchange column (TSKgel DEAE-5PW, 7.5 mm × 75 mm, from SigmaAldrich) that is connected to an Agilent HPLC1100 apparatus. Elute the column using a linear sodium chloride gradient by mixing buffer A (20 mM phosphate, pH 7.5) and buffer B (the high salt phosphate buffer) and collect all peaks manually. Analyze all collected peaks using Native PAGE (pH 8.3) (*see* **Note 37**) and bioluminescence measurement.

8. Quantify INSL3-Luc by bioluminescence measurement after appropriate dilution according to the specific activity of 1.5×10^5 counts/fmol (*see* **Note 38**).

3.4 Saturation Receptor-Binding Assays of INSL3-Luc

To test whether INSL3-Luc retains binding affinity with receptor RXFP2, we carried out saturation receptor-binding assays (*see* **Note 39**) using living human embryonic kidney (HEK) 293T cells transiently overexpressing human RXFP2 as receptor source. As shown in Fig. 2a, a typical saturation binding curve was obtained for INSL3-Luc, with a calculated dissociation constant (K_d) of 2.0 ± 0.1 nM ($n = 3$). Thus, INSL3-Luc retained high binding affinity with receptor RXFP2 although a large NanoLuc was attached. The calculated maximal binding capacity (B_{max}) was 3.6 ± 0.1 fmol/well ($n = 3$), equal to the average receptor density of ~22,000 receptors/cell (~10^5 cells/well). After the specific binding data were converted to a Scatchard plot, a linear curve was obtained, suggesting one-site binding of INSL3-Luc with receptor RXFP2 (Right inner panel). Additionally, nonspecific binding of INSL3-Luc was quite low, accounting for less than 10% of total binding (Left inner panel). Thus, INSL3-Luc represents a novel bioluminescent tracer for interaction studies of INSL3 with its receptor RXFP2.

1. Culture HEK293T cells in complete DMEM medium to 70% confluence in two 3.5-mm dishes for transfection (*see* **Note 40**). Transfect these cells with human RXFP2 expression construct pcDNA6/RXFP2 using a transfection reagent according to the user's manual (*see* **Note 41**).
2. Next day of transfection, suck off the medium, wash the cells with 2–3 mL warm PBS solution, and add 1 mL warm trypsin solution to each dish (*see* **Note 42**). Put the dishes into a 37 °C incubator for 2–3 min, gently shake the dish to detach the cells. Add 2 mL complete medium to each dish and gently pipette the cells suspension 2–3 times.
3. Transfer the trypsinized cells into a 15-mL sterile tube and centrifuge ($1000 \times g$, 2 min). Discard the supernatant and gently resuspend the cell pellet (from two 35-mm dishes) with 6–7 mL of complete medium. Aliquot the cell suspension into a 96-well plate (100 μL/well, 60–70 wells in total) and put the plate into a 37 °C CO_2 incubator for 24–36 h (*see* **Note 43**).
4. Serially dilute INSL3-Luc conjugate to following concentrations (*see* **Note 44**): 40, 20, 10, 5, 2.5, 1.25, 0.675, and 0 nM (Binding Solution only). Take eight 1.5-mL eppendorf tubes and label them as 1–8. To tube 1, add x μL INSL3-Luc conjugate (prepared in Subheading 3.3 and quantified by bioluminescence measurement), then add $(800 - x)$ μL Binding Solution and mix thoroughly. Transfer 400 μL mixture from tube 1 to tube 2, and then add 400 μL Binding Solution to tube 2 and mix thoroughly, so on until tube 7 (0.675 nM). Directly add 400 μL Binding Solution to tube 8. Other dilution patterns can also be used.

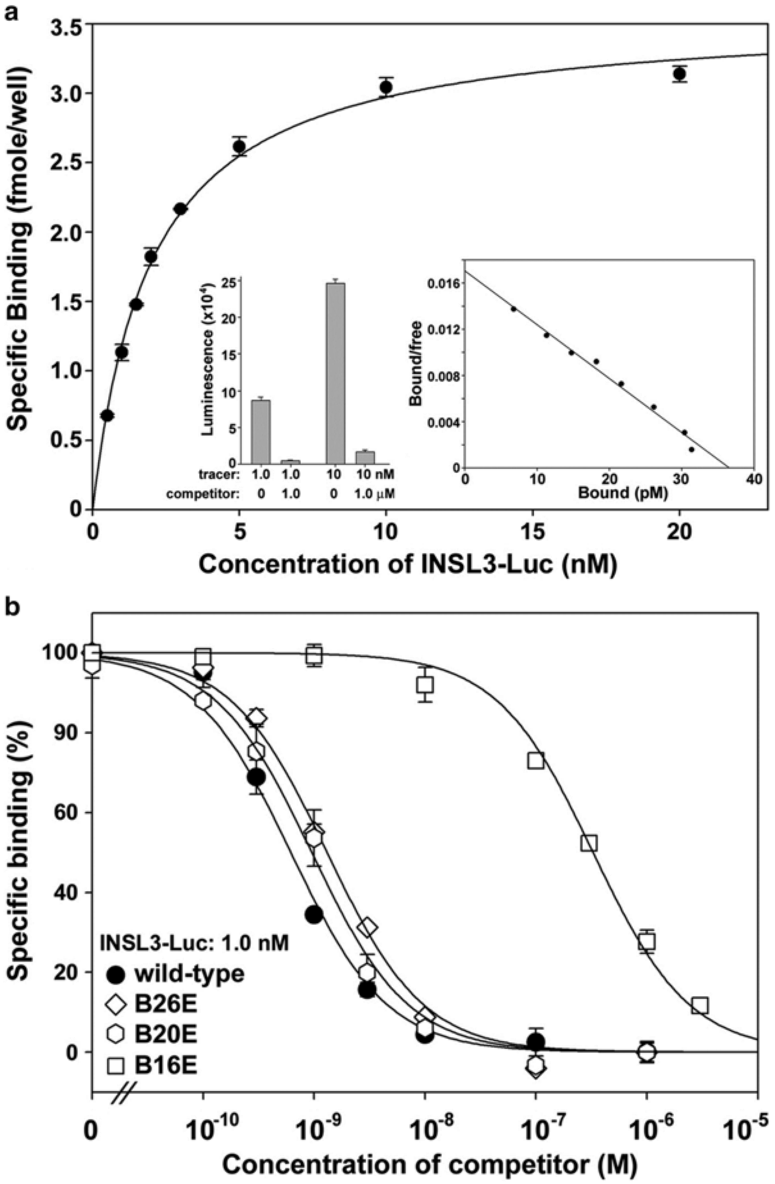

Fig. 2 (**a**) Saturation binding of INSL3-Luc with the receptor RXFP2. The measured specific binding data were expressed as the mean ± SE ($n = 3$) and fitted to a hyperbolic function $Y = B_{max}/(K_d + X)$ using SigmaPlot10.0 software. The linear Scatchard plot and the chart plot of total binding and nonspecific binding are shown as the inner panels. (**b**) Competition receptor-binding of INSL3 and its analogues using INSL3-Luc as a tracer. The measured data were expressed as the mean ± SE ($n = 3$) and fitted with sigmoidal curves using SigmaPlot10.0 software (Reproduced from ref. 17 with permission from Elsevier)

5. For total binding assay, gently remove medium from the first three wells of the 96-well plate with a pipette (*see* **Note 45**), immediately add 50 μL Binding Solution to each well, then transfer 50 μL diluted INSL3-Luc from tube 1 to each well (*see* **Note 46**) and gently mix. Remove medium from the second three wells, immediately add 50 μL Binding Solution to each well, then transfer 50 μL diluted INSL3-Luc from tube 2 to each well and gently mix. So on until tube 8.
6. For nonspecific binding assay, gently remove medium from the first three wells of the 96-well plate, immediately add 50 μL Competition Solution (Binding Solution containing 2.0 μM INSL3) to each well (*see* **Note 47**), then transfer 50 μL diluted INSL3-Luc from tube 1 to each well and gently mix. So on until tube 8.
7. Incubate the plate at 21–22 °C for 1–2 h (*see* **Note 48**). Thereafter, wash the plate as following: gently remove the binding solution with a pipette from first three wells; add 200 μL of ice-cold PBS solution to each well and gently remove the washing solution; add 200 μL of ice-cold PBS solution to each well again and gently remove the solution (*see* **Note 49**). Wash the next three wells and until all wells are washed.
8. After all well were washed, add 100 μL Lysis Buffer with room temperature (Promega) to each well (*see* **Note 50**), pipette the cell lysate and transfer 50 μL to a well of a white opaque 96-well plate.
9. Add 25-fold diluted substrate solution (diluted in PBS with room temperature) to the white opaque 96-well plate (50 μL/well) and immediately measure bioluminescence at a SpectraMax M5 plate reader using luminescence mode.
10. Process the measured saturation binding data as following: (1) Calibrate the measured bioluminescence data by subtracting the average value of the wells with zero tracer concentration (Binding Solution only) from all originally measured bioluminescence data (*see* **Note 51**). (2) Plot nonspecific binding curve using the calibrated bioluminescence data of nonspecific binding as Y-axis and tracer concentrations as X-axis. Fit the nonspecific binding data by a linear curve passing through the origin (*see* **Note 52**). (3) Plot the total binding curve using the calibrated bioluminescence data of total binding as Y-axis and tracer concentrations as X-axis. For one-site binding model, fit the total binding curve with $Y = B_{\max}X/(K_d + X) + N_{\text{non}}X$, where K_d is the dissociation constant, $B_{\max}$ is the maximal binding capacity, and N_{non} is a coefficient for nonspecific binding (*see* **Note 53**). (4) Calculate specific binding data by subtracting the calculated nonspecific binding data from the calibrated total binding data. (5) Plot the specific binding curve using the calculated bioluminescence data of

specific binding as Y-axis and the tracer concentrations as X-axis. For one-site binding model, fit the specific binding curve with $Y = B_{\max}X/(K_d + X)$. Alternatively, convert the measured bioluminescence data to bound tracer amount (fmol/well) by dividing the calibrated bioluminescence data with the specific activity of NanoLuc (1.5×10^5 counts/fmol) for further processing.

11. Convert the specific binding data to Scatchard plot as following. (1) Calculate the bound tracer concentrations (pM) by dividing the specific binding bioluminescence data (counts) with the product of tracer-specific activity (counts/fmol) and binding assay volume (mL) (*see* **Note 54**). (2) Calculate free tracer concentration (pM) by subtracting the bound tracer concentration (pM) from the total tracer concentration (pM) (*see* **Note 55**). (3) Calculate the ratio of bound tracer to free tracer (bound/free) by dividing the bound tracer concentration (pM) with the free tracer concentration (pM) (*see* **Note 56**). (4) Draw Scatchard plot using bound tracer concentrations (pM) as X-axis and bound/free values as Y-axis (*see* **Note 57**).

3.5 Competition Receptor-Binding Assays Using INSL3-Luc as Tracer

After confirmed that INSL3-Luc retains high binding affinity with receptor RXFP2, we used it as a novel nonradioactive tracer for competition receptor-binding assays to evaluate the receptor-binding potencies of various INSL3 analogues (*see* **Note 58**). As shown in Fig. 2b, typical sigmoidal competition curves were obtained for INSL3 and its analogues, with different IC_{50} values. Thus, INSL3-Luc is a sensitive nonradioactive tracer for accurate measurement of receptor-binding potencies of various INSL3 analogues.

1. Prepare HEK293T cells transiently overexpressing human RXFP2 as described in Subheading 3.4.
2. Prepare Tracer Solution by diluting INSL3-Luc into the Binding Solution to a final concentration of 2.0 nM (*see* **Note 59**).
3. Serially dilute competitor (INSL3 or its analogues in this case) to following concentrations: 2000, 200, 20, 2, 0.2, 0.02, and 0 nM (Binding Solution only) (*see* **Note 60**). Take seven 1.5-mL eppendorf tubes and label them as 1–7. To tube 1, add x μL stock solution of INSL3 or its analogue (*see* **Note 61**), then add (200–x) μL Binding Solution and mix thoroughly. Transfer 20 μL mixture from tube 1 to tube 2, and then add 180 μL of Binding Solution to tube 2 and mix thoroughly. So on until tube 6. Directly add 200 μL of Binding Solution to tube 7.
4. For competition binding assays, remove medium from the first three wells with a pipette, immediately add 50 μL Tracer Solution to each well, and then transfer 50 μL competitor from tube 1 to each well (*see* **Note 62**) and gently mix. Remove medium from the second three wells, immediately add 50 μL

Tracer Solution to each well, then transfer 50 μL competitor from tube 2 to each well and gently mix. So on until tube-7.

5. Incubate the plate at 21–22 °C for 1–2 h, then wash the cells and measure bioluminescence according to the procedures in Subheading 3.4.
6. Process the measured competition binding data as following. (1) Calibrate the measured bioluminescence data by subtracting the average of the wells with 1000 nM of wild-type INSL3 (*see* **Note 63**) from all original bioluminescence data. (2) Normalize the binding data by dividing all calibrated bioluminescence with the average value of the wells without competitor (Binding Solution only) (*see* **Note 64**). (3) Convert the competitor concentrations to logarithm scale in unit of *log*M, for examples, 1000 nM versus −6 and 1 nM versus −9. (4) Plot the competition binding data using software, such as SigmaPlot or Prism, using the normalized bioluminescence data as *Y*-axis and competitor concentrations in logarithm as *X*-axis. Fit the data with sigmoidal curves $Y = 100/(1 + 10^{X - log\mathrm{IC}_{50}})$ and the values of $log\mathrm{IC}_{50}$ can be calculated from the fitted curves by the software (*see* **Note 65**).

3.6 Overexpression of NanoLuc-fused LIF as a Bioluminescent Tracer

In above sections, we provided a chemical conjugation approach for preparation of NanoLuc-based protein or peptide tracers for novel bioluminescent ligand–receptor binding assays using INSL3 as an example (*see* **Note 66**). In the following sections, we will provide a genetic fusion approach for preparation of bioluminescent tracers using leukemia inhibitory factor (LIF) as an example [18] (*see* **Note 67**). LIF elicits pleiotropic effects on a diverse range of cells by activating a heterodimeric cell membrane receptor LIFR/gp130. LIF is an aggregation-prone protein and difficult for soluble overexpression in *E. coli*, fusion of NanoLuc at N-terminus of the mature human LIF significantly improved its soluble overexpression. As shown in Fig. 3, soluble and monomeric 6×His-NanoLuc-LIF could be efficiently overexpression in *E. coli* and be conveniently purified to homogeneity [18]. After removal of 6×His-NanoLuc fusion partner by enterokinase digestion, mature monomeric LIF protein with full biological activity was obtained at a final yield of ~5 mg per liter of *E. coli* culture broth. Besides *E. coli* cells, other host cells, such as mammalian cells, can also be used for overexpression of the NanoLuc-fused proteins as novel bioluminescent tracers (*see* **Note 68**).

1. Transform the expression construct pNLuc/LIF (*see* **Note 69**) into the *E. coli* strain Rosetta-gami 2(DE3) (*see* **Note 70**) and carry out induced overexpression at 25 °C overnight according to the procedures in Subheading 3.1.
2. After IPTG induction, collect *E. coli* cells by centrifugation (5000 × *g*, 10 min) and lyse them by sonication or French press according to the procedures in Subheading 3.1.

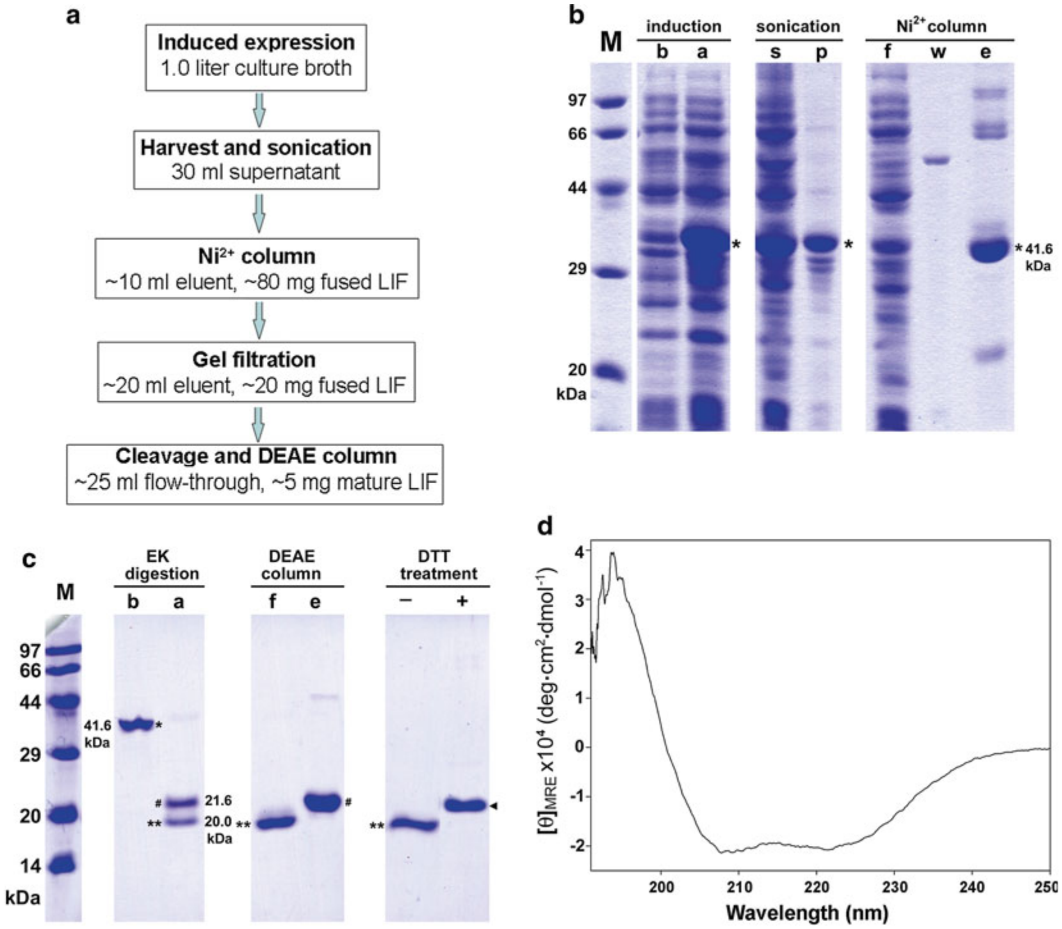

Fig. 3 Purification and characterization of the NanoLuc-fused LIF and the mature LIF. (**a**) Flowchart of the purification and maturation process. (**b**) Nonreducing SDS-PAGE analysis of 6×His-NanoLuc-LIF. *Lane b*, total cell lysate before IPTG induction; *lane a*, total cell lysate after IPTG induction; *lane s*, supernatant after sonication; *lane p*, pellet after sonication; *lane f*, flowthrough from the Ni^{2+} column; *lane w*, wash fraction by 30 mM imidazole; *lane e*, eluted fraction by 250 mM imidazole; *lane M*, protein marker. The *asterisk* indicates the band of 6×His-NanoLuc-LIF that has a theoretical molecular weight of 41.6 kDa. After electrophoresis, the gel was stained by Coomassie brilliant blue R250. (**c**) Nonreducing SDS-PAGE analyses of the mature LIF. *Lane b*, monomeric 6×His-NanoLuc-LIF eluted from gel filtration; *lane a*, after enterokinase digestion; *lane f*, flowthrough from the ion-exchange column; *lane e*, eluent from the ion-exchange column; *lane (–)*, mature LIF without DTT treatment; *lane (+)*, mature LIF treated with 20 mM DTT; *lane M*, protein marker. The *asterisk* indicates the band of 6×His-NanoLuc-LIF. The *double asterisk* indicates the band of mature LIF that has a theoretical molecular weight of 20.0 kDa. The *octothorpe* indicates the band of 6×His-NanoLuc-tag that has a theoretical molecular weight of 21.6 kDa. The *arrowhead* indicates the band of reduced LIF protein without disulfide bonds. After electrophoresis, the gel was stained by Coomassie brilliant blue R250. (**d**) Circular dichroism spectrum of the mature LIF (Reproduced from ref. 18 with permission from Elsevier)

3. Purify soluble 6×His-NanoLuc-LIF from the lysate supernatant by a Ni^{2+} column as described in Subheading 3.1.
4. Load the 6×His-NanoLuc-LIF fraction eluted from the Ni^{2+} column to a gel filtration column (TSKgel G2000SW$_{XL}$, 7.8 mm × 300 mm, SigmaAldrich, St. Louis, MO, USA) (*see* **Note 71**) that is connected to an Agilent HPLC1100 apparatus. Elute the column by 20 mM Tris–Cl (pH 8.5) containing 50 mM NaCl (*see* **Note 72**), manually collect all peaks and analyze them by nonreducing SDS-PAGE (*see* **Note 73**).
5. Add $CaCl_2$ stock solution and urea stock solution to monomeric 6×His-NanoLuc-LIF fraction to final concentrations of 2.0 mM and 1.6 M, respectively (*see* **Note 74**). Then, add enterokinase (New England Biolabs, Ipswich, MA, USA) to a final concentration of 2 ng/mL and carry out digestion at 25 °C overnight (*see* **Note 75**).
6. Load the digestion mixture onto a DEAE ion-exchange column (TSKgel DEAE-5PW, 7.5 mm × 75 mm, from SigmaAldrich) (*see* **Note 76**) that is connected to an Agilent HPLC1100 apparatus. Collect the flowthrough fraction (mature LIF fraction) and elute the bound fraction (6×His-NanoLuc-tag) by a sodium chloride gradient and analyze them by nonreducing SDS-PAGE.
7. Quantify the purified by 6×His-NanoLuc-LIF and mature LIF by BCA method using BSA as a standard. Measure bioluminescence of the purified 6×His-NanoLuc-LIF as described in Subheading 3.2. Calculate specific activity of 6×His-NanoLuc-LIF based on the measured bioluminescence and measured protein concentration (*see* **Note 77**).

3.7 Receptor-Binding Affinity of the NanoLuc-Fused LIF

In above section, we prepared 6×His-NanoLuc-LIF through soluble overexpression in *E. coli*. To test it whether retained high receptor-binding affinity, we carried out saturation receptor-binding assays using living murine leukemia M1 cells as a receptor source (*see* **Note 78**). As shown in Fig. 4a, 6×His-NanoLuc-LIF bound M1 cells in a typical saturation manner, with a calculated dissociation constant (K_d) of 33.1 ± 3.2 pM ($n = 3$), suggesting that 6×His-NanoLuc-LIF retained high binding affinity with LIFR/gp130 receptor although a large NanoLuc moiety was attached. The calculated maximal binding capacity (B_{max}) on 10^5 M1 cells was 8915 ± 225 counts, equal to ~350 receptors per M1 cell (specific activity of 6×His-NanoLuc-LIF was 1.5×10^5 counts/fmol). A linear Scatchard plot was obtained for binding of 6×His-NanoLuc-LIF with M1 cells (*see* Fig. 4b), suggesting that M1 cells only had high affinity binding site. Thus, 6×His-NanoLuc-LIF represents a novel bioluminescent tracer for studying the interactions of LIF with its receptor.

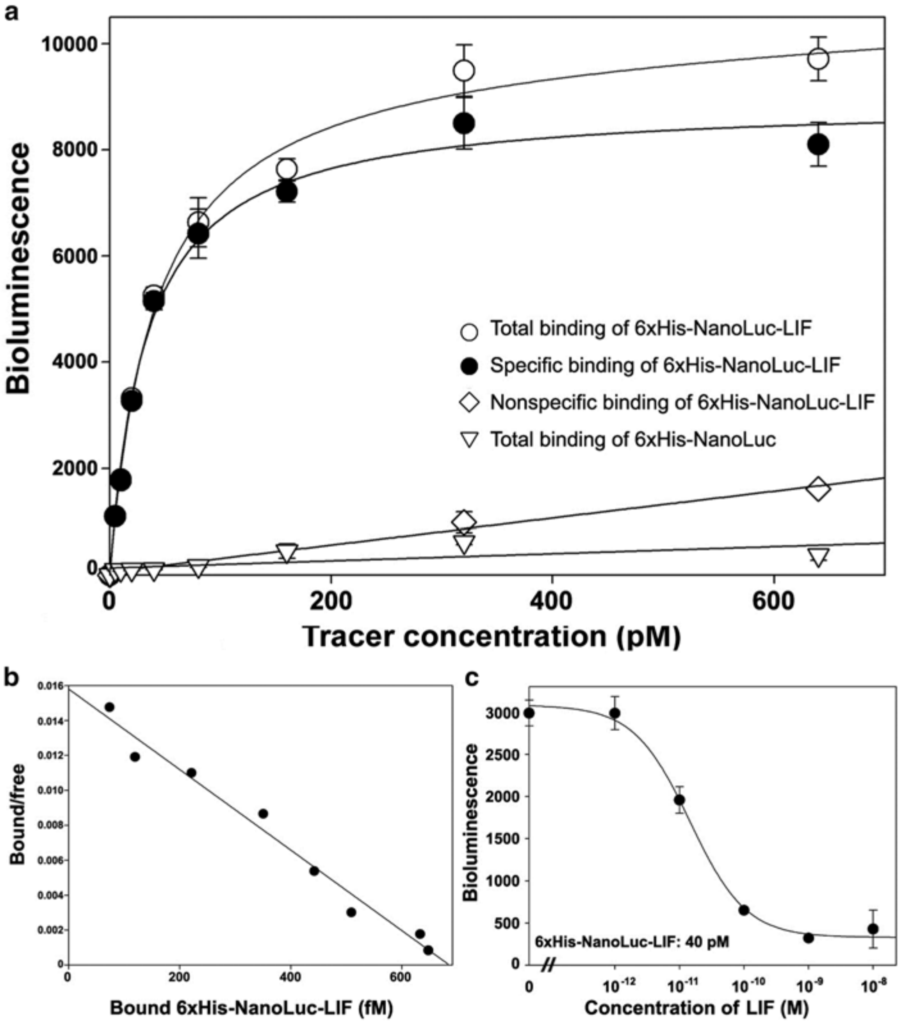

Fig. 4 Binding of the NanoLuc-fused LIF with the endogenously expressed LIFR/gp130 receptor on M1 cells. (**a**) Saturation binding with murine leukemia M1 cells. The measured bioluminescence data were expressed as mean ± SE ($n = 3$). The total binding data of 6×His-NanoLuc-LIF were fitted to $Y = B_{max}/(K_d + X) + N_{non}X$, and the specific binding data to $Y = B_{max}/(K_d + X)$ using SigmaPlot 10.0. The nonspecific binding data of 6×His-NanoLuc-LIF and the total binding data of 6×His-NanoLuc were fitted to linear curves using SigmaPlot 10.0. (**b**) Scatchard plot of the specific binding data of 6×His-NanoLuc-LIF with M1 cells. (**c**) Competition binding of mature LIF with M1 cells using 6×His-NanoLuc-LIF as a tracer. The measured bioluminescence data were expressed as mean ± SE ($n = 3$) and fitted to a sigmoidal curve using SigmaPlot 10.0 (Reproduced from ref. 18 with permission from Elsevier)

1. Culture suspension murine leukemia M1 cells in complete RPMI1640 medium in a 25-mm^2 flask at 37 °C in a CO_2 incubator to cell density of ~10^6 cells/mL.
2. Collect M1 cells by centrifugation (1000 ×*g*, 2 min) and resuspend them in Binding Solution (serum-free RPMI1640 medium plus 1 % BSA) at density of 4×10^6 cells/mL. Seed 50 μL of the cell suspension into each well of a 96-well filtration

plate (polyethersulfone membrane with 1.2 μm pore size, from Pall Incorporation, Port Washington, NY, USA) (*see* **Note 79**) that has been rinsed by the Binding Solution before use.

3. Serially dilute purified 6×His-NanoLuc-LIF to following concentrations: 2560, 1280, 640, 320, 160, 80, 40, 20, and 0 pM (Binding Solution only) using Binding Solution as described in Subheading 3.4.
4. For total binding assay, add 25 μL/well of Binding Solution and 25 μL/well of 2560 pM 6×His-NanoLuc-LIF to the first three wells of the 96-well filtration plate, and mix gently. Add 25 μL/well of Binding Solution and 25 μL/well of 1280 pM 6×His-NanoLuc-LIF to the second three wells, and mix gently (*see* **Note 80**). So on until the last tube with zero tracer concentration.
5. For nonspecific binding assay, add 25 μL/well of Competition Solution (Binding Solution plus 120 nM mature LIF) and 25 μL/well of 2560 pM 6×His-NanoLuc-LIF to the first three wells of the 96-well filtration plate, and mix gently. Add 25 μL/well of Competition Solution and 25 μL/well of 1280 pM 6×His-NanoLuc-LIF to the second three wells, and mix gently. So on until the last tube with zero tracer concentration.
6. After incubation at 21–22 °C for 1 h, centrifuge the filtration plate (400 × *g*, 2 min) in order to filter the solution. Add 200 μL of ice-cold PBS solution to each well and centrifuge the plate again. Repeat the above wash process once or twice (*see* **Note 81**).
7. Add 100 μL of ice-cold PBS solution to each well in order to resuspend the cells and then transfer 50 μL of the cell suspension to a white opaque 96-well plate (*see* **Note 82**). Put the plate at room temperature for 20–30 min to let the cell suspension reach room temperature.
8. Add 50 μL of 25-fold diluted substrate solution (diluted in room temperature Lysis Buffer, from Promega) to each well of the white opaque 96-well plate, well mix, and measure bioluminescence at a SpectraMax M5 plate reader using luminescence mode.
9. Process the measured saturation binding data as described in Subheading 3.4.

3.8 Competition Receptor-Binding Using the Novel Bioluminescent LIF Tracer

In above section, we demonstrated that 6×His-NanoLuc-LIF retained high binding affinity with LIF receptor, thus we used it as a novel nonradioactive tracer in competition receptor-binding assays. As shown in Fig. 4c, competition binding of the mature LIF with 6×His-NanoLuc-LIF on M1 cells was in a typical sigmoidal manner, with a calculated IC_{50} value of 15.8 ± 3.2 pM ($n = 3$). Thus, the bioluminescent LIF tracer was sensitive enough to monitor ligand–receptor interactions even using the endogenously expressed LIFR/gp130 as receptor source.

1. Prepare M1 cells and seed them in a 96-well filtration plate (2×10^5 cells/well) according to the procedures in Subheading 3.7.
2. Prepare Tracer Solution by diluting 6×His-NanoLuc-LIF into Binding Solution (serum-free RPMI1640 plus 1% BSA) to a final concentration of 160 pM.
3. Prepare the Competition Solution by serial dilution of mature LIF to following concentrations using Binding Solution: 40 nM, 4 nM, 400 pM, 40 pM, 4 pM, and 0 pM (Binding Solution only) according to procedures in Subheading 3.5.
4. For competition receptor-binding assay, add 25 μL/well of Tracer Solution and 25 μL/well of 40 nM Competition Solution to the first three wells and mix gently. Add 25 μL/well of Tracer Solution and 25 μL/well of 4 nM Competition Solution to the second three wells (*see* **Note 83**) and mix gently. So on until the last tube with zero competitor concentration.
5. After incubation at 21–22 °C for 1 h, wash the cells and measure bioluminescence according to procedures in Subheading 3.7.
6. Process the measured competition receptor-binding data as described in Subheading 3.5.

4 Notes

1. pH of the resultant solution will be 7.5 and don't need adjustment at most cases. The actual pH can be confirmed using a pH meter.
2. BSA is an essential carrier protein for dilution of NanoLuc or NanoLuc-based tracers, especially at low concentration range.
3. High concentration (milimolar range) of INSL3 is necessary for efficient reaction with modification reagent SPDP because it is a bimolecular reaction.
4. The N-hydroxysuccinimide (NHS) ester group in SPDP will be hydrolyzed quickly in aqueous solution, thus we dissolve it in nonaqueous solvent and store at low temperature.
5. The optimal pH for reaction of an NHS ester moiety with a primary amine moiety is 7–8. Don't use salt containing primary amine moiety, such as Tris or urea, in the buffer for NHS ester modification. Guanidine chloride will improve solubility of INSL3 in the modification reaction. If the protein or peptide has high solubility, guanidine chloride is not necessary.
6. Insure concentration of the SPDP-modified INSL3 is sufficiently high, at least 0.1 mM, for efficient conjugation with 6×His-Cys-NanoLuc.

7. The extinction coefficient of the SPDP-modified INSL3 is the sum of that of INSL3 (8480 M^{-1} cm^{-1}) and that of SPDP moiety (3780 M^{-1} cm^{-1} measured using SPDP).
8. EDTA can prevent oxidation of the exposed Cys of 6×His-Cys-NanoLuc by chelating metal ions that are catalysts for thiol oxidation. Low concentration of urea can increase protein solubility and also make the conjugation easier by rendering the structure of NanoLuc and INSL3 slightly more flexible. However, don't use high concentration of urea that can cause exposure of the buried Cys in NanoLuc. Urea is not necessary for some conjugation reactions.
9. Use appropriate basic medium for culturing different cells, for examples, DMEM medium for HEK293T cells and RPMI1640 medium for murine leukemia M1 cells.
10. BSA is an essential carrier protein for dilution of protein or peptide samples, especially at low concentration range. Prepare the Binding Solution using different basic media for different cells since living cells are used in our binding assays.
11. The unique exposed cysteine residue can also be introduced to the C-terminus of NanoLuc without disturbance to enzymatic activity and overexpression in *E. coli*. In a recent work, we designed a 6×His-NanoLuc-Cys, that carries a C-terminal cysteine through a long flexible hydrophilic arm, for chemical conjugation [19]. 6×His-NanoLuc-Cys is better than 6×His-Cys-NanoLuc for conjugation with protein or peptide hormones because it has a long flexible hydrophilic arm between NanoLuc and the exposed Cys.
12. Other *E. coli* strains derived from BL21(DE3), such as BL21(DE3)star and RosettaBlue(DE3), can also be used to overexpress NanoLuc.
13. Alternatively, spread 50–100 μL of the transformed cells on a solid LB plate containing 100 μg/mL of Amp, put the plate into a 37 °C incubator overnight. Next day, pickup several colonies into 50 mL liquid LB medium, add 100 μL of Amp stock solution, and cultured in a 37 °C shaker overnight with vigorous shaking (250 rpm).
14. Typically, 50–100 mg of purified NanoLuc can be obtained from 1 L of *E. coli* culture broth.
15. Low temperature (25–20 °C) is essential for soluble overexpression of NanoLuc in *E. coli*. If induced at 37 °C, NanoLuc will form inclusion bodies.
16. High concentration of salt can reduce nonspecific binding to Ni^{2+} column that is used for purification of the overexpressed NanoLuc.
17. Load appropriate amount of the supernatant to the Ni^{2+} column according to its capacity. Don't overload.

18. The NanoLuc fraction can be confirmed by SDS-PAGE, the band of 6×His-Cys-NanoLuc is around 20 kDa. It can also be confirmed by bioluminescence measurement after appropriate dilution.
19. In order to decrease the salt concentration for further purification by ion-exchange chromatography.
20. The unique exposed Cys in 6×His-Cys-NanoLuc might be blocked by small thiol-containing molecules, such as cysteine or reduced glutathionine (GSH), or by dimmerization of the enzyme. DTT treatment can remove these possible blockages from the unique exposed Cys residue.
21. Load an appropriate amount of NanoLuc to the ion-exchange column according to capacity of the column. Other anion ion-exchange columns can also be used for NanoLuc purification.
22. After two-step purification, a single protein band with an apparent molecular weight of ~20 kDa will appear on reducing SDS-PAGE. On nonreducing SDS-PAGE, a minor band with molecular weight of 40 kDa will also appear due to disulfide crosslinking of 6×His-Cys-NanoLuc during sample preparation and electrophoresis.
23. Concentration of the purified NanoLuc can also be determined by other total protein quantification methods, such as Lowry method and Bradford method.
24. The measured bioluminescence data on different plate readers may be quite different because arbitrary units are used for luminescence.
25. The ideal measured bioluminescence range is 10^3–10^6 counts/well at a SpectraMax M5 plate reader using a white opaque 96-well plate. The measured specific activity of NanoLuc is 1.5×10^5 counts/fmol, thus the suitable enzyme range for bioluminescence measurement is 0.01–10 fmol/well (0.2–200 pg/well). Appropriately dilute the enzyme according to its concentration measured by BCA or other methods.
26. White opaque 96-well plate is necessary for bioluminescence measurement. Black plate will absorb bioluminescence and thus decrease detection sensitivity; clear (transparent) plate will cause interference from wells to wells.
27. The measured bioluminescence will be slightly affected by components of the assay system. We use Lysis Buffer in the present assay because it is necessary for lysis of cells in later assays. The Lysis Buffer contains reducing reagents, likely GSH or DTT. Use the Lysis Buffer with room temperature because temperate affects NanoLuc activity.
28. Total volume of the bioluminescence assay is 100 μL/well. Promega suggested 2 μL substrate stock solution for each well,

but we found that 1 μL/well of substrate stock solution is enough at most cases. Use freshly diluted substrate. Use PBS solution with room temperature because temperate affects NanoLuc activity.

29. To obtain reliable data, read the plate 3–4 times within 5 min on the plate reader and use the data with the best reproducibility.
30. The easily labeled INSL3 has a single primary amine moiety at the A-chain N-terminus, thus various functional groups can be conveniently introduced to it's A-chain N-terminus by reaction with a reagent carrying a primary amine-specific moiety, such as an NHS ester.
31. Other bifunctional reagents, such as LC-SPDP, PEG4-SPDP, and PEG12-SPDP (Thermo Scientific, Waltham, MA, USA), containing a pyridyldithiol moiety and an NHS ester moiety can also be used for this experiment.
32. The disulfide linkage between NanoLuc and INSL3 can be broken by reducing reagents, such as DTT or β-mercaptoethanol.
33. To insure complete modification of INSL3, the molar ratio of SPDP to INSL3 is 10:1 in the modification reaction.
34. The un-reacted SPDP, its hydrolyzed product and some impurities all have absorbance at 280 nm, thus several peaks will be eluted from the column.
35. Insure concentration of the purified 6×His-Cys-NanoLuc is sufficiently high, at least 0.1 mM. If its concentration is not high enough, concentrate it using an ultrafiltration tube (cutoff molecular weigh of 3 kDa).
36. For different proteins or peptides, their molar ratio to NanoLuc can be appropriately adjusted to reach the highest conjugation efficiency.
37. NanoLuc carries net negative charges at pH 8.3 while INSL3 carries net positive changes at pH 8.3, thus the conjugate can be analyzed by native PAGE. It can also be analyzed by nonreducing SDS-PAGE.
38. Occasionally, conjugation of a protein or peptide might affect enzymatic activity of NanoLuc. To test this effect, measure the NanoLuc activity with or without DTT treatment. Take two aliquots of the conjugate, add 1/20-volume of 1 M DTT stock solution to one aliquot; add 1/20-volume of water to the other aliquot. After incubation at room temperature for 30 min, appropriately dilute them with Dilution Buffer and measure their bioluminescence using PBS instead of Lysis Buffer (Promega) because Lysis Buffer contains reducing reagents. If DTT treatment increased bioluminescence, the conjugated protein or peptide has detrimental effect on NanoLuc activity;

otherwise, the conjugated protein or peptide has no effects on NanoLuc activity. If the conjugated protein or peptide has detrimental effect, the conjugate can be quantified by bioluminescence measurement after DTT treatment using the standard protocol in Subheading 3.2.

39. From saturation binding assays, the dissociation constant (K_d), reflecting the binding affinity of INSL3-Luc with receptor RXFP2, can be calculated from the saturation binding curve. The maximal binding capacity (B_{max}), reflecting the active receptor number on cell membrane, can also be calculated from the saturation binding curve.
40. Cells from a 35-mm dish are enough for seeding 30–40 wells of a 96-well plate. Transfect enough HEK293T cells for binding assays.
41. A lot of commercially available transfection reagents can be used for this experiment, such as Lipofectamine 2000 (Invitrogen, Carlsbad, CA, USA). Insure the transfection efficiency over 80 %.
42. Don't over-digest the cells. The 0.25 % trypsin solution can be appropriately diluted by PBS solution if necessary.
43. Insure the cells grow to 100 % confluence in the 96-well plate before binding assay, otherwise HEK293T cells are prone to be washed away.
44. The range of tracer concentration used for saturation binding assays is typically from 10 K_d to 0.1 K_d, where K_d. is the dissociation constant of the tracer with its receptor.
45. Don't remove medium from all wells at one time, cells will dehydrate and die if exposed to the air for a long time.
46. The final INSL3-Luc concentrations in the saturation binding assays are 20 nM, 10 nM, 5 nM, 2.5 nM, 1.25 nM, 0.625 nM, 0.3125 nM and 0 nM, respectively, due to mixing with equal volume of Binding Solution or Competition Solution.
47. Large excess (~100-fold) of competitor (INSL3 in this assay) can occupy almost all of the specific binding sites, thus the measured tracer binding (INSL3-Luc in this assay) under this condition is due to nonspecific binding.
48. Low temperature can prevent internalization of the cell membrane receptors, but it also slows down the ligand binding process. For INSL3/RXFP2, incubation at 21–22 °C for 1–2 h is enough to reach binding equilibrium.
49. Cold solution will slow down the dissociation of the bound tracer from the cells. Wash cells as quickly as possible to diminish dissociation of the bound tracer.
50. If the conjugated protein or peptide disturbs NanoLuc activity, lyse the cells with Lysis Buffer plus 20 mM DTT to insure

breakage of the disulfide linkage between NanoLuc and the conjugated protein or peptide.

51. The measure bioluminescence data of the wells with zero tracer concentration will be very low, typically hundreds, because no tracer was added.
52. From the fitted linear curve, nonspecific binding value at a given tracer concentration can be easily calculated.
53. Software, such as SigmaPlot and Prism, can be used to process these data.
54. Use the average bioluminescence of the triplicate wells as "specific binding bioluminescence." The "binding assay volume" means the solution volume for each well in unit of mL. The "tracer specific activity" means bioluminescence per fmol of tracer measured on same plate reader using same assay system.
55. Convert the unit of the total tracer concentrations from nM to pM for calculation of the bound/free value.
56. Bound/free is a unit-less value so same unit should be used for the bound tracer and the free tracer.
57. For one-site binding model, the Scatchard plot is a linear curve whose intersection with X-axis is the $B_{\max}$ in unit of pM and whose slope is the K_d in unit of pM.
58. From competition assays, IC_{50} values, reflecting relative receptor binding potencies of various INSL3 analogues, can be calculated from the competition binding curves.
59. The working concentration of INSL-Luc in the competition assays is 1.0 nM due to mixing with equal volume of Competitor Solution. Use appropriate tracer concentration in competition assays to obtain large enough specific binding.
60. Other competitor concentration pattern can also be used provided it covers enough range and contains enough concentration points. Use appropriate competitor concentration range to obtain a complete sigmoidal curve.
61. The concentration of INSL3 or its analogues can be quantified by UV absorbance at 280 nm using the extinction coefficient calculated as $\varepsilon_{280\text{nm}}$ $(M^{-1}cm^{-1}) = 5500 \times$ number of Trp $+ 1490 \times$ number of Tyr $+ 125 \times$ number of disulfide. Dissolve sample in 1.0 mM aqueous HCl solution (pH 3.0) and measure its UV absorbance at a photometer directly or after appropriate dilution.
62. The working competitor concentrations are 1000 nM, 100 nM, 10 nM, 1 nM, 0.1 nM and 0.01 nM, respectively, due to mixing with equal volume of the Tracer Solution.
63. The measured bioluminescence at presence of 1.0 μM wild-type INSL3 is though as nonspecific binding.

64. The calibrated bioluminescence at absence of competitor is the largest specific binding. As increase of the competitor concentrations, the specific binding will be decreased in a sigmoidal manner when logarithmic scale of competitor concentrations (*X*-axis) are used in the plot.
65. IC_{50} values can be calculated from *log*IC_{50} values. IC50 reflects relative receptor-binding potencies of different ligands.
66. Some other protein or peptide hormones can also be chemically conjugated with an engineered NanoLuc carrying a unique exposed cysteine residue at either the N-terminus or the C-terminus. To diminish disturbance of NanoLuc, the conjugation site on protein or peptide should be carefully selected and the receptor-binding affinity of the conjugate should be experimentally tested.
67. Some other protein or peptide hormones can also be fused to NanoLuc through recombinant DNA technology, at either the C-terminus or the N-terminus of NanoLuc. The receptor-binding affinity of the NanoLuc-fused proteins should be experimentally tested because NanoLuc fusion might disturb their correct folding and receptor-binding.
68. In our recent work, we successfully prepared a bioluminescent erythropoietin (Epo) tracer by secretory overexpression of a C-terminally NanoLuc-fused human Epo in the transiently transfected HEK293T cells. The signal peptide of Epo precursor can efficiently mediate secretion of the monomeric glycosylated Epo-Luc fusion protein from transfected HEK293T cells. Epo-Luc retained high binding affinity with Epo receptor (forthcoming).
69. The LIF expression construct pNLuc/LIF was generated by ligation of a synthetic codon-optimized DNA fragment encoding mature human LIF into an *E. coli* expression vector pNLuc that carries coding sequence of 6×His-NanoLuc-tag upstream of the multiple cloning site. Other genes can also be ligated into this vector for overexpression of N-terminally 6×His-NanoLuc-tagged proteins in *E. coli*.
70. This *E. coli* strain favors formation of disulfide bonds in cytosol due to genetic modifications, but it has a lower growth rate compared with other expression strains, such as BL21(DE3). We found that soluble 6×His-NanoLuc-LIF could also be efficiently overexpressed in *E. coli* strain BL21(DE3).
71. Load appropriate sample volume according the user's manual of the column. For the column used in the present work, the loading volume is 1.0 mL or less. Other gel filtration columns can also be used for separation of the aggregated and monomeric 6×His-NanoLuc-LIF.

72. The elution buffer is compatible with later enterokinase digestion, thus the eluted monomeric 6×His-NanoLuc-LIF fraction will be subjected to enterokinase digestion without buffer change.
73. LIF has six cysteine residues that form three intramolecular disulfide bonds in the correctly folded molecules. A fraction of 6×His-NanoLuc-LIF doesn't form correct intramolecular disulfide bonds and thus forms oligomers through intermolecular disulfide crosslinking. Nonreducing SDS-PAGE is suitable for analysis of monomeric or oligomeric states of 6×His-NanoLuc-LIF.
74. Ca^{2+} is necessary for high activity of enterokinase. Urea can improve mature LIF solubility and thus prevent its aggregation after digestion.
75. Analyze an aliquot of the digestion mixture by nonreducing SDS-PAGE to determine the digestion efficiency.
76. Mature LIF carries net positive charges, so it doesn't bind the positively charged DEAE resin and thus flows through the column. The cleaved 6×His-NanoLuc-tag as well as a small fraction of un-digested 6×His-NanoLuc-LIF carries net negative charges and thus binds the positively charged DEAE resin.
77. The measured specific activity of 6×His-NanoLuc-LIF is $\sim 1.5 \times 10^5$ counts/fmol when measured on a SpectraMax M5 plate reader using a white opaque 96-well plate. Thus, the fused LIF has no detrimental effects on the NanoLuc activity.
78. M1 cells express endogenous heterodimeric LIFR/gp130 receptor.
79. Solution cannot flow through the filter membrane without vacuum or centrifugation.
80. The actual tracer concentrations in the saturation binding assay are 640 pM, 320 pM, 160 pM, 80 pM, 40 pM, 20 pM, 10 pM, 5 pM and 0 pM, respectively, due to mixing with 2 volumes of cell suspension and 1 volume of Binding Solution or Competition Solution.
81. The filtration approach for receptor-binding assays can also be applied to adherent cells that need to be detached by EDTA solution just before binding assays. Trypsin digestion is not good for binding assays because it maybe digest the cell membrane receptors.
82. Direct lysis of the cells in the filtration plate is not good because the filter membrane can absorb NanoLuc protein.
83. The actual tracer concentration in the competition binding assay is 40 pM, and the actual competitor concentrations are 10 nM, 1 nM, 100 pM, 10 pM, 1 pM, and 0 pM, respectively, due to mixing of 2 volumes of cells suspension, 1 volume of Tracer Solution and 1 volume of Competitor Solution.

Acknowledgments

We thank Promega Corporation for providing the plasmids encoding NanoLuc. This work was supported by the National Natural Science Foundation of China (31470767, 31270824) and the Fundamental Research Funds for the Central Universities (2000219098).

References

1. Frank LA, Krasitskaya VV (2014) Application of enzyme bioluminescence for medical diagnostics. Adv Biochem Eng Biotechnol 144:175–197
2. Badr CE (2014) Bioluminescence imaging: basics and practical limitations. Methods Mol Biol 1098:1–18
3. Scott D, Dikici E, Ensor M, Daunert S (2011) Bioluminescence and its impact on bioanalysis. Annu Rev Anal Chem (Palo Alto, Calif) 4:297–319
4. Hall MP, Unch J, Binkowski BF, Valley MP, Butler BL, Wood MG, Otto P, Zimmerman K, Vidugiris G, Machleidt T, Robers MB, Benink HA, Eggers CT, Slater MR, Meisenheimer PL, Klaubert DH, Fan F, Encell LP, Wood KV (2012) Engineered luciferase reporter from a deep sea shrimp utilizing a novel imidazopyrazinone substrate. ACS Chem Biol 7:1848–1857
5. Bylund DB, Toews ML (2011) Radioligand binding methods for membrane preparations and intact cells. Methods Mol Biol 746: 135–164
6. Hulme EC, Trevethick MA (2010) Ligand binding assays at equilibrium: validation and interpretation. Br J Pharmacol 161:1219–1237
7. Sykes DA, Dowling MR, Charlton SJ (2010) Measuring receptor target coverage: a radioligand competition binding protocol for assessing the association and dissociation rates of unlabeled compounds. Curr Protoc Pharmacol, Chapter 9: Unit 9.14
8. McKinney M, Raddatz R (2006) Practical aspects of radioligand binding. Curr Protoc Pharmacol, Chapter 1: Unit 1.3
9. de Jong LA, Uges DR, Franke JP, Bischoff R (2005) Receptor-ligand binding assays: technologies and applications. J Chromatogr B Analyt Technol Biomed Life Sci 829:1–25
10. Thibault G, Schiffrin E (2001) Radioligand binding assay. Methods Mol Med 51:305–314
11. Handl HL, Gillies RJ (2005) Lanthanide-based luminescent assays for ligand-receptor interactions. Life Sci 77:361–371
12. Selvin PR (2002) Principles and biophysical applications of lanthanide-based probes. Annu Rev Biophys Biomol Struct 31:275–302
13. Zhang WJ, Jiang Q, Wang XY, Song G, Shao XX, Guo ZY (2013) A convenient method for europium-labeling of a recombinant chimeric relaxin family peptide R3/I5 for receptor-binding assays. J Pept Sci 19:350–354
14. Zhang WJ, Gao XJ, Liu YL, Shao XX, Guo ZY (2012) Design, recombinant preparation and europium-labeling of a fully active easily-labeled INSL3 analogue for receptor-binding assays. Process Biochem 47:1856–1860
15. Zhang WJ, Luo X, Song G, Wang XY, Shao XX, Guo ZY (2012) Design, recombinant expression and convenient A-chain N-terminal europium-labelling of a fully active human relaxin-3 analogue. FEBS J 279:1505–1512
16. Zhang WJ, Luo X, Liu YL, Shao XX, Wade JD, Bathgate RA, Guo ZY (2012) Site-specific DOTA/europium-labeling of recombinant human relaxin-3 for receptor-ligand interaction studies. Amino Acids 43:983–992
17. Zhang L, Song G, Xu T, Wu QP, Shao XX, Liu YL, Xu ZG, Guo ZY (2013) A novel ultrasensitive bioluminescent receptor-binding assay of INSL3 through chemical conjugation with Nanoluciferase. Biochimie 95: 2454–2459
18. He SX, Song G, Shi JP, Guo YQ, Guo ZY (2014) Nanoluciferase as a novel quantitative protein fusion tag: application for overexpression and bioluminescent receptor-binding assays of human leukemia inhibitory factor. Biochimie 106:140–148
19. Liu Y, Shao XX, Zhang L, Song G, Liu YL, Xu ZG, Guo ZY (2015) Novel bioluminescent receptor-binding assays for peptide hormones: using ghrelin as a model. Amino Acids 47:2237–2243
20. Maguire JJ, Kuc RE, Davenport AP (2012) Radioligand binding assays and their analysis. Methods Mol Biol 897:31–77

Chapter 7

Bioluminogenic Imaging of Aminopeptidase N In Vitro and In Vivo

Wenxiao Wu, Laizhong Chen, Jing Li, Lupei Du, and Minyong Li

Abstract

Bioluminescence is a process that converts biochemical energy to visible light. Bioluminescence-based imaging technology has been widely applicable in the imaging of process envisioned in life sciences. As one of the most popular bioluminescence system, the firefly luciferin–luciferase system is exceptionally suitable for deep tissue imaging in living animals owing to its long wavelength emission light. Herein, we report the experimental detail of bioluminogenic imaging of aminopeptidase N activity both in vitro and in vivo.

Key words Aminopeptidase N, Bioluminescence, Caged luciferin, Living animal imaging

1 Introduction

Aminopeptidase N (APN/CD13) is a peptidase that plays important roles in both physiological and pathological progresses by hydrolyzing biological active substances and serves as a good target for anticancer drugs [1–8]. So far, many fluorogenic and colorimetric probes have been established for the detection of APN activity [9–11]. For instance, L-Leu-pNA and L-Leu-AMC are the commercially available substrates for in vitro APN activity assay [9, 12]. Our group reported a fluorescent probe, L-Ala-PABA-7HC, that demonstrated excellent applications in high-throughput screening of APN inhibitors on the basis of its high sensitivity and ratiometric property. However, none of the reported probes can be used for an in vivo activity assay since their short wavelength emission lights have poor tissue penetration capability.

Bioluminescent imaging (BLI) does not need excitation lights and usually emits long wavelength lights, thus is suitable for deep tissue imaging [13–15]. Herein, we report the detailed protocol of bioluminogenic imaging of aminopeptidase N activity both in vitro and in vivo by using several luciferin-based probes. All of these probes could be well recognized and hydrolyzed by APN [16].

Sung-Bae Kim (ed.), *Bioluminescence: Methods and Protocols*, Methods in Molecular Biology, vol. 1461,
DOI 10.1007/978-1-4939-3813-1_7, © Springer Science+Business Media New York 2016

More importantly, these probes could be activated by APN to generate bioluminescence in the presence of firefly luciferase in vitro and in vivo.

2 Materials

Milli-Q water and analytical grade reagents were used to prepare all aqueous solutions. The bioluminescence imaging was measured with an IVIS Kinetic imaging system which is equipped with a cooled charge coupled device (CCD) camera. The pseudocolored bioluminescent images (in photons/s/cm^2/scr) were superimposed over the gray scale photographs of the animals. Circular region of interests (ROIs) were drawn over the areas and quantified using Living Image software. The results were reported as total photon flux within an ROI in photons per sec.

1. Resolving 50 mM Tris–HCl buffer, pH 7.4: Weigh 0.6 g Tris, 1.3 mg $ZnCl_2$ and 95.2 mg $MgCl_2$ then transfer to the cylinder. Add water into the cylinder until the solid was dissolved. Mix and adjust pH with 0.1 M HCl to 7.4. Dilute to 100 mL with water. Store at 4 °C.
2. Resolving a 0.01 M phosphate buffer (PBS), pH 7.4: Weigh 7.9 g NaCl, 0.2 g KCl, 0.24 g KH_2PO_4 and 1.8 g K_2HPO_4 then transfer to the cylinder. Add water to a volume of 800 mL. Mix and adjust pH with 0.1 M HCl. Make up to 1 L with water. Store at 4 °C.
3. Stock solution of 2.85 mM APN probe **1**: Weigh 1.0 mg probe **1** into 1.5 mL Eppendorf tube. Add 1 mL Tris–HCl buffer. Store at 4 °C.
4. Stock solution of 3.36 mM APN probe **2**: Weigh 1.3 mg probe **2** into 1.5 mL Eppendorf tube. Add 1 mL Tris–HCl buffer. Store at 4 °C.
5. Stock solution of 2.60 mM APN probe **3**: Weigh 1.5 mg probe **3** into 1.5 mL Eppendorf tube. Add 1 mL Tris–HCl buffer. Store at 4 °C.
6. 0.005 IU/mL APN: 0.2 IU APN was dissolved by 390 μL Tris–HCl buffer.
7. 200 μg/mL luciferase containing 4 mM ATP: Weigh 2.2 mg adenosine 5′-triphosphate disodium salt (ATP disodium salt) into 1.5 mL Eppendorf tube. Add 1 mL Tris–HCl buffer. 0.1 mg luciferase was dissolved by 500 μL of 4 mM ATP in 1.5 mL Eppendorf tube (*see* **Note 1**).
8. 1.5 mg/mL Bestatin: Weigh 1.5 mg Bestatin into 1.5 mL Eppendorf tube, and add 1 mL Tris–HCl buffer.
9. 20 μM APN probe **1**: 17.5 μL of APN probe **1** stock solution was diluted to 2.5 mL using Tris–HCl buffer.

10. 20 μM APN probe **2**: 16 μL of APN probe **2** stock solution was diluted to 2.5 mL using Tris–HCl buffer.
11. 20 μM APN probe **3**: 14.8 μL of APN probe **3** stock solution was diluted to 2.5 mL using Tris–HCl buffer.
12. 1.0 mg/mL Bestatin: Weigh 2 mg Bestatin into 2 mL Eppendorf tube. Add 2 mL Tris–HCl buffer.
13. 12.5–400 μM APN probes **1**: 400 μM: 140 μL stock solution APN probe **1** were diluted to 1 mL using Tris–HCl buffer. 200 μM: 500 μL of 400 μM APN probe **1** were diluted to 1 mL using Tris–HCl buffer. 100 μM: 500 μL of 200 μM APN probe **1** were diluted to 1 mL using Tris–HCl buffer. 50 μM: 500 μL of 100 μM APN probe **1** were diluted to 1 mL using Tris–HCl buffer. 25 μM: 500 μL of 50 μM APN probe **1** were diluted to 1 mL using Tris–HCl buffer. 12.5 μM: 500 μL of 25 μM APN probe **1** were diluted to 1 mL using Tris–HCl buffer.
14. 12.5–400 μM APN probes **2**: 400 μM: 119 μL stock solution APN probe **2** was diluted to 1 mL using Tris–HCl buffer. Others as APN probe **1**.
15. 12.5–400 μM APN probes **3**: 400 μM: 153 μL stock solution APN probe **3** was diluted to 1 mL using Tris–HCl buffer. Others as APN probe **1**.
16. 2.5 mg/mL APN probe **1** or **2**: Weight 2.5 mg probe **1** or **2** into 1.5 mL Eppendorf tube. Add 1 mL normal saline.
17. 10 mg/mL Bestatin: Weight 5 mg Bestatin into 1.5 mL Eppendorf tube. Add 0.25 mL dimethyl sulfoxide and 0.25 mL normal saline (*see* **Note 2**).
18. Firefly luciferase (Promega), (*see* **Note 3**) store at −80 °C.
19. ATP (Aladdin), store at −20 °C.
20. APN (Merck), (*see* **Note 4**) store at −80 °C.
21. ES-2-FLuc cells (the Committee on Type Culture Collection of Chinese Academy of Sciences) expressing firefly luciferase (FLuc) (*see* **Note 5**).
22. Balb/c-nu male mice (Animal Center of China Academy of Medical Sciences, Beijing, China), 8 weeks of age (*see* **Note6**).

3 Methods

Carry out all procedures at room temperature unless otherwise specified.

3.1 In Vitro Bioluminescence Measurement

1. 50 μL bestatin (1.5 mg/mL) and 10 μL APN (0.005 IU/mL) were added into 96-well white-plates, incubated at 37 °C for 15 min; as a blank control, Tris buffer was added instead of APN solution under the same condition.

2. 90 μL of APN probes **1–3** (20 μM) was added in the wells, respectively, incubated at 37 °C for 1 h.
3. 50 μL of luciferase (200 μg/mL) containing 4 mM ATP was added in the wells equally, then the bioluminescence intensity was measured for 10 s integration time at 27 °C (*see* **Note 7**).
4. Relative total photon flux was calculated by dividing the total photon flux of the experimental condition by the total photon flux of the blank control (*see* Fig. 1).

3.2 Cell Bioluminescence Imaging

1. The ES-2-FLuc cells in logarithmic phase (*see* **Note 8**) and centrifugation were diluted into RPMI 1640 supplemented with 10% FBS for a cells-suspension (2 × 10^5/mL) (*see* **Note 9**).
2. 200 μL cells suspension was added into black clear flat bottom 96-well plates. As a blank control, the RPMI 1640 supplemented with 10% FBS was instead of the cells-suspension. The cells in the black 96-well plates were cultured at 37 °C in a humidified atmosphere in a 5% CO_2 incubator for 24 h (*see* **Note 10**).
3. Medium removed, the 96-well plates were washed once by 1 × PBS. The cells were incubated with or without 100 μL bestatin (1.0 mg/mL), incubating for 0.5 h in the incubator.

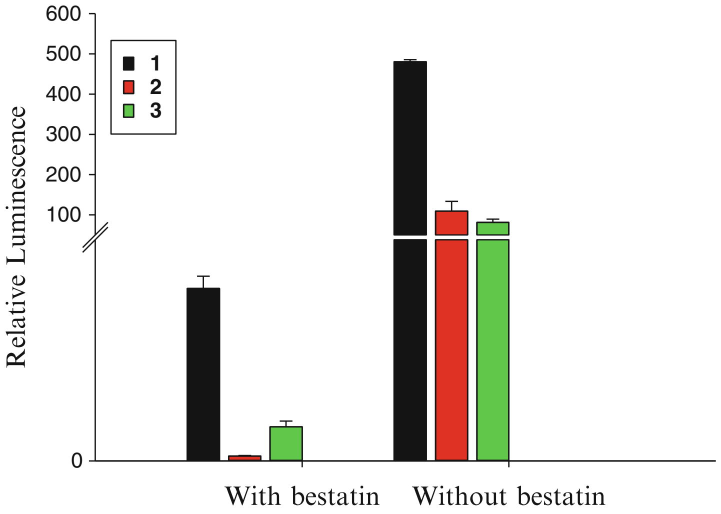

Fig. 1 Relative bioluminescence for probes **1–3** with or without bestatin. APN (0.005 IU/mL, 10 μL) incubated with bestatin (1.5 mg/mL, 50 μL) or without bestatin for 0.5 h, followed by probes **1–3** (20 μM, 90 μL) addition, then luciferase (100 μg/mL, 50 μL) in 50 mM Tris buffer with 10 mM $MgCl_2$, 0.1 mM $ZnCl_2$, and 2 mM ATP (pH 7.4) was added. The bioluminescent signal was measured immediately. Error bars are SD for three measurements. (Reproduced in part from Li et al. with permission from Anal. Chem. (ACS) [16])

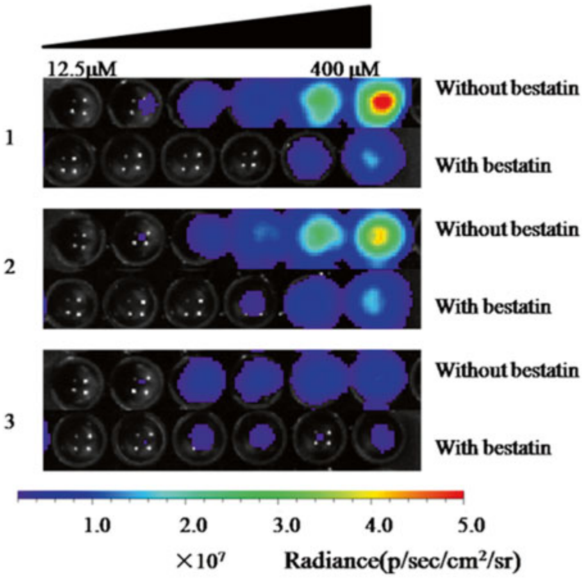

Fig. 2 ES-2-FLuc cells bioluminescent imaging incubated with various concentrations probes **1**–**3** (12.5–400 μM, 100 μL) without or with bestatin (1.0 mg/mL, 100 μL). (Reproduced in part from Li et al. with permission from Anal. Chem. (ACS) [16])

4. 100 μL different concentration of APN probes **1**, **2,** and **3** (12.5–400 μM) were added to each well and the luciferase activity was measured 20 min later using a Xenogen IVIS Spectrum imaging system (*see* Fig. 2).
5. Luminescent signal (photons/s) for each well was measured and plotted as average values (experiments conducted in triplicate) (*see* Fig. 3).

3.3 In Vivo Bioluminescent Imaging

1. ES-2-FLuc cells (1×10^7) dissolved in normal saline (0.1 mL) were implanted subcutaneously into the right armpit region of each 6-weeks-old female nude mouse (*see* **Note 11**). The tumor was harvested if its size is 1 cm³, and then was cut into pieces (*see* **Note 12**). The mice were disinfected locally before the puncture needle implants 10 mg tumor pieces subcutaneously into the right armpit region (*see* **Note 13**). Two weeks later, the tumor xenograft mice models were formed (*see* **Note 14**).
2. Mice bearing ES-2-FLuc subcutaneous tumors were anesthetized with isoflurane and 25 μL probe **1** or **2** (2.5 mg/mL in NS) was injected into the tumor, which was named intratumor injection (*see* **Note 15**), followed by bioluminescent imaging every 5 min for 30 min. The bioluminescent signal changed with the time (*see* Fig. 4).
3. The mice were intratumorally injected with 0.1 mL bestatin (10 mg/mL) followed 3 h later by an intratumorally injection of

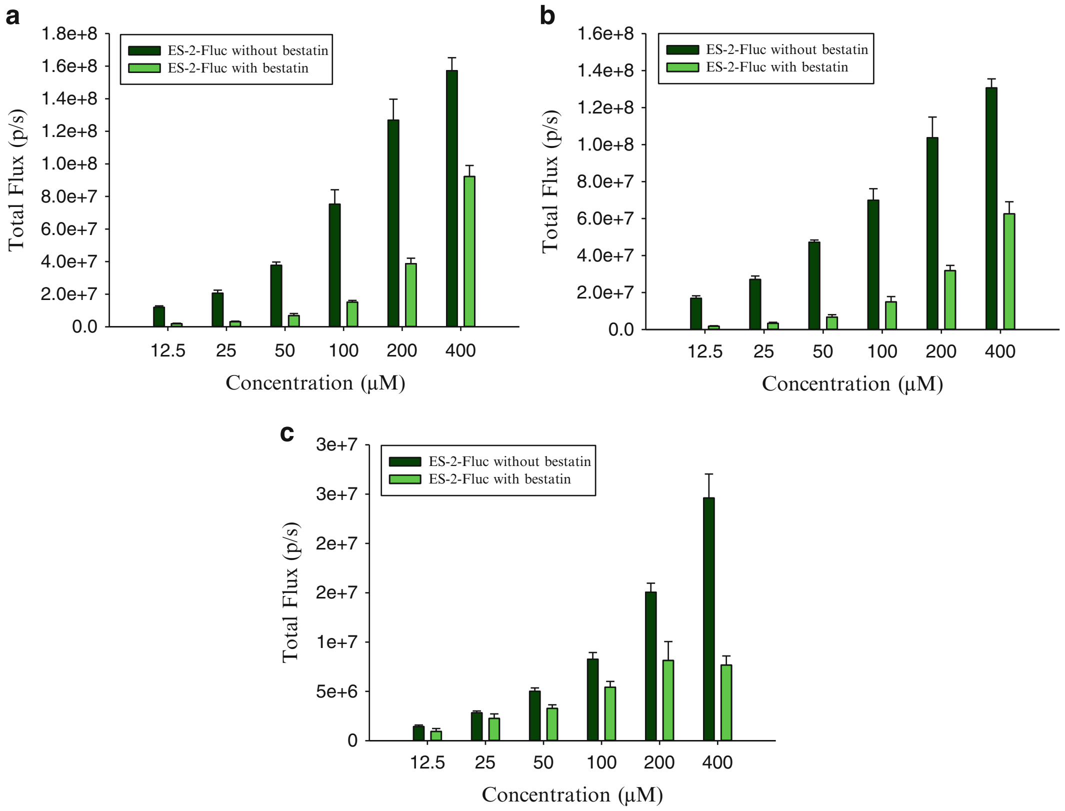

Fig. 3 (**a**) Quantification of bioluminescent signal from various concentrations probe **1** (12.5–400 μM, 100 μL) added to ES-2-FLuc cells without or with bestatin (1.0 mg/mL, 100 μL). (**b**) Quantification of bioluminescent signal from various concentrations probe **2** (12.5–400 μM, 100 μL) added to ES-2-FLuc cells without or with bestatin (1.0 mg/mL, 100 μL). (**c**) Quantification of bioluminescent signal from various concentrations probes **3** (12.5–400 μM, 100 μL) added to ES-2-FLuc cells without or with bestatin (1.0 mg/mL, 100 μL). (Reproduced in part from Li et al. with permission from Anal. Chem. (ACS) [16])

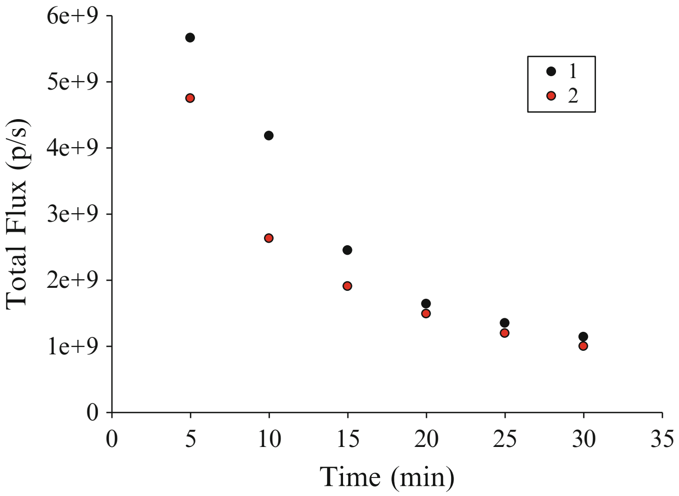

Fig. 4 Total photon output from a nude mouse implanted with ES-2-FLuc xenografts after intraperitoneal injection of probe **1** and **2** (2.5 mg/mL, 25 μL). (Reproduced in part from Li et al. with permission from Anal. Chem. (ACS) [16])

25 μL probe **1** or **2** (2.5 mg/mL). Controls for the bestatin experiment were completed by intratumorally injecting vehicle (0.1 mL) followed by the probe **1** or **2** 3 h later. Light production was measured 25 min after the injection of probes (*see* Fig. 5).

4. The relative total photon flux for each condition was calculated by dividing the total photon flux after the injection of bestatin or vehicle by the total photon flux before the injection of bestatin or vehicle (*see* Fig. 6).

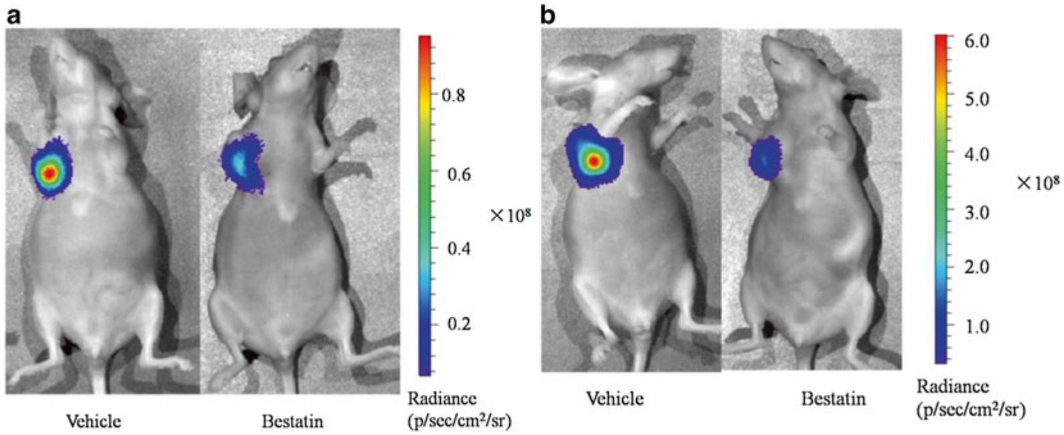

Fig. 5 (**a**) Representative bioluminescent imaging of APN activity in ES-2-FLuc tumor xenograft for probe **1** (2.5 mg/mL, 25 μL) without or with bestatin (10 mg/mL, 0.1 mL). (**b**) Representative bioluminescent imaging of APN activity in ES-2-FLuc tumor xenograft for probe **2** (2.5 mg/mL, 25 μL) without or with bestatin (10 mg/mL, 0.1 mL). (Reproduced in part from Li et al. with permission from Anal. Chem. (ACS) [16])

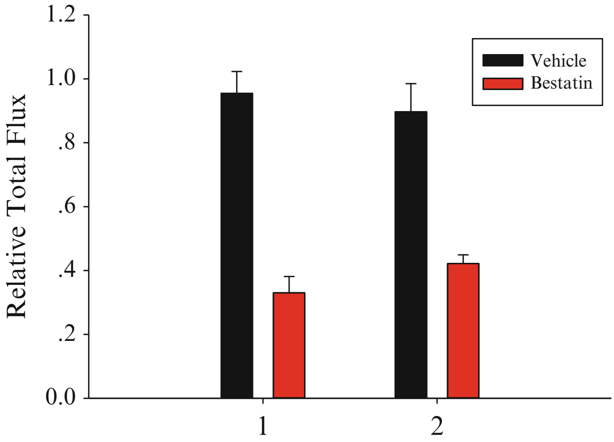

Fig. 6 Relative bioluminescence emission for mice injected with probe **1** (2.5 mg/mL, 25 μL) and **2** (2.5 mg/mL, 25 μL) without or with bestatin (10 mg/mL, 0.1 mL) ($n = 2$). (Reproduced in part from Li et al. with permission from Anal. Chem. (ACS) [16])

4 Notes

1. The luciferase is melt in 4 °C for keeping the activity.
2. Dimethyl sulfoxide is regarded as a co-solvent. If the probe is water soluble, the co-solvent can be not used.
3. In order to avoiding multigelation, 5 mg luciferase was subpackaged into 5 ml Eppendorf tube, 60 μg/tube.
4. In order to avoiding multigelation, 10 IU APN was dissolved into 500 μL Tris–HCl, pH 7.4, then the solution was subpackaged into 1.5 mL Eppendorf tube, 10 μL/tube (0.2 IU).
5. The ES-2-FLuc cells were cultured in RPMI 1640 supplemented with 10% fetal bovine serum (FBS) at 37 °C in a humidified atmosphere in a 5% CO_2 incubator.
6. Mice were group-housed on a 12:12 light–dark cycle at 22 °C with free access to food and water (sterilized distilled water).
7. The temperature during measuring measurement need be kept in 27 °C.
8. The cells need to be used after 3-generation subculture.
9. The attachment ability of ES-2-FLuc cells is very weak, thus 25 cm^2 cell culture dish that be filled with cells only needs 0.7 mL 0.25% trypsin for 30 s.
10. After incubating for 24 h in the incubator, every plate was carpeted with cells.
11. The weight of the mouse is about 19 ± 1 g. Before injection, the cells suspension must be diluted by normal saline; the injection site and tumor site are within a short distance about 1 cm; injection finished, the needle needs to be pulled out slightly.
12. The mucous membranes covering the tumor must be removed, and the necrosis in the tumor must be removed. The pieces are too small to measure the size.
13. The injection site and tumor site are within a short distance of about 1 cm.
14. The ideal diameter of the tumors is about 0.6 cm.
15. The syringe needle must be enough slender, which is minimally invasive to the tumor. When the needle tip reached the center of the tumor, the solution was injected into the tumor slowly, and then the needle was pulled out slowly. In order to avoiding the solution spilling from the tumor, the injection needs to be done carefully.

Acknowledgement

This work was supported by grants from the Program of New Century Excellent Talents in University (No. NCET-11-0306), the Shandong Natural Science Foundation (No. JQ201019), the Program for Changjiang Scholars and Innovative Research Team in University (No. IRT13028), the Major Project of Science and Technology of Shandong Province (No. 2015ZDJS04001), the Shandong Key Research & Development Project (No. 2015GSF118166) and the Independent Innovation Foundation of Shandong University, IIFSDU (No. 2010JQ005 and 2014JC008). The first two authors contributed to this article equally.

References

1. Pasqualini R, Koivunen E, Kain R, Lahdenranta J, Sakamoto M, Stryhn A, Ashmun RA, Shapiro LH, Arap W, Ruoslahti E (2000) Aminopeptidase N is a receptor for tumor-homing peptides and a target for inhibiting angiogenesis. Cancer Res 60:722–727
2. Antczak C, De Meester I, Bauvois B (2001) Transmembrane proteases as disease markers and targets for therapy. J Biol Regul Homeost Agents 15:130–139
3. Mechtersheimer G, Moller P (1990) Expression of aminopeptidase N (CD13) in mesenchymal tumors. Am J Pathol 137:1215–1222
4. Riemann D, Kehlen A, Langner J (1999) CD13–not just a marker in leukemia typing. Immunol Today 20:83–88
5. Nunez L, Amigo L, Mingrone G, Rigotti A, Puglielli L, Raddatz A, Pimentel F, Greco AV, Gonzalez S, Garrido J, Miquel JF, Nervi F (1995) Biliary aminopeptidase-N and the cholesterol crystallisation defect in cholelithiasis. Gut 37:422–426
6. Noble F, Banisadr G, Jardinaud F, Popovici T, Lai-Kuen R, Chen H, Bischoff L, Parsadaniantz SM, Fournie-Zaluski MC, Roques BP (2001) First discrete autoradiographic distribution of aminopeptidase N in various structures of rat brain and spinal cord using the selective iodinated inhibitor [125I]RB 129. Neuroscience 105:479–488
7. Vlahovic P, Stefanovic V (1998) Kidney ectopeptidases. Structure, functions and clinical significance. Pathol Biol (Paris) 46:779–786
8. Kotlo K, Shukla S, Tawar U, Skidgel RA, Danziger RS (2007) Aminopeptidase N reduces basolateral Na+-K+ -ATPase in proximal tubule cells. Am J Physiol Renal Physiol 293:F1047–F1053
9. Zhang Z, Harada H, Tanabe K, Hatta H, Hiraoka M, Nishimoto S (2005) Aminopeptidase N/CD13 targeting fluorescent probes: synthesis and application to tumor cell imaging. Peptides 26:2182–2187
10. Femfert U, Cichocki P (1972) Substrate activation in the hydrolysis of L-alanine-4-nitroanilide catalyzed by aminopeptidase M. FEBS Lett 27:219–220
11. Lejczak B, Kafarski P, Zygmunt J (1989) Inhibition of aminopeptidases by aminophosphonates. Biochemistry 28:3549–3555
12. Poumarat JS, Houillier P, Rismondo C, Roques B, Lazar G, Paillard M, Blanchard A (2002) The luminal membrane of rat thick limb expresses AT1 receptor and aminopeptidase activities. Kidney Int 62:434–445
13. Prescher JA, Contag CH (2010) Guided by the light: visualizing biomolecular processes in living animals with bioluminescence. Curr Opin Chem Biol 14:80–89
14. Keyaerts M, Caveliers V, Lahoutte T (2012) Bioluminescence imaging: looking beyond the light. Trends Mol Med 18:164–172
15. Badr CE, Tannous BA (2011) Bioluminescence imaging: progress and applications. Trends Biotechnol 29:624–633
16. Li J, Chen L, Wu W, Zhang W, Ma Z, Cheng Y, Du L, Li M (2014) Discovery of bioluminogenic probes for aminopeptidase N imaging. Anal Chem 86:2747–2751

Chapter 8

Firefly Luciferase-Based Sequential Bioluminescence Resonance Energy Transfer (BRET)-Fluorescence Resonance Energy Transfer (FRET) Protease Assays

Bruce Branchini

Abstract

We describe here the preparation of ratiometric luminescent probes that contain two well-separated emission peaks produced by a sequential bioluminescence resonance energy transfer (BRET)-fluorescence resonance energy transfer (FRET) process. The probes are single soluble fusion proteins consisting of a thermostable firefly luciferase variant that catalyzes yellow-green (560 nm maximum) bioluminescence and a red fluorescent protein covalently labeled with a near-Infrared fluorescent dye. The two proteins are connected by a decapeptide containing a protease recognition site specific for factor Xa, thrombin, or caspase 3. The rates of protease cleavage of the fusion protein substrates were monitored by recording emission spectra and plotting the change in peak ratios over time. Detection limits of 0.41 nM for caspase 3, 1.0 nM for thrombin, and 58 nM for factor Xa were realized with a scanning fluorometer. This method successfully employs an efficient sequential BRET-FRET energy transfer process based on firefly luciferase bioluminescence to assay physiologically important protease activities and should be generally applicable to the measurement of any endoprotease lacking accessible cysteine residues.

Key words Bioluminescence, BRET, Caspase, Factor Xa, Firefly, FRET, Luciferase, Protease, mKate, Thrombin

Abbreviations

AF680	Alexa Fluor 680 C2-maleimide
BFFP-	BRET-FRET fusion protein, a fusion protein consisting of an N-terminus hexa-His tagged mKate S158A variant joined to PpyWT-TS through the decapeptide linker GSAP4P3P2P1GSG where P4P3P2P1 is DEVD (C3), LVPR (Th), IEGR (Xa), or GSGS (GS)
BFS-	The BRET-FRET substrates corresponding to the BFFP-proteins labeled with AF680
BRET	Bioluminescence resonance energy transfer
FRET	Fluorescence resonance energy transfer
CCD	Charge-coupled device
LC/ESMS	Tandem HPLC-electrospray ionization mass spectrometry

Sung-Bae Kim (ed.), *Bioluminescence: Methods and Protocols*, Methods in Molecular Biology, vol. 1461,
DOI 10.1007/978-1-4939-3813-1_8, © Springer Science+Business Media New York 2016

LH_2	D-firefly luciferin
Luc	*Photinus pyralis* luciferase (E. C. 1.13.12.7)
nIR	Near-infrared
PBSA buffer	20 mM sodium phosphate buffer (pH 7.2) containing 150 mM NaCl, 5 mM EDTA and 0.8 M ammonium sulfate
PpyWT	Recombinant *Photinus pyralis* luciferase containing the additional N-terminal peptide GPLGS
PpyWT-TS	PpyWT containing the mutations T214A, A215L, I232A, F295L, and E354K
RFP	Red fluorescent protein (mKate S158A variant)
SRET	Sequential BRET-FRET.

1 Introduction

A varied group of biological organisms emit light (bioluminescence) that spans the visible spectrum [1, 2]. We describe here a method based on the development of new biomaterials based on the firefly luciferase system from *Photinus pyralis* (Luc), which produces yellow-green light with $\lambda_{max} = 560$ nm from firefly luciferin (LH_2), Mg-ATP, and oxygen [3]. Our method employs a thermostable Luc variant and is a rare example [4–6] of a sequential bioluminescence resonance energy transfer (BRET)—fluorescence resonance energy transfer (FRET) process that does not require nanomaterials. BRET and FRET involve nonradiative energy transfer from a bioluminescent or fluorescent donor to an acceptor. The efficiency of these processes depends on the spectral overlap, relative orientation, and inverse sixth-power of the distance between the donor and acceptor [7]. For BRET, efficiency can be expressed as the ratio of fluorescence acceptor emission to bioluminescence emission [8]. We have developed luminescent reagents for enzyme assays that can be used in a

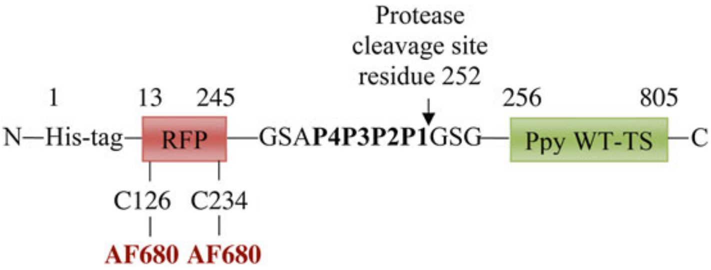

Fig. 1 Schematic representation of the fusion protein substrates. The P4P3P2P1 peptide sequences correspond to: BFS-Xa, IEGR; BFS-C3, DEVD; BFS-Th, LVPR, and BFS-GS, GSGS. The *arrow* indicates the cleavage site for the three proteases. BFS-GS, which does not contain a specific protease site, served as a control for substrate specificity and stability. The *numbers* above the schematic diagram indicate the amino acid sequences of the fusion proteins. Reproduced in part from Branchini et al. with permission from Anal. Biochem. (Elsevier) [5]

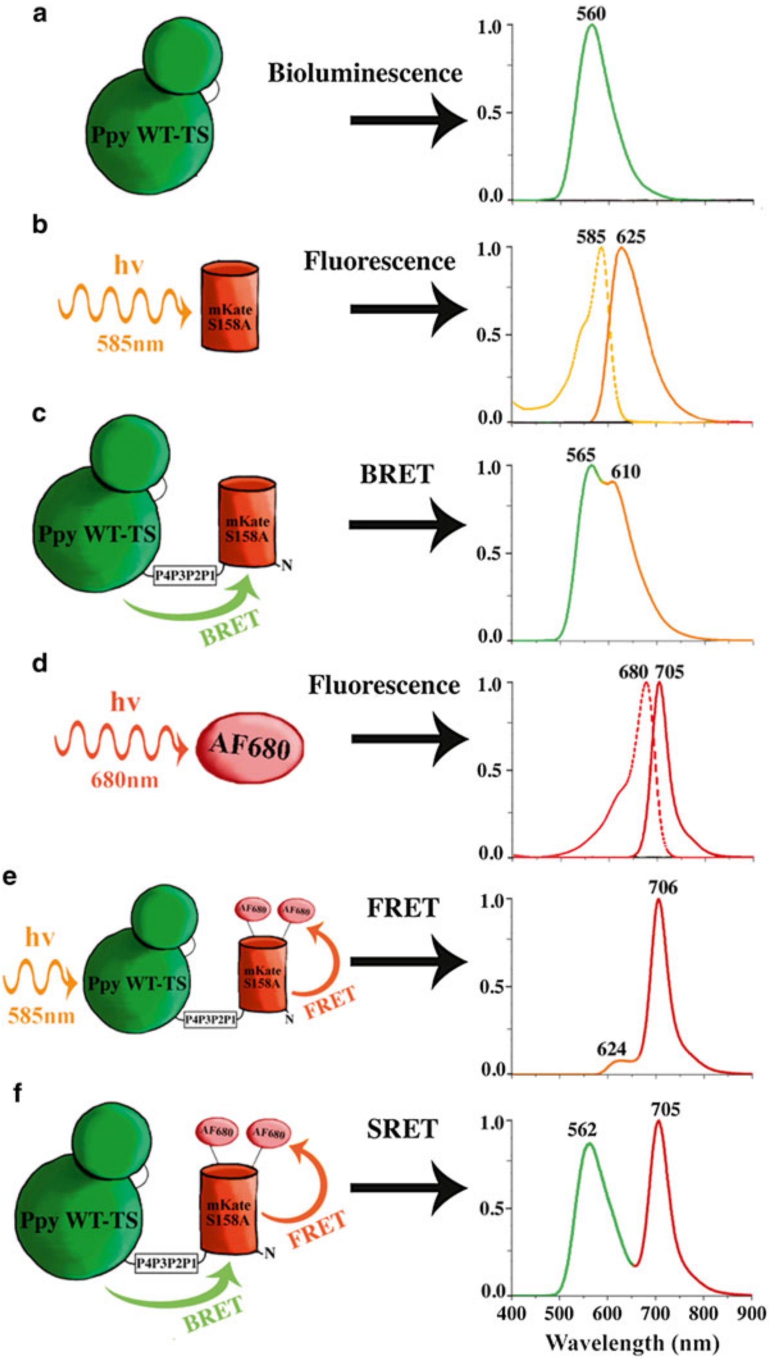

Fig. 2 Normalized absorption, emission, and fluorescence spectra. The following spectra were obtained as described in Methods and demonstrate: (**a**) the bioluminescence of PpyWT-TS following addition of LH_2 and Mg-ATP; (**b**) RFP absorbance and fluorescence (excitation 585 nm); (**c**) BRET produced by unlabeled fusion protein substrate following addition of LH_2 and Mg-ATP; (**d**) AF680 absorbance and fluorescence (excitation 680 nm); (**e**) FRET produced by 585 nm excitation of fusion protein substrate; (**f**) SRET of BFS-Th following addition of LH_2 and Mg-ATP. Reproduced in part from Branchini et al. with permission from Anal. Biochem. (Elsevier) [5]

ratiometric format taking advantage of the high sensitivity and low background of bioluminescence, while avoiding difficulties with the standardization of intensity units. Ratiometric probes require two distinct signals and are self-referencing because the ratio of the two signals is independent of the probe concentration [9, 10]. Our method uses ratiometric luminescent probes for monitoring proteolytic activity that contain two well-separated emission peaks produced by a sequential BRET-FRET process (SRET). The probes are single soluble fusion proteins consisting of a red fluorescent protein (RFP) labeled with the Alexa Fluor dye AF680 and PpyWT-TS [11], a thermostable Luc variant. The two proteins are connected by a decapeptide containing a protease recognition site (*see* Fig. 1). We explored the potential utility of the assay concept with representative serine proteases factor Xa and thrombin involved in blood coagulation and the cysteine protease caspase 3, which plays a key role in apoptosis [12]. We describe a SRET method (*see* Fig. 2) that offers excellent sensitivity and selectivity that is achieved in a ratiometric format.

2 Materials

The following materials used in the method include:

1. Chemicals/buffers—Mg-ATP (bacterial source, Sigma-Aldrich, St. Louis, MO); Alexa Fluor® 680 C2-maleimide (AF680) dye, Invitrogen, Carlsbad, CA; firefly luciferin (LH_2) was a generous gift from Promega, Inc., Madison, WI; PBSA buffer, 20 mM sodium phosphate buffer (pH 7.2) containing 150 mM NaCl, 5 mM EDTA and 0.8 M ammonium sulfate; and assay buffer, 0.50 mL of a 25 mM glycylglycine buffered (pH 7.8) solution of LH_2 (150 μM) and Mg-ATP (2 mM).
2. Molecular biology reagents—pQE-30 expression vector, Qiagen, Valencia, CA; mutagenic oligonucleotides, Integrated DNA technologies, Coralville, IA; pGEX-6P-2 expression vector, GE Healthcare, Piscataway, NJ; QuikChange® Lightning Site-Directed Mutagenesis kit, Stratagene, La Jolla, CA; and the mKate S158A variant gene (GenBank Accession # EU383029) flanked by *Bam*HI and *Xho*I restriction endonuclease sites in the pUC57 vector was synthesized by GenScript USA, Inc, Piscataway, NJ.
3. Proteins—human thrombin and human caspase 3, Sigma-Aldrich, St. Louis, MO; and restriction endonucleases, TPCK-treated trypsin, and factor Xa protease, New England Biolabs, Beverly, MA.
4. Protein purification—the recombinant GST-fusion proteins *P. pyralis* luciferase (PpyWT) and the thermostable variant PpyWT-TS were expressed and purified as previously reported [11] (*see* **Notes 1** and **2**); the mKate S158A variant (RFP) was similarly expressed and purified in yields of 4–5 mg/0.25 L

culture. The fusion proteins BFFP-Xa, BFFP-C3, BFFP-Th, and BFFP-GS were expressed from the plasmids described below and were purified in yields of 3.5–4.5 mg/0.25 L culture as described [13] previously except that biotin was not added to the growth media (*see* **Notes 3** and **4**).

3 Methods

3.1 Cloning of the Fusion Proteins BFFP-Xa, BFFP-C3, BFFP-Th, and BFFP-GS

1. The vector containing the gene encoding the fusion protein BFFP-Xa, consisting of an N-terminus hex-His tagged mKate S158A variant joined to PpyWT-TS through the decapeptide linker GSAIEGRGSG, was constructed as follows. The synthesized mKate S158A variant gene in the pUC57 vector was digested with *Bam*HI and *Xho*I and ligated into the corresponding cloning sites in a modified version [13] of the pQE-30 plasmid.
2. A Gly codon and *Afe*I site were then inserted prior to the stop codon of the mKate gene using primer #1 (*see* Table 1) and its respective reverse complement.
3. The PpyWT-TS gene in the pGEX-6P-2 expression vector [11] was modified by inserting an *Afe*I restriction site followed by the codons for linker residues IEGRGSG upstream of the start codon using primer #2 (*see* Table 1) and its respective reverse complement.

Table 1
DNA primer sequences

Primer #	Primer sequence
1[a]	5′-A CTG GGC CAT AAA CTG AAC **GGA AGC GCT** TAA CTC GAG ACC CCG GGT CG-3′
2[a]	5′-G CCC CTG GGA TCC **AGC GCT ATC GAA GGT CGT GGA TCC GGA** ATG GAA GAC GCC AAA AAC-3′
3[b]	5′-CTG AAC GGA AGC **GCA GAC GAA GTT GAT** GGA TCC GGA ATG GAA GAC GCC-3′
4[b]	5′-CTG AAC GGA AGC **GCA CTC GTA CCT CGT** GGA TCC GGA ATG GAA GAC GCC-3′
5[b]	5′-CTG AAC GGA AGC **GCA GGC TCA GGT AGT** GGA TCC GGA ATG GAA GAC GCC AAA AAC-3′

[a] Bold text represents the inserted codons and underline represents the AfeI site

[b] Bold text represents the mutated bases and underline represents the removal of the AfeI site

4. The plasmids containing the altered mKate and PpyWT-TS genes were digested with *Afe*I and *Xho*I and, after purification with a Qiagen QIAquick kit, the modified PpyWT-TS gene fragment was ligated into the pQE-30 plasmid producing the expression vector for BFFP-Xa (*see* **Note 5**).
5. The vectors containing the genes encoding the fusion proteins BFFP-C3, BFFP-Th, and BFFP-GS were prepared from the corresponding BFFP-Xa expression vector by mutating the codons for the tetrapeptide protease recognition site within the decapeptide linker. The primers (*see* Table 1) and their respective reverse compliments that were used to make the fusion proteins are: BFFP-C3 by introducing the DEVD peptide codons with primer #3; BFFP-Th by introducing the LVPR peptide codons with primer #4; and BFFP-GS by introducing the GSGS peptide codons with primer #5 (*see* **Note 6**).

3.2 Covalent Labeling with AF680 to Produce BFS Fusion Protein Substrates

1. Stock solutions of AF680 (10 mM, determined by UV using $\epsilon_{684\text{nm}} = 175{,}000\ \text{M}^{-1}\ \text{cm}^{-1}$ [14]) were prepared in sterile deionized water, divided into 30 μL aliquots, lyophilized and stored at −20 °C.
2. The labeling reactions to produce BFS-C3, BFS-Th, BFS-Xa, and BFS-GS were performed at 10 °C in PBSA buffer (*see* **Note 7**). Labeling reactions were initiated by addition of 1 mL of 30 μM fusion protein in PBSA buffer to a lyophilized aliquot of AF680 (0.3 mM final concentration), gently mixed, and incubated for 30 min.
3. Reactions were quenched by addition of 20 μL of glutathione solution (2 mM final concentration), and after 15 min were exhaustively dialyzed against PBSA buffer (8 changes, 1 L each) (*see* **Notes 8–11**).

3.3 Ratiometric Assays of Caspase 3, Factor Xa, and Thrombin Activity

1. The rates of protease cleavage of fusion protein substrates (*see* **Notes 12** and **13**) were monitored by changes in luminescence intensity ratios. Mixtures (0.05 mL) of 2.0 μM fusion protein substrates and proteases (BFS-C3 with 0.408–8.17 nM caspase 3; BFS-Xa with 58.0–465.0 nM factor Xa; and BFS-Th with 1.0–20.0 nM thrombin) were incubated in PBSA at 20 °C and 5 μL aliquots were withdrawn at the times indicated in Fig. 5 and added to cuvettes containing assay buffer (*see* **Note 14**).
2. Samples were briefly mixed and placed in the sample compartment of a Horiba Jobin-Yvon *i*HR imaging spectrometer and emission spectra were recorded. Peak ratios were determined from the intensities of the 560 nm (bioluminescence) and 706 nm (SRET) peaks.
3. The relationships between protease concentration and change in luminescence intensity ratio were determined using both the imaging spectrometer and a PerkinElmer LS55 luminescence

spectrometer in endpoint analysis assay format. Mixtures (0.05 mL) of fusion protein substrates and varying concentrations (*see* Fig. 6) of target proteases were incubated in PBSA at 20 °C for 15 min and 5 or 10 μL aliquots were withdrawn and added to cuvettes containing 0.50 mL of assay buffer (*see* **Note 15**).

4. Samples were briefly mixed and placed in the sample compartment of a Horiba Jobin-Yvon *i*HR imaging or into a scanning fluorometer and emission spectra were recorded as detailed above (*see* **Notes 16** and **17**).

4 Notes

1. During the affinity chromatography process to ensure good protein yields with high specific activity, it is important to keep the centrifuge tube containing the resuspended cells in a beaker of ice while performing the sonication step in order to minimize localized heating. Also, while washing the resin-bound protein, it is important to leave ~5 mL of PBS wash solution above the pelleted resin to avoid inadvertently removing resin.
2. Concentrations of PpyWT and PpyWT-TS were determined with the Bio-Rad Protein Assay system using BSA as the standard. Specific activity measurements were determined as previously reported [15, 16] except that the integration time was 15 min and the final LH_2 concentration was 0.5 mM.
3. Fusion protein substrate concentrations were determined by UV using the RFP chromophore ($\epsilon_{585\ \mathrm{nm}} = 51{,}000\ \mathrm{M}^{-1}\ \mathrm{cm}^{-1}$ for the mKate S158A variant [17]). The absorbance value at 585 nm must be reduced by 19 % of the maximum value of AF680 in order to correct for spectral overlap.
4. Mass spectral analyses were performed by tandem HPLC-electrospray ionization mass spectrometry (LC/ESMS) using a ThermoFinnigan Surveyor HPLC system and a ThermoFinnigan LCQ Advantage mass spectrometer. Post run data analysis was performed using ThermoFinnigan BioWorks Browser 3.0 deconvolution software. The found molecular masses (Da) of the following proteins were within the allowable experimental error (0.01 %) of the calculated values (in parenthesis): BFFP-Xa, 89,131 (89,138); BFFP-C3, 89,138 (89,141); BFFP-Th, 89,142 (89,148); BFFP-GS, 88,962 (88,971); and RFP, 26,596 (26,599).
5. Please contact the author about obtaining the expression vector containing BFFP-Xa.
6. With the likely limitation that Cys residues cannot be included in the linker region, it should be possible to design primers for

the BFFP-Xa template to introduce peptide codons to construct specific substrates for the measurement of other endoproteases of interest.

7. Ammonium sulfate was included because it substantially reduced noncovalent incorporation of nIR dye.

8. The dye-labeled fusion proteins could be stored in PBSA buffer at 5 °C for at least 2 months maintaining at least 90 % of the original activity.

9. The dye/protein ratios of the fusion protein substrates were estimated from the μmol of AF680 determined by UV using $\epsilon_{684\text{nm}} = 175{,}000\ \text{M}^{-1}\ \text{cm}^{-1}$ [14] and the μmol of protein determined by UV using $\epsilon_{585\ \text{nm}} = 51{,}000\ \text{M}^{-1}\ \text{cm}^{-1}$ for the mKate S158A variant [17] (*see* **Note 2**). The substrate nIR dye/protein ratios were 1.8 ± 0.3 and the labeling sites of the fusion protein substrates with AF680 were identified as Cys126 and Cys234. These residues correspond to positions 114 and 222 of RFP.

10. Each fusion protein substrate was also analyzed by LC/ESMS using a BioBasic-C4 (100 × 1 mm) column eluted at a flow rate of 50 μL/min with an acetonitrile gradient of 10 %/min. Absorbance was monitored at 280 and 680 nm and the long wavelength signal was only observed co-eluting with protein indicating the absence of any noncovalently incorporated AF680. The MS analysis of each substrate produced two signals in ~ 2:1 ratio corresponding to mass increases of 1958 Da and 979 Da, respectively. Based on the mass of AF680 (979 Da), the mass increases of 1958 Da and 979 Da corresponded to 2:1 and 1:1 dye/protein incorporation ratios, respectively.

11. Emission spectra produced by bioluminescence, BRET, and SRET were obtained using a Horiba Jobin-Yvon *i*HR imaging spectrometer equipped with a liquid N_2 cooled CCD detector and the excitation source turned off. Data were collected at 25 °C in a 0.8 mL quartz cuvette over the wavelength range 400–935 nm with the emission slit width set to 25 nm. Fluorescence emission spectra were measured with the excitation source set to 585 nm and the excitation and emission slits set to 1 nm. BRET ratios of the fusion proteins prior to labeling with AF680 were estimated by dividing the BRET peak intensity at 610 nm by the residual bioluminescence peak intensity at 565 nm. FRET efficiencies were determined by comparing fluorescence spectra of 1.0 μM solutions of fusion proteins prior to labeling with AF680 with the corresponding fusion protein substrate (labeled with AF680). The FRET efficiencies of the fluorescence at 625 nm from RFP in the unlabeled fusion proteins (F_D) and in the corresponding substrates ($F_{D\text{-}A}$) were calculated according to the equation $E = 1 - F_{D\text{-}A}/F_D$ [7]. SRET ratios for the fusion proteins were calculated

from emission spectra by dividing the intensity of the residual bioluminescence peak at 560 nm by the intensity of the SRET emission peak at 705 nm.

12. The activities of the substrates can be tested prior to conducting assays on unknown samples by incubating them with commercially available enzymes. The time course of cleavage of BFS-Xa (2.0 μM) by factor Xa (0.2 μM) at 20 °C in 0.05 mL PBSA can be monitored by withdrawing 5 μL aliquots of incubation mixtures and adding them to 0.50 mL of assay buffer. After mixing for 10 s, emission spectra are recorded and representative results are shown in Fig. 3. BFS-C3 and BFS-Th can be similarly evaluated and the details and typical results are shown in Fig. 4. The spectral properties and specific activities obtained with the substrates are summarized in Table 2.
13. The relative rates of cleavage of the fusion protein substrates (substrate specificity) were determined by incubating each one (2.0 μM) at 20 °C with 2.0 μM protease (caspase 3, thrombin, and factor Xa) in PBSA buffer. Aliquots (5 μL) were withdrawn at various intervals over 30 min and added to cuvettes containing 0.50 mL of assay buffer. Samples were briefly mixed and placed in the sample compartment of a Horiba Jobin-Yvon *i*HR imaging spectrometer and emission spectra were recorded. The changes in 560 nm/760 nm peak ratios per min were

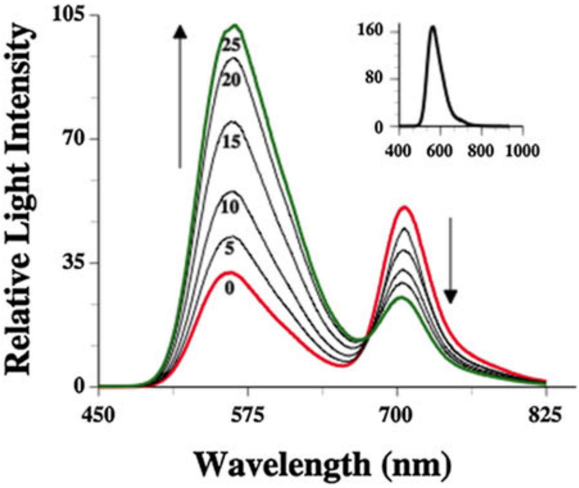

Fig. 3 Time course of cleavage of BFS-Xa by factor Xa. BFS-Xa (2.0 μM) and factor Xa (0.2 μM) were incubated at 20 °C in 0.05 mL PBSA. At the times (min) indicated in the figure, emission spectra were initiated by adding 5 μL aliquots of reaction mixtures to assay buffer. The *inset* shows the emission spectrum obtained from a 5 μL aliquot of the cleavage reaction mixture after 24 h of incubation at 20 °C. Reproduced in part from Branchini et al. with permission from Anal. Biochem. (Elsevier) [5]

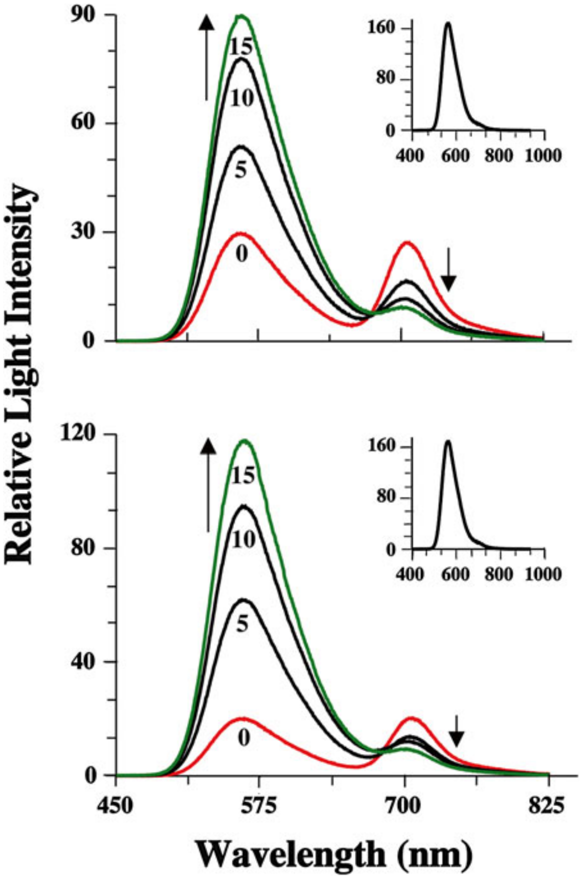

Fig. 4 Time courses of cleavage of BFS-C3 and BFS-Th by caspase 3 and thrombin. BFS-C3 (2.0 mM) and caspase 3 (0.2 mM) (*upper diagram*) and BFS-Th (2.0 mM) and thrombin (0.2 mM) (*lower diagram*) were incubated at 20 °C in 0.05 mL PBSA. Over 15 min at the times indicated in the figure, 5 mL aliquots were withdrawn and emission spectra were measured in assay buffer. The *insets* show the emission spectra obtained from 5 mL aliquots of each the cleavage reaction mixture after 24 h of incubation at 20 °C. Reproduced in part from Branchini et al. with permission from Anal. Biochem. (Elsevier) [5]

determined and are expressed as % of the rate obtained with BFS-C3 and caspase 3 (0.58/min), defined as 100%. The results are summarized in Table 3.

14. Linear responses were obtained over 15 min (*see* Fig. 5) and for at least 1 h for 58–465 nM factor Xa with BFS-Xa, 0.41–8.2 nM caspase 3 with BFS-C3 and 1.0–20 nM thrombin with BFS-Th. The SRET substrates could be used to monitor protease activity in a convenient endpoint format (*see* Fig. 6).
15. Similar endpoint analysis results were obtained (*see* Fig. 6) using a scanning fluorometer even though the initial luminescence

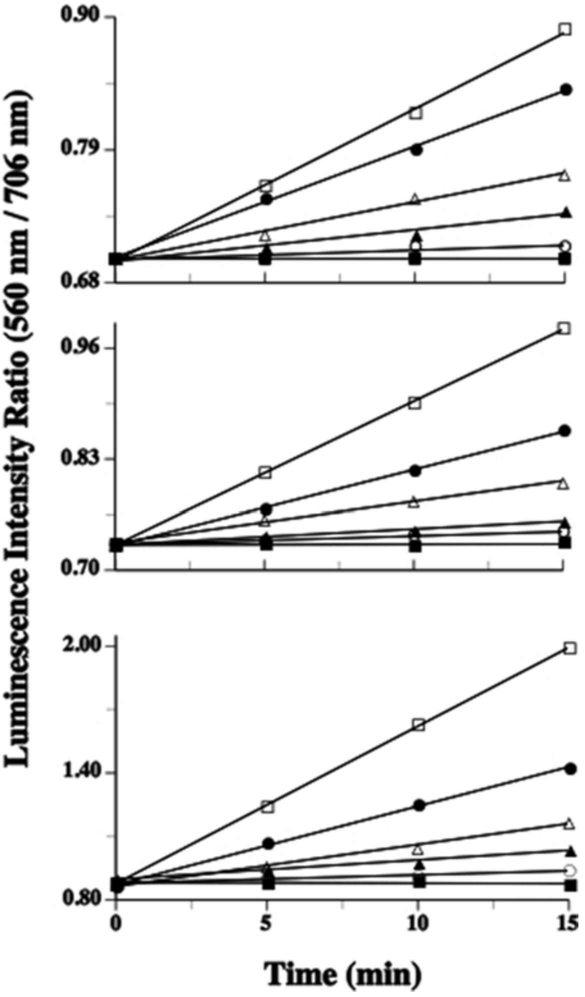

Fig. 5 Rates of protease cleavage of fusion protein substrates monitored by changes in luminescence intensity ratios. Mixtures (0.05 mL) of fusion protein substrates (2.0 μM) and proteases were incubated in PBSA at 20 °C. Aliquots (5 μL) were withdrawn and added to solutions containing LH_2 and Mg-ATP to generate the emission spectra used to calculate 560 nm/706 nm peak ratios. *Top*, BFS-Xa incubated with factor Xa (*filled square*, none; *open circle*, 58.0 nM; *filled triangle*, 116.0 nM; *open triangle*, 233.0 nM; *filled circle*, 349.0 nM; and *open square*, 465.0 nM); *Middle*, BFS-C3 incubated with caspase 3 (*filled square*, none; *open circle*, 0.408 nM; *filled triangle*, 0.817 nM; *open triangle*, 2.04 nM; *filled circle*, 4.08 nM; and *open square*, 8.17 nM); and Bottom, BFS-Th incubated with thrombin (*filled square*, none; *open circle*, 1.0 nM; *filled triangle*, 2.5 nM; *open triangle*, 5.0 nM; *filled circle*, 10.0 nM; and *open square*, 20.0 nM). Reproduced in part from Branchini et al. with permission from Anal. Biochem. (Elsevier) [5]

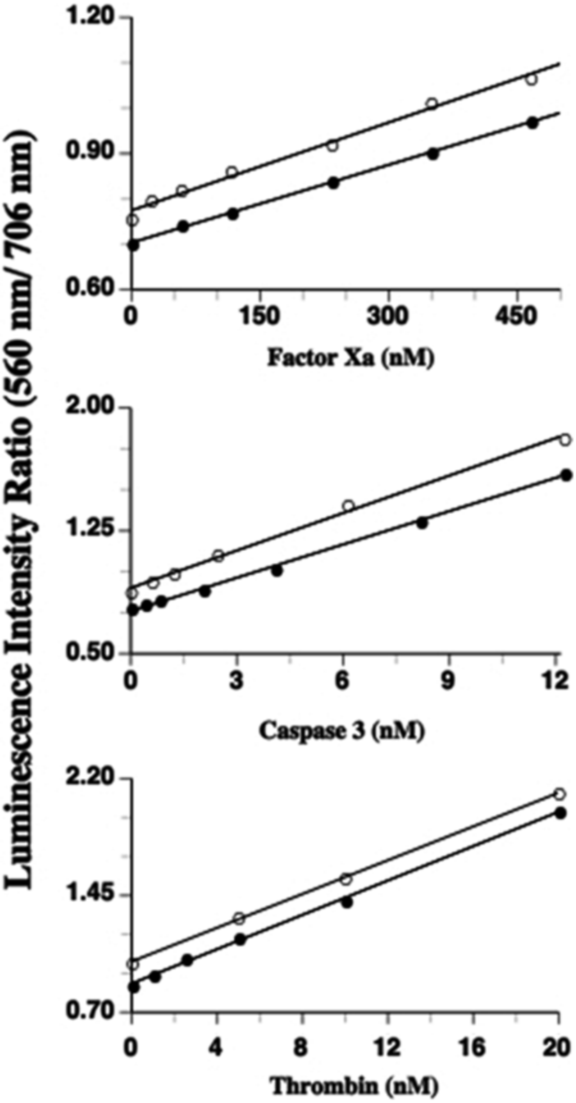

Fig. 6 Relationship between protease concentration and change in luminescence intensity ratio. Mixtures (0.05 mL) of fusion protein substrates and varying concentrations of proteases (BFS-Xa with factor Xa, BFS-C3 with caspase 3 and BFS-Th with thrombin) were incubated in PBSA at 20 °C for 15 min and 5 μL (*filled circle*) or 10 μL (*open circle*) aliquots were withdrawn and added to cuvettes containing 0.50 mL of assay buffer and Mg-ATP (2 mM). Samples were briefly mixed and placed in the sample compartment of: (*filled circle*) a Horiba Jobin-Yvon *i*HR imaging spectrometer or (*open circle*) after 1 min into a PerkinElmer LS55 luminescence spectrometer and emission spectra were recorded as described in Methods. Reproduced in part from Branchini et al. with permission from Anal. Biochem. (Elsevier) [5]

Table 2
Spectral properties and specific activities obtained with fusion protein substrates

Protein	Relative integrated specific activity[a] (15 min)	Emission maxima[b] (nm ± 1)	Peak ratio (560 nm/706 nm)	BRET ratio[c]	FRET efficiency[d]
PpyWT	100	560	–	–	–
PpyWT-TS	102	560	–	–	–
BFS-Xa	103	562, 707	0.70	0.85	0.83
BFS-Th	97	562, 705	0.88	0.82	0.82
BFS-C3	93	562, 705	0.73	0.82	0.86
BFS-GS	95	560, 706	0.78	0.84	0.83

[a] Specific activity values were expressed relative to PpyWT defined as 100

[b] For the fusion protein substrates, the second value is the SRET maximum

[c] Measurements were made as described in Methods. BRET ratios can be used to approximate the efficiency of energy transfer

[d] The range of FRET efficiency values is 0–1.0

Table 3
Relative protease activities toward fusion protein substrates

	Relative activity[a,b] (%)		
Substrate	Factor Xa	Caspase 3	Thrombin
BFS-Xa	11.8	nd	0.02
BFS-C3	nd	100	nd
BFS-Th	nd	nd	86.7
BFS-GS	nd	nd	nd

[a] Proteases (2 μM) and substrates (2 μM) were incubated at 20 °C and rates of change of peak ratios were calculated as described in Methods

[b] Values were calculated from the change in peak ratio/min and are expressed as % of the rate obtained with caspase 3 and BFS-C3 (0.58/min), defined as 100%. If the measured rate was not greater than 1.5 times the background rate of 1.0×10^{-5}/min (no protease added), the result was reported as nd, none detected

560 nm:705 nm peak ratios were higher because of the lower sensitivity of the PMT detector to the long wavelength peak. While detection limits of 0.41 nM for caspase 3, 1.0 nM for thrombin, and 58 nM for factor Xa were obtained with a scanning fluorometer, five- to tenfold lower protease concentrations were detected with an imaging spectrometer equipped with a cooled CCD detector. Moreover, the endpoint assays were performed with short incubation times (15 min), in small volumes (50 μL) using only 2 μM substrate.

16. If a recording spectrofluorimeter is used, it is best to wait 1 min (to ensure slow decay kinetics) before acquiring spectra. Very good results were obtained with a Perkin Elmer LS50 spectrometer operated in the "bioluminescence" mode as previously described [18] using a wavelength range of 500–750 nm and a scan speed of 250 nm/min. The excitation source was turned off and the emission slit was set to 10 nm.
17. The assays described here could also be conveniently performed on a simple luminometer equipped with two narrow bandpass filters and a red-sensitive PMT. It also may be possible to monitor protease activity in biological fluids by measuring the disappearance of the SRET peak because of the expected transmission advantage of the nIR signal.

Acknowledgements

I gratefully acknowledge the financial support provided by the National Science Foundation (MCB 1410390), the Air Force Office of Scientific Research (FA9550-14-1-0100) and the Hans & Ella McCollum'21 Vahlteich Endowment. The technical contributions of Justin C. Rosenberg, Danielle M. Fontaine, Kelsey P. Taylor, Tara L. Southworth, and Samantha J. Linder were essential to the development of the SRET substrates.

References

1. Hastings JW (1996) Chemistries and colors of bioluminescent reactions-a review. Gene 173:5–11
2. Widder EA (2010) Bioluminescence in the ocean: origins of biological, chemical, and ecological diversity. Science 328:704–708
3. Branchini BR, Behney CE, Southworth TL, Fontaine DM, Gulick AM, Vinyard DJ, Brudvig GW (2015) Experimental Support for a single electron-transfer oxidation mechanism in firefly bioluminescence. J Am Chem Soc 137:7592–7595
4. Carriba P, Navarro G, Ciruela F, Ferre S, Casado V, Agnati L, Cortes A, Mallol J, Fuxe K, Canela EI, Lluis C, Franco R (2008) Detection of heteromerization of more than two proteins by sequential BRET-FRET. Nat Methods 5:727–733
5. Branchini BR, Rosenberg JC, Ablamsky DM, Taylor KP, Southworth TL, Linder SJ (2011) Sequential bioluminescence resonance energy transfer-fluorescence resonance energy transfer-based ratiometric protease assays with fusion proteins of firefly luciferase and red fluorescent protein. Anal Biochem 414:239–245
6. Navarro G, McCormick PJ, Mallol J, Lluis C, Franco R, Cortes A, Casado V, Canela EI, Ferre S (2013) Detection of receptor heteromers involving dopamine receptors by the sequential BRET-FRET technology. Methods Mol Biol (Clifton, NJ) 964:95–105
7. Lakowicz JR (2006) Principles of fluorescence spectroscopy, 3rd edn. Springer Science + Business Media LLC, New York, NY
8. Chalfie M, Kain S (2006) Green fluorescent protein: properties, applications, and protocols, vol 47, 2nd edn, Methods of biochemical analysis. Wiley-Interscience, Hoboken, NJ
9. Tsien RY, Poenie M (1986) Fluorescence ratio imaging - a new window into intracellular ionic signaling. Trends Biochem Sci 11:450–455
10. Domaille DW, Zeng L, Chang CJ (2010) Visualizing ascorbate-triggered release of labile copper within living cells using a ratiometric fluorescent sensor. J Am Chem Soc 132: 1194–1195

11. Branchini BR, Ablamsky DM, Murtiashaw MH, Uzasci L, Fraga H, Southworth TL (2007) Thermostable red and green light-producing firefly luciferase mutants for bioluminescent reporter applications. Anal Biochem 361:253–262
12. Neurath H (1999) Proteolytic enzymes, past and future. Proc Natl Acad Sci U S A 96:10962–10963
13. Branchini BR, Ablamsky DM, Rosenberg JC (2010) Chemically modified firefly luciferase is an efficient source of near-infrared light. Bioconjug Chem 21:2023–2030
14. Haugland RP, Spence MTZ, Johnson ID, Basey A (2005) The handbook: a guide to fluorescent probes and labeling technologies, 10th edn. Molecular Probes, Eugene, OR
15. Branchini BR, Southworth TL, Khattak NF, Michelini E, Roda A (2005) Red- and green-emitting firefly luciferase mutants for bioluminescent reporter applications. Anal Biochem 345:140–148
16. Branchini BR, Ablamsky DM, Rosenman JM, Uzasci L, Southworth TL, Zimmer M (2007) Synergistic mutations produce blue-shifted bioluminescence in firefly luciferase. Biochemistry 46:13847–13855
17. Chu J, Zhang ZH, Zheng Y, Yang J, Qin LS, Lu JL, Huang ZL, Zeng SQ, Luo QM (2009) A novel far-red bimolecular fluorescence complementation system that allows for efficient visualization of protein interactions under physiological conditions. Biosens Bioelectron 25:234–239
18. Branchini BR, Southworth TL, Murtiashaw MH, Wilkinson SR, Khattak NF, Rosenberg JC, Zimmer M (2005) Mutagenesis evidence that the partial reactions of firefly bioluminescence are catalyzed by different conformations of the luciferase C-terminal domain. Biochemistry 44:1385–1393

Chapter 9

Monitoring Intracellular pH Change with a Genetically Encoded and Ratiometric Luminescence Sensor in Yeast and Mammalian Cells

Yunfei Zhang, J. Brian Robertson, Qiguang Xie,
and Carl Hirschie Johnson

Abstract

"pHlash" is a novel bioluminescence-based pH sensor for measuring intracellular pH, which is developed based on Bioluminescence Resonance Energy Transfer (BRET). pHlash is a fusion protein between a mutant of *Renilla* luciferase (RLuc) and a Venus fluorophore. The spectral emission of purified pHlash protein exhibits pH dependence in vitro. When expressed in either yeast or mammalian cells, pHlash reports basal pH and cytosolic acidification. In this chapter, we describe an in vitro characterization of pHlash, and also in vivo assays including in yeast cells and in HeLa cells using pHlash as a cytoplasmic pH indicator.

Key words pH, BRET, Luminescence, Resonance transfer, Ratiometric

1 Introduction

Intracellular pH (pH_i) is a very important modulator for cells to maintain proper function. Most proteins, especially enzymes, are affected by even subtle pH changes. To maintain stable intracellular pH values, all cells have mechanisms to pump protons in or out across cellular membranes. Moreover, the distribution of protons is not uniform within a cell and depends on the nature of subcellular compartments [1]. Current methods for measuring intracellular pH include: (I) a classical microelectrode technique that relies on a specific apparatus that is not present in most labs; (II) fluorescent dyes, such as BCECF (2′7′-bis-2-carboxyethyl-5- (and -6)-carboxyfluorescein) and SNARF (seminaphthorhodafluor) [2], which are popular because of their convenience and accessibility for many labs; (III) genetically encodable fluorescent pH-sensitive GFPs (e.g., "pHluorin" or "Pt-GFP") [3–5], which overcome some of the limitations of fluorescent dyes (such as being able to measure the pH within subcellular compartments).

Sung-Bae Kim (ed.), *Bioluminescence: Methods and Protocols*, Methods in Molecular Biology, vol. 1461,
DOI 10.1007/978-1-4939-3813-1_9, © Springer Science+Business Media New York 2016

We are developing luminescence-based pH probes. Since luciferases are enzymes, many luciferases show the significant pH dependency of activity that is common to most enzymes. Some luciferases like firefly luciferase show both changes in activity and shifts in spectra with pH change [6], while other luciferases show activity changes but have little spectral shift, e.g. RLuc [7], *Gaussia* luciferase (GLuc) [8], PpyRE8 [9] and NanoLuc [10]. The activity of most of these luciferases peaks near neutral pH (e.g., pH 7.0–7.5).

By fusing a bright mutant of *Renilla* luciferase ("RLuc8") [11] via an Ala-Glu-Leu linker to the circularly permuted Venus fluorophore ("cpVenus") [12], we developed a fusion protein, called "pHlash," that shows a dramatic pH-dependent change in vitro in its spectrum of emission–as the pH increases, the spectral ratio shifts increasingly to the yellow (*see* Fig. 1). pHlash utilizes Bioluminescence Resonance Energy Transfer (BRET) [13], which makes its response ratiometric like that of pHluorins [3–5]; however, pHlash avoids fluorescence excitation since it is luminescent and BRET-based. In the absence of fluorescence excitation, problems associated with this irradiation are avoided, such as autofluorescence, photobleaching, and photo-response/toxicity. The spectral response of pHlash is specific for pH–neither $CaCl_2$, $MgCl_2$, NaCl, nor KCl had a significant effect on the spectra or pH dependency of pHlash [14]. In this chapter, we describe the in vitro pH calibration assay of purified pHlash protein; as well as in vivo assays to monitor the intracellular pH changes in yeast cells and HeLa cells using pHlash as the pH indicator.

2 Material

2.1 Constructs Information

1. The pHlash construct encodes a fusion protein of RLuc8 [11] and cpVenus (cp173Venus) [12] linked by the sequence GCCGAGCTC encoding the amino acids Ala-Glu-Leu.
2. Plasmid used for protein expression in *E. coli*: pRSETb-pHlash (Addgene, Plasmid #61550), built from pRSETb (Invitrogen).
3. Plasmid used for expression in yeast cells (*Saccharomyces cerevisiae* strain CEN.PK113-7D): pRS305-hph-P*ACT1*pHlash (*see* **Note 1**).
4. Plasmid used for expression in HeLa cells: pcDNA3.1+-pHlash (Addgene, Plasmid #61552), built from pcDNA3.1+ (Invitrogen).

2.2 Protein Expression and Purification

1. To express His-tagged fusion proteins (N-terminal fusions of His6) of pHlash, *E. coli* strain BL21 (DE3) cells were used to transform those constructs.
2. 50-mL flask and 2-L flask.
3. LB medium with ampicillin (60 μg/mL).

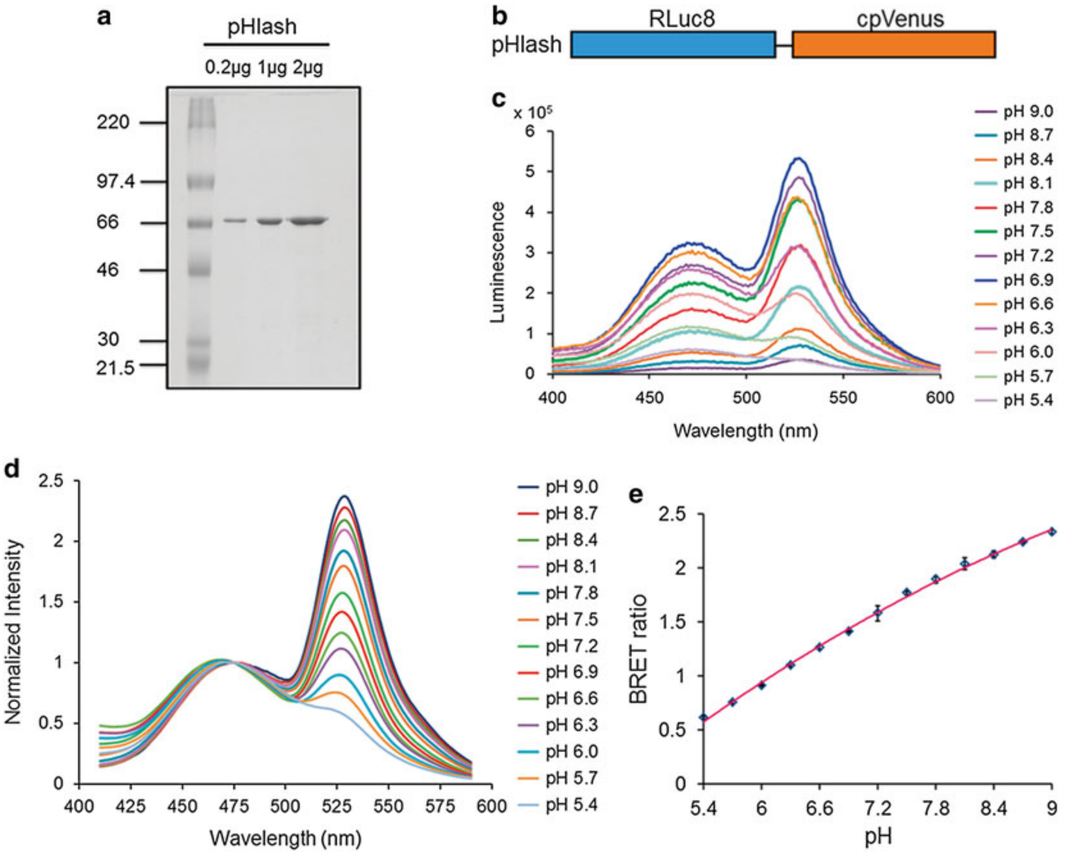

Fig. 1 pH response of purified pHlash protein in vitro. (**a**) SDS-PAGE gel of purified His-tagged pHlash protein stained with Coomassie Blue dye. Leftmost lane is molecular weight standards with kDa indicated, while the other lanes are the purified pHlash protein loaded at 0.2, 1, and 2 μg per lane. (**b**) Construct of the pHlash fusion protein. RLuc8 was linked to cpVenus by the sequence Ala-Glu-Leu. (**c**) Raw data (not normalized) of luminescence emission spectra of purified pHlash protein with 10 μM nCTZ at different pH values (pH 5.4–9.0) in 50 mM BIS-Tris-propane, 100 mM KCl, and 100 mM NaCl. (**d**) Normalized luminescence emission spectra of pHlash measured as in panel C. Luminescence intensity was normalized to the peak at 475 nm. (**e**) The BRET ratio (luminescence at 525 nm:475 nm) as a function of pH is shown for pHlash in vitro. Error bars are +/− S.D., but in most cases the error bars are so small that they are obscured by the symbols (*n* = 3)

4. TALON metal affinity resin (Clontech).
5. Equilibration/Wash buffer: 50 mM sodium phosphate, 300 mM NaCl, pH 7.0.
6. Elution buffer: 50 mM sodium phosphate, 300 mM NaCl, 150 mM imidazole, pH 7.0.
7. 10 % SDS-PAGE gel.
8. Dialysis cassette (20 K MWCO) (Thermo Scientific).
9. Dialysis buffer: 30 mM MOPS, 5 % Glycerol, pH 7.2.
10. BSA standard solution and Protein Assay Dye Reagent Concentrate (Bio-Rad).

2.3 In Vitro Characterization of pHlash

1. QuantaMaster QM-7/SE spectrofluorometer (Photon Technology International, Birmingham NJ).
2. Calibration buffer: 50 mM BIS-Tris-propane, 10 mM KCl, and 100 mM NaCl (*see* **Note 2**). pH was adjusted with 1 N HCl to 13 different pH values ranging from 5.4 to 9.0 (*see* **Note 3**).
3. Substrates for luciferase: native coelenterazine (nCTZ) (NanoLight, Pinetop, AZ) (*see* **Note 4**).
4. 1.5-mL disposable plastic cuvettes.

2.4 In Vivo pH Calibration of Yeast Strain Expressing pHlash

1. Yeast strain: *Saccharomyces cerevisiae* strain CEN.PK113-7D.
2. Yeast complete synthetic medium (CSM) (100 mL): 650 mg Nitrogen base (without amino acids), 11 mg complete amino acids mix, 2 g glucose.
3. Yeast permeabilization buffer: 50 mM MES, 50 mM HEPES, 50 mM KCl, 50 mM NaCl, 0.2 M ammonium acetate, 10 mM NaN_3, 10 mM 2-deoxyglucose, 75 μM monensin, and 10 μM nigericin, titrated to 8 different pH values adjusted with 1 M NaOH from 5.5 to 9.0 [15] (*see* **Note 5**).
4. BCECF-AM (Molecular Probes, Eugene OR).
5. YPD medium: 1 % yeast extract, 2 % peptone, and 2 % D-Glucose.
6. QuantaMaster QM-7/SE spectrofluorometer (Photon Technology International, Birmingham NJ).
7. 1.5-mL disposable plastic cuvettes.
8. 4.5-mL glass cuvette.
9. Magnetic micro stir bar (~7 mm length).

2.5 In Vivo Experiments with HeLa Cells Expressing pHlash

1. HeLa cells (obtained from ATCC, ATCC® Number: CCL-2™).
2. Culture medium: Dulbecco's Modified Eagle's Medium (DMEM) (Invitrogen) supplemented with 10% fetal bovine serum (FBS) (Invitrogen).
3. FuGene 6 (Invitrogen, Carlsbad, CA).
4. Recording media: DMEM medium without phenol red (Invitrogen) supplemented with 10% FBS.
5. ViviRen™ (a serum-insensitive version of coelenterazine-h; Promega, Madison WI) (*see* **Note 6**).
6. pH calibration buffer: 100 mM KCl, 100 mM NaCl, 1.36 mM $CaCl_2$, 4.5 g/L glucose, 20 μM nigericin, and 50 mM BIS-Tris-propane (pH 5.5–9.0).
7. QuantaMaster QM-7/SE spectrofluorometer (Photon Technology International, Birmingham NJ).
8. 4.5-mL glass cuvette.
9. Magnetic micro stir bar (~7 mm length).
10. MES buffer: 50 mM MES, 130 mM KCl, 1 mM $MgCl_2$, 25 mM NaCl, pH 6.1.

2.6 BRET Imaging

1. Dual-View™ micro-imager (Optical Insights, Tucson AZ, USA).
2. Modified electron bombardment-charge coupled device (EB-CCD) camera (Hamamatsu Photonic Systems, Bridgewater NJ, USA) [16].
3. IX-71 inverted microscope (Olympus America Inc., Melville NY, USA) with an Apo N 60× objective, NA 1.49 (oil immersion, Olympus).
4. Temperature-controlled (22–37 °C) light-tight box.
5. 35-mm Glass Bottom Cell Culture Dish (MatTek Corporation).
6. HeLa cells transfected with pcDNA3.1+/pHlash.

3 Methods

3.1 Protein Expression and Purification

1. In a 50-mL flask, inoculate *E. coli* strain BL21 (DE3) cells bearing pRSETb/pHlash in 10 mL LB medium with ampicillin (60 μg/mL). Grow the starter culture overnight at 37 °C with agitation.
2. In a 2-L flask, dilute the overnight culture into 500 mL fresh LB medium with ampicillin (60 μg/mL).
3. Grow the culture at 37 °C with agitation until an OD_{600} of 0.6 is reached. Add 1 mM isopropyl-β-d-thiogalactopyranoside (IPTG) to induce the expression at 25 °C with gentle agitation.
4. After incubation with IPTG for 5 h at 25 °C, harvest the cells by centrifugation at 6000 × *g* for 15 min. Suspend the pellet with 25 mL Equilibration buffer.
5. Disrupt the cells by sonication (1 min for 8 times, with 30 s interval, keep the sample on ice).
6. To remove the cell debris, centrifuge the sample at 22,000 × *g* for 40 min. Transfer the supernatant to a new 50-mL tube, and then add 5 mM imidazole to the supernatant.
7. Incubate the supernatant with balanced TALON metal affinity resin with gentle shaking at 4 °C for 1 h.
8. Load the sample into one empty column and let the resin settle down. Collect the flow-through and then wash the resin with at least 20 bed volumes of Equilibration/Wash buffer containing 10 mM imidazole.
9. Elute the protein according to the manufacturer's protocol (*see* **Note** 7).
10. After the gradient elution, 10 μL samples from each eluted fraction should be assayed by SDS-PAGE to confirm which fraction(s) contains pHlash. Fractions with high yield and purity can be combined (*see* **Note 8**).

11. Dialyse eluted pHlash protein in 1 L 30 mM MOPS buffer (pH 7.2) (containing 5% glycerol) at 4 °C to remove imidazole (*see* **Note 8**). After 12 h dialysis, transfer the dialysis cassette (or dialysis bag) to fresh MOPS buffer and incubate for another 12 h.
12. Quantify the purified pHlash protein using the Bio-Rad protein assay, then flash-freeze it with liquid nitrogen. Store the samples at −80 °C for later use.

3.2 In Vitro pH Calibration of pHlash

1. For measurement of BRET emission, use a QuantaMaster QM-7/SE spectrofluorometer with the slit width set to 16 nm. The excitation beam of the QuantaMaster is not needed and can be turned off.
2. Set the following parameters for pH calibration. Select "Emission Scan" mode (*see* **Note 9**) and set the wavelength from 400 nm to 600 nm in 1 nm steps with 0.1 s integration for each step.
3. For each individual measurement, prepare a 1.5 mL disposable cuvette. Dilute purified pHlash protein (1 μg in 2 μL of the MOPS storage buffer) 250-fold to achieve a final concentration of 1 μg purified protein per 500 μL calibration buffer. Mix the sample well with a pipette.
4. Add fresh coelenterazine (nCTZ) to the sample to a final concentration of 10 μM before each measurement (*see* **Note 10**). Mix the sample quickly, then insert the cuvette, and start the measurement immediately.
5. Repeat the measurements with calibration buffers at different pH.
6. To analyze data from Emission Scan mode, smooth the curve using a ± 10 nm running average and then normalize the luminescence intensity from each measurement curve to each curve's peak at 475 nm (*see* Fig. 1d). The BRET ratio is obtained by dividing the luminescence intensity at 525 nm by the luminescence intensity at 475 nm.
7. Plot the BRET ratio from each curve as a function of the pH to generate a standard curve (*see* Fig. 1e) that can be used to estimate pH of experimental samples when their BRET ratios are determined.

3.3 In Vivo pH Calibration of Yeast Strain Expressing pHlash

3.3.1 Genetic Construct for Yeast Expression

Transform the desired strain of yeast with the *LEU2* integrating plasmid pRS305-hph-P*ACT1*pHlash and select for resistance on YPD medium that includes 200 μg/mL hygromycin (*see* **Note 1** for how this plasmid was constructed). Once transformed and selected, the resulting yeast cells have a stable integration of the construct, which allows pHlash experiments to be conducted in a medium or buffer of choice without the need for antibiotics or auxotrophic requirements.

3.3.2 In Vivo pH Calibration

1. Prepare a 2 mL starter culture of yeast strain expressing pHlash and let it grow overnight at 28–30 °C with agitation. Dilute the starter culture tenfold with fresh Yeast complete synthetic medium and incubate for 5 h.
2. Harvest the yeast cells by centrifugation at 1000 × *g* for 5 min, wash with distilled water.
3. In vivo pH calibration should be performed in yeast cells expressing pHlash that have been slightly permeabilized to protons by incubating in yeast permeabilization buffer [15]. For each pH value to be tested, use yeast cells harvested from 1 mL culture (*see* **Note 11**), and resuspend the cells with 1 mL yeast permeabilization buffer. Incubate at room temperature with gentle rotation for 30 min.
4. Use the QuantaMaster QM-7/SE spectrofluorometer to measure the BRET ratio of the in vivo calibration samples in "Emission Scan" mode as previously described in **step 2** in Subheading 3.2 and **step 6** in Subheading 3.2. Or alternatively the "Two-Wavelength Switching" mode (described hereafter) can be used to ensure that the in vivo BRET ratios are stable (*see* **Note 9**). To use Two-Wavelength Switching mode, shut off the excitation beam and set the slit width to 16 nm. Select Two-Wavelength Switching mode, and set the wavelength to record at 475 nm and 525 nm, with 0.5 s integration. The QuantaMaster will selectively monitor these two wavelengths continuously or for a set amount of time.
5. Transfer each sample into a 4.5-mL glass cuvette. A stir bar placed on the bottom of the cuvette allows gentle stirring to maintain the cells in suspension. Add fresh nCTZ to the sample to a final concentration of 10 μM before each measurement. Insert the cuvette and start the measurement in Two-Wavelength Switching mode. Continue to record until a stable BRET ratio is achieved. Figure 2b shows examples of stable BRET ratios recorded in Two-Wavelength Switching mode.
6. Plot the BRET ratio of each pH unit tested to generate a standard curve like that shown in (*see* Fig. 2a). This standard curve can be used to estimate the intracellular pH of experimental samples of yeast when their BRET ratios are determined.
7. If desired, the standard curve and in vivo experiments can be corroborated by BCECF-AM (Molecular Probes, Eugene OR) in permeabilized nontransformed yeast cells as shown in (*see* Fig. 2a and c). For in vivo calibration using BCECF-AM, incubate yeast cultures in YPD medium (at pH 7.5) with 50 μM BCECF-AM at 30 °C for 30 min, wash and suspend in yeast permeabilization buffer. Incubate at room temperature with gentle rotation for 30 min. Measure fluorescence with dual excitation at 440 nm and 490 nm and record emission at 535 nm with the QuantaMaster QM-7/SE spectrophotometer.

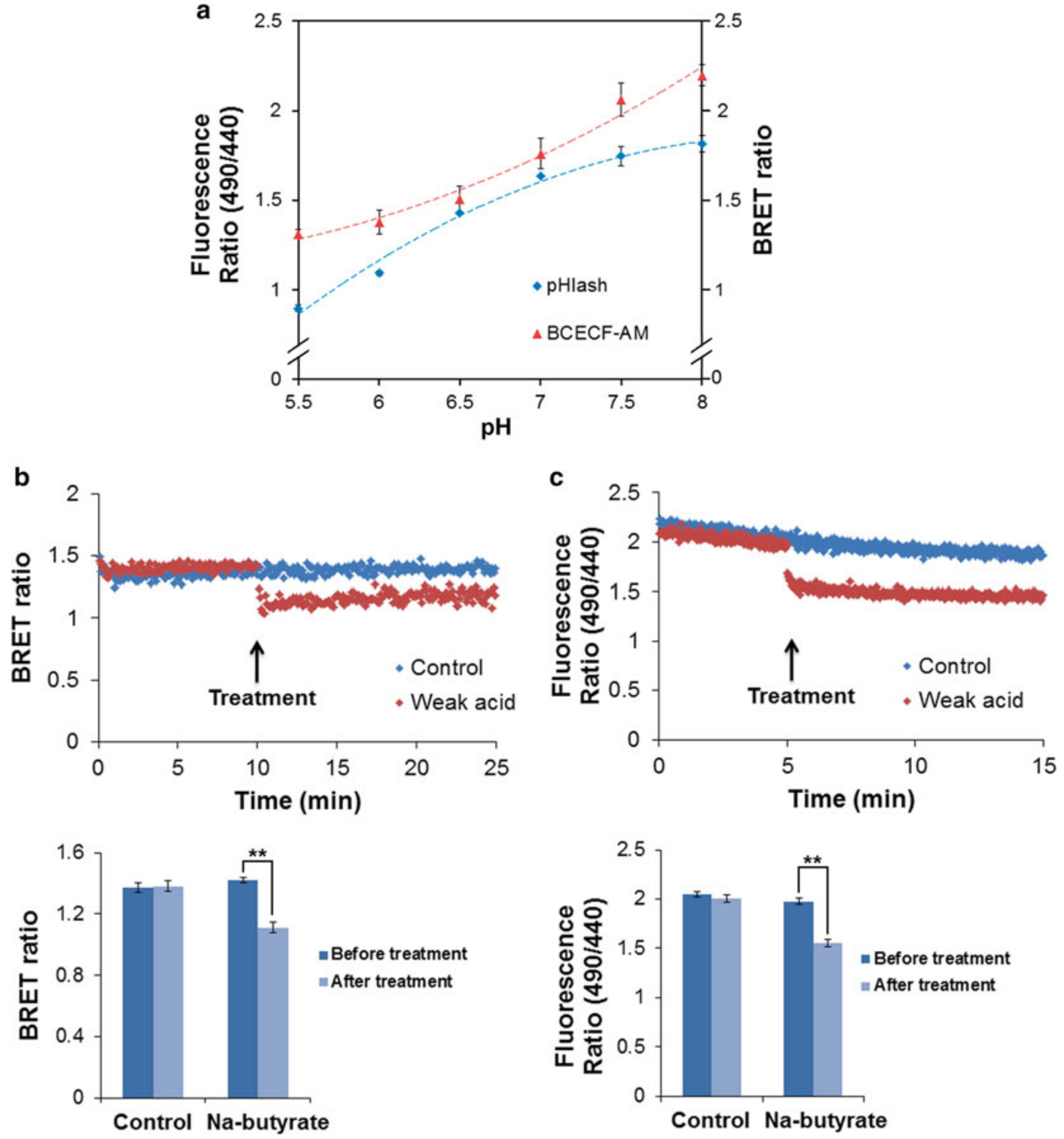

Fig. 2 Response of yeast pH to weak acid treatment. (**a**) pH response of BCECF-AM loaded yeast cells (red) compared with pHlash transformed yeast cells (blue). (**b**) Response of pHlash -expressing yeast cells to weak acid. Yeast cells were suspended in 20 mM MES buffer (pH 5.0) with 10 μM nCTZ. After 10 min baseline recording, 20 μM final concentration of Na-butyrate (pH 5.0) was added (upper portion of the panel). An equal volume of pH 5.0 buffer was added as control. The change in BRET ratio of pHlash reports the intracellular acidification after treatment with Na-butyrate, and is quantified in the lower portion. (**c**) Response of BCECF-AM loaded yeast cells to weak acid (20 μM sodium butyrate, upper portion). Yeast cells were suspended in 20 mM MES buffer (pH 5.0). After 10 min baseline recording, 20 μM final concentration of Na-butyrate (pH 5.0) was added (total added volume was 20 μL, which is the same volume as that for the pH 5.0 buffer that was used as a control). In panels **a**, **b**, and **c**, error bars are +/− S.D., but in some cases the error bars are so small that they are obscured by the symbols ($n=3$ for panel **a**, $n=5$ for panels **d** and **e**). ** $p<0.01$

3.3.3 Performance Confirmation by Perturbation of pH with Na-butyrate

If desired to confirm that yeast cytosolic pH as indicated by pHlash is responding in real time to pH perturbation, pHlash-expressing yeast cells can be suspended in 20 mM MES buffer (pH 5.0) with 10 μM nCTZ. Using the Two-Wavelength Switching mode to monitor dual emission at 475 nm and 525 nm with 0.5 s integration, add 20 μM final concentration of Na-butyrate (pH 5.0) (*see* Fig. 2b, red points). For a control recording, add a volume of 20 mM MES buffer (pH 5.0) equal to that of the Na-butyrate solution used above (but without Na-butyrate; *see* Fig. 2b, blue points). The change in BRET ratio of pHlash reports the intracellular acidification after treatment with Na-butyrate (*see* Fig. 2b, lower portion).

3.4 In Vivo Experiments with HeLa Cells Expressing pHlash

3.4.1 HeLa Cell Culture and Transfection

1. Grow HeLa Cells in 35-mm cell culture dishes in DMEM medium (Invitrogen) with 10% FBS at 37 °C with 5% CO_2 until they reach 80% confluence.
2. Dilute 3 μL FuGene6 with serum-free DMEM medium. Mix gently and keep at room temperature for 5 min.
3. Add 1 μg of plasmid DNA to the mixture. Mix gently and then spin down shortly. Incubate at room temperature for 30 min.
4. Add the mixture to cells in 35-mm dishes. Swirl gently to mix. Return the dish to the incubator.
5. 24–48 h after transfection, cells can be used for BRET measurement or imaging (*see* **Note 12**).

3.4.2 In Vivo pH Calibration

1. 24–48 h after transfection, wash the cells with Dulbecco's Phosphate-Buffered Saline (DPBS) and then trypsinize the cells for 5–10 min. Transfer the cells to 1.5 mL tube and centrifuge at 900 × *g* for 5 min.
2. Resuspend the cells with pH calibration buffers such that extracellular pH values cover a range of 5.5 to 9.0.
3. Incubate the cells in the calibration buffer for 10 min. Add ViviRen™ (substrate) to the assay buffer to a final concentration of 2.5 μM.
4. Use a QuantaMaster QM-7/SE spectrophotometer to measure dual emission at 475 nm and 525 nm for 10 min. A stir bar placed on the bottom of the cuvette gently stirs the cells to maintain them in suspension.
5. Generate a standard curve by plotting the BRET ratio as a function of pH to cover the range of buffers tested. This standard curve can be used to estimate intracellular pH of other pHlash-expressing HeLa cells from experimental conditions.

3.4.3 Imaging of BRET in HeLa Cells

1. Prepare apparatus for BRET imaging (*see* **Note 13** for detailed information). Set the temperature controller of the light-tight box to 37 °C.
2. Prepare pHlash-expressing HeLa cells for imaging (*see* **Note 12**).

3. In brightfield, focus on a group of cells using the inverted microscope using the Dual-View™ in"Bypass Mode."
4. Switch to excitation mode and look for cells with bright fluorescence (of the cpVenus moeity) (*see* **Note 14**). Move the target cell to the center view, focus quickly, and turn off the excitation light.
5. Drop in ViviRen™-containing medium directly to the dish without touching the dish. Close the box and switch the Dual-View™ out of "Bypass Mode" by pushing the filter holder inside the Dual-View™. Close the box for imaging.
6. For single HeLa cell imaging, collect and integrate 10 sequential 2 s exposures by choosing the median value for each pixel over the sequence of 10 exposures. Then subtract background with ImageJ by using a single pixel from the nonsample region of the image as a background value.
7. Calculation of BRET ratio: A pixel-by-pixel BRET ratio can be calculated with ImageJ, and the numerical ratios visualized with a pseudocolor look-up-table (LUT) (*see* Fig. 3a).

3.4.4 Response of pHlash to Acidification of the Cytoplasm in HeLa Cells

1. In a 4.5 mL glass cuvette, initiate a time-course recording from pHlash transfected HeLa cells with 2.5 μM ViviRen™ in pH 6.1 MES buffer. A stir bar placed on the bottom of the cuvette provides gentle stirring to maintain the cells in suspension.
2. Record the luminescence at 475 nm and 525 nm using the QM-7/SE spectrofluorometer with the excitation beam turned off. After recording for 3 min, add nigericin to a final concentration of 10 μM in 5 μL ethanol (*see* Fig. 3c).
3. For control, prepare another batch of cells and record as before. After recording for 3 min, add the same volume of pH 6.1 MES buffer (including 5 μL ethanol) as that for the nigericin solution described in **step 2** in Subheading 3.4.4 (*see* Fig. 3b).

4 Notes

1. A yeast integrating vector that includes pHlash driven by a constitutively expressed promoter (pRS305-hph-P*ACT1*pHlash) was constructed from the pRS305-hph-P*GAL1*CBG99 backbone [17] as follows. The yeast *ACT1* promoter was amplified by PCR from *S. cerevisiae* genomic DNA (strain S288C) using the 5′ primer ttcactCCCGGGTAAGTAAATAAGACACACGCGAG that contained an *Xma*I overhang, and 3′ primer atgattAGATCTTGTTAATTCAGTAAATTTTCGATC that contained a *Bgl*II overhang. This PCR product was used to replace P*GAL1* of pRS305-hph-P*GAL1*CBG99. A PCR product containing the pHlash CDS was then added in place of the CBG99 CDS of the backbone. This pHlash PCR product was generated from the

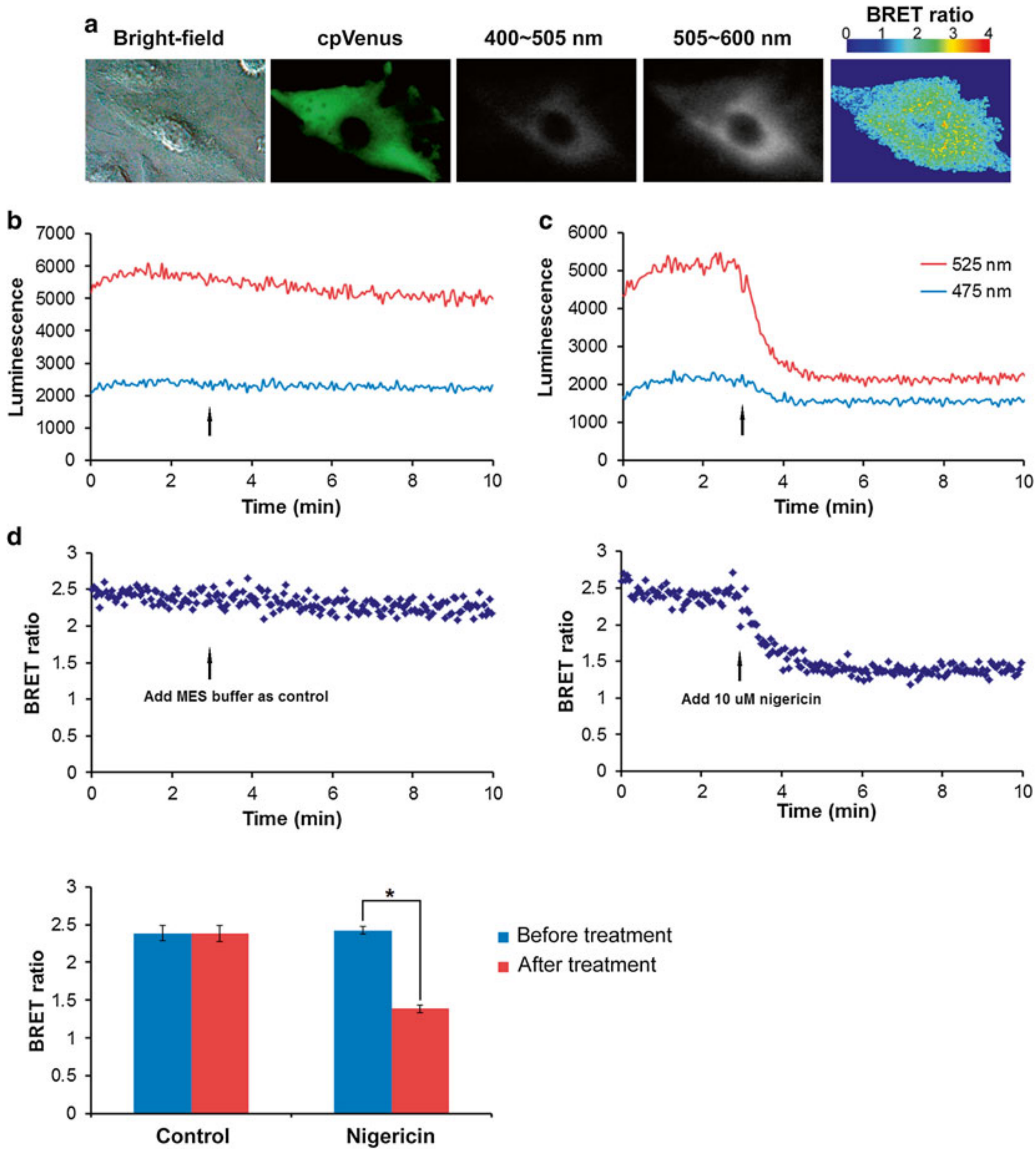

Fig. 3 Response of pHlash to acidification of the cytoplasm in HeLa cells. (**a**) BRET imaging of single pHlash-expressing HeLa cell. Panels from left to right are bright-field, fluorescence from cpVenus, 400–505 nm luminescence, 505–600 nm luminescence, and BRET ratio image. (**b** and **c**) Time-course recording of total luminescence from pHlash -transfected HeLa cells with 2.5 μM ViviRen™ as substrate in pH 6.1 MES buffer (50 mM MES, 130 mM KCl, 1 mM $MgCl_2$, 25 mM NaCl). Luminescent signals were recorded at 475 nm and 525 nm using the QM-7/SE spectrofluorometer. (**b**) Control recording . After 3 min baseline recording, 100 μL MES buffer was added as control. (**c**) Response of pHlash to acidification. After 3 min baseline recording, 10 μM final concentration of nigericin (in 100 μL MES buffer) was added. (**d**) Histogram shows change in BRET ratio change of pHlash -expressing HeLa cells treated with nigericin compared with control. Error bars are +/− S.D

template plasmid pcDNA3.1+-pHlash (Addgene) using the 5′ primer atgattAGATCTATGGCTTCCAAGGTGTACGAC that contained a *Bgl*II overhang, and the 3′ primer ttcactTCTAGATTACTCGATGTTGTGGCGG that contained an *Xba*I overhang. The result was pRS305-hph-P*ACT1*pHlash, a plasmid that integrates into the native yeast *LEU2* gene when the plasmid is linearized with *Afl*II and transformed by the standard lithium acetate method. Yeast transformants can be selected on YPD containing 200 μg/mL hygromycin.

2. BIS-Tris-propane has two pK_a values at 25 °C, 6.8 and 9.0, which give it a wide buffering range from approximately pH 6.0 to 9.5.
3. For in vitro pH calibration, we chose the pH range from 5.4 to 9.0 because the activity of RLuc8 luciferase peaks at neutral pH (~pH 7.0), and decreases at both low and high pH. Beyond the pH 5.4–9.0 range, luminescence is very dim.
4. nCTZ is very sensitive to light and not stable in solution. Stocks are stored at −80 °C. We prepare fresh working solutions before each experiment, and wrap the tubes with aluminum foil to protect nCTZ from light. Keep the working solution on ice. We usually use 10 μM nCTZ for both in vitro and in vivo experiments.
5. Monensin and nigericin are dissolved in ethanol. The stock solutions are stored at −20 °C and added to the permeabilization buffer before use.
6. ViviRen™ is very sensitive to light. We make a 10 mM stock solution in DMSO. Aliquots are stored at −80 °C. We prepare a fresh working solution before each experiment and wrap the tube with aluminum foil to protect the solution from light. During the experiment, the substrate is maintained on ice. For single cell BRET imaging, we use 10 μM ViviRen™ as substrate; and when recording with the QuantaMaster QM-7/SE spectrofluorometer, we reduced the concentration to 2.5 μM.
7. For 500 mL *E. coli* culture, we used 2 mL TALON metal affinity resin (1 mL bed volume). For protein elution, we used an imidazole gradient from 20 mM to 150 mM.
8. The elution buffer we used contained 150 mM imidazole. To remove imidazole, the buffer was exchanged to 30 mM MOPS buffer by dialysis at 4 °C.
9. Calibration curves were derived from measurements of the BRET by two different methods: (I) Emission Scan Mode in the QM-7/SE spectrofluorometer, where the spectrum was continuously scanned from 400 to 600 nm; (II) Two-Wavelength Switching Mode in the QM-7/SE spectrofluorometer, where the monitoring of luminescence emission was alternately switched between 475 nm and 525 nm for measurement of time

courses. In Two-Wavelength Switching Mode in the QM-7/SE spectrofluorometer, the switching requires additional time, so the average time for one cycle to measure luminescence at both 475 nm and 525 nm is about 1.5 s. The calibration curve obtained with the Emission Scan Mode is more linear than that obtained with the Two-Wavelength Switching Mode. However, the Two-Wavelength Switching Mode was needed for the time-course measurements.

10. After adding nCTZ to the sample, mix quickly by swirling the cuvette for 3 s and then start the measurement immediately. Perform each measurement in the same time so that the results obtained can be directly compared.
11. We perform yeast in vivo pH calibration with 8 different pH values from pH 5.5 to 9.0. For each pH value to be tested, we harvest yeast cells from 1 mL yeast culture, wash with distilled water and resuspend with1 mL yeast permeabilization buffer.
12. 24–48 h after transfection, we trypsinize and transfer the cells to 35-mm glass bottom dishes. Culture the cells in DMEM medium without phenol red supplemented with 10% FBS until the cells adhere to the bottom of the dishes.
13. BRET imaging was accomplished using a Dual-View™ micro-imager and a modified EB-CCD camera as described previously [16, 18]. The Dual-View™ consists of a dichroic mirror, which was here selected to split the incoming image at 505 nm (dichroic Q505LPxr) and interference filters to further refine wavelengths below 505 nm (HQ505SP) and above 505 nm (HQ505LP). The use of the Dual-View™ therefore allows the simultaneous acquisition of luminescence images at two wavelengths. A "BRET ratio" image of emission in the two ranges can be calculated thereafter without the complication that the total luminescence intensity may change over the time course of the exposure. Our EB-CCD camera had a GaAsP photocathode with low ion feedback and cooling to −25 °C (Hamamatsu Photonic Systems, Bridgewater NJ, USA). This EB-CCD camera model C7190-13 W has a resolution of 512 × 512 pixels with a pixel size of 24 × 24 μm. The acquisition software was Photonics-WASABI (Hamamatsu). The Dual-View™ and EB-CCD were attached to the bottom port of an IX-71 inverted microscope (Olympus America Inc., Melville NY, USA). This setup allows the measurement of fluorescence using an epifluorescence attachment (EX 500/20 nm, EM 520 LP). The entire IX-71 microscope was enclosed in a temperature-controlled (22–37 °C) light-tight box. The IX-71 microscope was used with an Apo N 60× objective, NA 1.49 (oil immersion, Olympus).
14. Here we use a Light-Emitting Diode flashlight as an excitation source for fluorescence microscopy [19] so that the light source can be rapidly switched on and off without bulb afterglow. This

allows one to immediately begin acquisition of bioluminescent images following fluorescent identification of target samples, and it offers dimer excitation with safer wavelengths for protecting the samples.

References

1. Roos A, Boron WF (1981) Intracellular pH. Physiol Rev 61:296–434
2. Fricker MD, Plieth C, Knight H, Blancaflor E, Knight MR, White NS, Gilroy S (1999) Fluorescence and luminescence techniques to probe ion activities in living plant cells. In: Mayson WT (ed) *Fluorescent and Luminescent Probes for Biological Activity.* Academic Press, San Diego, pp 569–596
3. Miesenbock G, De Angelis DA, Rothman JE (1998) Visualizing secretion and synaptic transmission with pH-sensitive green fluorescent proteins. Nature 394:192–195
4. Kneen M, Farinas J, Li Y, Verkman AS (1998) Green fluorescent protein as a noninvasive intracellular pH indicator. Biophys J 74:1591–1599
5. Schulte A, Lorenzen I, Böttcher M, Plieth C (2006) A novel fluorescent pH probe for expression in plants. Plant Methods 2:1–13
6. Ugarova NN, Maloshenok LG, Uporov IV, Koksharov MI (2005) Bioluminescence spectra of native and mutant firefly luciferases as a function of pH. Biochemistry (Moscow) 70:1534–1540
7. Matthews JC, Hori K, Cormier MJ (1977) Purification and properties of *Renilla* reniformis luciferase. Biochemistry 16:85–91
8. Verhaegen M, Christopoulos TK (2002) Recombinant *Gaussia* luciferase. Overexpression, purification and analytical application of a bioluminescent reporter for DNA hybridization. Anal Chem 74:4378–4385
9. Branchini BR, Ablamsky DM, Rosenberg JC (2010) Chemically modified firefly luciferase is an efficient source of near-infrared light. Bioconjugate Chem 21:2023–2030
10. Hall MP, Unch J, Binkowski BF, Valley MP, Butler BL, Wood MG, Otto P, Zimmerman K, Vidugiris G, Machleidt T, Robers MB, Benink HA, Eggers CT, Slater MR, Meisenheimer PL, Klaubert DH, Fan F, Encell LP, Wood KV (2012) Engineered luciferase reporter from a deep sea shrimp utilizing a novel imidazopyrazinone substrate. ACS Chem Biol 7:1848–1857
11. Loening AM, Fenn TD, Wu AM, Gambhir SS (2006) Consensus guided mutagenesis of *Renilla* luciferase yields enhanced stability and light output. Protein Eng Des Sel 19:391–400
12. Nagai T, Yamada S, Tominaga T, Ichikawa M, Miyawaki A (2004) Expanded dynamic range of fluorescent indicators for Ca^{2+} by circularly permuted yellow fluorescent proteins. Proc Natl Acad Sci U S A 101:10554–10559
13. Xu Y, Piston D, Johnson CH (1999) A bioluminescence resonance energy transfer (BRET) system: application to interacting circadian clock proteins. Proc Natl Acad Sci U S A 96:151–156
14. Zhang Y, Xie Q, Roberson JB, Johnson CH (2012) pHlash: A new genetically encoded and ratiometric luminescence sensor of intracellular pH. PLoS One 7, e43072
15. Brett CL, Tukaye DN, Mukherjee S, Rao R (2005) The yeast endosomal $Na^+(K^+)/H^+$ exchanger Nhx1 regulates cellular pH to control vesicle trafficking. Mol Biol Cell 16:1396–1405
16. Xu X, Soutto M, Xie Q, Servick S, Subramanian C et al (2007) Imaging protein interactions with bioluminescence resonance energy transfer (BRET) in plant and mammalian cells and tissues. Proc Natl Acad Sci U S A 104: 10264–10269
17. Krishnamoorthy A, Robertson JB (2015) Dual color monitoring overcomes limitations of single bioluminescent reporters in fast growing microbes and reveals phase-dependent protein productivity during metabolic rhythms of yeast. Appl Environ Microbiol 81: 6484–6495
18. Xie Q, Soutto M, Xu X, Zhang Y, Johnson CH (2011) Bioluminescence resonance energy transfer (BRET) imaging in plant seedlings and mammalian cells. Methods Mol Biol 680:3–28
19. Roberson JB, Zhang Y, Johnson CH (2009) Light-emitting diode flashlights as effective and inexpensive light sources for fluorescence microscopy. J Microsc 236:1–4

Chapter 10

A Protein–Protein Interaction Assay FlimPIA Based on the Functional Complementation of Mutant Firefly Luciferases

Yuki Ohmuro-Matsuyama and Hiroshi Ueda

Abstract

There is a significant focus on detecting and assaying protein–protein interactions (PPIs) in biology and biotechnology. Protein-fragment complementation assay (PCA) is one of the most widely used methods to detect PPI by splitting the enzyme-coding or fluorescent protein-coding polypeptide, as well as Förster resonance energy transfer (FRET). Here, we describe a novel PPI assay FlimPIA (firefly luminescent intermediate-based protein–protein interaction assay) by a unique approach of splitting the two major catalytic steps (half reactions) of firefly luciferase (FLuc).

Key words Protein–protein interaction, Firefly luciferase, Substrate channeling, Reaction intermediate, Luciferyl adenylate

1 Introduction

The human interactome is predicted to contain 150,000 to 300,000 protein–protein interactions (PPIs) [1, 2]. To discover and investigate PPI, exploration of novel PPI assay is considered highly important.

Firefly luciferase (FLuc) is a monooxygenase that produces excited state oxyluciferin (OxL) from firefly d-luciferin (LH_2) by multistep catalysis. The reactions can be divided into two half-reactions, ATP-driven luciferin adenylation and subsequent oxidative reaction as shown in Fig. 1a.

Recent reports revealed that the adenylation reaction and the subsequent oxidative luminescent reaction are each catalyzed by two different FLuc conformations [3, 4]. FLuc is consisted of N- and C- terminal domains connected by a hinge region [5, 6], and the latter rotates ~140° according to the reactions to proceed from the adenylation to the oxidative luminescent reactions (*see* Fig. 1b). By dividing the half reactions each catalyzed by different conformations, we made a novel PPI assay, FlimPIA.

Sung-Bae Kim (ed.), *Bioluminescence: Methods and Protocols*, Methods in Molecular Biology, vol. 1461,
DOI 10.1007/978-1-4939-3813-1_10, © Springer Science+Business Media New York 2016

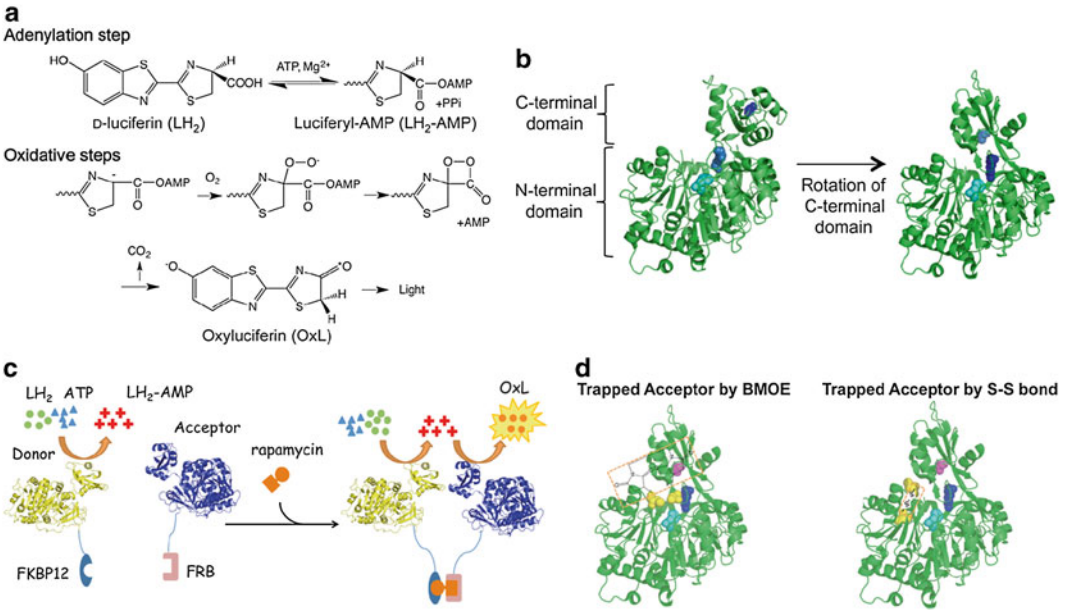
a
Adenylation step
ATP, Mg2+
D-luciferin (LH2)
Luciferyl-AMP (LH2-AMP)
Oxidative steps
Light
Oxyluciferin (OxL)
b
C-terminal domain
N-terminal domain
Rotation of C-terminal domain
c
LH2 ATP
LH2-AMP
Donor
Acceptor
rapamycin
OxL
FKBP12
FRB
d
Trapped Acceptor by BMOE
Trapped Acceptor by S-S bond

Fig. 1 Working mechanism of FlimPIA. (**a**) Chemical reactions catalyzed by firefly luciferase (FLuc). FLuc produces excited state oxyluciferin (OxL) from d-Luciferin (LH_2) by a two-step catalysis: the adenylation step and the oxidative steps. (**b**) The conformation of FLuc for each catalytic step. FLuc is composed of a large N-terminal domain and a smaller C-terminal domain, which rotates ~140° according to the reactions to proceed from the adenylation reaction to the oxidative luminescent reaction: Key Lys residues (K529 and K443) are shown in *light* and *dark blue*, respectively. H245 is shown in cyan. (**c**) Schematic representation of FlimPIA. FLuc (Donor) exhibits very low activity in the oxidative steps, while FLuc (Acceptor) exhibits low activity in the adenylation step. When they are in close proximity, LH_2-AMP produced by the Donor is more efficiently oxidized by the Acceptor, which results in stronger light emission upon interaction. (**d**) The entrapped Acceptors by BMOE (*left*) and a disulfide bond (*right*). Residues shown in the yellow are used for the linkage. Reproduced from Ohmuro-Matsuyama et al. with permission from American Chemical Society. [11]

We devised two FLuc mutants, the "Donor" of the reaction intermediate luciferyl adenylate (LH_2-AMP), and the "Acceptor" of LH_2-AMP, and applied them to FlimPIA. After screening of several mutant enzymes in the reports [7–10] and their combinations, H245D/K443A/L530R with very low oxidative luminescent activity was chosen as a Donor. For the first generation FlimPIA, K529Q with low adenylation activity was employed as the Acceptor (*see* Fig. 1b).

To apply these mutants to PPI assay, one each of an interacting protein pair was fused to the N-terminus of the Donor and the Acceptor. When the distance between the Donor and the Acceptor became shorter by the interaction, the more abundant LH_2-AMP around the Donor lead to the production of OxL by the Acceptor, which resulted in higher luminescence (*see* Fig. 1c) [11].

However, the first generation FlimPIA suffered from the background signal due to the original Acceptor. To reduce this background signal caused from the remaining adenylation activity of the original Acceptor, one each of residues in N- and C-terminal domain, respectively, is substituted with Cys, to entrap the conformation of the Acceptor to the oxidation one, either chemically (Acceptor-cc1, -cc2) or by disulfide bonding (Acceptor-cc3), (*see* Fig. 1d) [12]. Branchini et al. could capture FLuc into the oxidation conformation by chemical trapping using a crosslinking reagent 1,2-bis (maleimide) ethane (BMOE) [3]. Here, Acceptor-cc1 is made according to the same strategy. FlimPIA using Acceptor-cc1 has successfully abolished most of its background luminescence, while it showed considerably reduced luminescent intensity compared with the original Acceptor due to the substitution of all native Cys for avoiding mis-trapping. To solve this problem, the original Acceptor retaining all native Cys is made (Acceptor-cc2). However, the crosslinking reaction by BMOE needs careful tuning of the reaction to get effective background suppression, even if Acceptor-cc1 is used. Then, as an alternative and more practical method, the conformation of the Acceptor is captured through a disulfide bond, which has a short Cα-Cα distance that can be specifically formed (Acceptor-cc3). Both the merits and the demerits of the improved Acceptors are summarized in Table 1.

FlimPIA was revealed to have several advantages over conventional PPI assays [12, 13]. First, the probes are fourfold more stable than those of PCA using split FLuc (FLuc PCA) at 37 °C. Second, the signal is more than tenfold higher than that of FLuc PCA. Third, the signal-to-background ratio (S/B ratio) is higher than that of FRET. Fourth, the sensitivity is higher than that of FLuc PCA. Finally, the detectable dimension between the interacting proteins (7 nm) is larger than that of FP-based FRET or FLuc PCA.

Table 1
Comparison of three acceptors

	Merits	Demerits
Acceptor-cc1	• Negligible background luminescence • Highest S/B ratio among the three Acceptors.	• Lowest luminescent intensity. • The determination of reaction condition to attain sufficiently high crosslinking yield is somewhat difficult.
Acceptor-cc2	• Highest luminescent intensity among the three Acceptors.	• The long linker length (BMOE ~ 8.0 Å) might allow undesirable miss-crosslinking between one Cys in BD and another in the FLuc. • Lower S/B ratio than that of Acceptor-cc1.
Acceptor-cc3	• No chemical reaction needed. • Low possibility of undesirable miss-crosslinking between one Cys in BD and another in the Fluc.	• Lower S/B ratio than that of Acceptor-cc1.

2 Materials

Prepare all solutions using ultrapure water (made by purifying deionized water to attain resistivity of 18 MΩ cm at 25 °C). For all the reagents, use them of the highest grade available.

1. ATP and LH_2 are from Sigma, St. Louis, MO. 3-Morpholinopropanesulfonic acid (MOPS) (Dojindo, Kumamoto, Japan).
2. QuikChange Site-Directed Mutagenesis kit and QuikChange Multi Site-Directed Mutagenesis kit (Agilent Technologies, Santa Clara, CA).
3. *E. coli* JM109 competent cells (SciTrove, Tokyo, Japan).
4. SHuffle T7 express lysY competent cells (New England Biolabs, Tokyo, Japan).
5. Rapamycin (LKT Laboratories, St. Paul, MN).
6. 1,2-Bismaleimidoethane (BMOE) (Pierce Biotechnology, Thermo Fisher Scientific, Waltham, MA).
7. Isopropyl-β-d-thiogalactopyranoside (IPTG) (Wako, Osaka, Japan).
8. The white half-area multiwell plate (Costar 3693) (Corning-Costar, Osaka, Japan).
9. pGEM-luc (Promega, Madison, WI).
10. pET32b (Merck, Darmstadt, Germany).
11. The ultrasonifier (Taitec, Saitama, Japan).
12. TALON Metal Affinity Resin and TALON Disposable Gravity Column (Clontech, CA).
13. Toyopearl HW-40S gel (Tosoh, Tokyo, Japan).
14. TALON extraction buffer: 300 mM NaCl, 50 mM Sodium phosphate, adjusted to pH 7.0.
15. TALON elution buffer: 150 mM of imidazole in TALON extraction buffer.
16. MOPS buffer: 100 mM MOPS, 10 mM $MgSO_4$, pH 7.3.
17. Substrate solution (2×): 20 mM ATP, and 150 μM LH_2 in MOPS buffer.
18. The reaction mixture (1×) to synthesize LH_2-AMP: 10 mM ATP, 300 μM LH_2, 1 mg/mL bovine serum albumin and 2 μM of the Donor in MOPS buffer.
19. MR buffer: 50 mM sodium phosphate, 100 mM NaCl, 1 mM EDTA, pH 7.0.

To apply the Donor and the Acceptor to a PPI assay, each enzyme should be fused with a pair of binding domains (BDs). Here, the protocol is described for a well-known interacting protein pair, the FK506-binding protein 12 (FKBP12) and the FKBP-rapamycin-associated protein (FRB), as an example (*see* **Note 1**). They associate in an antibiotic rapamycin-dependent manner. Synthetic genes for *E. coli* codon-optimized human FKBP12 and FRB, appended with *Nco*I/*Sfi*I and *Not*I sites at the 5′ and 3′ ends, respectively, were synthesized by Mr gene GmbH, Regensburg, Germany (now under Life Technologies). However, other qualified supplier of synthetic DNA will be also used.

For the measurement, we use a multiwell luminometer AB-2350 equipped with an injector (ATTO, Tokyo, Japan). The fluorescent spectrometer FP-8500 is from Jasco, Tokyo, Japan.

3 Method

3.1 Construction of FKBP/FRB Fused FLuc Expression Vector

1. Amplify the DNA fragment encoding FLuc derived of *Photinus pyralis* by PCR using pGEX-Ppy [7] or pGEM-luc as a template, and primers NotG4SBack encoding a G_4S linker and *Not*I site and XhoFor containing *Xho*I site.
2. Digest the amplified fragment with the corresponding restriction enzymes, *Not*I and *Xho*I, and subclone into pET32b between the *Not*I and *Xho*I sites.
3. Digest the synthetic fragments encoding FKBP12 and FRB (binding domains, BDs) cDNAs with *Nco*I and *Not*I, and ligate each fragment with pET32b digested with *Nco*I and *Not*I (*see* **Note 2**).
4. Transform JM109 competent cells with the ligation mixture.
5. Culture the cells on LB agar plate containing 100 μg/mL ampicillin (LBA agar plate) overnight at 37 °C.
6. Pick some colonies, and culture in 4 mL LB liquid medium containing 100 μg/mL ampicillin (LBA medium) overnight.
7. Extract the plasmid, and confirm the nucleotide sequence of whole open reading frame.

3.2 Construction of pET32/BD/ Donor

1. To make H245D/K443A/L530R/E354K mutant as the Donor, conduct a series of site-directed mutagenesis with QuikChange Site-directed kit according to the manufacturer's protocol. Use pET32/BD/FLuc as the template, and the primers H245D, K443A, L530R, and E354K, with their complementary strands (*see* **Note 3**).
2. After PCR, add 1 μL of *Dpn*I (~10 U) to the reaction mixture to digest the methylated template, by incubating for 1 h at 37 °C. Transform JM109 competent cells, with a part of the digested template.
3. Culture the cells on LBA agar plate.

4. Pick some colonies and culture each colony in 4 mL LBA medium.
5. Extract the plasmid and confirm the nucleotide sequences.

3.3 Construction of pET32/BD/Acceptor

1. To make a K529Q mutant as the Acceptor, perform QuikChange site-directed mutagenesis using pET32/BD/FLuc as a template and the following primer pairs with their complementary strands: K529Q, and E354K used in **step 1** in Subheading 3.2.
2. Follow the **steps 2**–**5** in Subheading 3.2.

3.4 Construction of pET32/BD/Acceptor-cc1

1. To remove all Cys residues and also add thermo-stabilization mutations to the Acceptor enzyme, conduct a series of site-directed mutagenesis with QuikChange Multi Site-directed mutagenesis kit according to the manufacturer's instructions. Use pET32/BD/FLuc as a template, and following oligonucleotides as the primers: for substitution to Cys: Y447CPac– and I108CNar+; for thermo-stabilization, 232mutMro–, 295mutMsc+; for substitution of original Cys, C81S, C251S, C391S; for both, 214-216mutSac+.
2. Follow the **steps 2**–**5** described in Subheading 3.2 (Table 2).

3.5 Construction of pET32/BD/Acceptor-cc2

1. Substitute the residues of the original Acceptor at position 108 and 447 to Cys as described in Subheading 3.4.
2. Follow the **steps 2**–**5** described in Subheading 3.2.

3.6 Construction of pET32/BD/Acceptor-cc3

1. Substitute the residues of the original Acceptor at position 204 and 402 with Cys by QuikChange site-directed mutagenesis using the primers, L204CEcoT+ and V402CMro– for substitution of Cys.
2. Follow the procedure of **steps 2**–**5** described in Subheading 3.2.

3.7 Construction of FLuc N-terminal Domain Expression Vector

1. To make an expression vector for the FLuc N-terminal domain (N-domain, to be used in Subheading 3.9), obtain the DNA fragment encoding the N-domain sequence (1–437 aa) of FLuc by PCR using FKBP/FRB-fused FLuc expression vector as a template, and the primers NotG4SBack and 437XhoFor containing *Xho*I site.
2. Digest the amplified fragment with *Not*I and *Xho*I, and ligate with pET32b digested with *Not*I and *Xho*I.
3. Transform JM109 competent cells with the ligation mixture, and follow the **steps 5**–**7** in Subheading 3.1.

3.8 Expression and Purification of the Enzymes

1. Transform SHuffle T7 Express lysY competent cells with pET32/BD/Donor and pET32/BD/Acceptor (*see* **Note 4**).
2. Incubate the transformed *E. coli* on a LBA agar plate at 30 °C for 24 h.

Table 2
List of oligonucleotide primers used[a]

	Sequence
NotG4SBack	5′-ggcgcgccgcggccgccggtggtggtggtagcatggaagacgccaaaaacataaag-3′
XhoFor	5′-ggcgcgcctcgagctttccgcccttcttggcct-3′
H245D	5′-gttccattccatGacggttttggaatgt-3′
K443A	5′-gacctcttgaagtctttaattGCatacaaaggatatcaggtggc-3′
L530R	5′-ccgaaaggtcttaccggtaaacTcgacgcaagaaaaatca-3′
E354K	5′-ttctgattacacccaGAggggatgattaa-3′
K529Q	5′-ccgaaaggtcttaccggtCRRctcgacgcaagaaaatcagagag-3′
232mutMro-	5′-cctatttttggcaatcaaatcGCGccggatactgcgattttaagtg-3′
295mutMsc+	5′-ccaaccctattttcattcctGGCcaaaagcactctgattgac-3′
C81S	5′-cacaaatcacagatcgtcgtaagcagCgaaaactctcttcaattc-3′
C251S	5′-gaatgtttactacactcggatatCtgatatctggatttcgagtcgtc-3′
C391S	5′-cagagaggcgaattatCtgtcagagggcctatgattatg-3′
214-216mutSac+	5′-ggtgtggcccttccgcatagaGctCTcGCcgtcagattctcgcatgcc-3′
Y447CPac-	5′-gaagtctttaataaaatacaaaggatAtcaggtggcccccgctg-3′
I108CNar+	5′-ggagttgcagtggcgcccgcgaacgacTGttataatgaacgtg-3′
L204CEcoT+	5′-tctggatctactgggtGCccCaagggtgtggcccttccg-3′
V402CMro-	5′-cctatgattatgtccggttatTGCaacaaCccggaagcgaccaac-3′
437XhoFor	5′-ggcgcgcctcgaggcggtcaactatgaagaagtg-3′

[a] The underlined nucleotides are the restriction sites for subcloning. The capital letters represent mutated nucleotides (*see* **Note 14**)

3. Pick one colony up, and culture it in 4 mL LBA medium at 30 °C.
4. Centrifuge 0.4 mL of **step 3**, and collect the pellet to remove secreted β-lactamase from the pre-cultured *E. coli*.
5. Resuspend the pellet with 100 mL of LBA medium in a 500-mL flask, and culture in 30 °C.
6. When the OD_{600} reaches 0.4–0.6, add 40 μM of IPTG, and culture the cells at 16 °C.
7. Centrifuge and collect the cells, and resuspend the pellet with 10 mL of the TALON extraction buffer.
8. Sonicate the *E. coli* on ice using an ultrasonifier for 2 min (50% interval) five times (*see* **Note 5**).
9. Centrifuge the sonicated solution at 11,000 × *g* for 20 min.
10. Add 200 μL of TALON Metal Affinity Resin to the supernatant, and rotate or shake gently for 20 min.

11. Centrifuge at 700 ×*g* for 2 min, and resuspend the resin with 10 mL of TALON extraction buffer.
12. Rotate or shake gently for 10 min.
13. Repeat **steps 11** and **12** two times.
14. Centrifuge at 700 ×*g* for 2 min, and collect the resin.
15. Suspend the resin with 3 mL of TALON extraction buffer, and put the suspension into a TALON 2-mL Disposable Gravity Column.
16. Allow to drain until it reaches the top of the resin bed.
17. Wash the column with 2 mL of TALON extraction buffer.
18. Elute the enzyme with 500 μL of TALON elution buffer (*see* **Note 6**).

3.9 Synthesis, Detection, and Purification of LH_2-AMP [7]

1. The reaction mixture is made up with a final volume of 500 μL.
2. Incubate the mixture at 37 °C for 5 min, and add 50 μL of 1 M HCl to stop the reaction (*see* **Note** 7).
3. Apply the mixture to a small column containing 2 mL of Toyopearl HW-40S gel equilibrated with water, which is adjusted to pH 3.5 using HCl, and collect fractions of 1 μL using water (pH 3.5) (*see* **Note 8**).
4. To identify the fractions containing LH_2-AMP, react a part of each fraction with 1 μM of the N-domain of FLuc (*see* Subheading 3.2) in MOPS buffer, because the reaction of N-domain with LH_2-AMP displays a higher luminescent intensity than the reaction with LH_2 and ATP (*see* **Note 9**).
5. To confirm the fraction containing LH_2-AMP and determine the concentration of LH_2-AMP in the fraction, measure the fluorescent spectrum and intensity of each fraction using a fluorescence spectrometer, FP-8500. When these fractions are excited at 327 nm, the peak of the fluorescent spectrum of LH_2-AMP is at approximately 535 nm. On the other hand, the peak of the fluorescent spectrum of LH_2 is at approximately 529 nm. From the fluorescent intensity of the fraction containing LH_2-AMP at 535 nm, the concentration of LH_2-AMP in the fraction can be estimated by using the fluorescent intensity of LH_2 at 529 nm as a standard. When the peak values of LH_2-AMP and x nM of LH_2 are y and z, respectively, the concentration of LH_2-AMP can be determined as follows (*see* **Note 10**).

$$\text{The concentration of } LH_2\text{-AMP (nM)} = \frac{x \times y}{z \times 0.45}$$

3.10 Chemical Crosslinking of Acceptor-cc1 and Acceptor-cc2

1. Change the buffer containing the purified Acceptor to an MR buffer by ultrafiltration or dialysis.
2. React 5 μM of the Acceptor with 20 μM of BMOE at 20 °C for 1 h.

3.11 Measurement of Overall Luminescent Activity

1. Suspend the enzyme in a MOPS buffer.
2. Dispense 50 μL of the solution to a well of 96-well plate or a tube for a luminometer.
3. Measure the light intensity after injection of 50 μL of 2× substrate solution. When the adenylation activity of the Acceptor is suppressed, lower luminescent intensity is detected.

3.12 Measurement of Oxidative Luminescent Activity

1. Suspend the enzyme in MOPS buffer.
2. Dispense 50 μL of the solution to a well of 96-well plate or a tube for a luminometer.
3. Measure the light intensity after injection of 50 μL of LH_2-AMP diluted in MOPS buffer.

3.13 FlimPIA

1. Suspend Donor and Acceptor with or without equimolar amount of rapamycin in the MOPS buffer.
2. Dispense the mixture (50 μL) to a well of 96-well plate or a tube for a luminometer.
3. Measure the light intensity after injection of 50 μL of 2× substrate solution with a periodical integration of 0.1 s with a luminometer, up to 4 s (*see* Figs. 2 and 3) (*see* **Notes 11–13**). Measure the samples with and without interaction, i.e. ± equimolar rapamycin, to calculate S/B ratio.

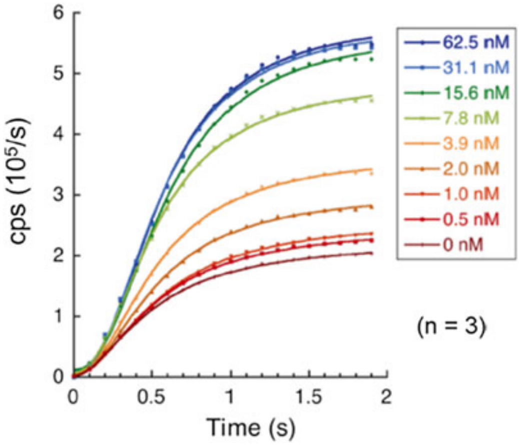

Fig. 2 FlimPIA with the conventional Acceptor. FKBP/Donor and FRB/Acceptor (50 nM each) was added with the indicated concentrations of rapamycin. The longitudinal axis; the luminescent intensity; the horizontal axis; time after adding substrates. Reproduced from Ohmuro-Matsuyama et al. with permission from American Chemical Society [11]

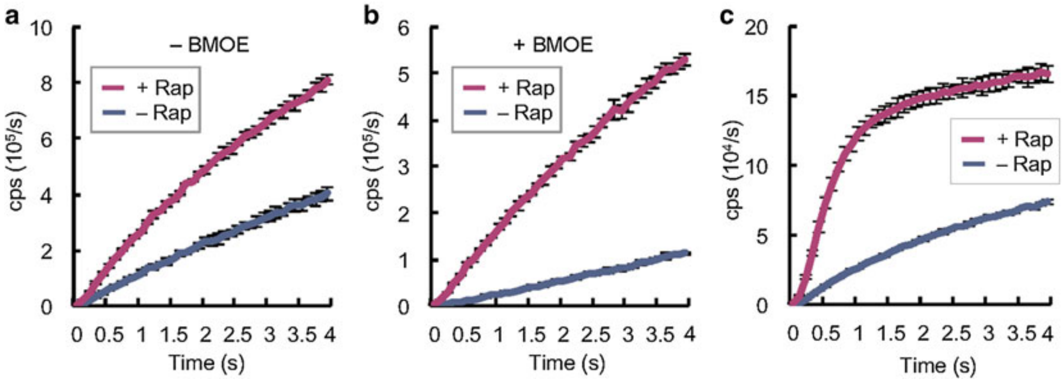

Fig. 3 FlimPIA with the improved Acceptors. (**a**) FlimPIA with Acceptor-cc2. The mixture of FKBP/Donor and FRB/Acceptor-cc2 (50 nM each) was added with/without 50 nM rapamycin (*n* = 3). (**b**) FlimPIA with Acceptor-cc2. The mixture of FKBP/Donor and trapped FRB/Acceptor-cc2 (50 nM each) was added with/without 50 nM rapamycin (*n* = 3). (**c**) FlimPIA with Acceptor-cc3. The mixture of FKBP/Donor and FRB/Acceptor-cc3 (50 nM each) was added with/without 50 nM rapamycin (*n* = 3). Reproduced from Ohmuro-Matsuyama et al. with permission from American Chemical Society [11]

4 Notes

1. Rapamycin, a potent immunosuppressive reagent, binds to two proteins: to FKBP12 and subsequently to FRB.
2. BD should be fused to the N-terminal of FLuc, because the S/B ratio becomes significantly lower when it is fused to the C-terminus. The fusion to the C-terminal of FLuc hampers the rotation of the C-terminal domain in the process from the adenylation to the oxidative luminescent reactions.
3. E354K is a mutation to confer thermostability.
4. SHuffle T7 Express lysY is an engineered *E. coli* B strain to express proteins containing disulfide bonds in the cytoplasm. Constitutively expressed disulfide bond isomerase DsbC promotes the correction of mis-oxidized proteins into their correct form, and also works as a chaperone that can assist in the folding of proteins that do not require disulfide bonds.
5. From this step to **step 18**, the samples must be kept on ice.
6. The purified enzyme in the buffer containing 15 % glycerol can be stored for several months at −80 °C.
7. The oxidative luminescent reaction of Donor is almost abolished, therefore LH_2-AMP is accumulated in the reaction mixture.
8. The fractions containing LH_2-AMP elute earlier than the fractions containing LH_2 and ATP.
9. The N-domain derived of *Photinus pyralis* shows a very weak and slow increase of bioluminescence when added with LH_2

and ATP. However, it emits quicker and brighter luminescence upon adding LH_2-AMP. Therefore we can selectively quantify LH_2-AMP in the sample.

10. LH_2-AMP can be stored at −80 °C before use up to 3 months.
11. The signal intensity and S/B ratio of FlimPIA are strongly influenced by the concentration of probes. Optimize the concentration between 10 nM and 1 μM.
12. The signal intensity and S/B ratio of FlimPIA are also influenced by the temperature. Set the temperature of the luminometer between 30 and 32 °C.
13. The maximum S/B ratio is usually observed between 0.3 and 1 s after injecting substrates. The longer reaction time (>1 s) gives the higher background luminescence due to the accumulation of LH_2-AMP in the reaction mixture.
14. Each primer is named as follows: The products obtained with the primers 232mutMro− and V402CMro− will lose an *Mro*I restriction site, while the product amplified with 295mutMsc+ will gain a new *Msc*I restriction site, etc.

Acknowledgment

We thank B. Branchini for providing inspiration for the project. This project was supported by SENTAN, JST, Japan, and partly by the "Leave a Nest" Microtech Nichion award.

References

1. Venkatesan K, Rual JF, Vazquez A, Stelzl U, Lemmens I, Hirozane-Kishikawa T, Hao T, Zenkner M, Xin X, Goh KI, Yildirim MA, Simonis N, Heinzmann K, Gebreab F, Sahalie JM, Cevik S, Simon C, de Smet AS, Dann E, Smolyar A, Vinayagam A, Yu H, Szeto D, Borick H, Dricot A, Klitgord N, Murray RR, Lin C, Lalowski M, Timm J, Rau K, Boone C, Braun P, Cusick ME, Roth FP, Hill DE, Tavernier J, Wanker EE, Barabasi AL, Vidal M (2009) An empirical framework for binary interactome mapping. Nat Methods 6:83–90
2. Zhan QC, Petrey D, Deng L, Qiang L, Shi Y, Thu CA, Bisikirska B, Lefebvre C, Accili D, Hunter T, Maniatis T, Califano A, Honig B (2012) Structure-based prediction of protein-protein interactions on a genome-wide scale. Nature 490:556–560
3. Branchini BR, Rosenberg JC, Fontaine DM, Southworth TL, Behney CE, Uzasci L (2011) Bioluminescence is produced from a trapped firefly luciferase conformation predicted by the domain alternation mechanism. J Am Chem Soc 133:11088–11091
4. Sundlov JA, Fontaine DM, Southworth TL, Branchini BR, Gulick AM (2012) Crystal structure of firefly luciferase in a second catalytic conformation supports a domain alternation mechanism. Biochemistry 51:6493–6495
5. Conti E, Franks NP, Brick P (1996) Crystal structure of firefly luciferase throws light on a superfamily of adenylate-forming enzymes. Structure 4:287–298
6. Nakatsu T, Ichiyama S, Hiratake J, Saldanha A, Kobashi N, Sakata K, Kato H (2006) Structural basis for the spectral difference in luciferase bioluminescence. Nature 440:372–376
7. Ayabe K, Zako T, Ueda H (2005) The role of firefly luciferase C-terminal domain in efficient coupling of adenylation and oxidative steps. FEBS Lett 579:4389–4394
8. Branchini BR, Murtiashaw MH, Magyar RA, Anderson SM (2000) The role of lysine 529, a

conserved residue of the acyl-adenylate- forming enzyme superfamily, in firefly luciferase. Biochemistry 39:5433–5440

9. Branchini BR, Southworth TL, Murtiashaw MH, Wilkinson SR, Khattak NF, Rosenberg JC, Zimmer M (2005) Mutagenesis evidence that the partial reactions of firefly bioluminescence are catalyzed by different conformations of the luciferase C-terminal domain. Biochemistry 44:1385–1393
10. Fujii H, Noda K, Asami Y, Kuroda A, Sakata M, Tokida A (2007) Increase in bioluminescence intensity of firefly luciferase using genetic modification. Anal Biochem 366:131–136
11. Ohmuro-Matsuyama Y, Nakano K, Kimura A, Ayabe K, Ihara M, Wada T, Ueda H (2013) A protein-protein interaction assay based on the functional complementation of mutant firefly luciferases. Anal Chem 85:7935–7940
12. Ohmuro-Matsuyama Y, Hara Y, Ueda H (2014) Improved protein-protein interaction assay FlimPIA by the entrapment of luciferase conformation. Anal Chem 86:2013–2018
13. Ohmuro-Matsuyama Y, Chung CI, Ueda H (2013) Demonstration of protein-fragment complementation assay using purified firefly luciferase fragments. BMC Biotechnol 13:31

Chapter 11

Single-Chain Probes for Illuminating Androgenicity of Chemicals

Sung-Bae Kim and Hiroaki Tao

Abstract

The present protocol introduces a single-chain probe carrying a functional peptide in the N-terminal domain of the androgen receptor (AR NTD) for illuminating androgenicity of ligands. In the single-chain probe, a functional peptide in the AR NTD was genetically fused to the ligand-binding domain of AR (AR LBD) via a flexible linker, and then sandwiched between the N- and C-terminal fragments of split-firefly luciferase (FLuc) dissected at D415. This single-chain probe exerts (1) a high signal-to-background ratio and (2) sensitive discrimination between agonists and antagonists, where the dimerization of AR LBD is not involved. The present protocol guides a fundamental methodology on how to discriminate weak protein–protein (peptide) binding, and provides a new insight into the intramolecular folding inside monomeric AR.

Key words Single-chain probe, Bioluminescence, Androgen receptor, Androgenicity, Firefly luciferase

1 Introduction

Androgen receptor (AR) is a member of the nuclear receptor (NR) super family that acts as a ligand-dependent transcriptional regulator. Upon stimulation with androgen, monomeric AR undergoes an androgen-specific intramolecular interaction between the N-terminal domain (NTD) and the ligand-binding domain (LBD) [1, 2].

This androgen-induced intramolecular interaction is mediated by two LXXLL-like peptide sequences in the AR NTD, i.e., ^{23}FQNLF^{27} and ^{433}WHTLF^{437} (L = leucine (hydrophobic), F = phenylalanine (hydrophobic), X = any amino acid). A previous sequence analysis of AR NTD revealed five predicted amphipathic α-helices that resemble LXXLL core sequences at residues 21–34, 177–201, 351–359, 395–405, and 432–434 [3–5]. However, their interactions with AR LBD are unfortunately weak, and thus difficult to be estimated with conventional methodologies.

The present protocol introduces an advanced methodology to illuminate weak protein–protein interactions (PPIs) in mammalian

Sung-Bae Kim (ed.), *Bioluminescence: Methods and Protocols*, Methods in Molecular Biology, vol. 1461, DOI 10.1007/978-1-4939-3813-1_11, © Springer Science+Business Media New York 2016

cells with a single-chain probe. In the single-chain probe, the functional peptide of interest is fused to the AR LBD and sandwiched between the N- and C-terminal fragments of firefly luciferase (FLuc). The probe exerts an excellent signal-to-background ratio (S/B ratio) with a 100-times-improved detection limit to androgens. The detailed procedure is specified with the corresponding examples sensing androgenicity of natural steroid hormones and man-made chemicals.

2 Reagents

2.1 Mammalian Cells

1. Chinese hamster ovary-derived CHO cells.
2. Human cervical carcinoma-derived HeLa cells.
3. African green monkey kidney fibroblast-derived COS-7 cells.
4. Human breast cancer-derived MCF-7 cells.

2.2 Ligands for Stimulating Single-Chain Probes

1. Flutamide, a synthetic, nonsteroidal antiandrogen.
2. Cyproterone acetate (CPA), a synthetic, steroidal antiandrogen.
3. 5α-dihydrotestosterone (DHT), a natural endogenous androgen.

2.3 Cell Growing Reagents

1. Penicillin-Streptomycin (P/S).
2. Dulbecco's modified eagle's medium (DMEM; Sigma).
3. Steroid-free fetal bovine serum (FBS).

2.4 Genetic Engineering Reagents

1. pcDNA 3.1(+) vector (Invitrogen), a mammalian expression vector.
2. pTransLucent vector (Panomics), a reporter vector comprising the AR-recognition element (ARE) and cDNA encoding FLuc as a reporter.
3. A cDNA template encoding a full-length AR.
4. BigDye Terminator Cycle Sequencing kit, a sequencing reagent kit,
5. TransIT-LT1 (Mirus), a lipofection reagent

2.5 Assay Reagents

1. Bright-Glo, an assay kit comprising D-Luciferin (Promega).

3 Methods

3.1 Design of a Single-Chain Probe for Imaging Ligand-Activated Intramolecular Folding of Androgen Receptor

A single-chain probe illuminating a ligand-activated molecular folding of androgen receptor (AR) is designed as follows (*see* Figs. 1 and 2):

1. Download the amino acid sequence of human AR from a public database, NCBI.
2. Predict the α-helical structure in the N-terminal domain (NTD) with a public 2-dimension prediction algorism (e.g., Hierarchical

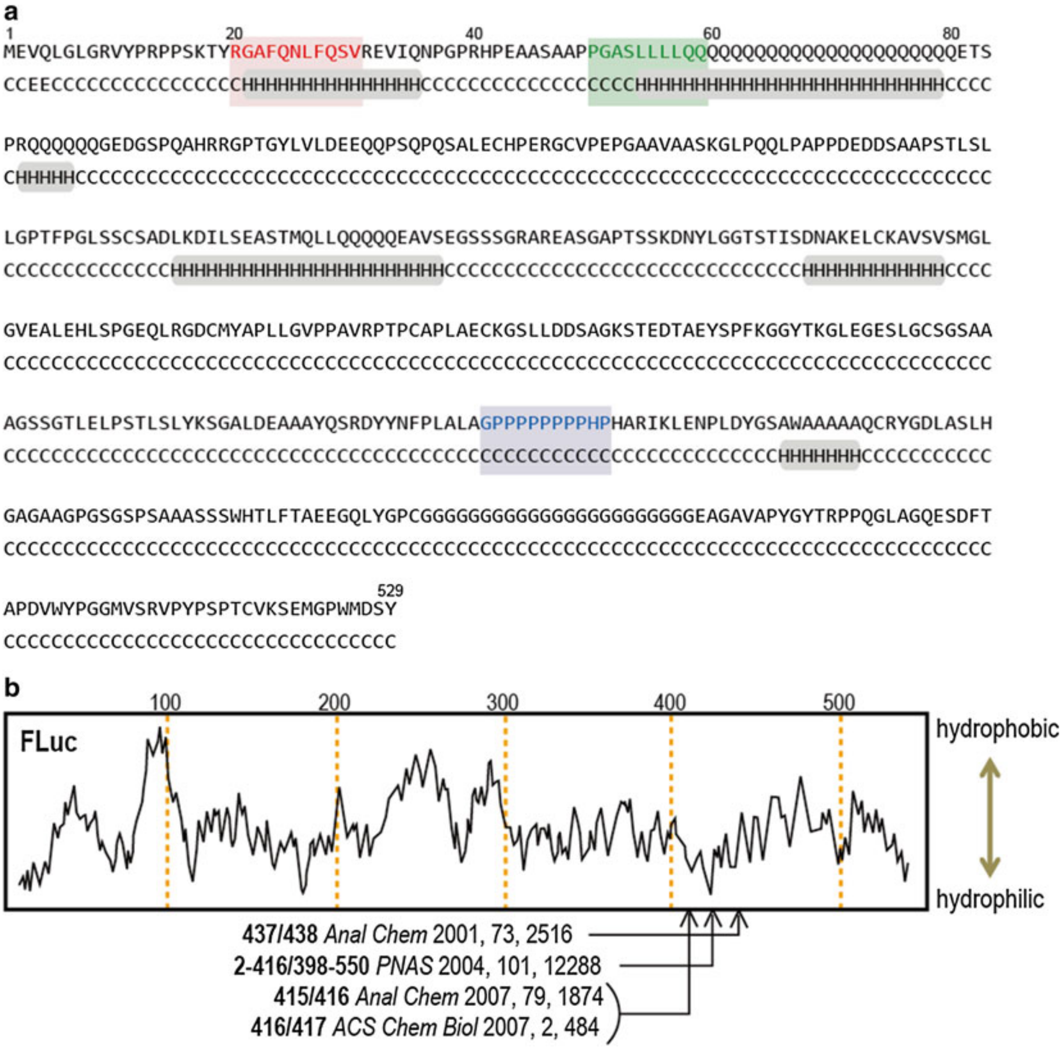

Fig. 1 (**a**) Mapping of the amino acid sequence and the corresponding Hierarchical Neural Network Codes (HNNC) in the N-terminal domain of human androgen receptor (AR). The amino acid sequences incorporated in the plasmids, pLeu-rich and pPro-rich were PGASLLLLQQ and GPPPPPPPPHP, respectively. (**b**) A hydrophilicity search of firefly luciferase revealing a hydrophilic region in the middle of the sequence. The sequence was projected by the scale of Kyte and Doolittle [5]. The targetted hydrophilic region is around 400–450 AA. The *arrows* show known dissection sites for bioassays in literatures. Reproduced in part from Kim et al. with permission from Anal. Sci. [3]

Neural Network codes (HNNC) [1]) and choose short helical and/or hydrophobic sites (ca. 10 amino acids) in the sequences like leucine- or proline-rich regions (*see* Fig. 1 and **Note 1**).

3. Confirm the significance of the predicted leucine- or proline-rich regions above with a conventional reporter-gene assay Reporter-gene assay as follow:
   (a) Purchase or prepare a mammalian expression vector carrying a cDNA encoding a full-length AR.

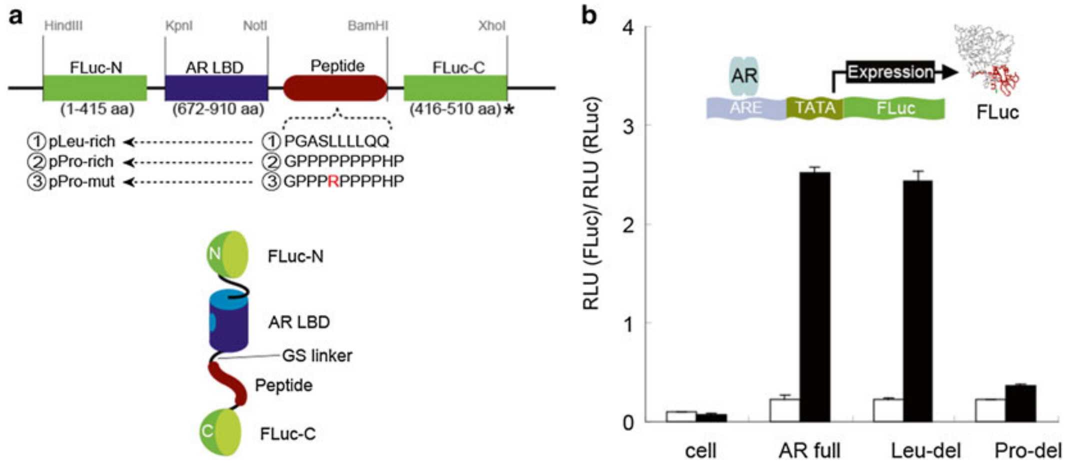

Fig. 2 (**a**) Schematic structures of the cDNA constructs encoding single-chain probes. The plasmids constructed from a single-molecule-format backbone were named pLeu-rich (^{50}PGASLLLLQQ^{59}), pPro-rich (^{373} GPPPPPPPPHP^{382}), and pPro-mut (^{373}GPPP**R**PPPPHP^{382}), according to the component peptides. Abbreviations: *FLuc-N*, N-terminal fragment of firefly luciferase; *FLuc-C*, C-terminal fragment of firefly luciferase; *AR LBD*, ligand-binding domain of androgen receptor; *Peptide*, a specific peptide sequence for binding AR LBD. (**b**) A reporter-gene assay for estimating the transcriptional activities of intact AR (AR full), leucine- (Leu-del) and proline-deficient AR (Pro-del). DHT-stimulated ARs are translocated into the nucleus for transcription. The luminescent activities by firefly luciferase (FLuc; reporter) were normalized with those of *Renilla* luciferase (a Dual-luciferase assay (Promega)) ($n = 3$). The intensities after the stimulation of 10^{-5} mol/L 5α-dihydrotestosterone (DHT) or vehicle (0.1 % DMSO) were specified in closed and open bars, respectively. Reproduced in part from Kim et al. with permission from Anal. Sci. [3]

(b) Remove the site encoding the proline-rich region (GPPPPPPHP) in the sequence encoding AR in the vector with PCR and appropriate primers (i.e., a proline-deficient fragment of AR).

(c) Seperately, delete the site encoding the original leucine-rich region (PGASLLLL) in the cDNA encoding AR with PCR and appropriate primers (i.e., a leucine-deficient AR variant).

(d) Grow COS-7 cells in a 24-well plate and cotransfect them with the mixture of the three component vectors: i.e., (1) a reporter vector (pTransLucent, Panomics) (2) a vector encoding *Renilla* luciferase as an internal reference (0.2 μg per each well), and (3) a plasmid carrying cDNA encoding full length AR (positive control), the leucine-deficient AR, or the proline-deficient AR.

(e) Six hours after transfection, the cells were stimulated with 10^{-6} M DHT and further incubate them for 12 h.

(f) Determine the reporter expression levels with a Dual-luciferase assay kit (Promega). Figure 2b is the typical result of this reporter-gene assay (*see* **Note 2**).

4. Separately, conduct a hydrophilicity search of FLuc with a web service (e.g., the scale of Kyte and Doolittle) for estimating the hydrophilic region in the 3/4 position of the sequence and decide a putative dissection site in the hydrophilic region (*see* **Note 3**).
5. Fuse the helical and/or hydrophobic sequence to the C-terminal end of the AR LBD, and sandwich them between the N- and C-terminal fragments of FLuc.
6. Add a GS linker between the domains and construct a single-chain structure.

3.2 Plasmid Construction

The above designed plasmids (pLeu-rich and pPro-rich) in Section 3.1 are fabricated by subcloning each specific cDNA fragments encoding the parts into pcDNA 3.1(+) vector (Invitrogen). The specific steps were as follows:

1. Conduct a polymerase chain reaction (PCR) to amplify the cDNAs of the N-terminal (FLuc-N; 1–415 AA) and the C-terminal (FLuc-C; 416–510 AA) domains of FLuc comprising unique restriction sites (i.e., *Hind*III/*Kpn*I and *BamH*I/*Xho*I) at both ends of the domains using adequate primers and a template cDNA of full-length FLuc.
2. Modify the cDNA encoding human AR LBD (672–910 AA) by PCR to introduce unique *Kpn*I and *Not*I sites at the respective 5′ and 3′ ends of the domains.
3. Synthesize-to-order cDNA oligomers encoding specific leucine- and proline-rich peptides, ^{50}PGASLLLLQQ^{59,} and ^{373}GPPPPPPPPHP^{382} comprising *Not*I and *BamH*I sites at the 5′ and 3′ ends (*see* **Note 4**).
4. Ligate the cDNA fragments digested by the corresponding restriction enzymes and subclone the consequent chimeras into pcDNA 3.1(+) vector (Invitrogen).
5. Sequence the constructed plasmids to ensure fidelity with a BigDye Terminator Cycle Sequencing kit and a genetic analyzer ABI Prism310 (Applied Biosystems).
6. Name the plasmids pLeu-rich and pPro-rich, respectively, according to the linked functional peptides (*see* **Note 5**).

3.3 Androgen Sensitivities of HeLa Cells Carrying pPro-Rich or pLeu-Rich

Androgenicity of ligands is determined with the above probes as follow (*see* Fig. 3a).

1. Culture human cervical carcinoma-derived HeLa cells in 12-well plates in Dulbecco's modified eagle's medium (DMEM; Sigma) supplemented with 10% steroid-free fetal bovine serum (FBS) and 1% penicillin-streptomycin (P/S) at 37 °C in a 5% CO_2 incubator (Sanyo).

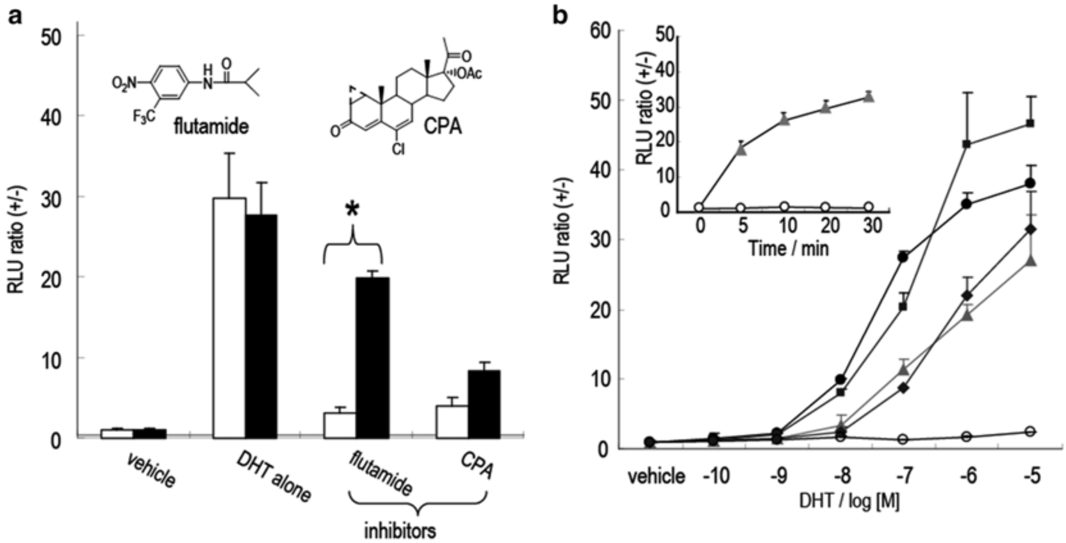

Fig. 3 (**a**) An effect of native androgen and synthetic chemicals on the bioluminescence intensities from HeLa cells carrying pPro-rich (*closed bars*) or pLeu-rich (*open bars*) in the presence of 10^{-6} mol/L DHT ($n = 3$). The tested antagonists were cyproterone acetate (CPA) and flutamide. The asterisk shows the selective antagonistic effect of flutamide on the AR LBD–leucine-rich peptide binding. Vehicle means a culture medium carrying 0.1 % DMSO (negative control). (**b**) Determination of the androgen sensitivity of the four different cell lines (CHO, HeLa, NIH 3T3, and MCF-7 cells) carrying pPro-rich ($n = 3$). The cell lines were stimulated with a 10^{-5} mol/L of DHT for 20 min for initiating AR LBD–proline-rich peptide binding and the subsequent emission of bioluminescence light ($\lambda_{max} = 615$ nm). "[M]" means molar concentrations (mol/L). HeLa cells carrying pAR-dim (negative control) expressing two consecutive AR LBDs were symboled "*open circle.*" Abbreviations: *CHO*, chinese hamster ovary cell (*filled square*); *HeLa*, human cervical carcinoma cell (*filled triangle*); *COS-7*, African green monkey kidney fibroblast cell (*filled diamond*); *MCF-7*, human breast cancer cell (*filled circle*). Inset shows the kinetics of bioluminescence intensities from HeLa cells carrying pPro-rich in response to vehicle (*open circle*) and DHT (*filled triangle*). Reproduced in part from Kim et al. with permission from Anal. Sci. [3]

2. Transfect the cells in the 12-well plates with pPro-rich or pLeu-rich using a transfection reagent (TransIT-LT1 (Mirus)) and extensively incubated for 16 h (*see* **Note 6**).
3. Prestimulate the HeLa cells in each well with a vehicle (0.1 % DMSO) or 5×10^{-5} mol/L antagonist (final conc; flutamide and cyproterone acetate (CPA)) for 5 min (*see* **Note 7**).
4. Additionally, stimulate all of the cells except for the positive control with a 10^{-6} mol/L DHT for 20 min (*see* **Note 8**).
5. Determine the luminescence intensities of each well using a substrate kit (Bright-Glo; Promega) and a luminometer (Minilumat LB9506; Berthold).
6. Normalize the obtained firefly luminescence intensities in form of "relative luminescence unit (RLU) ratio (+/−)," i.e., the ratio of RLU (+)/ RLU (−), where RLU (+) and RLU (−) mean the luminescence intensity from a 1 μg protein of cell lysate after HeLa cells were incubated with or without a ligand, respectively.

3.4 Comparison of the Androgen Sensitivity of Various Cell Lines Carrying pPro-Rich

One may examine the androgen sensitivities of various mammalian cell lines to demonstrate the influence of the cell context on the AR LBD–peptide binding as follows (*see* **Note 9** and Fig. 3b).

1. Grow four kinds of mammalian cell lines in a 12-well plate to a 90% confluent: i.e., (1) Chinese hamster ovary-derived CHO cells, (2) human cervical carcinoma-derived HeLa cells, (3) African green monkey kidney fibroblast-derived COS-7 cells, and (4) human breast cancer-derived MCF-7 cells.
2. Transiently transfect each cell line with pPro-rich using a transfection reagent (Mirus), and incubate in a cell incubator for 16 h.
3. Stimulate the cells with varying concentrations of DHT for 20 min.
4. Estimate the recovered FLuc activities using the Bright-Glo substrate kit and a luminometer (*see* **Note 10**). One may monitor the time-course of the bioluminescence intensities from the HeLa cells carrying pPro-rich in response to DHT as follows (*see* Fig. 3b Inset).
5. Transfect HeLa cells cultured in a 12-well plate with pPro-rich, and incubate in 37 °C for 16 h.
6. Stimulate the cells on each well with 10^{-5} mol/L DHT for 0, 5, 10, 20, or 30 min.
7. Determine the respective luminescence intensities of the cells by the addition of the substrate solution.

3.5 Reversibility of the AR LBD–Proline-Rich Peptide Binding in Response to DHT

One may evaluate the reversibility of AR LBD–proline-rich peptide binding in the single-chain probe (pPro-rich) through a repeated treatment and the withdrawal of DHT as follow (*see* Fig. 4).

1. Transfect HeLa cells cultured in a 24-well plate with pPro-rich using the transfection reagent (Mirus).
2. At 16 h after extensive incubation, stimulate all of the cells with 10^{-5} mol/L DHT for 20 min except for a negative control with the vehicle (0.1% DMSO).
3. Replace the culture medium on the wells with a fresh one and incubate the cells in the cell incubator.
4. At 20, 40, 60, and 120 min after the medium change, determine the luminescence intensities using the Bright-Glo substrate kit.
5. Stimulate the remaining cells in the 24-well plate once again with 10^{-5} mol/L DHT for 20 min.
6. Replace again the culture medium in the plate wells with a fresh one for removing DHT.
7. At 20, 40, 60, and 120 min after the second medium change, determine the recovered FLuc activities using the Bright-Glo substrate kit.

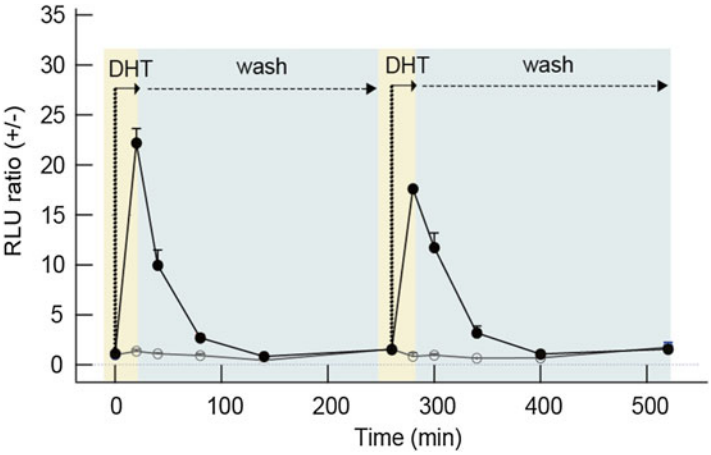

Fig. 4 Time course of the bioluminescence intensities from the cells carrying pPro-rich by the deprivation of DHT 20 min after the stimulation with 10^{-5} mol/L DHT (*closed dots*) or 0.1 % DMSO (*open dots*) ($n=3$). After repeated stimulation and deprivation of 10^{-5} mol/L DHT, the fluctuations of the luminescence intensities were monitored for 2 h. Reproduced in part from Kim et al. with permission from Anal. Sci. [3]

4 Notes

1. Typically, a sequence with a length of 10–11 amino acids is appropriate.
2. The result shows the contribution of the found proline- and leucine-rich regions to the transcription efficiency of AR. It is an indirect evidence of binding between AR LBD and the proline (leucine)-rich region, as androgen-activated AR exerts an intramolecular folding before dimeration and recruiting of the coactivators.
3. Upon deciding the dissection site of FLuc, known dissection sites in literatures may be referred.
4. Many domestic companies provide a service for synthetic DNAs in cheap prices.
5. As a negative control, one may make a mutant-bearing version of pPro-rich, where the plasmid comprises the sequence ^{373}GPPP**R**PPPPHP^{382}. This mutant plasmid may be named “pPro-mut” (Fig. 2a).
6. Long incubation time generally causes an overexpression of the probes, elevating the background intensity of bioluminescence and worsening the S/N ratios.
7. Every antagonists induce a distinctive conformational change of AR LBD, exerting various assembly models of coactivators.

8. The incubation time, 20–30 min, comprises all of the time spans for (1) a membrane permeation of androgen, (2) AR LBD–androgen binding, (3) subsequent association of AR LBD with a peptide, and (4) complementation of the flanking N- and C-terminal fragments of split FLuc.
9. The driving force of the peptide–AR LBD binding is considered the hydrogen bond [2] and the hydrophobic interaction between the two components [2–4].
10. The variance of the ligand sensitivity of the cells although pPro-rich was equally transfected may be reasoned as follows: (1) The expression level of the probe differs according to the host cell lines and (2) variance in the physiological contexts of cell lines upon determining the androgenicity of ligands.

Acknowledgements

This work was supported by grants from Japan Society for the Promotion of Science (JSPS), grant numbers 26288088, 16K-14051, and 15KK0029.

References

1. Guermeur Y, Geourjon C, Gallinari P, Deleage G (1999) Improved performance in protein secondary structure prediction by inhomogeneous score combination. Bioinformatics 15:413–421
2. Dubbink HJ, Hersmus R, Verma CS, van der Korput HA, Berrevoets CA, van Tol J, Ziel-van der Made AC, Brinkmann AO, Pike AC, Trapman J (2004) Distinct recognition modes of FXXLF and LXXLL motifs by the androgen receptor. Mol Endocrinol 18:2132–2150
3. Kim SB, Umezawa Y, Tao H (2009) Determination of the androgenicity of ligands using a aingle-chain probe carrying androgen receptor N-terminal peptides. Anal Sci 25:1415–14204
4. Langley E, Zhou ZX, Wilson EM (1995) Evidence for an anti-parallel orientation of the ligand-activated human androgen receptor dimer. J Biol Chem 270: 29983–29990
5. He B, Kemppainen JA, Wilson EM (2000) FXXLF and WXXLF sequences mediate the NH2-terminal interaction with the ligand binding domain of the androgen receptor. J Biol Chem 275: 22986–22994

Chapter 12

Multicolor Imaging of Bifacial Activities of Estrogens

Sung-Bae Kim and Yoshio Umezawa

Abstract

The present protocol introduces multicolor imaging of bifacial activities of an estrogen. For the multicolor imaging, the authors fabricated two single-chain probes emitting green or red bioluminescence (named Simer-G and -R, respectively) from click beetle luciferase (CBLuc) green and red: Simer-R consists of the ligand binding domain of estrogen receptor (ER LBD) and the Src homology-2 (SH2) domain of Src, which are sandwiched between split-CBLuc red (CBLuc-R). On the other hand, Simer-G emitting red light consists of the ER LBD and a common consensus sequence of coactivators (LXXLL motif), which are inserted between split-CBLuc green (CBLuc-G). This probe set creates fingerprinting spectra from the characteristic green and red bioluminescence in response to agonistic and antagonistic activities of a ligand of interest. The present protocol further provides a unique methodology to calculate characteristic estrogenicity scores of various ligands from the spectra.

Key words Bioluminescence, Multicolor imaging, Luciferase, Single-chain probe, Estrogen receptor, Click beetle

1 Introduction

A crosstalk between distinct signaling pathways is a complex feature of ligand-activated signal transduction pathways in mammalian cells. This intrinsic nature implicates that the roles of a ligand are much more complex and multifacial than ever expected in the physiological circumstances of living cells. Thus, it is rational to simultaneously determine such multiple, occasionally bifacial activities of a ligand in living cells to understand the ligand actions. However, such multi-stimulative, bifacial activities of a ligand for various signaling pathways are hard to estimate, owing to the lack of a suitable methodology.

In this chapter, we introduce a unique bioanalytical method with single-chain multicolor probes for simultaneous determination of multiple effects of a ligand with red and green. The basic molecular design was fabricated by us for the first time for determining protein–protein interactions [1]. The probe contains N- and C-terminal fragments of a split-luciferase, between which any

Sung-Bae Kim (ed.), *Bioluminescence: Methods and Protocols*, Methods in Molecular Biology, vol. 1461,
DOI 10.1007/978-1-4939-3813-1_12, © Springer Science+Business Media New York 2016

two proteins of interest were inserted. The probe is characterized as a single-chain bioluminescent probe, in which all the components required for signal sensing and light emission are integrated.

In this chapter, we exemplify simultaneous illumination of the genomic and nongenomic signaling pathways of the estrogen receptor (ER) (*see* **Note 1**) with single-chain multicolor probes carrying click beetle luciferases red and blue (CBLuc red and blue). These probes were named "Simer" (**S** ingle-chain **M**ulticolor probe with **E**strogen **R**eceptor), and the assay can be called a Simer assay.

2 Materials

2.1 Mammalian Cells

1. HeLa cell derived from human cervical cancer.
2. COS-7 cell derived from African green monkey kidney.
3. NIH 3T3 cell derived from a mouse embryonic fibroblast.
4. MCF-7 cell derived from human mammary epithelium.

2.2 Ligands for Stimulating Single-Chain Multicolor Imaging Probes

1. 4-Hydroxytamoxifen (OHT), estrogen antagonist.
2. ICI 182780, estrogen antagonist.

2.3 Reagents Related with Genetic Engineering

1. pCBR-Control vector (Promega) encoding click beetle luciferase red.
2. *E. coli* strain DH5α, a competent cell.
3. pCBG99-Control vector (Promega) encoding click beetle luciferase green.
4. TransIT-LT1 (Mirus) as a lipofection reagent.

2.4 The Other Reagents

1. Dimethyl sulfoxide (DMSO).
2. Bright-Glo reagent kit (Promega).
3. Phosphate buffered saline (PBS).

3 Methods

3.1 Basic Designs of Single-Chain Multicolor Imaging Probes

A blueprint structure of single-chain multicolor probes should be designed beforehand as follows (*see* Fig. 1):

1. Download the amino acid sequence of CBLuc Green and Red from a public database, NCBI (*see* **Note 2**).
2. Determine the hydrophilicity scale through pasting the full amino acid sequences of CBLuc Green and Red besides FLuc into the window of ExPASy Proteomics service (Swiss Institute

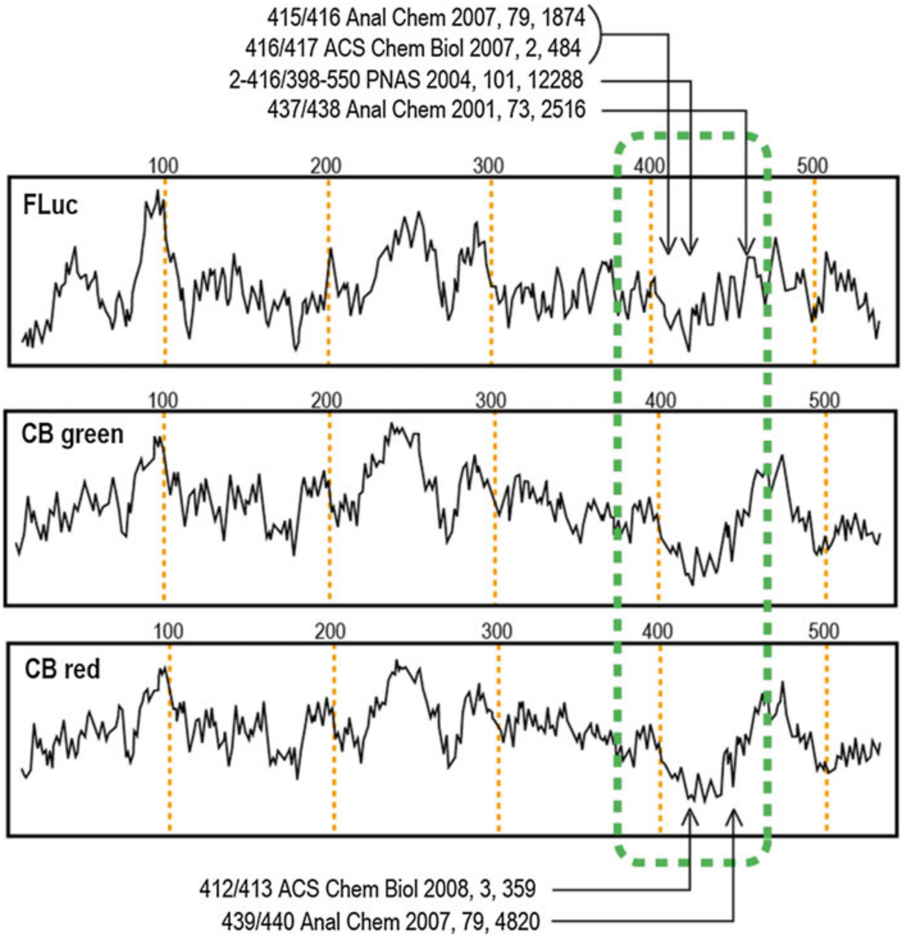

Fig. 1 A hydrophilicity search of beetle luciferases revealing a hydrophilic region in the 400–450 AA region of the sequence. The sequence was projected by the scale of Kyte et al. [2]. The hydrophilic region was highlighted with a *dotted box*. The *arrows* show known dissection sites for bioassays in literatures

of Bioinfomatics; SIB) for obtaining the scale of Kyte and Doolittle [2].

3. Superimpose the hydrophilicity scales of CBLuc Green and Red on that of FLuc and identify potential dissection sites in the remarkably hydrophilic region in the 3/4 region of the scale from the N-terminal end (*see* **Notes 3** and **4**).
4. Split the sequence of CBLuc Green at the above identified dissection site, and sandwich a protein pair of interest representing a genomic signal pathway of ER (i.e., ER LBD and an LXXLL motif (*see* **Note 5**)) between split fragments. Add an appropriate flexible linker between the ER LBD and the LXXLL motif (*see* **Note 6**). This probe is named "Simer-G".
5. Split the sequence of CBLuc Red at the above identified dissection site, and sandwich a protein pair of interest represent-

ing a nongenomic signal pathway of ER (i.e., ER LBD and Src homology-2 domain (SH2) (*see* **Note 7**)) between the split fragments. Add an appropriate flexible linker between the ER LBD and the SH2 (*see* **Notes 8–10**). This probe is named “Simer-R”.

6. Further integrate the key elements of the two probes emitting red and green in a single molecule backbone as shown in Fig. 2 for making a single-chain multicolor probe emitting red and/or green light. This probe is named “Simer-RG”.

3.2 A Plasmid Encoding a Single-Chain Probe for Illuminating Nongenomic Activities of Estrogen

Based on the above design (Section 3.1), one may generate plasmids encoding single-chain multicolor imaging probes for illuminating nongenomic activities of hormones by a series of polymerase chain reactions (PCRs) as follows.

1. Generate the cDNAs encoding N-terminal fragment (1–412 aa) and C-terminal fragments (413–542 aa) of CBLuc Red by PCR to introduce unique restriction sites, *Hin*dIII/*Kpn*I, or *Bam*HI/*Xho*I at both ends of the fragments using adequate primers and the template vector, pCBR-Control (Promega).
2. Separately synthesize the cDNAs encoding ER LBD (305–550 aa) and Src SH2 (150–248 aa) respectively by PCR to add adequate restriction sites, *Nhe*I/*Bam*HI and *Kpn*I/*Nhe*I (*Not*I), at both ends.

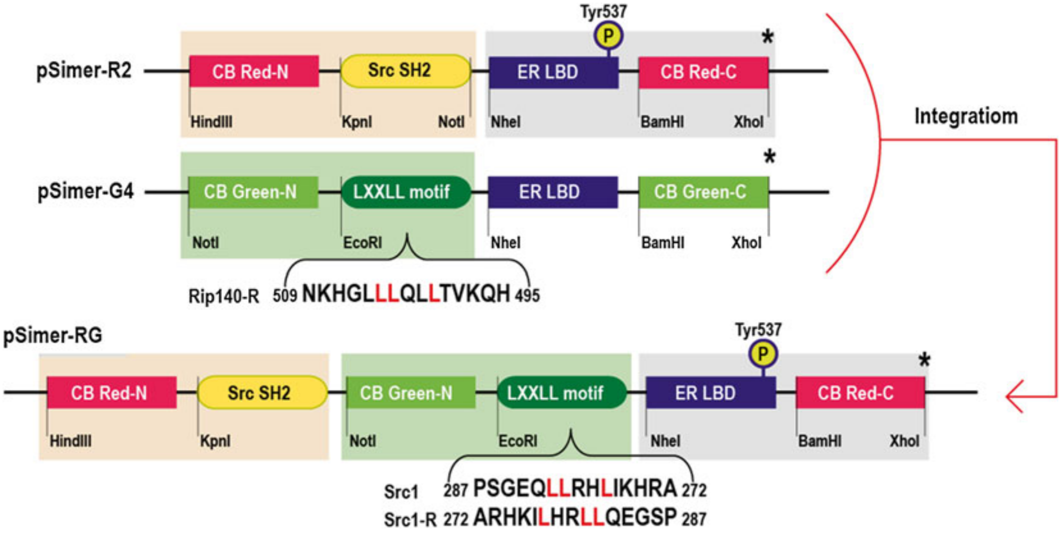
Tyr537
P
*
pSimer-R2
CB Red-N
Src SH2
ER LBD
CB Red-C
HindIII
KpnI
NotI
NheI
BamHI
XhoI
Integratiom
*
pSimer-G4
CB Green-N
LXXLL motif
ER LBD
CB Green-C
NotI
EcoRI
NheI
BamHI
XhoI
Rip140-R 509 NKHGLLLQLLTVKQH 495
pSimer-RG
Tyr537
P
*
CB Red-N
Src SH2
CB Green-N
LXXLL motif
ER LBD
CB Red-C
HindIII
KpnI
NotI
EcoRI
NheI
BamHI
XhoI
Src1 287 PSGEQLLRHLIKHRA 272
Src1-R 272 ARHKILHRLLQEGSP 287

Fig. 2 Schematic diagrams of cDNA constructs encoding single-chain probes. The component cDNA domains of each plasmid were specified with restriction sites. The present series of plasmids were named “pSimer,” which means a plasmid encoding a *Single-chain* bioluminescent probe with *E*strogen *R*eceptor

3. Subclone the PCR-amplified cDNA fragments in the corresponding restriction enzyme-digested pcDNA 3.1(+) vector backbone (*see* **Note 11**). The plasmid was named pSimer-R2. After expression, it may be called Simer-R2.

3.3 A Plasmid Encoding a Single-Chain Probe for Illuminating Genomic Activities of Estrogen

Make the cDNA constructs for pSimer-G series plasmids according to the above design (Section 3.1) for illuminating genomic activities of hormones by a series of polymerase chain reactions (PCRs) as follows.

1. Generate the cDNAs encoding N- and C-terminal fragments of CB Green respectively by PCR to introduce unique restriction sites, *Not*I/*Eco*RI and *Bam*HI/*Xho*I at both ends of the fragments using adequate primers and the template vector, pCBG99-Control (Promega).
    (a) Separately synthesize the cDNAs encoding ER LBD (305–550 aa) and an LXXLL motif (^{509}NKHGL$\underline{\text{LL}}$QL$\underline{\text{L}}$ TVKQH^{495}, a reverse peptide sequence of Rip140) respectively by PCR to add adequate restriction sites, *Nhe*I/*Bam*HI and *Eco*RI/*Nhe*I, at both ends (*see* **Note 12**).
2. Ligate and subclone the PCR-amplified cDNA fragments in the pcDNA 3.1(+) vector (Invitrogen) that was digested with the corresponding restriction enzymes.
3. Confirm Tthe fidelity of the cDNA construct in the plasmids is confirmed by sequencing it with a genetic analyzer ABI PRISM 310 (Applied Biosystems, Tokyo, Japan). The plasmid was named pSimer-G4. After expression, it is may be called Simer-G4.

3.4 A Plasmid Encoding a Single-Chain Probe for Illuminating Both Genomic and Nongenomic Activities of an Estrogen (Simer-RG)

Fabricate a plasmid encoding Simer-RG on the basis of the backbone of Simer-G4 and -R2 (*see* Fig. 1b for the molecular design) according to the following procedure.

1. Assemble the construct of pSimer-RG2 on the basis of the cDNA constructs of pSimer-G4 and -R2 as shown in Fig. 2 and Section 3.1.
2. Ligate the cDNA fragment encoding the N-terminal fragment of CBLuc Green and LXXLL motif between *Not*I and *Nhe*I of a pSimer-R2 backbone (*see* **Note 13**).
3. Confirm the fidelity of the cDNA sequences in the plasmids by sequencing them with a genetic analyzer ABI PRISM 310 (Applied Biosystems, Tokyo, Japan). They were named pSimer-RG2. The expressed fusion protein is may be called SIMER-RG2.

3.5 Determination of Ligand Sensitivity of Cells Carrying Each Plasmid

The ligand sensitivities of mammalian cells carrying each constructed plasmid were estimated as follows:

1. Transfect an aliquot of pSimer-R2 into the following mammalian cells, HeLa, COS-7, NIH 3T3, or MCF-7, using *Trans*IT-LT1 (i.e., 0.5 μg plasmid for each well of 24-well plate).
2. Incubate the cells carrying each plasmid in a 5 % CO_2 incubator for 16 h.
3. Stimulate the cells on the 24-well plate with a specific ligand or vehicle (0.1 % DMSO) for 15 min (*see* **Notes 14–16**).
4. Develop the bioluminescence intensities by Simer-R2 expressed in each cell line on the 24-well plate using a Bright-Glo substrate solution (Promega) as follows.
   (a) Wash the cells on the 24-well plate once with PBS.
   (b) Add the 40 μL substrate solution prepared according to manufacturer's instruction to each well of the plates.
   (c) After incubation for 3 min at 37 °C, record the developed bioluminescence intensities from the cell lysates with a luminometer (Minilumat LB9506; Berthold) (*see* **Note 17**).
5. Normalize the RLU values in form of fold intensity as follows.
   (a) Determine the amounts of proteins sequentially using a Bradford reagent (Bio-Rad) after the measurements of bioluminescence intensity.
   (b) Normalize the bioluminescence intensities (RLUs) by a vehicle (0.1 % (v/v) DMSO) and a ligand against the corresponding amount of proteins, which is expressed as "RLU/ μg protein."
   (c) Convert the individual optical intensities into a form of fold intensity, i.e., "RLU ratio (+/−)," which means the bioluminescence ratio of RLU (+) to RLU (−), where RLU (+) and RLU (−) are the RLU per 1 μg protein of the cell lysates treated with a ligand and a vehicle, respectively.
6. The selectivity of Simer-R2 to various ligands shows that the probe exhibited selective recognition for a known estrogen antagonist, OHT or ICI 182780, in any cell lines. Figure 3 shows the typical example.

3.6 Monitoring Spectra of Bioluminescence Intensities Triggered by Each Ligand

The spectra are taken on the basis of the following protocol.

1. Grow COS-7 cells in a six-well plate to 90 % confluent.
2. Transfect the cells on each well transiently with a 2.5 μg of a mixture of pSimer-R2 and pSimer-G4 (Case 1; *see* Fig. 4a for the working mechanism) or pSimer-RG2 (Case 2; *see* Fig. 5a for the working mechanism)
3. 16 h after the transfection, stimulate the cells with each ligand (10^{-6} M) for 20 min (*see* **Note 18**).

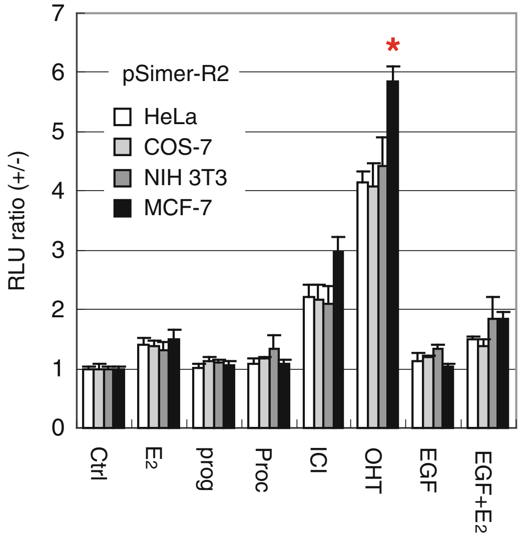

Fig. 3 Bioluminescence intensities of various cell lines carrying pSimer-R2 in response to ligands. Abbreviations: *Ctrl*, control; *E_2*, 17β-estradiol; prog, progesterone; proc, procymidone; *ICI*, ICI 182780; *OHT*, 4-hydroxytamoxifen; *EGF*, epidermal growth factor ($n = 3$). Reproduced in part from Kim et al. with permission from ACS Chemical Biology [3]

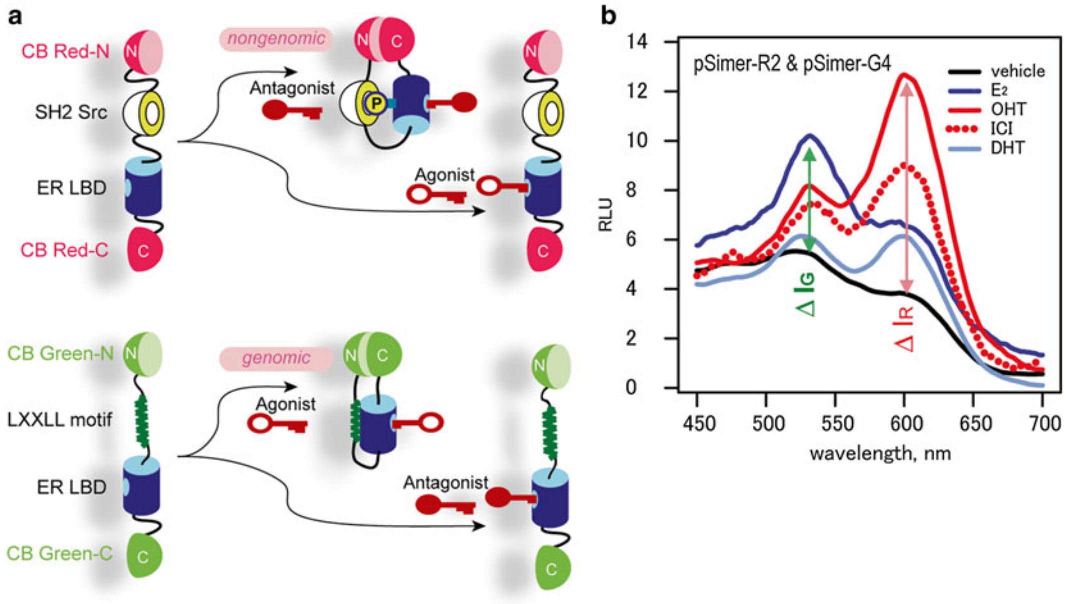
a
CB Red-N
SH2 Src
ER LBD
CB Red-C
nongenomic
Antagonist
Agonist
N
C
P
CB Green-N
LXXLL motif
ER LBD
CB Green-C
genomic
Agonist
Antagonist
b
pSimer-R2 & pSimer-G4
vehicle
E2
OHT
ICI
DHT
RLU
0
2
4
6
8
10
12
14
Δ IG
Δ IR
450
500
550
600
650
700
wavelength, nm

Fig. 4 (**a**) The ligand-sensing mechanism of a single-chain probe set. The probes exert different molecular structures according to agonist and antagonist. Abbreviations: *Src SH2*, SH2 domain of Src; *ER LBD*, ligand-binding domain of estrogen receptor; *CB Red-N*, N-terminal domain of click beetle luciferase red; *CB Green-C*, C-terminal domain of click beetle luciferase green. (**b**) The bioluminescence spectra of COS-7 cells carrying pSimer-R2 and pSimer-G4 in response to various ligands. These spectra enable us to score agonistic and antagonistic activities of ligands on the basis of bioluminescence intensity gaps (Δ LI) at 540 and 610 nm. The scores were specified in Table 1. Reproduced in part from Kim et al. with permission from ACS Chemical Biology [3]

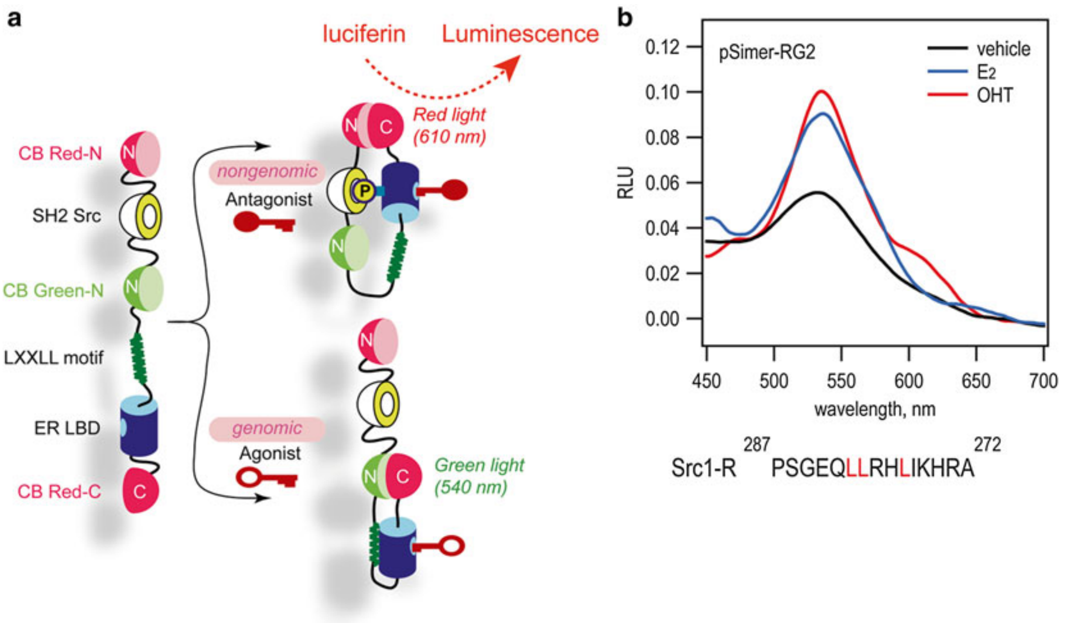
a
luciferin
Luminescence
Red light (610 nm)
CB Red-N
SH2 Src
CB Green-N
LXXLL motif
ER LBD
CB Red-C
nongenomic
Antagonist
genomic
Agonist
Green light (540 nm)
N
C
P
b
pSimer-RG2
vehicle
E2
OHT
RLU
0.12
0.10
0.08
0.06
0.04
0.02
0.00
450
500
550
600
650
700
wavelength, nm
287
272
Src1-R PSGEQLLRHLIKHRA

Fig. 5 (**a**) Working mechanism of a single-chain multicolor probe. The probe varies the molecular conformation according to agonist or antagonist. (**b**) The bioluminescence spectra of COS-7 cells carrying pSimer-RG2 in response to ligands. Reproduced in part from Kim et al. with permission from ACS Chemical Biology [3]

Table 1
List of estrogenicity scores of various estrogens and chemicals

Agonist		Antagonist		Crosstalk		EDC	
E_2	1.80	OHT	0.38	DHT	1.17	PCB	1.03
DES	1.27	Genistein	0.82	T	0.57	Flutamide	0.37
Estrone	0.95	ICI 182780	1.08	Progesterone	1.06	CPA	1.19
				Cortisol	0.68	RU486	1.33

Estrogenicity score (ES) = $(LI_{540} - IC_{540})/(LI_{610} - IC_{610})$
Abbreviations: *E2* 17β-estradiol; *OHT* 4-hydroxytamoxifen; *DHT* 5α-dihydrotestosterone; *T* testosterone; *PCB* polychlorinated biphenyls; *CPA* cyproterone acetate; *DES* diethylstilbestrol; *EDC* endocrine disrupting chemicals

4. Add an aliquot of Bright-Glo substrate solution (400 μL) to each well of the 6-well plate and incubate for 3 min.
5. Record bioluminescence spectra from the expressed probes with a spectrometer (FP-750; Jasco) (*see* **Note 19**). The typical spectra of each case are shown in Figs. 4b and 5b.
6. Normalized the bifacial activities of a ligand with respect to the maximal optical intensities (λ_{max}) at ~540 nm (green) and ~610 nm (red) in response to each ligand, through scoring

agonistic and antagonistic activities of a ligand (named Estroginicity Score): i.e., ES = $(LI_{540}–IC_{540})/(LI_{610}–IC_{610})$, where LI_{540} and LI_{610} respectively indicate the bioluminescence intensity at 540 and 610 nm upon stimulation with a ligand (*see* **Note 20**).

7. The typical ES scores are listed in the Table 1.

4 Notes

1. Estrogens exert their effects through the actions of ERs such as dimerization and coactivator recruitment for gene expression (genomic actions). But a number of other effects of estrogens such as kinase activation in the cytosol are so rapid that they cannot be related with direct gene expression (nongenomic actions), which are mediated through membrane-associated ERs.
2. As an optimal luciferase for this probe, we took advantage of click beetle luciferase (CBLuc). CBLuc is less-sensitive to pH, temperature, and heavy metals, and emits a stable light with D-Luciferin in physiological circumstances [4, 5].
3. The hydrophilicity scales of CBLuc Green and Red show a similar profile with that of FLuc. As information on the successful dissection sites for FLuc is known, one may decide a potential dissection region in CBLuc Green and Red from the corresponding split sites in FLuc by this superimpose.
4. Although crystallographic data of CBLuc were not reported, the structure of CBLuc is almost the same as that of FLuc from the viewpoint of the following homology factors between CBLuc and FLuc: (1) they are both members of a superfamily of acyl-adenylate-forming enzymes, and (2) the two hydrophobicity diagrams of the amino acids based on the scale of Kyte et al. [2] are almost superimposed.
5. The LXXLL motif is a core consensus sequence of coactivators, where “L” means leucine and “X” means any amino acids.
6. The binding of ER LBD with an LXXLL motif of coactivators indexes genomic activities of an estrogen. The activity of split-CBLuc Green inside the probes is temporarily lost. Upon stimulation with an agonist, the ER LBD interacts with the LXXLL motif inside the probe, and thus reconstitutes red bioluminescence at 610 nm through the complementation between the adjacent N- and C-terminal fragments.
7. The SH2 domain is the known phosphorylation recognition domain (Src homology-2 (SH2) domain) of a proto-oncogene tyrosine-protein kinase, Src.

8. The binding between ER LBD and SH2 represents a nongenomic activity of an estrogen. Ligand-activated tyrosine phosphorylation of ER LBD is recognized by the SH2 of Src. Upon stimulation with an antagonist, the ER LBD interacts with its counterpart Src SH2 inside the probe, and recover red bioluminescence.
9. In case of CBLuc Green and Red, the C-terminal regions are almost equivalent each other, and thus is sharable in a single-chain probe. The C-terminal region does not affect color.
10. An appropriate flexible linker less than 10 amino acids is helpful for relaxing possible steric hindrance or special mismatch in the single-chain probes: i.e., (1) a steric hindrance during the intramolecular complementation of the split CBLuc fragments; and (2) a special mismatch between the fragments. These might cause poor fold intensities upon determination of protein–protein interactions inside a single-chain probe.
11. The subcloning may be conducted with a common *E. coli* strain like DH5α as the bacterial host for the plasmid constructions.
12. The information about amino acid sequence consisting of the LXXLL motifs in the ER coactivators, Src1, can be taken from GenBank. The specific sequence is ^{946}VCNESLLLQKLVN FS^{932}, i.e., a reverse peptide sequence of Src1.
13. The author examined an optimal GS linker length between the LXXLL motif and ER LBD and found that a 10 GS linker is appropriate.
14. The stimulation time, 20 min, is largely shortened in comparison with that of the scheme of protein-fragment splicing assay (PSA), which require at least 2 h [6, 7]. Thus, the present method is applicable to a high-throughput analysis of the activities of bioactive small molecules, which even activate temporal, short-time molecular events.
15. The stimulation is conducted by replacing the culture media with a fresh culture media dissolving a ligand.
16. The ligand stimulation time needs ca. 15 min to reach a plateau after addition of 10^{-5} M OHT (*see* Fig. 2c). This time says that the probe takes 15 min to complete all the steps for recovering luciferase activities, i.e., from the plasma membrane permeation of a ligand, ER LBD–ligand binding, phosphorylation (Tyr537) of ER LBD, ER LBD–Src SH2 binding until a protein complementation between the flanking N- and C-terminal fragments of CBLucs.
17. The luminometer provides the bioluminescence intensities with a relative luminescence unit (RLU) because the photons are multiplied in the light-detecting unit of the luminometer.

18. After the cotransfection, the probes from pSimer-R2 and -G4 emit red or green bioluminescence in response to antagonists or agonists, respectively. As some of the ligands have a bifacial activity, such a ligand shows their own characteristic spectra distinctive from the others.
19. The vertical axis is expressed with an arbitrary unit (AU) per wavelength (nm).
20. Through this ES value, we can easily categorize ligands in agonistic and antagonistic groups and compare the bifacial activities of a ligand.

Acknowledgements

This work was supported by grants from Japan Society for the Promotion of Science (JSPS), grant numbers 26288088, 15K K0029, and 16K14051.

References

1. Kim SB, Awais M, Sato M, Umezawa Y, Tao H (2007) Integrated molecule-format bioluminescent probe for visualizing androgenicity of ligands based on the intramolecular association of androgen receptor with its recognition peptide. Anal Chem 79:1874–1880
2. Kyte J, Doolittle RF (1982) A simple method for displaying the hydropathic character of a protein. J Mol Biol 157:105–132
3. Kim SB, Umezawa Y, Kanno KA, Tao H (2008) An integrated-molecule-format multicolor probe for monitoring multiple activities of a bioactive small molecule. ACS Chem Biol 3:359–372
4. Viviani VR, Uchida A, Viviani W, Ohmiya Y (2002) The influence of Ala243 (Gly247), Arg215 and Thr226 (Asn230) on the bioluminescence spectra and pH-sensitivity of railroad worm, click beetle and firefly luciferases. Photochem Photobiol 76:538–544
5. Kim SB, Otani Y, Umezawa Y, Tao H (2007) Bioluminescent indicator for determining protein-protein interactions using intramolecular complementation of split click beetle luciferase. Anal Chem 79:4820–4826
6. Kim SB, Ozawa T, Watanabe S, Umezawa Y (2004) High-throughput sensing and noninvasive imaging of protein nuclear transport by using reconstitution of split Renilla luciferase. Proc Natl Acad Sci U S A 101:11542–11547
7. Ozawa T, Takeuchi TM, Kaihara A, Sato M, Umezawa Y (2001) Protein splicing-based reconstitution of split green fluorescent protein for monitoring protein-protein interactions in bacteria: improved sensitivity and reduced screening time. Anal Chem 73:5866–5874

Chapter 13

Circular Permutation Probes for Illuminating Phosphorylation of Estrogen Receptor

Sung-Bae Kim and Hiroaki Tao

Abstract

The present protocol demonstrates a new strategy for imaging ligand-triggered protein phosphorylation using circularly permutated luciferases (cpLuc): (1) a luciferase is first fragmented into two segments for creating new N- and C-terminal ends in the hydrophilic region, (2) the original N- and C-terminal ends are circularly permutated and linked via a GS linker, whereas the new ends made by fragmentation are correspondingly linked with two proteins of interest. When the new ends of the cpLuc are linked with the ligand-binding domain of estrogen receptor (ER LBD) and Src homology two domain of Src (SH2), the estrogen can trigger phosphorylation of the ER LBD and consequent intramolecular ER LBD–SH2 binding. This interaction triggers an approximation of the adjacent fragments of split-cpLuc recovering the enzyme activity. This probe design greatly improves signal-to-noise (S/N) ratios upon tracing weak protein–protein interactions (PPIs) in mammalian cells.

Key words Circular permutation, Phosphorylation, Luciferase, Estrogen receptor, Bioluminescence

1 Introduction

Recent revolutionary advances in the enzyme-manipulation technologies now allow researchers to carry out quantitative examination of the molecular dynamics and cell signaling in living cells [1].

As a creative approach for probing molecular events, a circular permutation (CP) of bioluminescent enzymes can be an effective technique. The putative active site region of many luciferases is known hydrophilic for recruiting the specific substrates from aquaphase [2]. As the putative active-site region is dissected into two fragments, the activity of the enzyme may be temporally lost. A dissected active site can be placed in the opposite side of the other dissected site in the single-chain probe backbone, by CP as shown in Fig. 1a. Upon stimulation of the ligand, the fragmented luciferase recovers its activity via an intramolecular complementation (*see* Fig. 1). As the possibility of encounter between the fragmented active sites by CP is rare in a basal condition, this allows a dramatically suppressed background activity

Sung-Bae Kim (ed.), *Bioluminescence: Methods and Protocols*, Methods in Molecular Biology, vol. 1461,
DOI 10.1007/978-1-4939-3813-1_13, © Springer Science+Business Media New York 2016

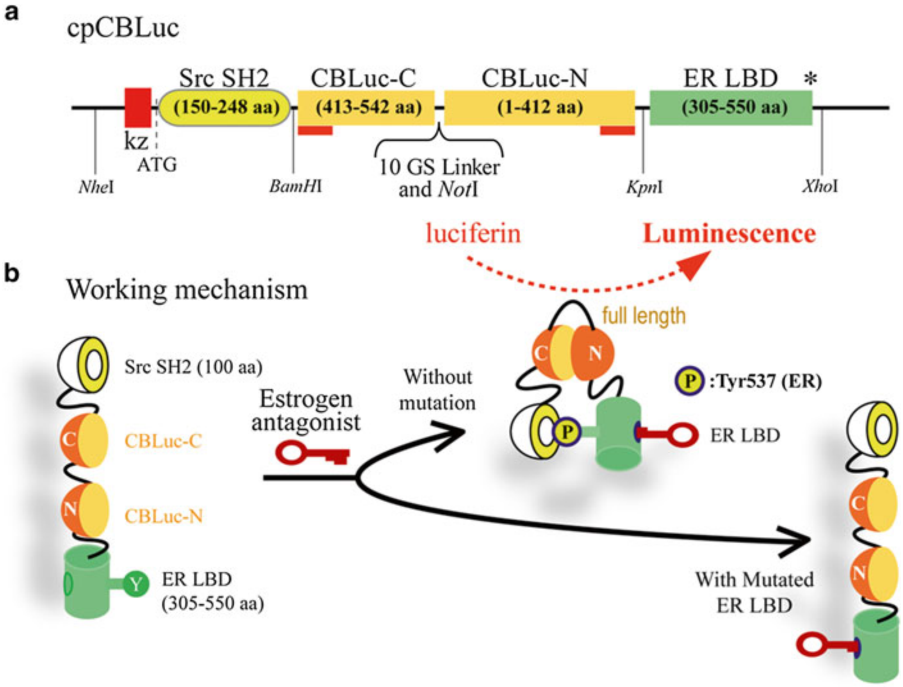
a
cpCBLuc
Src SH2
(150-248 aa)
CBLuc-C
(413-542 aa)
CBLuc-N
(1-412 aa)
ER LBD
*
(305-550 aa)
kz
ATG
NheI
BamHI
10 GS Linker
and NotI
KpnI
XhoI
b
Working mechanism
luciferin
Luminescence
full length
Src SH2 (100 aa)
C
CBLuc-C
N
CBLuc-N
ER LBD
(305-550 aa)
Y
Estrogen
antagonist
Without
mutation
C
N
P
P :Tyr537 (ER)
ER LBD
With Mutated
ER LBD
C
N

Fig. 1 (**a**) Schematic diagram of single-chain circular permutation (CP) probes. The original N- and C-terminals of CBLuc were fused with a 10 GS linker. On the other hand, its new terminal ends were created at I413. A dissection site is placed in the opposite side of the other dissected site in the probe backbone (red bars showing the putative active site, circular permutation). The dissection sites are fused with a pair of proteins of interest. Abbreviations: *Src SH2*, the SH2 domain of Src; *CBLuc-N and -C*, the N- and C-terminal fragment of click beetle luciferase. (**b**) Comprehensive illustration of the ligand-sensing mechanism of CPC and CPC-mut. Ligand-activated ER LBD is phosphorylated at Y537. This phosphorylation triggers Src SH2–ER LBD interactions, accompanying reconstitution of the split fragments of CBLuc. This intramolecular binding does not occur if the phosphorylation site is mutated (CPC-mut)

of the single-chain circular permutation (CP) probe and an enhancement of the signal-to-background (S/B) ratios.

Based on the knowledge, the present chapter guides on how to create a single-chain probe with circularly permutated split-luciferases derived from *Pyrearinus termitilluminans* (click beetle luciferase (CBLuc); Promega).

2 Materials

2.1 Ligands for Stimulating the CP Probes

1. 4-Hydroxytamoxifen (OHT).
2. 17β-estradiol (E_2).
3. Vehicle (0.1 % DMSO).
4. Estrone.
5. 5α-dihydrotestosterone (DHT).
6. Cortisol.

2.2 Reaction Buffers

1. CutSmart buffer (New England Biolabs).
2. PBS buffer (Wako Purechemicals).
3. Hank's balanced salt solution (HBSS) buffer (Gibco).

2.3 Reagents for Growing Mammalian Cells

1. Dulbecco's modified eagle's medium (DMEM; Sigma).
2. Steroid-free fetal bovine serum (FBS).
3. Penicillin-streptomycin (P/S).

2.4 Genetic Engineering Reagents

1. A mammalian expression vector, pcDNA 3.1(+) vector (Invitrogen).
2. A custom-made plasmid, pCPC.
3. Restriction enzymes (New England Biolabs): *Hind*III and *Xho*I.
4. BigDye Terminator Cycle Sequencing kit (Applied Biosystems).
5. A lipofection reagent, TransIT-LT1 (Mirus).

2.5 The Others

1. COS-7 cells derived from African green monkey kidney.
2. Bright-Glo substrate solution (Promega).

3 Methods

3.1 Molecular Design of CP Probes

A suitable dissection site of a luciferase for CP probes can be estimated with following method.

1. Download the amino acid sequence of click beetle luciferase (CBLuc) from a public database, NCBI.
2. Determine the hydrophilicity scale of the full sequence through pasting the full sequence into the window of ExPASy Proteomics service (Swiss Institute of Bioinfomatics; SIB) for obtaining the scale of Kyte and Doolittle [3] (*see* **Note 1**).
3. Identify a remarkably hydrophilic region in the middle of the scale (*see* **Note 2**).
4. Choose several candidate dissection sites near the "flexible" amino acids like glycine in the identified hydrophilic region (*see* **Note 3**).
5. Dissect the sequence of CBLuc at the chosen dissection site (e.g., between I439 and K440 in CBLuc) and place a split-sequence of CBLuc in the opposite side of the other split-sequence (circular permutation) (*see* **Note 4**).
6. Link the original N- and C-termini of the CBLuc sequence with a "glycine-serine (GS)" linker, and fuse a protein pair of interest to the new N- and C-termini made by the dissection. In the present protocol, we exemplify a binding model between the ligand-binding domain of estrogen receptor (ER LBD) and the Src homology 2 domain of Src (SH2) as the protein pair of interest (*see* **Notes 5–7**).

3.2 Generation of Plasmids Encoding various CP Probes

A cDNA construct encoding the designed CP probe above is generated by polymerase chain reaction (PCR) as follows.

1. Design a series of primers to generate unique restriction sites at the 5′ and 3′ ends of the component cDNA fragments shown in Fig. 1a (*see* **Notes 8** and **9**).
2. Conduct a series of PCRs to generate the cDNA fragments with the following ingredients: (1) cDNA encoding CBLuc as a template and the corresponding primers; (2) cDNA encoding full-length ER as a template and the corresponding primers; or (3) cDNA encoding *v*-Src as a template and the corresponding primers.

   Optionally, a flexible GS linker may be made between the cDNA fragments by a consecutive PCR.
3. Digest the PCR products with the corresponding restriction enzymes (*see* **Note 10**).
4. Tandemly ligate the enzyme-digested cDNA fragments and subclone into the pcDNA 3.1(+) (Invitrogen) as shown in Fig. 1a. Here, the plasmid was named pCPC according to the name of CBLuc that were Circularly Permutated in the probe. The expressed fusion probe is named CPC.
   (a) The Y537 in ER LBD can be mutated by a site-directed mutagenesis and name pCPC-mut. The mutated probe may be called CPC-mut after expression.
   (b) Further, a plasmid encoding the construct without CP is fabricated for a negative control as shown in Fig. 3b. The plasmid may be named pCPC-ctrl. The probe after expression may be named CPC-ctrl.
5. Determine the sequence of the plasmids constructed for this study to ensure fidelity, using a BigDye Terminator Cycle Sequencing kit and a genetic analyzer ABI Prism310 (Applied Biosystems).

3.3 Determination of Androgenicity of a Ligand with CPC

Androgenicity of ligands is determined with the optical intensity by CPC as follows (Fig. 2).

1. Culture COS-7 cells derived from African green monkey kidney in a 24-well plate with Dulbecco's modified eagle's medium (DMEM; Sigma), supplemented with 10% steroid-free fetal bovine serum (FBS) and 1% penicillin-streptomycin (P/S) at 37 °C in a 5% CO_2 cell incubator (Sanyo).
2. Transiently transfect the COS-7 cells with pCPC or pCPC-mut (0.2 μg/well) using a transfection reagent, TransIT-LT1 (Mirus).

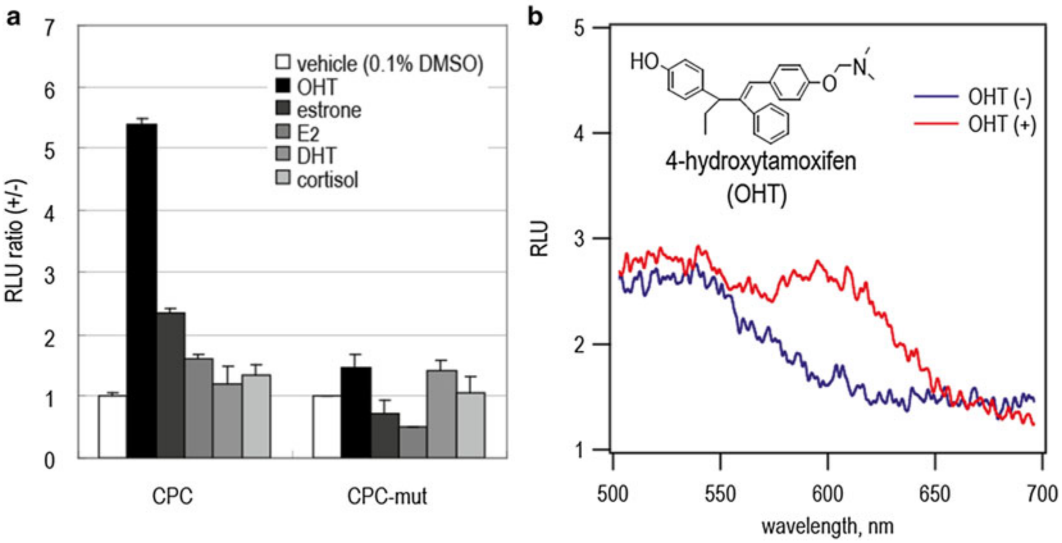

Fig. 2 (**a**) Mutagenesis study for the association of ER LBD with Src SH2 domain. Tyrosine 537 in ER LBD is replaced with lysine, and the plasmid is named pCPC-mut. The luminescence intensities from COS-7 cells carrying pCPC or pCPC-mut are compared in response to various ligands ($n = 3$). (**b**) Spectra from the COS-7 cells carrying CPC before and after stimulation of OHT. Reproduced in part from Kim et al. with permission from Bioconjugate Chem [6]

3. Incubate the cells extensively in the CO_2 incubator for 16 h.
4. Stimulate the cells carrying pCPC with 10^{-6} M of OHT, estrone, E_2, DHT, or cortisol (final concentration) for 20 min (*see* **Note 11**).
5. Eliminate the culture media and wash once the wells on the plate with a PBS buffer.
6. Add a Bright-Glo substrate solution (Promega) to each well of the plate and integrate the luminescence intensities for 15 s using a luminometer (Minilumat LB9506; Berthold). The brief procedure for the use of the Bright-Glo substrate solution comprising a lysis reagent is as follows:
   (a) Add a 40 μL of the substrate (D-Leuciferin) solution to each well of the plates.
   (b) 3 min after substrate addition, tap the plate gently, and transfer the subsequent cell lysates to a test tube and determine the luminescence intensities with a luminometer (*see* **Notes 12–14**).
   (c) The corresponding bioluminescence spectra may be determined with a conventional spectrophotometer (Fig. 2b).

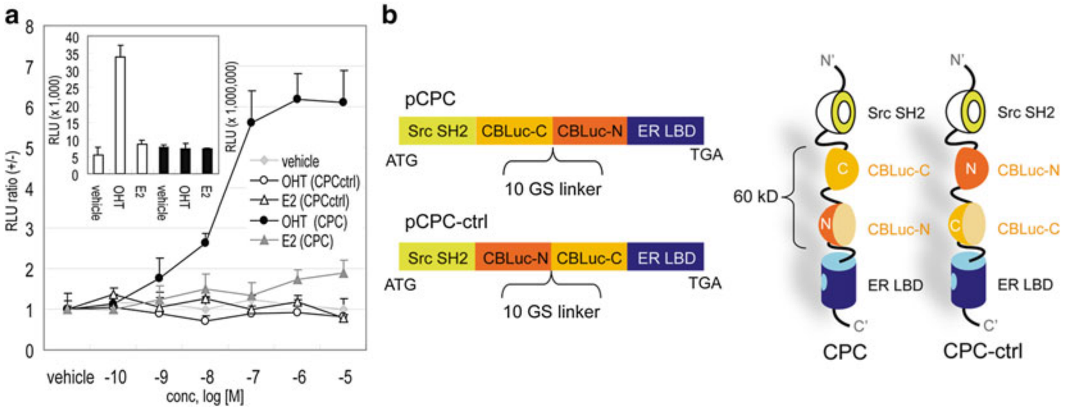

Fig. 3 Ligand sensitivity of CPC. (**a**) Comparison of ligand sensitivity of CPC and CPC-ctrl. The left X-axis shows the fold intensities according to varying concentrations of ligands. Inset shows the absolute luminescence intensities from the cells carrying CPC in response to various ligands. The left *open bars* show the luminescence intensities by CPC, whereas the right *closed bars* indicate the intensities by CPC-ctrl. (**b**) Comprehensive illustration of the molecular structures of CPC and CPC-ctrl. Abbreviations: *OHT*, 4-hydroxytamoxifen; *E_2*, 17β-estradiol; *DHT*, dihydrotestosterone; *Src SH2*, Src homology 2 (SH2) domain of Src; *ER LBD*, ligand binding domain of estrogen receptor; *CBLuc-N and -C*, N- and C-terminal domains of click beetle luciferase. Reproduced in part from Kim et al. with permission from Bioconjugate Chem [6]

3.4 Dose–Response Curves of CPC to Ligands and the Comparison with CPC-Ctrl

The ligand selectivity of CPC in COS-7 cells is determined with varying concentrations of steroids (*see* Fig. 3).

1. Transiently transfect COS-7 cells grown in the 24-well plates with pCPC or pCPC-ctrl.
2. 16 h after transfection, stimulate the cells with varying concentrations of a ligand (E_2, OHT, or vehicle (0.1% DMSO)) for 20 min.
3. Eliminate the culture media and wash once the wells on the plate with a PBS buffer.
4. Inject 40 μL of a Bright-Glo substrate solution (Promega) into each well and incubate 3 min before measurement of the optical intensities.
5. Integrate the luminescence intensities for 15 s with a luminometer (Minilumat LB9506; Berthold).

3.5 Ligand-Binding Kinetics of CPC and Its Filter-Screened Bioluminescence Intensities

The kinetics of ligand–CPC binding in living mammalian cells and its filter-screened bioluminescence are determined as follow (*see* Fig. 4).

1. Transfect COS-7 cells cultured in a 24-well, glass-bottom plate with pCPC and incubated for 16 h.

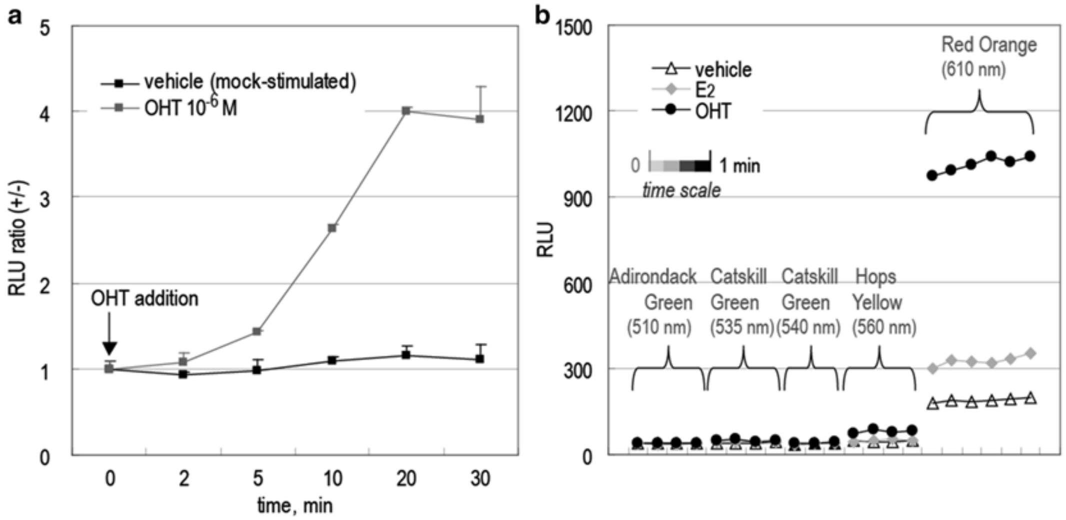

Fig. 4 Ligand-binding kinetics of CPC. (**a**) Time-course of OHT–CPC binding was examined. At 2, 5, 10, 20, and 30 min after OHT–CPC binding, the luminescence variances were monitored. (**b**) Relative luminescence intensities after being screened by bandpass filters. The light from the cells carrying CPC passed well through a 610 nm bandpass filter, indicating the signal is *red-orange light*. Reproduced in part from Kim et al. with permission from Bioconjugate Chem [6]

2. The ligand-CPC binding kinetics is determined as follow:
    (a) Stimulate the cells with vehicle (0.1% DMSO) or 10^{-6} M OHT for 0, 2, 5, 10, 20, or 30 minutes.
    (b) Eliminate the culture media and wash once the wells with a PBS buffer.
    (c) Inject 40 L of the Bright-Glo substrate solution into each well and incubate 3 min before measurement of the optical intensities.
    (d) Determine the optical intensities for 15 s with a luminometer (Minilumat LB9506; Berthold).
3. The filter-screened bioluminescence is determined as follow:
    (a) Saturate the cells of Step 1 with a 500 μL Hank's balanced salt solution (HBSS) buffer containing coelenterazine and one of the following stimulators: vehicle (0.1 % DMSO), 10^{-6} M E_2, or 10^{-6} M OHT.
    (b) 20 min after stimulation with the ligand, monitor the relative luminescence intensities from the cells with a series of bandpass filters, whose wavelengths are as follows: 510 ± 10 nm, 535 ± 10 nm, 540 ± 10 nm, 560 ± 10 nm, and 610 ± 10 nm (*see* **Note 15**).

4 Notes

1. Similar web software for predicting 2D structures of proteins are available in various public websites including NCBI and SIB.
2. A remarkably hydrophilic region in the scale of a luciferase sequence is considered to be advantageous over recruiting the specific substrate in an aqueous phase upon light-emitting reaction.
3. A flexible hinge region is preferred as a dissection site of luciferases. Although information on the 3D structure is not available, amino acids carrying small or no side chains like glycine may be a potential dissection site in the hydrophilic region.
4. In this molecular design, the potential active site region was divided into two fragments, causing a temporary loss of activity. A dissected active site of CBLuc was located in the opposite side of the other dissected site in the probe backbone, with respect to CP. In this conformation, the encountering chance between the fragmented active sites is extremely decreased in the basal conditions. This structure contributes to (1) the dramatic decrease of the basal activity of the probe, and (2) the improved signal-to-background ratios in our study.
5. Any protein–protein binding models may be acceptable as the binding pair of interest. Considering that this is an intramolecular protein–protein interaction, CP probes have a potential to illuminate relatively weak protein–protein binding models, which is impossible to be determined with a conventional bioassays.
6. The phosphorylation of estrogen receptor (ER) at Y537 is recognized by the adjacent SH2 domain. This intramolecular protein–protein interaction triggers reconstitution of the split-CBLuc. This phosphorylation-mediated binding can be proved with a reference probe carrying point-mutated ER LBD at Y537F.
7. Any protein pair may be attached at the new N- and C-termini. The pair includes FRB and FRBP, and *Xenopus laevis* calmodulin and M13.
8. Many public websites helping primer design exist, where one may check the feasibility of their own primers.
9. A flexible linker between the cDNA fragments may be set by this primer design. Typical flexible linkers consist of glycine (G) and serine (S), and thus called “GS” linker.
10. A double digestion of the PCR products saves time and labor. New England Biolabs (NEB) provides a CutSmart buffer, with which most of double digestions are available.

11. The total response time, 20 min, comprised the total time for (1) penetration of OHT across the plasma membrane, (2) OHT–ER LBD binding and conformation change of ER LBD, (3) subsequent binding of ER LBD with Src SH2, and (4) intramolecular complementation between the fragments of CBLuc. The large portion of the total response time, 20 min, was consumed during the penetration of OHT into the cytosol.
12. The injected solution cocktail of Bright-Glo (Promega) lyses the cells during the 3 min.
13. On/off system of conventional fluorescent probes with circularly permutated GFP (cpGFP) is considered to depend on the altered quantum yield of fluorescence by solvent penetration into the chromophore [4, 5]. In contrast, the recovery of luminescence in the present probes is based on the physical approximation after dissociation between the completely separated fragments of a split luciferase, and not on the hydrophobicity variance like cpGFP.
14. The detection limit is greatly improved, compared with conventional single-chain probes. It may be explained with the fact that CP of CBLuc decreases the basal interactions between the ER LBD and SH2 in the absence of a ligand.
15. The spectra of reconstituted CBLuc show that red-orange light was enhanced by OHT and the λ_{max} was the same as that of intact CBLuc. This result is correspondent with the results with bandpass filters.

Acknowledgements

This work was supported by grants from Japan Society for the Promotion of Science (JSPS), grant numbers 26288088, 16K-14051, and 15KK0029.

References

1. Weissleder R, Ntziachristos V (2003) Shedding light onto live molecular targets. Nat Med 9:123–128
2. Kim SB (2012) Labor-effective manipulation of marine and beetle luciferases for bioassays. Protein Eng Des Sel 25:261–269
3. Kyte J, Doolittle RF (1982) A simple method for displaying the hydropathic character of a protein. J Mol Biol 157:105–132
4. Kotlikoff MI (2007) Genetically encoded Ca^{2+} indicators: using genetics and molecular design to understand complex physiology. J Physiol 578:55–67
5. Souslova EA, Chudakov DM (2007) Genetically encoded intracellular sensors based on fluorescent proteins. Biochemistry (Mosc) 72: 683–697
6. Kim SB, Sato M, Tao H (2008) Circularly permutated bioluminescent probes for illuminating ligand-activated protein dynamics. Bioconjug Chem 19:2480–2486

Chapter 14

Fabrication of Molecular Strain Probes for Illuminating Protein–Protein Interactions

Sung-Bae Kim and Rika Fujii

Abstract

A unique bioluminescent imaging probe is introduced for illuminating molecular tension appended by protein–protein interactions (PPIs) of interest. A full-length luciferase is sandwiched between two proteins of interest via minimal flexible linkers. The ligand-activated PPIs append intramolecular tension to the sandwiched luciferase, boosting or dropping the enzymatic activity in a quantitative manner. This method guides construction of a new lineage of bioassays for ligand-activated PPIs.

Key words Luciferase, Bioluminescence, Molecular tension, Protein–protein interactions

1 Introduction

To date, several potential techniques have been established for determining protein–protein interactions (PPIs), including (1) Bioluminescence resonance energy transfer (BRET) based on energy transfer between bioluminescent donor and fluorescent acceptor proteins [1–3]; (2) mammalian/yeast two-hybrid assay reflecting interactions between "Prey" and "Bait" proteins [4]; (3) Protein-fragment complementation assay (PCA) making use of split-reporter protein and its conditional reconstitution [5, 6].

We previously developed a unique bioluminescent probe called "strain probe" for illuminating PPIs [7]. We initially hypothesized that any luciferase has talent to change its enzymatic activity according to the molecular tension artificially appended by PPIs. This molecular tension may cause distortion of the active site, which modulates the enzymatic activity.

In this protocol, we introduce how to fabricate *molecular tension probes* emitting bioluminescence in response to molecular tension a ppended by PPIs in detail.

Sung-Bae Kim (ed.), *Bioluminescence: Methods and Protocols*, Methods in Molecular Biology, vol. 1461,
DOI 10.1007/978-1-4939-3813-1_14, © Springer Science+Business Media New York 2016

1.1 Basic Concept for Designing Molecular Tension Probes

The basic design of *molecular tension probes* consists of four different ingredients, i.e., a full-length luciferase, a pair of proteins of interest (called proteins "A" and "B"), and a flexible linker, where the luciferase is sandwiched between the two proteins of interest via a minimal length of flexible linkers (*see* Fig. 1). The luciferase is tensed by the ligand-activated PPIs. The minimal flexible linkers as possible connecting the ingredients are advantageous to efficiently convert the molecular tension to practical distortion of the sandwiched luciferase.

All luciferases basically have talent to vary their enzymatic activity more or less according to the molecular tension appended by an intramolecular PPI. A globular marine luciferase may be advantageous over beetle luciferases, which consist of N- and C-terminal domains connected by a flexible hinge region [8] (*see* Fig. 1a). A globular marine luciferase like *Renilla reniformis* luciferase (RLuc) easily receives tension from PPIs, whereas the flexible region in beetle luciferases relaxes the intramolecular tension (*see* **Note 1**). The active site of RLuc8 is close from the C-terminal end [9], thus is prone to be influenced by protein-tagging and molecular tension appended by adjacent proteins.

In this protocol, we exemplify a *molecular tension probe* that is made of RLuc8 as a model luciferase sandwiched between the ligand-binding domain of the human estrogen receptor (ER LBD) and the

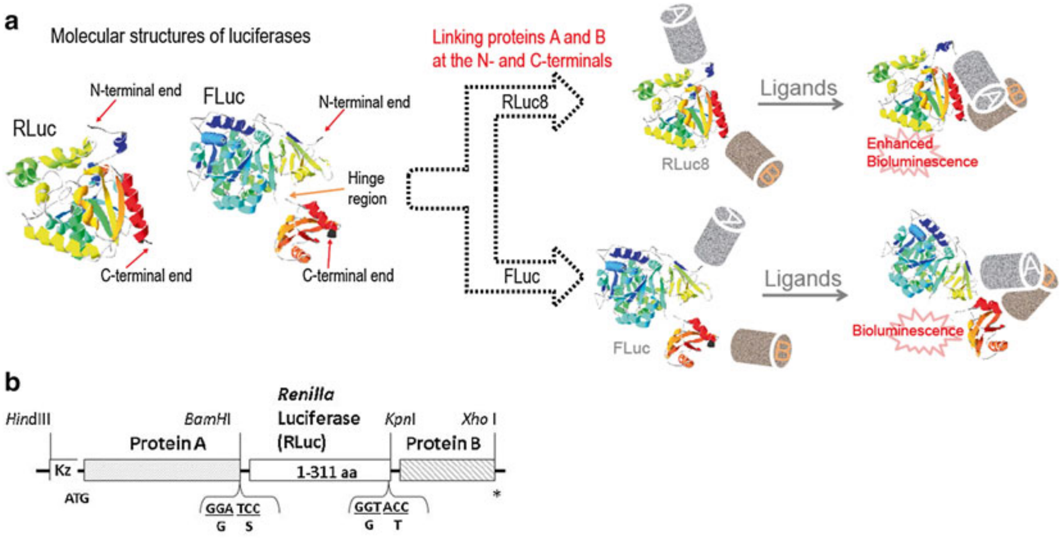
a
Molecular structures of luciferases
RLuc
N-terminal end
C-terminal end
FLuc
N-terminal end
Hinge region
C-terminal end
Linking proteins A and B at the N- and C-terminals
RLuc8
FLuc
RLuc8
Ligands
Enhanced Bioluminescence
FLuc
Ligands
Bioluminescence
A
B
b
HindIII
BamHI
Renilla Luciferase (RLuc)
KpnI
Xho I
Protein A
Protein B
Kz
1-311 aa
ATG
GGA TCC
G S
GGT ACC
G T
*

Fig. 1 (**a**) The working mechanism of *molecular tension probes*. Any luciferase may be sandwiched between two proteins A and B of interest. A ligand triggers an interaction between proteins A and B, which appends tense to the sandwiched luciferase. (**b**) A schematic diagram of the cDNA construct showing the segments. The linkers between the segments were minimized. It was designed that the restriction sites are the only linkers to connect each segment in the construct. Abbreviations: *RLuc8*, A *Renilla* luciferase variant carrying eight mutations; *FLuc*, a firefly luciferase; *Kz*, kozak sequence; *ER LBD*, the ligand binding domain of estrogen receptor; *SH2*, the Src homology domain 2 of *v*-Src

Src homology domain 2 of *v*-Src (SH2). Upon ligand activation, Tyr537 of ER LBD is phosphorylated and recognized by the counterpart SH2 domain. This molecular tension varies the bioluminescence intensity of the sandwiched RLuc8 (*see* Fig. 1).

2 Reagents

1. A mammalian expression vector, pcDNA 3.1(+) (Invitrogen).
2. Restriction enzymes (New England Biolabs); *Hind*III, *BamH*I, *Kpn*I, *Xho*I.
3. An African green monkey kidney-derived COS-7 cells.
4. Dulbecco's modified Eagle's medium (DMEM).
5. Fetal bovine serum (FBS; Gibco).
6. Penicillin-streptomycin (P/S; Gibco).
7. A repofection reagent, TransIT-LT1 (Mirus).
8. 17β-estradiol (E_2), an endogenous estrogen.
9. 4-Hydroxytamoxifen (OHT), a synthetic antiestrogen.
10. Phosphate-buffered saline (PBS; pH 7.4, 0.02 M).
11. A lysis buffer (E291A, Promega).
12. An assay buffer (E290B, Promega).
13. 100× native coelenterazine (nCTZ) (Promega).
14. A Bradford reagent for staining proteins (Wako Pure Chemicals).
15. A Hank's buffered salt solution (HBSS) buffer (Gibco).

3 Methods

3.1 Preparation of the DNA Constructs Encoding a Molecular Tension Probe

The cDNA constructs encoding *molecular tension probes* is fabricated by conventional genetic engineering techniques including polymerase chain reaction (PCR) with an adequate primer set and its subcloning into a mammalian expression vector as follows (*see* Fig. 1).

1. Generate the cDNA segments encoding full-length *Renilla* luciferase 8 (1–311 aa; RLuc8) by PCR using a corresponding primer set flanked with unique restriction sites, *BamH*I and *Kpn*I, for introducing unique restriction sites at the 5′- and 3′-terminals, respectively.
2. Seperately fabricate the cDNA segments encoding the ER LBD and the SH2 domain of *v*-Src by PCR using corresponding primer sets flanked with the unique restriction sites, *Hind*III/*BamH*I, and *Kpn*I/*Xho*I, respectively.
3. Digest the above cDNA segments and the multiple cloning site (MCS) of a mammalian expression vector pcDNA 3.1(+) (Invitrogen) with the corresponding restriction enzymes,

*Hind*III/*Bam*HI; *Bam*HI/*Kpn*I; *Kpn*I/*Xho*I; *Hind*III/*Kpn*I, respectively (*see* **Note 2**).

4. Gel-purify the digested cDNA segments and the expression vector.
5. Ligate the cDNA segments into the expression vector *p*cDNA 3.1(+) to fabricate a cDNA construct encoding the *molecular tension probe* (single coding sequence) (*see* Fig. 1b).
6. Confirm the sequences of the cDNA constructs in pcDNA 3.1(+) vector with a genetic sequencer (GenomeLab GeXP, Beckman Coulter) (*see* **Note 3**). The expressed probe may be called ERS.

3.2 Bioluminescence Spectra of COS-7 Cells Carrying *p*Ers

The ligand-driven variance of optical spectra can be determined with a mammalian culture cell line, COS-7 cells, carrying *the molecular tension probe* as follows (*see* Fig. 2a).

1. Grow COS-7 cells derived from African green monkey kidney fibroblast (*see* **Note 4**) in a Dulbecco's modified Eagle's medium (DMEM) supplemented with 10 % fetal bovine serum (FBS; Gibco), and 1 % penicillin-streptomycin (P/S; Gibco) at 37 °C in 5 % CO_2.
2. Subclone the cells in 12-well culture plates, and transiently transfect them in each well with an aliquot (1 μg) of *p*Ers using a transfection reagent, TransIT-LT1 (Mirus).
3. Incubate the cells for 16 h in a cell incubator (5 % CO_2, 37 °C) (*see* **Note 5**).
4. Stimulate the cells on the 12-well plates for 20 min with the vehicle (0.1 % DMSO), 1 μM of 17β-estradiol (E_2; estrogen) or 1 μM of 4-hydroxytamoxifen (OHT; antiestrogen). Wash the cells once with phosphate-buffered saline (PBS; pH 7.4, 0.02 M).

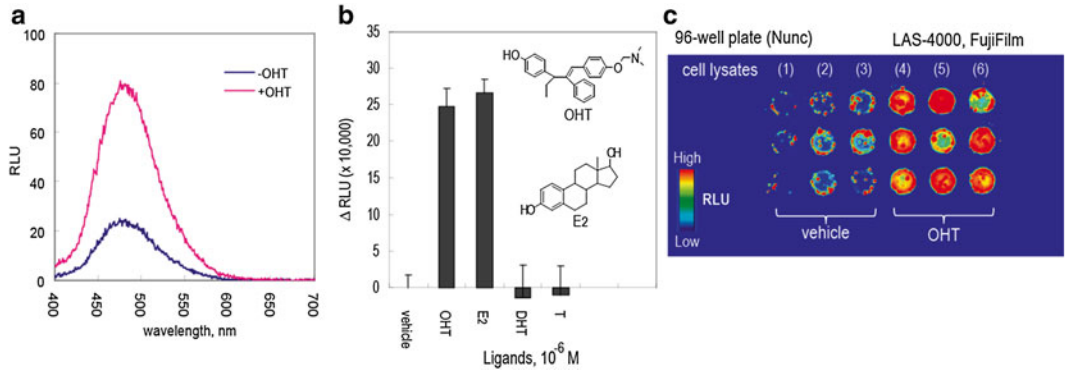

Fig. 2 (**a**) Variance in the bioluminescence emission spectra before and after addition of 1 μM 4-hydroxytamoxifen (OHT). (**b**) Ligand selectivity of ERS. The luminescence intensities were compared after activation of ERS with various ligands. The figure was reproduced in part from Kim et al. with permission from Bioconjugate Chem. [7]. (**c**) An optical image of the lysates of COS-7 cells after stimulation with vehicle or OHT (*n* = 9)

5. Lyse the cells with a lysis buffer (E291A, Promega) for 15 min at room temperature.
6. Transfer an aliquot (50 μL) of the lysates into a 1.5 mL microtube and determine the bioluminescence spectra with a spectrophotometer (*see* **Note 6**) immediately after addition of an aliquot (400 μL) of an assay buffer (E290B, Promega) dissolving native coelenterazine (nCTZ) into the microtube.

3.3 Determination of Estrogenic Activity of Chemicals with a Molecular Tension Probe

Estrogenicity of hormones and synthetic chemicals is visualized with a *molecular tension probe*, ERS, as follows (*see* Fig. 2b).

1. Grow COS-7 cells in a 96-well plate in a cell incubator (5% CO_2, 37 °C).
2. Transiently transfect the COS-7 cells in the plate with an aliquot of pErs (0.2 μg/well) using the lipofection reagent (TransIT-LT1, Mirus) and incubate them in the cell incubator for 16 h.
3. Stimulate the cells with the vehicle, 10^{-6} M of E_2, or 10^{-6} M of OHT for 20 min (*see* **Note 7**).
4. Wash the cells once in the plate with PBS, and lyse them with a lysis buffer (E291A, Promega) for 15 min.
5. Transfer the cell lysates to a 1.5 mL microtube and determine the subsequent bioluminescence intensities with a luminometer (Glomax 20/20, Promega) immediately after adding an assay solution (E290B, Promega) dissolving nCTZ.
6. Measure the total protein amounts in the applied cell lysates with a Bradford reagent for the following normalization.
7. Normalize the bioluminescence intensities as follows: The RLuc luminescence intensities were expressed as a ratio of relative luminescence unit (RLU), that is, RLU (+)/RLU (−), where RLU (+) and RLU (−) are the luminescence intensities with 1 μg of cell lysate after the cells were incubated with and without a ligand, respectively; the RLU is an amplified value of photon counts generated from the luminometer (arbitrary unit) (*see* Fig. 2b).

The procedure from **steps 5** to 7 may be substituted by the following alternative (*see* Fig. 2c).

5a. Transfer an aliquot of the cell lysates to a fresh 96-well optical bottom plate (*see* **Note 8**).

6a. Simultaneously inject an aliquot (50 μL) of the assay buffer dissolving nCTZ into the cell lysates on the plate using a multichannel pipette (*see* **Note 9**) and immediately transfer the plate in an image analyzer (LAS-4000, FujiFilm).

7a. Determine the optical intensities on the plate with the equipped controlling software (Image reader ver. 2.0) and analyze the optical images with the analysis software (Multi Gauge ver. 3.1).

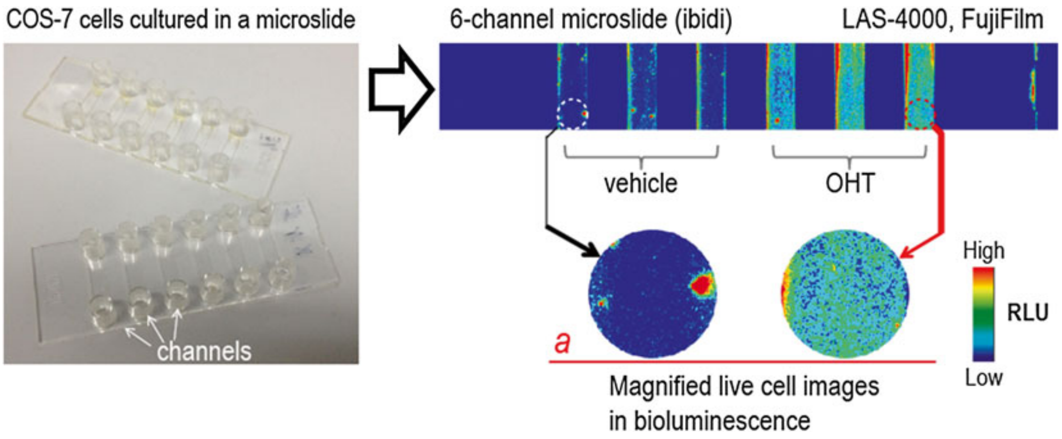
COS-7 cells cultured in a microslide
channels
6-channel microslide (ibidi)
LAS-4000, FujiFilm
vehicle
OHT
a
Magnified live cell images in bioluminescence
High
RLU
Low

Fig. 3 A bioluminescence image (BLI) of COS-7 cells carrying the tension probe on a microslide (μ-Slide IV$^{0.4}$, ibidi). The three channels on the *left* and *right* are stimulated with vehicle and ligand, respectively ($n=3$). The *inset a* shows a magnified optical image of the microslide

8a. Normalize the optical intensities per area (originally expressed in RLU/mm^2) to the integrated time (sec) and applied protein amounts (μg): i.e., RLU/s/mm^2 or RLU/μg/s/mm^2.

3.4 Bioluminescence Imaging (BLI) of Living Mammalian Cells with a Molecular Tension Probe

Live-cell images by ERS are conducted with the following procedure (*see* Fig. 3).

1. Grow COS-7 cells in a six-channel microslide (μ-slide VI$^{0.4}$, ibidi) until a 80 % fluency (*see* **Note 10**).
2. Transiently transfect the cells with pErs using a lipofection reagent (TransIT-LT1, Mirus) and incubate them in a cell incubator (5 % CO_2, 37 °C) for 16 h.
3. Stimulate the cells in the channels with vehicle (0.1 % DMSO) or 10^{-6} M OHT for 20 min before image acquisition.
4. Wash the cells in the channels once with a Hank's buffered salt solution (HBSS) buffer (Gibco) and then fill the channels simultaneously with 80 μL of an HBSS buffer dissolving nCTZ using a multichannel pipet.
5. Immediately transfer the microslide into the dark box of an image analyzer (LAS-4000mini, FujiFilm) and determine the optical images with the equipped software (Image reader ver2.0 and Multi Gauge ver3.1).

4 Notes

1. The C-terminal domain of firefly luciferase (FLuc) is rotated to release luciferin in the light-emitting process [10], which is hampered by the molecular tension in the probe.

2. A double digestion is convenient with the Cutsmart buffer of New England Biolab (NEB).
3. In this protocol, the made probes are named "ERS" from the consecutive initial letters of the components, i.e., *E*R LBD-*R*Luc8-*S*H2. The corresponding plasmid may be named *p*Ers.
4. Any mammalian cell lines are basically applicable for this protocol.
5. The incubation time influences on the signal-to-background (S/B) ratios. A better S/B ratio is achieved by avoiding the overexpression.
6. Recommended is a spectra photometer equipped with a cooled CCD camera which simultaneously acquires the whole range of wavelength, instead of scanning the wavelength range.
7. A concentration ranging from 10^{-5} to 10^{-7} M of steroid is appropriate for the stimulation.
8. An optical-bottom microplate manufactured for bioluminescence is recommended for suppression of the background bioluminescence.
9. 8- or 12-channel pipettes are useful for the simultaneous injection.
10. Because of the small culture medium volume in the channels of the microslide, the culture medium is prone to be condensed by evaporation. The culture medium needs to be refreshed every 12 h for easing the condensation.

Acknowledgements

This work was supported by grants from Japan Society for the Promotion of Science (JSPS), grant numbers 26288088, 16K14051, and 15KK0029.

References

1. Hoshino H, Nakajima Y, Ohmiya Y (2007) Luciferase-YFP fusion tag with enhanced emission for single-cell luminescence imaging. Nat Methods 4:637–639
2. Gammon ST, Villalobos VM, Roshal M, Samrakandi M, Piwnica-Worms D (2009) Rational design of novel red-shifted BRET pairs: platforms for real-time single-chain protease biosensors. Biotechnol Prog 25:559–569
3. De A, Ray P, Loening AM, Gambhir SS (2009) BRET3: a red-shifted bioluminescence resonance energy transfer (BRET)-based integrated platform for imaging protein-protein interactions from single live cells and living animals. FASEB J 23:2702–2709
4. Pichler A, Prior JL, Luker GD, Piwnica-Worms D (2008) Generation of a highly inducible Gal4 → FLuc universal reporter mouse for *in vivo* bioluminescence imaging. Proc Natl Acad Sci U S A 105:15932–15937
5. Luker KE, Smith MC, Luker GD, Gammon ST, Piwnica-Worms H, Piwnica-Worms D (2004) Kinetics of regulated protein-protein interactions revealed with firefly luciferase complementation imaging in cells and living animals. Proc Natl Acad Sci U S A 101:12288–12293

6. Kim SB, Umezawa Y, Kanno KA, Tao H (2008) An integrated-molecule-format multicolor probe for monitoring multiple activities of a bioactive small molecule. ACS Chem Biol 3:359–372
7. Kim SB, Sato M, Tao H (2009) Molecular tension-indexed bioluminescent probe for determining protein-protein interactions. Bioconjug Chem 20:2324–2330
8. Nakatsu T, Ichiyama S, Hiratake J, Saldanha A, Kobashi N, Sakata K, Kato H (2006) Structural basis for the spectral difference in luciferase bioluminescence. Nature 440:372–376
9. Loening AM, Wu AM, Gambhir SS (2007) Red-shifted *Renilla reniformis* luciferase variants for imaging in living subjects. Nat Methods 4:641–643
10. Sundlov JA, Fontaine DM, Southworth TL, Branchini BR, Gulick AM (2012) Crystal structure of firefly luciferase in a second catalytic conformation supports a domain alternation mechanism. Biochemistry 51:6493–6495

Chapter 15

An ALuc-Based Molecular Tension Probe for Sensing Intramolecular Protein–Protein Interactions

Sung-Bae Kim, Ryo Nishihara, and Koji Suzuki

Abstract

Optical imaging of protein–protein interactions (PPIs) facilitates comprehensive elucidation of intracellular molecular events. The present protocol demonstrates an optical measure for visualizing molecular tension triggered by any PPI in mammalian cells. A unique design of single-chain probes was fabricated, in which a full-length artificial luciferase (ALuc®) was sandwiched between two model proteins of interest, e.g., FKBP and FRB. A molecular tension probe comprising ALuc23 greatly enhances the bioluminescence in response to varying concentrations of rapamycin, and named "tension probe (TP)." The basic probe design can be further modified towards eliminating the C-terminal end of ALuc and was found to improve signal-to-background ratios, named "combinational probe." TPs may become an important addition to the tool box of bioassays in the determination of protein dynamics of interest in mammalian cells.

Key words Bioluminescence, Protein–protein interactions, Tension probe, Bioluminescent imaging, Combinational probe

1 Introduction

Optical imaging of the protein–protein interactions (PPIs) facilitates comprehensive elucidation of intracellular molecular events [1]. To date, PPIs have been visualized with various strategies using fluorescent proteins and luciferases, which include *F*luorescence *R*esonance *E*nergy *T*ransfer (FRET) [2], *B*ioluminescence *R*esonance *E*nergy *T*ransfer (BRET) [3], and *P*rotein-fragment *C*omplementation *A*ssay (PCA) [4, 5].

PCA is an emerging technology for determining the occurrence of PPIs in mammalian cell lines, where a monomeric luciferase is split into two fragments for a temporal loss and conditional reconstitution of the activities only upon PPI [6, 7]. To date, many luciferases including firefly luciferase (FLuc) [4, 5], *Renilla reniformis* luciferase (RLuc) [8], and artificial luciferase (ALuc®) [9] (*see* **Note 1**) have been utilized for PCA. However, this methodology requires a complex probe design and a tedious optimization process for

Sung-Bae Kim (ed.), *Bioluminescence: Methods and Protocols*, Methods in Molecular Biology, vol. 1461,
DOI 10.1007/978-1-4939-3813-1_15, © Springer Science+Business Media New York 2016

seeking a suitable dissection site and restores merely 0.5–5 % of the original optical intensity after complementation [10, 11]. The sophisticated molecular design limits the general applicability of an optimized PPI model to other bioassays. A bioluminescent probe using the full length of luciferases without luciferase dissection provides an ideal optical means allowing a maximal optical intensity.

In the present protocol, we guide on how to fabricate an efficient molecular tension probe with ALucs, which varies its enzymatic activity by molecular tension physically induced by PPIs (*see* **Note 2**). We first fabricated a model bioluminescent probe comprising full-length ALucs sandwiched between the *FK*506-*b*inding *p*rotein (FKBP) and the *F*KBP-*r*apamycin-*b*inding domain of mTOR (FRB) as a model protein pair (*see* Fig. 1a). The model luciferase, ALuc®, was selected because of its excellent optical intensity and stability [9, 12] (*see* **Note 3**). Rapamycin triggers a FKBP–FRB interaction, which induces molecular tension to the sandwiched full-length ALuc®. The tensed ALuc enhances the optical intensities in a ligand-dependent manner (*see* Fig. 1b). This unique tension probe was named "molecular *t*ension *p*robe (abbreviated *TP* for short). Further, a series of combinational probes were fabricated, where several amino acids at the C-terminal end in the probe is eliminated and designed to be compensated by the homological N-terminal end of FRBP, which was named a "combinational probe."

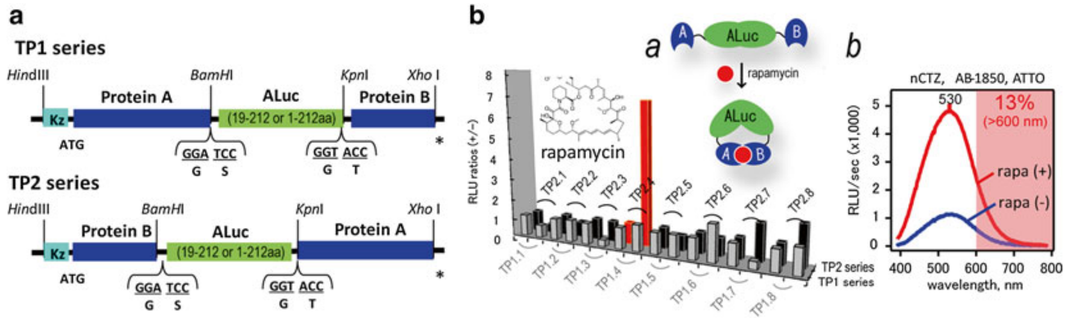

Fig. 1 (**a**) Schematic structures of cDNA constructs of bioluminescent template candidates for sensing molecular tension. Tension probes v1 and v2 differ in the order of proteins A and B of interest. Abbreviations: *TP1* and *TP2*, Tension probes ver. 1 and ver. 2; *Kz*, kozak sequence. (**b**) Optical intensity variance of 16 kinds of template candidates before and after ligand stimulation ($n = 3$). The *gray* and *black bars* indicate TP1 and TP2 series templates, respectively. The signs "+" and "−" at the *X*-axis represent the presence or absence of rapamycin, respectively. The *red bars* highlight the dramatic elevation of bioluminescence from a tension probe named "TP2.4." The *inset a* shows that the basic working mechanism of molecular tension probes in mammalian cells. The proteins *A* and *B* in the tension probe are approximated in response to a ligand. The protein binding causes molecular strain to the sandwiched ALuc®. The molecular tension dramatically enhances bioluminescence. The *inset b* shows the bioluminescence spectra of TP2.4 before and after rapamycin stimulation. The maximal optical intensity is found at 530 nm. Abbreviations: *TP1.1*, Tension probe ver. 1.1; *TP2.1*, Tension probe ver. 2.1, etc. Reproduced in part from Kim et al. with permission from Bioconjugate Chemistry [15]

2 Reagents

1. Restriction enzymes (New England Biolads): *Hind*III, *BamH*I, *Kpn*I, *Xho*I.
2. A DNA ligation kit (Takara Bio).
3. *p*cDNA 3.1(+) mammalian expression vector (Invitrogen).
4. African green monkey kidney-derived COS-7 cells.
5. Dulbecco's modified Eagle's medium (DMEM).
6. Fetal bovine serum (FBS; Gibco).
7. Penicillin–streptomycin mixture (P/S; Gibco).
8. A lipofection reagent (TransIT-LT1; Mirus).
9. Rapamycin, an inhibitor of the Ser/Thr protein kinase.
10. A lysis buffer, included in a *Renilla* luciferase assay kit (E291A, Promega).
11. An assay solution, included in a *Renilla* luciferase assay kit (E290B, Promega).
12. A *Renilla* luciferase assay kit comprising 100× native coelenterazine (nCTZ) (E2820, Promega).
13. An Hanks' Balanced Salt Solution(HBSS) buffer (Gibco).
14. A 96well optical bottom microplate for bioluminescence measurement (Thermo Scientific).

3 Methods

3.1 Construction of Plasmids

We generated a series of DNA constructs encoding 19 kinds of different molecular designs for estimating their potential as molecular tension probes able to sense PPIs (*see* Table 1). The basic molecular structures of TP1 and TP2 series probes differ in the consecutive order of their component proteins from the N-terminal end. The schematic diagrams of the cDNA constructs are illustrated in Fig. 1a.

1. As a template for polymerase chain reaction (PCR), obtain the cDNAs encoding the following components from the corresponding providers: ALucs 16, 23, 24, 30 were from our previous studies [9, 12]; the human FKBP (12 kD, Genbank access number: AAP36774.1) and FRB (11 kD, PDB access number: 1AUE_A) were custom-synthesized by Eurofins Genomics (Tokyo) on the basis of the sequence information of a public database (NCBI) (*see* **Note 4**).
2. Generate a series of cDNA segments encoding the components shown in Table 1 by PCR using corresponding primers to introduce unique restriction sites, *Hind*III/*BamH*I, *BamH*I/*Kpn*I, or *Kpn*I/*Xho*I at the 5′ and 3′ ends, respectively (*see* **Note 5**).

Table 1
Detailed list of the components of the molecular tension probes, fabricated in this study

Probe name	Protein A[a]	Inserted luciferase	Length of luciferase[b]	Internal secretion peptide (SP)[c]	Protein B[a]	Figure numbers in use
TP1.1	12.246 pt	ALuc16	*1–212 (full)*	+	FRB	Fig. 1
TP1.2	FKBP	ALuc16	*19–212*	–	FRB	Fig. 1
TP1.3	FKBP	ALuc23	*1–212 (full)*	+	FRB	Fig. 1
TP1.4	FKBP	ALuc23	*19–212*	–	FRB	Fig. 1
TP1.5	FKBP	ALuc24	*1–212 (full)*	+	FRB	Fig. 1
TP1.6	FKBP	ALuc24	*19–212*	–	FRB	Fig. 1
TP1.7	FKBP	ALuc30	*1–212 (full)*	+	FRB	Fig. 1
TP1.8	FKBP	ALuc30	*19–212*	–	FRB	Fig. 1
TP2.1	FRB	ALuc16	*1–212 (full)*	+	FKBP	Fig. 1
TP2.2	FRB	ALuc16	*19–212*	–	FKBP	Fig. 1
TP2.3	FRB	ALuc23	*1–212 (full)*	+	FKBP	Fig. 1
TP2.4	**FRB**	**ALuc23**	**19–212**	–	**FKBP**	Figs. 1, 2, 3, and 4
TP2.5	FRB	ALuc24	*1–212 (full)*	+	FKBP	Fig. 1
TP2.6	FRB	ALuc24	*19–212*	–	FKBP	Fig. 1
TP2.7	FRB	ALuc30	*1–212 (full)*	+	FKBP	Fig. 1
TP2.8	FRB	ALuc30	*19–212*	–	FKBP	Fig. 1
TP3.1	FRB	ALuc23	*19–209*	–	FKBP	Fig. 3
TP3.2	FRB	ALuc23	*19–207*	–	FKBP	Fig. 3
TP3.3	**FRB**	**ALuc23**	19–198	–	**FKBP**	Fig. 3

ER LBD the ligand-binding domain of estrogen receptor, *SH2* the SH2 domain of *v*-Src

[a] Proteins A and B refer to the proteins at the N- and C-terminal ends of the tension probe

[b] "Length of Luciferase" indicates the amino acid numbers of the inserted luciferase

[c] The signs "+" and "–" represent the presence or absence of secretion peptide (SP)

3. Restrict the cDNA segments by the corresponding restriction enzymes (NEB), ligated with a ligation kit (Takara Bio), and finally subcloned into a *p*cDNA 3.1(+) mammalian expression vector (Invitrogen) using the *Hind*III and *Xho*I sites. The probes are categorized into three groups (TP1, TP2, and TP3 series) according to the molecular designs (*see* Table 1 and **Note 6**). The corresponding plasmids may be called pTP1, pTP2, and pTP3, respectively.
4. Confirm the DNA sequences of all the constructs with a genetic analysis system (GenomeLab GeXP, Beckman Coulter).

3.2 Evaluation of an Optimal Molecular Design for Molecular Tension Probes

Sixteen kinds of molecular designs are examined for fabricating efficient molecular tension probes (*see* Fig. 1b).

1. Culture the African green monkey kidney-derived COS-7 cells in a 96-well plate (Nunc) in a Dulbecco's modified Eagle's medium (DMEM) supplemented with 10 % fetal bovine serum (FBS; Gibco), and 1 % penicillin-streptomycin (P/S; Gibco) at 37 °C in a cell incubator (5 % CO_2; Sanyo).
2. Transfect the cells on the plate transiently with an aliquot (0.2 μg/well) of the pcDNA 3.1(+) vector encoding one of the TP1 and TP2 series probes using a lipofection reagent (TransIT-LT1; Mirus), and incubated for 16 h at 37 °C in 5 % CO_2 before the following experiments.
3. Stimulate the cells on the plate with vehicle (0.1 % ethanol dissolved in the culture medium) or 10^{-6} M of rapamycin for 4 h and lyse with a lysis buffer (Promega) (*see* **Note 7**).
4. Transfer an aliquot (10 μL) of the lysates into a fresh 96-well optical bottom microplate (Thermo Scientific) and simultaneously mix with 50 μL of assay solution (Promega) containing native coelenterazine (nCTZ) with a multichannel pipette (Gilson) (*see* **Note 8**).
5. Place the plate immediately into the chamber of an image analyzer (LAS-4000, FujiFilm) equipped with a cooled CCD camera system (−25 °C).
6. Determine the optical intensities with the image acquisition software (Image Reader v2.0) and analyze with the specific image analysis software (Multi Gauge v3.1).
7. TP2.4 exhibits 6.7-fold enhanced bioluminescence intensity in the presence of 10^{-6} M of rapamycin compared to the presence of vehicle alone (0.1 % ethanol dissolved in the culture medium). In contrast, TPs comprising the secretion peptide (SP) at the N-terminal end generally exerts poor optical variation in response to 10^{-6} M rapamycin (*see* **Notes 9** and **10**).

The corresponding optical spectra can be taken in the presence or absence of rapamycin as follows (*see* Fig. 1b, inset *b*). The protocol shares the same procedure as the above **steps 1** and **2**.

1. Stimulate the COS-7 cells expressing TP2.4 with 10^{-5} M of rapamycin for 4 h and lyse with the lysis buffer.
2. Mix 5 μL of the lysate with 35 μL of the assay solution (Promega) containing nCTZ in a 200 μL microtube.
3. Integrate the corresponding optical intensities for 30 s with a high-precision spectrophotometer (AB-1850, ATTO) equipped with a cooled charge-coupled device (CCD) camera that enables one-shot capture of the entire wavelength (*see* **Note 11**).

3.3 Ligand-Dependent Elevation of Optical Intensities of TP2.4

The following protocol allows determining the ligand-driven feature of the optical intensities of TP2.4 with varying concentrations of rapamycin (*see* Fig. 2).

1. Prepare the COS-7 cells expressing TP2.4 as described above for Fig. 1b.
2. Stimulate the cells with vehicle (0.1 % ethanol) or varying concentrations of rapamycin from 10^{-9} to 10^{-4} M for 4 h.
3. Lyse the cells with a lysis buffer (Promega) after washing once with a PBS buffer and transfer an aliquot (10 μL) of the lysates into a fresh 96-well optical-bottom plate (Thermo Scientific).
4. Mix the lysates in the plate simultaneously with 50 μL of assay solution (Promega) containing nCTZ with a multichannel pipette (Gilson).
5. Transfer the plate immediately into the chamber of the image analyzer and record the optical intensities.
6. Normalize the optical intensities (relative luminescence unit; RLU) to protein amount (μg), integration time (sec), and area (mm^2), i.e., the unit is expressed in RLU/μg/s/mm^2 (*see* **Note 12**).
7. Rapamycin increased the optical intensities even at low concentrations like 10^{-9} M, with the signal reaching a plateau at 10^{-5} M (*see* **Note 13**).

3.4 Fabrication of a Combinational Probe for Illuminating Protein–Protein Interactions

Because the C-terminal end of ALuc23 shares high sequential homology with the adjacent N-terminal end of FKBP inside TP2.4 (alignment score: 26, ClustalW v2.1), a combinational probe may be constructed through the following procedure (*see* **Note 14**). One can modify the TP2.4 to fabricate a combinational probe with the synergistic property of the molecular tension probe and a conventional protein-fragment complementation assay (PCA) as follows (*see* Fig. 3).

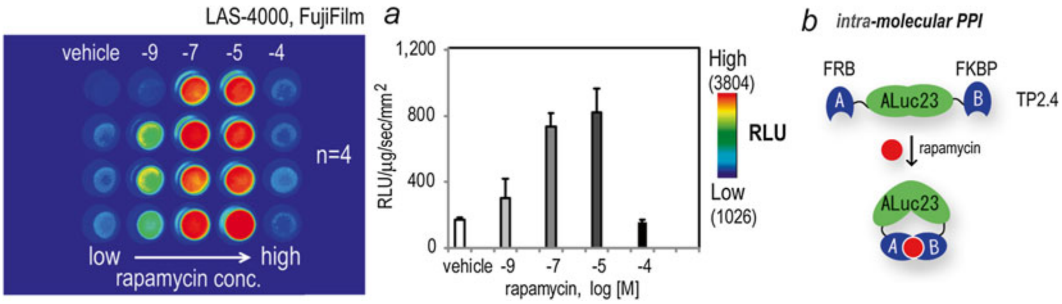

Fig. 2 The optical intensities of TP2.4 in response to varying concentrations of rapamycin ($n = 4$). *Inset a* indicates the absolute optical intensities adjusted by protein amount (μg), integration time (sec), and light-emitting area (mm^2). *Inset b* illustrates the working mechanism of the tension probes. Rapamycin provokes an intramolecular protein–protein interaction. Reproduced in part from Kim et al. with permission from Bioconjugate Chemistry [15]

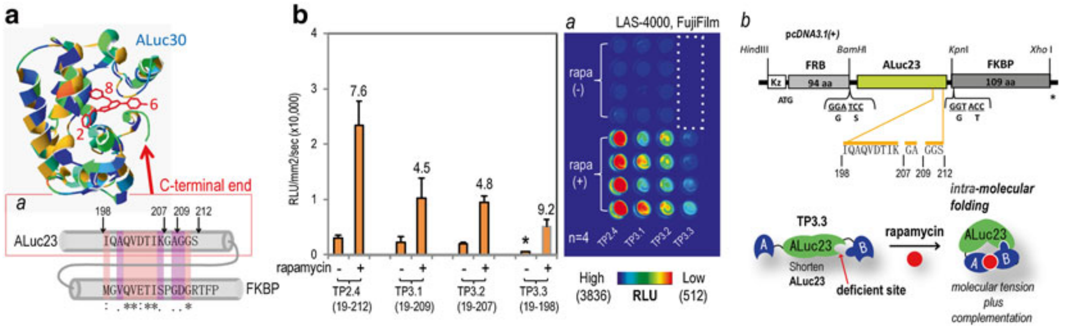

Fig. 3 (**a**) Predicted super two-dimensional structure of ALuc30 [12]. The *inset a* highlights the C-terminal end of ALuc30, which shares high sequential homology with the N-terminal end of FKBP. (**b**) Optical intensities of TP3 series in the presence or absence of rapamycin ($n = 4$). TP3 series templates contain a shortened C-terminal end of ALuc23 between FRB and FKBP, compared with the TP2 series. The *white dotted box* in the optical image indicates extremely suppressed background intensity. The corresponding amino acid length of the ALuc23 is specified in the parenthesis. The *asterisk* indicates the greatly diminished optical intensity. The *inset a* shows the corresponding optical image. The *inset b* shows the schematic diagram of the cDNA construct of a combinational bioluminescent probe, highlighting the eliminated amino acids of ALuc23. The drawing bellow illustrates a working mechanism of combinational bioluminescent probes. Reproduced in part from Kim et al. with permission from Bioconjugate Chemistry [15]

1. Fabricate a series of new trancated cDNA fragments encoding ALuc23 by PCR with respect to eliminating several amino acids at the C-terminal end of ALuc23 in TP2.4, as shown in Fig. 3b, inset *b* and name pTP3.1 to 3.3 (*see* Table 1).
2. Generate new pcDNA3.1(+) plasmids by replacing cDNA of the full-length ALuc23 in TP2.4 with the corresponding truncated cDNA fragments of ALuc23.
3. Prepare the COS-7 cells expressing one of the above-described TP3 probes (i.e., TP2.4, TP3.1, TP3.2, and TP3.3) in a 96-well optical bottom microplate with the same method as described above (*see* Fig. 3b, inset *b*).
4. Stimulate the cells in the plate with vehicle (0.1% Ethanol) or 10^{-6} M of rapamycin for 4 h, and determine the optical intensities from the cell lysates with the image analyzer as described above.
5. The maximal S/B ratio of 9.2 is found with TP3.3 embedding the shortest ALuc fragment (18–198 AA) (*see* **Note 15**).

3.5 Live-Cell Image of COS-7 Cells Carrying TP2.4

1. Conduct the bioluminescence imaging (BLI) with living COS-7 cells carrying TP2.4 in a multichannel microslide (μ-slide VI$^{0.4}$, ibidi) (*see* Fig. 4).
2. Transfect the COS-7 cells grown on the 6-channel microslide transiently with pTP2.4 and incubate for 2 days.
3. The cells on the left three channels and right three channels were then stimulated with vehicle (0.1% ethanol) or 10^{-6} M rapamycin for 4 h, respectively.

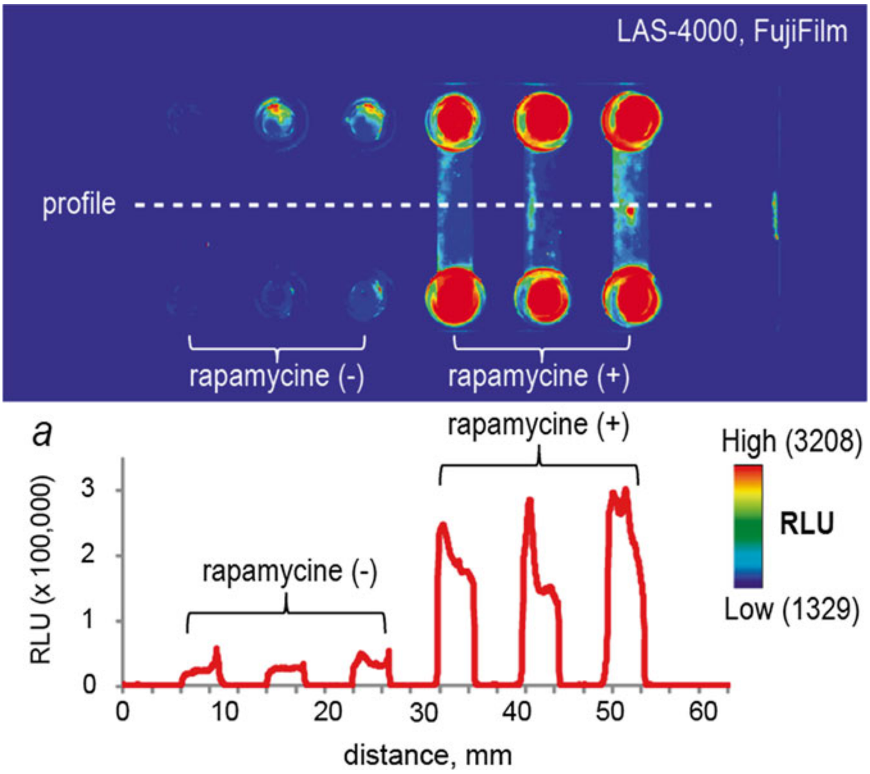

Fig. 4 Rapamycin-driven optical intensity variance of living COS-7 cells on a microslide. TP2.4 emits rapamycin-dependent bioluminescence. The *inset a* shows a profile of the optical image of the optical slide. Reproduced in part from Kim et al. with permission from Bioconjugate Chemistry [15]

4. Replace the culture media in the slide channels with an HBSS buffer containing nCTZ.
5. Transfer the slide immediately into the image analyzer and take the consequent optical image every 5 min in a high precision and 30 s integration mode.
6. The right three channels stimulated with 10^{-6} M rapamycin exhibit about six fold stronger optical intensities (i.e., 6.1 ± 0.7) in the slide, compared to the left three channels stimulated with the vehicle (0.1 % ethanol).

4 Notes

1. ALucs are originally established through extracting frequently occurring amino acids from multiple sequence alignment of highly conserved copepod luciferases from zooplanktons, which were collected at the southern deep-sea of Hokkaido, Japan (13 species) by our colleagues in AIST and two other conventional copepod luciferases (two species) [13, 14].

2. Beetle luciferases are excluded in the evaluation because they are said generally darker than copepod luciferases and comprise a long flexible region, naturally easing molecular tension.
3. ALucs are predicted to consist of two repeated mirror image-like catalytic domains, besides a highly variable domain at the N-terminal region including a unique secretion peptide (SP) according to the multiple alignment [9, 12].
4. The PPIs include homo- and hetro-dimerization of FRB and FKBP12.
5. Minimize the linkers connecting the probe components as possible to efficiently develop intramolecular tension inside the single-chain probe.
6. The cDNA constructs encoding TP1 and TP2 series probes differ in the consecutive order of the segments from the 5′ end (*see* Fig. 1a). The constructs encoding TP3 series probes are characteristic in that they carry cDNA segments encoding ALuc23 with a shortened C-terminal end, compared with the others.
7. The 4 h of incubation time to reach the optical plateau comprise all the periods for (a) plasma membrane (PM) permeation of rapamycin, (b) rapamycin-induced intramolecular binding between FRB and FKBP, and (c) the sandwiched ALuc–substrate interaction and corresponding emission of bioluminescence. Steps (b) and (c) are unlikely to be a rate-determining step because it reaches a plateau in less than 2 min, according to surface plasmon resonance (SPR) studies [16, 17]. The remaining step (a) is the rate-determining step. The PM permeability of chemicals greatly depends on the hydrophobicity. Variance of the stimulation times between steroid and rapamycin, i.e., 20 min vs. 4 h, is considered to reflect the PM permeability of the chemicals.
8. Because the appended molecular tension presumably modifies the internal shape of the active site, TPs may have a unique substrate selectivity and kinetics to coelenterazine analogues.
9. The SP-bearing TPs are secreted into the extracellular compartment, although the SP is in the middle of the TPs. According to our evaluation, 86% of the TP2.3 bearing SP is secreted into the extracellular compartment, whereas only 4% of the TP2.4 without SP is leaked into the extracellular compartment.
10. The other demerit of SP in TPs is that the SPs may act as natural flexible linker inside the probes and thus, may ease the intramolecular tension raised by the FKBP–FRB interaction, considering that the SP is located at the flexible N-terminal boundary.
11. The optical intensity in the spectra is greatly enhanced by rapamycin and the maximum optical intensity ($\lambda_{\max}$) was found at ca. 530 nm. About 13% of the overall light emission was located in the red and near-infrared region at a wavelength

longer than 600 nm, which is highly tissue-permeable and commonly referred to as "optical window."

12. The specific image analysis software (Multi Gauge v3.1; FujiFilm) allows setting region of interest (ROI) on the optical image for calculating the optical intensity per area (mm^2).
13. Rapamycin at 10^{-4} M resulted in only a basic level of optical intensities, close to those observed upon treatment with vehicle alone (0.1% ethanol). The poor optical intensity is interpreted as being caused by cell death induced by the excess amount of rapamycin.
14. The "combinational" means that the probe comprises both features of molecular tension probes and protein-fragment complementation assays (PCAs).
15. The improved S/B ratio is achieved by the greatly diminished "background" intensity, rather than the "signal" intensity developed by rapamycin. The basic optical signal intensity of TP3.3 induced by the vehicle was as low as that of the optical bottom plate itself (*see* Fig. 3b, inset *a*; dotted line).

Acknowledgements

This work was partly supported by JSPS KAKENHI Grants Number 26288088, 16K14051, and 15KK0029.

References

1. Ozawa T, Yoshimura H, Kim SB (2013) Advances in fluorescence and bioluminescence imaging. Anal Chem 85:590–609
2. Vogel SS, Thaler C, Koushik SV (2006) Fanciful FRET. Sci STKE 2006(331):re2
3. Hoshino H, Nakajima Y, Ohmiya Y (2007) Luciferase-YFP fusion tag with enhanced emission for single-cell luminescence imaging. Nat Methods 4:637–639
4. Luker KE, Smith MC, Luker GD, Gammon ST, Piwnica-Worms H, Piwnica-Worms D (2004) Kinetics of regulated protein–protein interactions revealed with firefly luciferase complementation imaging in cells and living animals. Proc Natl Acad Sci USA 101: 12288–12293
5. Kim SB, Awais M, Sato M, Umezawa Y, Tao H (2007) Integrated molecule-format bioluminescent probe for visualizing androgenicity of ligands based on the intramolecular association of androgen receptor with its recognition peptide. Anal Chem 79:1874–1880
6. Tarassov K, Messier V, Landry CR, Radinovic S, Serna Molina MM, Shames I, Malitskaya Y, Vogel J, Bussey H, Michnick SW (2008) An *in vivo* map of the yeast protein interactome. Science 320:1465–1470
7. Kim SB, Umezawa Y, Kanno KA, Tao H (2008) An integrated-molecule-format multicolor probe for monitoring multiple activities of a bioactive small molecule. ACS Chem Biol 3:359–372
8. Kaihara A, Umezawa Y (2008) Genetically encoded bioluminescent indicator for ERK2 dimer in living cells. Chem Asian J 3:38–45
9. Kim SB, Torimura M, Tao H (2013) Creation of artificial luciferases for bioassays. Bioconjug Chem 24:2067–2075
10. Paulmurugan R, Gambhir SS (2005) Firefly luciferase enzyme fragment complementation for imaging in cells and living animals. Anal Chem 77:1295–1302
11. Kim SB, Otani Y, Umezawa Y, Tao H (2007) Bioluminescent indicator for determining

protein–protein interactions using intramolecular complementation of split click beetle luciferase. Anal Chem 79:4820–4826

12. Kim SB, Izumi H (2014) Functional artificial luciferases as an optical readout for bioassays. Biochem Biophys Res Commun 448:418–423
13. Takenaka Y, Masuda H, Yamaguchi A, Nishikawa S, Shigeri Y, Yoshida Y, Mizuno H (2008) Two forms of secreted and thermostable luciferases from the marine copepod crustacean, Metridia pacifica. Gene 425: 28–35
14. Takenaka Y, Yamaguchi A, Tsuruoka N, Torimura M, Gojobori T, Shigeri Y (2012) Evolution of bioluminescence in marine planktonic copepods. Mol Biol Evol 29:1669–1681
15. Kim SB, Nishihara R, Citterio D, Suzuki K (2016) Genetically encoded molecular tension probe for tracing protein–protein interactions in mammalian cells. Bioconjug Chem 27(2): 354–362.
16. Banaszynski LA, Liu CW, Wandless TJ (2005) Characterization of the FKBP center dot Rapamycin center dot FRB ternary complex. J Am Chem Soc 127:4715–4721
17. Wear MA, Walkinshaw MD (2007) Determination of the rate constants for the FK506 binding protein/rapamycin interaction using surface plasmon resonance: An alternative sensor surface for Ni -nitrilotriacetic acid immobilization of His-tagged proteins. Anal Biochem 371:250–252

Chapter 16

Live Cell Bioluminescence Imaging in Temporal Reaction of G Protein-Coupled Receptor for High-Throughput Screening and Analysis

Mitsuru Hattori and Takeaki Ozawa

Abstract

G protein-coupled receptors (GPCRs) are notable targets of basic therapeutics. Many screening methods have been established to identify novel agents for GPCR signaling in a high-throughput manner. However, information related to the temporal reaction of GPCR with specific ligands remains poor. We recently developed a bioluminescence method for the quantitative detection of the interaction between GPCR and β-arrestin using split luciferase complementation. To monitor time-course variation of the interactions, a new imaging system contributes to the accurate evaluation of drugs for GPCRs in a high-throughput manner.

Key words G protein-coupled receptor, Bioluminescence, Complementary technology, Protein–protein interaction, High-throughput screening, EM-CCD camera

1 Introduction

G protein-coupled receptors (GPCRs) are the largest transmembrane spanning receptor protein family in humans. They play important roles in various processes including cellular metabolism, neurotransmission, and chemoattraction [1–3]. Actually, GPCRs have a function in the conversion of vast diversity of extracellular stimuli into intracellular downstream signals, resulting in regulation of numerous physiological functions [4]. Many GPCRs are examined specifically because of their relation to human diseases, as evidenced by the fact that GPCRs are a main target for the establishment of drugs [5]. In fact, approximately 40% of GPCRs are current targets for therapeutic drugs related to the signal transduction [6].

For over 150 GPCRs, specific ligands have not been identified. They are called orphan receptors [7]. Consequently, various methods have been developed to identify important reagents for GPCR signals, most of which are intended for application to high-throughput screening (HTS) [8]. In conventional HTS, the main purpose is simply a

Sung-Bae Kim (ed.), *Bioluminescence: Methods and Protocols*, Methods in Molecular Biology, vol. 1461,
DOI 10.1007/978-1-4939-3813-1_16, © Springer Science+Business Media New York 2016

judgment of whether the reagent activates or inhibits the signal of target GPCR or not. However, particularly addressing the type of GPCRs, the reaction profile with the ligand differs in each [9]. Moreover, the temporal variation of GPCR signaling is indispensable information for the elucidation of the physiological effects of drugs.

Split luciferase fragment complementation assay is quite useful to monitor the temporal variation of GPCR signaling in living cells [10–12]. In principle, a luciferase protein is dissected into two fragments that have less enzymatic activity. These fragments are fused with GPCR and β-arrestin, which belongs to a small cytoplasmic protein interacting with GPCR for desensitization [13]. Upon stimulation of GPCR by a specific ligand, interaction of GPCR with β-arrestin brings the two luciferase fragments into proximity, leading to fragment complementation. The interactions are detectable temporally by bioluminescence.

The split luciferase complementation method is applied to quantitative and competitive assays used with a multiwell microtiter plate [14]. According to standard protocols used to measure bioluminescence, a conventional plate reader with a photomultiplier is often used, in which photon counting is performed one by one in each well. This procedure always includes a time lag between samples. The time lag is an important difficulty related to acquisition of accurate information from the luminescence profile in the case of temporal bioluminescence assays with living cells.

To overcome such issues, we developed a method to use a highly sensitive luminescence imaging system for detection of luminescence signals from whole wells of a multiwell microtiter plate [15]. Using an electron-multiplying charge-coupled device (EM-CCD) camera, temporal variation of bioluminescence from the interaction of GPCR with β-arrestin was obtained simultaneously. Accordingly, the imaging of multiple samples can contribute to evaluation of the reagents for GPCRs in a high-throughput manner.

2 Materials

2.1 DNA Plasmids

We established the plasmids encoding split luciferase probes with the same materials in our previous reports [14]. The present method especially defined the materials as explained below.

1. cDNA of luciferase, click beetle in green (Brazilian *Pyrearinus termitilluminans*, Emerald luciferase (ELuc), $\lambda_{\max} = 537$ nm; Toyobo Co. Ltd.) (*see* **Note 1**).
2. cDNAs of GPCR, β2-adrenergic receptor (ADRB2), and an isoform of β-arrestins, β-arrestin2 (*see* **Notes 2** and **3**).

We prepared the plasmids encoding ADRB2 connected with the C-terminal fragment of ELuc and β-arrestin2 connected with the N-terminal fragment (*see* Fig. 1).

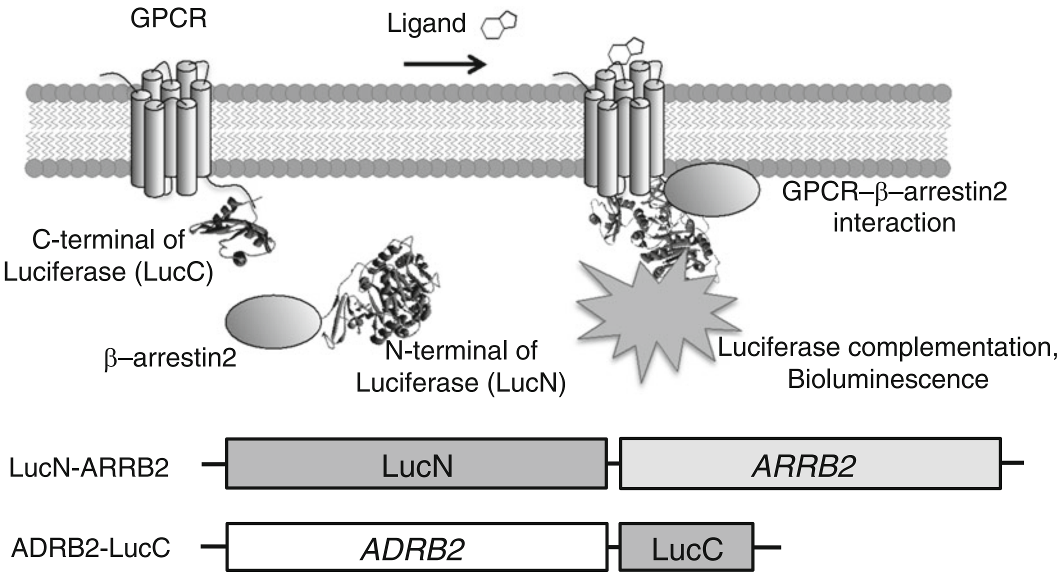
GPCR
Ligand
C-terminal of Luciferase (LucC)
β–arrestin2
N-terminal of Luciferase (LucN)
GPCR–β–arrestin2 interaction
Luciferase complementation, Bioluminescence
LucN-ARRB2
LucN
ARRB2
ADRB2-LucC
ADRB2
LucC

Fig. 1 Schematic illustration and construction of probes in the split complementary strategy to detect the protein–protein interaction of GPCR with β-arrestin2. The N-terminal and C-terminal of split luciferase fragments are fused, respectively, with β-arrestin2 (ARRB2) and GPCR, ADRB2

2.2 Preparation for Live Cell Assay with Multiwell Plate

HEK293 cells were cultured and the stable cell line expressing split luciferase probes was established using the same materials as described in our previous reports [14].

1. HEK293 cells (stable cell line) derived from human embryonic kidney cells.
2. D-MEM (Sigma) supplemented with 10% heat-inactivated FBS (Gibco BRL), 100 U/mL penicillin, and 100 mg/mL streptomycin (Gibco BRL).
3. Hank's balanced salt solution (HBSS; Gibco BRL) with 10% heat-inactivated FBS.
4. Agonist (isoproterenol) and antagonist (propranolol) (Wako Pure Chemical Inds. Ltd.).
5. d-Luciferin potassium salt (Wako Pure Chemical Inds. Ltd.)

2.3 Multiwell Plate Imaging with Bioluminescence Imaging System

1. Multifunctional in vivo imaging system (Miis; Molecular Devices Corp.) (*see* **Note 4**).
2. EM-CCD camera (iXon Ultra888; Andor Technology) cooled at −80 °C (*see* **Note 5**).
3. Metamorph software (Universal Imaging Corp.).

3 Methods

The imaging strategy is to obtain a high signal-to-noise ratio from cells. Therefore, we choose a stable cell line expressing both GPCR and β-arrestin2 connected with split luciferase fragments for the assay [10, 14]. We introduced the gene into HEK293 cells using antibiotics for selection (*see* **Note 6**). The GPCR probe is located at the plasma membrane. The β-arrestin2 probe is distributed in the cytosol. When the specific ligand binds to GPCR in the probe, β-arrestin2 probe translocates to the activated GPCR and forms the complex. Luciferase fragment complementation is induced in this timing, thereby generating bioluminescence (*see* Fig. 1).

In this protocol, ADRB2 was used as a test GPCR protein in the split luciferase fragment probe. The agonist and antagonist of ADRB2, isoproterenol, and propranolol were prepared for stimulation or inhibition of GPCR signaling dose-dependently. Using live cell imaging system, numerous cell samples in wells can be visualized simultaneously to evaluate the time-dependent variation of GPCR signaling with the agonist and antagonist.

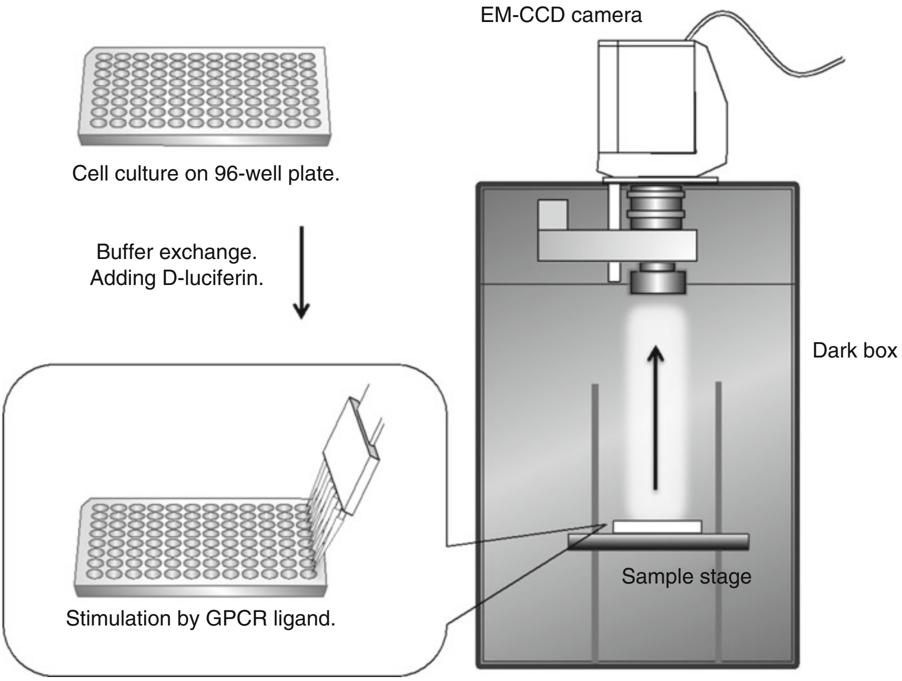

Fig. 2 Technical protocols of temporal bioluminescence imaging. Cells stably expressing GPCR and β-arrestin2 probes are cultured on a 96-well plate. Temporal variation of bioluminescence depending on ligand dosing is detected using the EM-CCD camera

1. HEK293 cells stably expressing ADRB2 and β-arrestin2 luminescence probes are cultured on 96-well plate in D-MEM at 37 °C in an atmosphere of 5 % CO_2 for 24 h (*see* **Notes 7–9**).
2. Live cell imaging system and Metamorph software are set up. An EM-CCD camera imaging system is set at −80 °C (*see* **Note 10**).
3. The medium is replaced with 100 μL/well of HBSS with 10 % (v/v) FBS and 10 mM (M = mol/L) of d-Luciferin.
4. The cell plate is set on the stage of the imaging system. The focus is adjusted using the background luminescence (*see* **Note 11** and Fig. 2). The luminescence detection error in the area of CCD is confirmed beforehand (*see* **Note 12**).
5. Some wells are treated with the antagonist, propranolol, of which the concentration is increased stepwise among the wells.

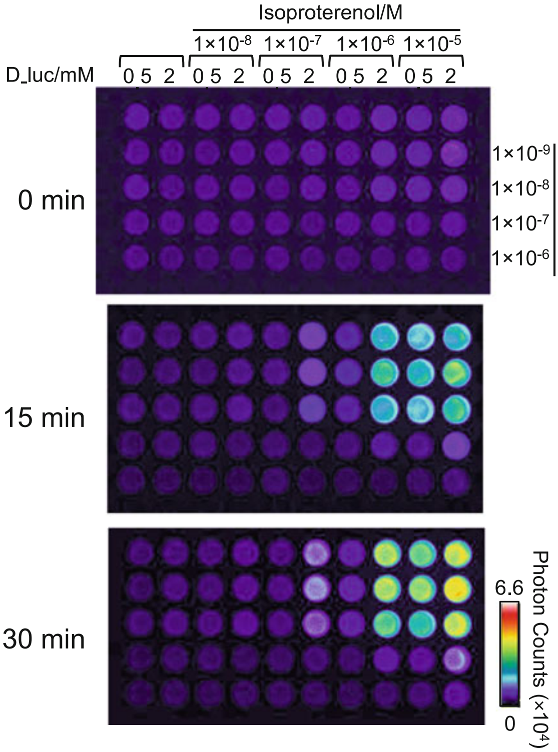

Fig. 3 Bioluminescence images of cells stably expressing GPCR (ADRB2) and β-arrestin2 probes on a 96-well plate. The luminescence from cells was detected by an EM-CCD camera with isoproterenol and propranolol dosing. Three time points of luminescence images are shown as pseudo-colors (0, 15, and 30 min). The concentrations of d-Luciferin (d-Luc) and each ligand are shown at the sides of the images. Images were modified from an earlier report under the permission of Analytical Sciences [15]

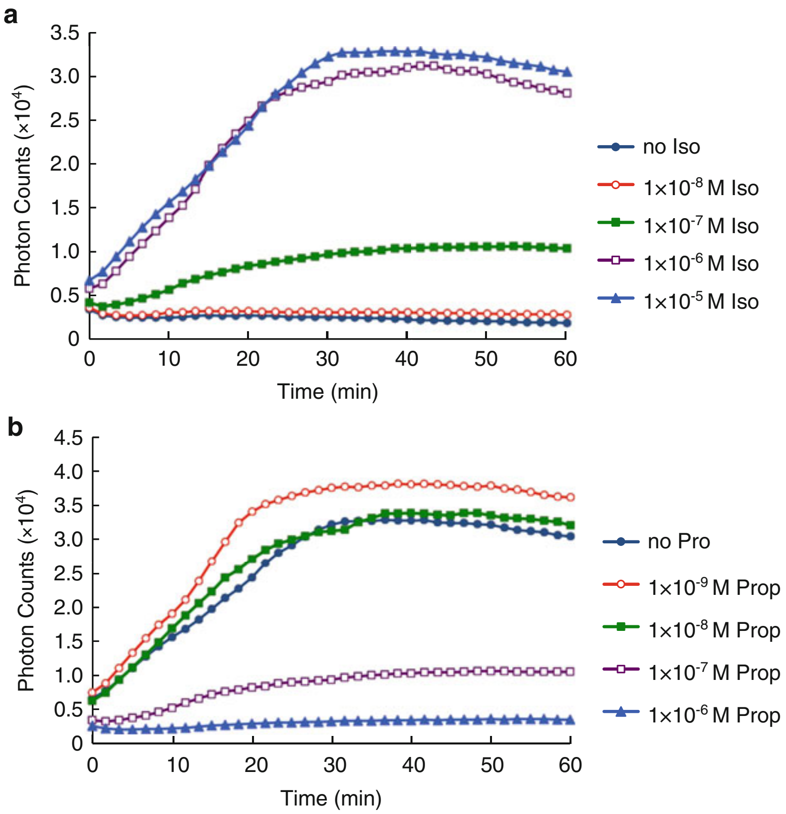

Fig. 4 Time-course variation of bioluminescence that responds to the interaction frequency of ADRB2 and β-arrestin2. All data were measured based on results in Fig. 3. (**a**) Temporal analysis of the interaction of ADRB2 with β-arrestin2 in different condition of isoproterenol (Iso). Data were measured from five regions of wells without propranolol (Pro). (**b**) Temporal analysis of inhibition for Iso in the presence of different concentration of Pro. Data from wells treated with 1×10^{-5} M of Iso were selected

6. Cells are incubated on the stage at room temperature for 10 min.
7. The agonist, isoproterenol is added to the wells with a different concentration in each (*see* **Note 13**).
8. The luminescence image is taken using time lapse imaging (*see* **Note 14** and Fig. 3).
9. Luminescence counts for respective time points are calculated from the region of wells with Metamorph software (*see* **Note 15** and Fig. 4).

4 Notes

1. ELuc is a bright luciferase of the type using d-Luciferin. For luminescence imaging, high intensity provides an excellent signal-to-noise ratio.
2. The cDNAs of probes are usually inserted respectively into expression vectors of pcDNA4/V5-His and pcDNA3.1/myc-His.
3. We can also demonstrate that GPCR is useful for the complementary strategy, such as somatostatin type 2 receptor, apelin receptor, adrenergic receptors (α2a, β2), cholecystokinin B receptor, endothelin receptors (types A, B), μ-opioid receptor, endothelial differentiation G-protein/coupled receptor 3, and angiotensin II receptor type I. These GPCR probes have already confirmed the luminescence reaction in living cells [10, 12, 16].
4. Standard in vivo imaging systems for living subjects are available for the assay. A white light source is necessary for bright-field imaging.
5. Sensitivity and resolution of EM-CCD camera are important to measure bioluminescence counts accurately.
6. We usually used 0.8–2 mg/mL G418 and 0.04–0.2 mg/mL Zeocin for selection and 0.8 mg/mL G418 and 0.04 mg/mL Zeocin for culture.
7. Before preparation, the experimental plan should be designed well. Actually, 3–6 wells with same condition of ligands are needed to calculate the standard deviations in quantitative assay. The range of concentrations of the ligand is important to show the sigmoidal dose–response curve.
8. We recommend the use of an 8-channel or 12-channel pipette for addition of the solution to the wells.
9. The cell number was about 1×10^6 cells/well.
10. The EM-CCD camera temperature is crucially important to support the sensitivity of bioluminescence. A water-cooling system is available for the camera as an option.
11. The focus of bioluminescence image is subtly different from that of the bright-field image.
12. A lens aberration sometimes occurred depending on the magnification.
13. Administration of the ligand is performed directly on the stage.
14. The exposure time and the interval depend on the cell condition and the type of GPCRs. We took images every 100 s, with 10 s exposure for each.
15. The calculation protocol can be performed automatically if the plate position on the stage is fixed in every assays.

Acknowledgements

We thank Molecular Devices Corp. for active support related to the technical aspects of imaging. This work was supported by the Japan Society for the Promotion of Science (JSPS) and MEXT, Japan.

References

1. Grisshammer R (2013) Why we need many more G protein-coupled receptor structures. Expert Rev Proteomics 10:1–3
2. Conn PJ, Christopoulos A, Lindsley CW (2009) Allosteric modulators of GPCRs: a novel approach for the treatment of CNS disorders. Nat Rev Drug Discov 8:41–54
3. Musnier A, Blanchot B, Reiter E, Crepieux P (2010) GPCR signalling to the translation machinery. Cell Signal 22:707–716
4. Stevens RC, Cherezov V, Katritch V, Abagyan R, Kuhn P, Rosen H, Wuthrich K (2013) The GPCR network: a large-scale collaboration to determine human GPCR structure and function. Nat Rev Drug Discov 12:25–34
5. Hopkins AL, Groom CR (2002) The druggable genome. Nat Rev Drug Discov 1:727–730
6. Foord SM, Bonner TI, Neubig RR, Rosser EM, Pin JP, Davenport AP, Spedding M, Harmar AJ (2005) International union of pharmacology. XLVI. G protein-coupled receptor list. Pharmacol Rev 57:279–288
7. Allen JA, Roth BL (2011) Strategies to discover unexpected targets for drugs active at G protein-coupled receptors. Annu Rev Pharmacol Toxicol 51:117–144
8. Zhang R, Xie X (2012) Tools for GPCR drug discovery. Acta Pharmacol Sin 33:372–384
9. Hattori M, Tanaka M, Takakura H, Aoki K, Miura K, Anzai T, Ozawa T (2013) Analysis of temporal patterns of GPCR–β-arrestin interactions using split luciferase-fragment complementation. Mol Biosyst 9:957–964
10. Misawa N, Kafi AKM, Hattori M, Miura K, Ozawa T (2010) Rapid and high-sensitivity cell-based assays of protein–protein interactions using split click beetle luciferase complementation: an approach to the study of G-protein-coupled receptors. Anal Chem 82:2552–2560
11. Hida N, Awais M, Takeuchi M, Ueno N, Tashiro M, Takagi C, Singh T, Hayashi M, Ohmiya Y, Ozawa T (2009) High-sensitivity real-time imaging of dual protein–protein interactions in living subjects using multicolor luciferases. PLoS One 4:e5868
12. Takakura H, Hattori M, Takeuchi M, Ozawa T (2012) Visualization and quantitative analysis of G protein-coupled receptor–β-arrestin interaction in single cells and specific organs of living mice using split luciferase complementation. ACS Chem Biol 7:901–910
13. Hatori M, Ozawa T (2015) Bioluminescent tools for the analysis of G-protein-coupled receptor and arrestin interactions. RSC Adv 5:12655–12663
14. Takakura H, Hattori M, Tanaka M, Ozawa T (2015) Cell-based assays and animal models for GPCR drug screening. Methods Mol Biol 1272:257–270
15. Hattori M, Ozawa T (2015) High-throughput live cell imaging and analysis for temporal reaction of G protein-coupled receptor based on split luciferase fragment complementation. Anal Sci 31:327–330
16. Kafi AKM, Hattori M, Misawa N, Ozawa T (2011) Dual-color bioluminescence analysis for quantitatively monitoring G-protein-coupled receptor and β-arrestin interactions. Pharmaceuticals 4:457–469

Chapter 17

Imaging Histone Methylations in Living Animals

Thillai V. Sekar and Ramasamy Paulmurugan

Abstract

Histone modifications (methylation, acetylation, phosphorylation, sumoylation, etc.,) are at the heart of cellular regulatory mechanisms, which control expression of genes in an orderly fashion and control the entire cellular regulatory networks. Histone lysine methylation has been identified as one of the several posttranslational histone modifications that plays crucial role in regulating gene expressions in facultative heterochromatic DNA regions while maintaining structural integrity in constitutive heterochromatic DNA regions. Since histone methylation is dysregulated in various cellular diseases, it has been considered a potential therapeutic target for drug development. Currently there is no simple method available to screen and preclinically evaluate drugs modulating this cellular process, we recently developed two different methods by adopting reporter gene technology to screen drugs and to preclinically evaluate them in living animals. Method detects and quantitatively monitors the level of histone methylations in intact cells, is of a prerequisite to screen small molecules that modulate histone lysine methylation. Here, we describe two independent optical imaging sensors developed to image histone methylations in cells and in living animals. Since we used standard PCR-based cloning strategies to construct different plasmid vectors shown in this chapter, we are not providing any details regarding the construction methods, instead, we focus on detailing various methods used for measuring histone methylation-assisted luciferase quantitation in cells and imaging in living animals.

Key words Histone methylation, Optical imaging, Reporter genes, Luciferase, Split reporters, Protease, Degron, In vivo imaging

1 Introduction

Histone lysine methylation mainly occurs to six different lysine residues located in the N-terminal tails of Histone 3 (H3K4, H3K9, H3K27, H3K36, and H3K79) and Histone 4 (H4K20). In mammalian cells these modifications primarily control chromatins structural organizations in transcriptionally inactive heterochromatic regions and gene expression in euchromatic regions [1–4]. These histone lysine methylation marks are implicated with major cellular diseases including cancer. Global hypermethylation or hypomethylation in various histone lysine methylation marks have been observed with the onset and progression of many cancer

Sung-Bae Kim (ed.), *Bioluminescence: Methods and Protocols*, Methods in Molecular Biology, vol. 1461,
DOI 10.1007/978-1-4939-3813-1_17, © Springer Science+Business Media New York 2016

types [5–7]. In the past two decades, many aspects of histone lysine methylation have been investigated and the outcome of this extensive research has identified histone lysine methylation as a potential therapeutic target for treating various cellular diseases including cancer. Histone methyltransferases and demethylases are two groups of enzymes, which determine the state of histone methylation in all of these methylation marks. The important role of these enzymes in various histone methylation marks has been disclosed with the development of different knockout mouse models [8]. Small molecule inhibitors, such as Bix01294 [9] and JIB-04 [10], have been recently identified using indirect drug-screening methods and evaluated them for their roles in regulating histone methylations. However, the pace of designing drugs targeting this important therapeutic target is stalled, because of unavailability of sensitive and robust screening and evaluation methods.

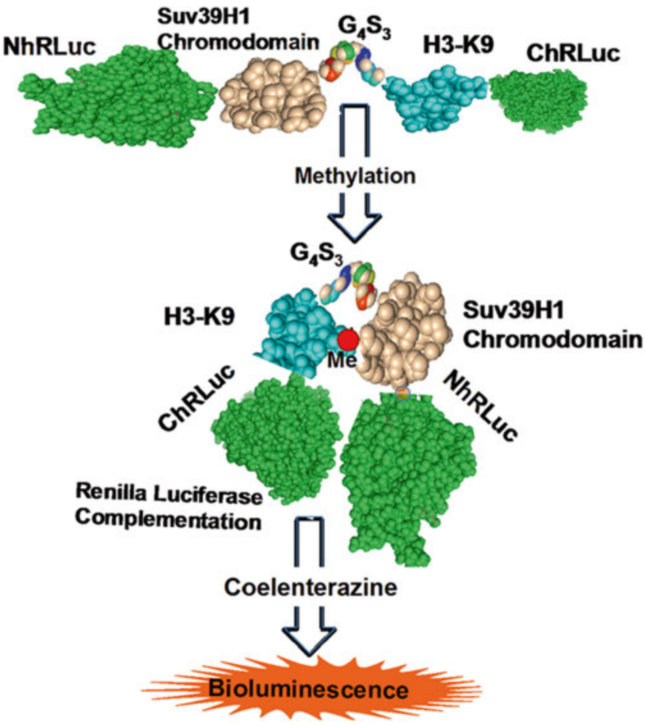

Fig. 1 Schematic illustration of the design of split-*Renilla* luciferase complementation sensor for imaging H3K9 histone methylation. In this sensor N- and C-terminal fragments of *Renilla* luciferase (NhRLuc and ChRLuc) are connected by chromodomain from Suv39H1 protein and 1–13 amino acid substrate peptide from H3 protein, which are in turn linked, by $(G_4S)_3$ linker peptide. The fusion protein when expressed in cells the substrate domain is methylated by cellular methyltransferase enzymes. This process is specific to each methylation mark. The methylated peptide in turn recruit chromodomain specific to the mark located within the fusion protein and induce intramolecular conformational change to the protein which in turn lead to complementation between the reporter fragments

Here we elaborate the protocols employed for quantitatively measuring histone lysine methylations using imaging sensors based on two different conceptual designs, which exploit the biology of histone lysine methylations [11, 12]. We used the well-established split-reporter protein complementation strategy [13–15] to design the first intramolecular folding-based histone lysine methylation imaging sensor where methylation of N-terminal methyltransferase substrate peptide located within the histone protein of the sensor (*see* Fig. 1 and **Notes 1** and **2**). In our second sensor design, we used C-terminal degron of mouse ornithine decarboxylase as protease recognition sequence for proteasomal degradation of the sensor system. The protein to which degron is appended will be degraded by proteasome when there is no methylation occur to the substrate peptide located within the sensor, but the protein degradation will be blocked when methylation of sensor which in turn lead to change in the conformation of the sensor protein (*see* Fig. 2

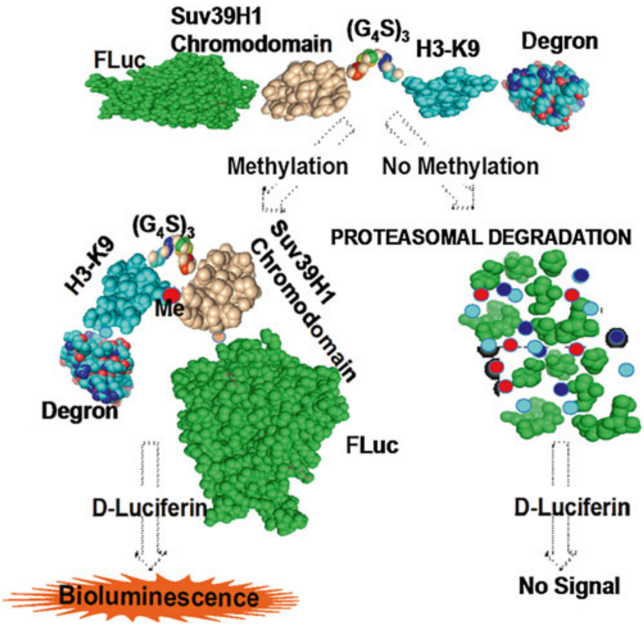

Fig. 2 Schematic illustration of the design of degron-protease-blockade histone methylation imaging sensor. The scheme shows the outcome of H3K9 and its respective mutant (H3L9) sensor upon methylation by methyltransferase enzymes, The sensor is a fusion protein in which full-length firefly luciferase is fused to H3K9 peptide, a 15-amino acid linker, Suv39h1-chromodomain, and a 37-amino acid degron protease recognition sequence at the COOH-terminal. Upon methylation of H3K9 peptide by methyltransferase recruits the inbuilt Suv39h1 chromodomain and creates a conformational lock which blocks degron-mediated proteasomal degradation of H3K9 sensor fusion protein, as a result intact FLuc protein is accumulated in the cells. H3L9 sensor, which lacks K9-for methylation, undergoes constitutive proteasomal degradation due to lack of H3K9-Suv39h1 conformational lock eventually shows low or no FLuc signal

and **Note 3**). Both these sensors were validated with suitable control mutant sensors and by using methyltransferase inhibitors (Bix01294 and UNC0638) and demethylase inhibitor (JIB-04).

2 Materials

2.1 *In Vitro* and *In Vivo* Imaging of Histone Methylation by Split-Renilla Luciferase (Split-RLuc) Complementation Sensor

1. Plasmid vectors pcPur-NhRLuc-Suv39H1-$(G_4S)_3$-H3K9-ChRLuc [H3K9] and pcPur-NhRLuc-Suv39H1-$(G_4S)_3$-H3L9-ChRLuc [H3L9] (*see* Fig. 3a and **Note 4**).
2. HEK293T cells (ATCC®, Manassas, VA) derived from human embryonic kidney cells.
3. Dulbecco's modified eagle medium (DMEM) with 10% fetal bovine serum and 1% penicillin and streptomycin solution (GIBCO BRL, Frederick, MD).
4. Lipofectamine 2000 and serum free OptiMEM medium (Life Technologies, Grand Island, NY).
5. 37 °C incubator with 5% CO_2 (Thermo scientific, Sunnyvale, CA).
6. Histone Methyltransferase inhibitors such as Bix01294, UNC0638 (Cayman chemical, Ann Arbor, MI), and demethylase inhibitor JIB-04 (Sigma, St. Louis, MO).
7. Passive lysis buffer (Promega, Madison, WI), Coelenterazine (CTZ) (Nanolight, Pinetop, AZ), d-Luciferin (Biosynth, Itasca, IL), and LARII substrate (Promega, Madison, WI).
8. Bio-Rad protein assay kit (Bio-Rad, Hercules, CA).
9. Luminometer (Turner T20/20, Sunnyvale, CA), microcentrifuge (Thermo scientific, Sunnyvale, CA), vortex mixer, spectrophotometer (Agilent Technologies, Santa Clara, CA), and Infinite-1000 microplate reader (Tecan Systems, San Jose, CA).
10. Growth factor reduced matrigel (BD Biosciences, San jose, CA), anesthesia platform.
11. 4–5 weeks old nude mice (Charles River, San Diego, CA).
12. Optical imaging instrument with cooled CCD camera and living image in vivo imaging analysis software (PerkinElmer, Waltham, MA).
13. HEK293T cells stably coexpressing H3K9 or H3L9 sensor with FLuc-EGFP normalizing protein.

2.2 Degron-Blockade Optical Imaging

1. In addition all materials described in Subheading 2.1 we also need materials shown below.
2. Plasmid vectors pcPur-FLuc2-Suv39H1-$(G_4S)_3$-H3K9-Degron and pcPur-FLuc2-Suv39H1-$(G_4S)_3$-H3L9-Degron (*see* Fig. 3b and **Note 4**).
3. HEK293T cells (ATCC, Manassas, VA) stably expressing the sensors.

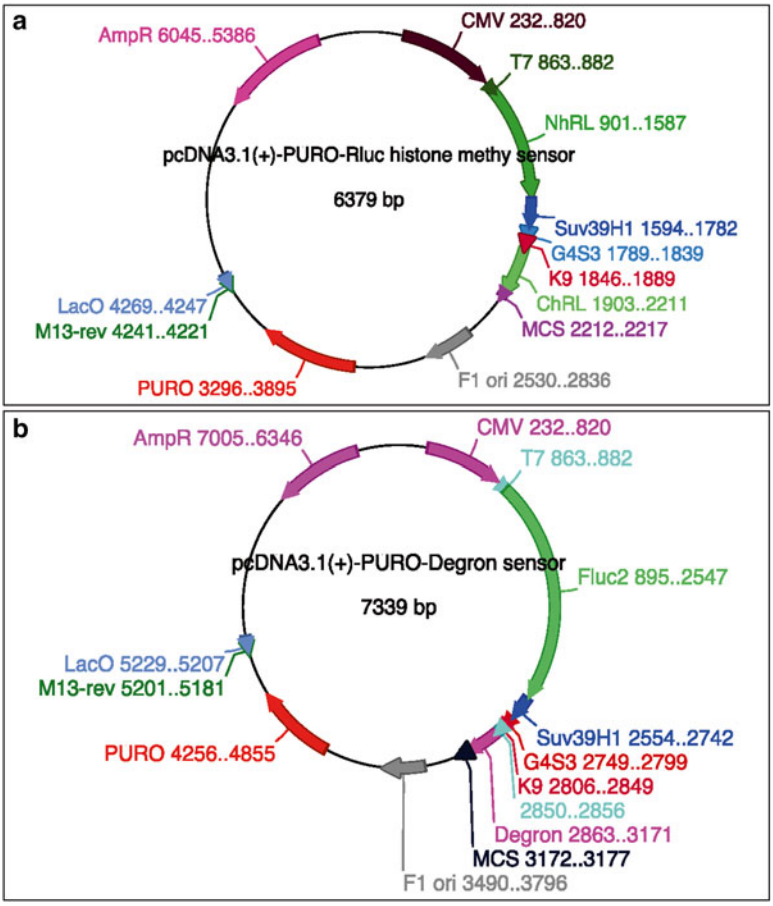
a
AmpR 6045..5386
CMV 232..820
T7 863..882
NhRL 901..1587
pcDNA3.1(+)-PURO-Rluc histone methy sensor
6379 bp
Suv39H1 1594..1782
G4S3 1789..1839
K9 1846..1889
ChRL 1903..2211
MCS 2212..2217
F1 ori 2530..2836
PURO 3296..3895
LacO 4269..4247
M13-rev 4241..4221
b
AmpR 7005..6346
CMV 232..820
T7 863..882
pcDNA3.1(+)-PURO-Degron sensor
7339 bp
Fluc2 895..2547
LacO 5229..5207
M13-rev 5201..5181
PURO 4256..4855
Suv39H1 2554..2742
G4S3 2749..2799
K9 2806..2849
2850..2856
Degron 2863..3171
MCS 3172..3177
F1 ori 3490..3796

Fig. 3 Vector maps illustrate the genetic components of plasmid vectors expressing. (**a**) split-RLuc complementation, and (**b**) Degron protease blockade histone methylation imaging sensors

3 Methods

3.1 Generation of HEK293T Cells Stably Coexpressing Histone Methylation (H3K9) or Mutant (H3L9) Renilla Luciferase (RLuc) Complementation Sensor with FLuc-EGFP Normalizing Protein

1. Plasmids (5 μg each) expressing fusion proteins of H3K9 (pcPur-NhRLuc-Suv39H1-$(G_4S)_3$-H3K9-ChRLuc) or H3L9 (pcPur-NhRLuc-Suv39H1-$(G_4S)_3$-H3L9-ChRLuc) sensors and normalizing FLuc-EGFP plasmid were cotransfected in HEK293T cells plated at 70 % confluence in a 10 cm plate 24 h before transfection by using lipofectamine 2000 transfection agent using manufacturer-suggested protocol. The cells were incubated at 37 °C with 5 % CO_2 for 24 h.
2. 24 h after transfection, cells were trypsinized and plated to a 1:3 subculture ratio in 10 cm plates, and puromycin (Life Technologies, Grand Island, NY) was added to a concentration of 500 ng/mL.

3. The cells were further incubated for 48 h. The dead cells were washed and added fresh medium with 500 ng/mL of puromycin. At this stage more than 80% of cells died. The steps were repeated till no further cell death was observed. At this stage the cells were FACS sorted for FLuc-EGFP expression and plated at low dilution (2000 cells/10 cm plate in 10 mL medium with 500 ng/mL puromycin).
4. The cells were incubated further for 2 weeks with medium change once in every 3 days.
5. At this stage colonies of 2–3 mm in diameter were formed from individual cells.
6. Single colony of transfected cells were selected and expanded by plating first in 12-well plate followed by 10 cm plate.
7. The cells isolated from several colonies that express H3K9 and H3L9 sensors were tested for the identification of clones express equal level of sensor fusion proteins by immunoblot analysis using anti-FLuc antibody.
8. The clones (H3K9 and H3L9) expressed equal level of sensor fusion proteins while expressing FLuc-EGFP normalizing proteins were used for further in vitro and in vivo evaluations for histone methylation imaging.

3.2 In Vitro Evaluation of Split-RLuc Complementation Sensor by Luminometer and Optical CCD Camera Imaging (In Response to Histone Methyltransferase and Demethylase Inhibitors)

1. Plated HEK293T cells (1.5×10^5 cells/well) stably coexpressing the histone methylation imaging sensor or its respective mutant sensor with normalizing FLuc-EGFP (H3K9-FLuc-EGFP and H3L9-FLuc-EGFP) in 12-well plates in DMEM with 10% FBS on day 1 and incubated at 37 °C with 5% CO_2 for the cells to attach and attain normal morphology.
2. 24 h later the medium was changed to DMEM with 2% FBS and the cells (triplicate for each condition) were treated with different concentrations of Bix01294 (0, 0.5, 1, 2, 3, and 4 μM), UNC0638 (0, 1, 2, 3, 5, and 8 μM) and JIB-04 (0, 0.1, 0.2, 0.3, 0.4, 0.5, and 0.6 μM) and further incubated for 24 h and used for assessing luciferase activity by luminometer after lysing the cells, and by using CCD camera imaging in intact cells. The cells treated with DMSO are used as vehicle control.

3.2.1 Luminometer Assay

1. After required time of incubation with drugs, the cells were lysed in 200 μL of 1× passive lysis buffer by keeping in shaker for 20 min at 4 °C. The lysates from each well was transferred to 1.5 mL microfuge tube and centrifuged at 9,600 × *g* for 5 min at 4 °C to remove all cell debris. The supernatant was transferred to fresh microfuge tube and kept in ice till the luminometer assay was completed.
2. 20 μL of lysate from each tube was transferred to a fresh microfuge tube for luminometer assay.

3. The lysate was quickly mixed with 100 μL of CTZ (10 μg/mL of CTZ in PBS; CTZ stock must be prepared at 1 mg/mL in 100% ethanol and stored in air tight container at −20 °C) and measured the photon signal for 10 s.
4. Similarly FLuc signals from the same lysate was measured by mixing 20 μL of lysate with 100 μL of LARII substrate in 1.5 mL microfuge tube and measuring the photons for 10 s.
5. 10 μL of every sample was used for protein estimation in 96-well plate using Bio-Rad protein assay reagent. Sample was mixed with 100 μL of assay reagent and incubated at RT for 5 min. Optical density was measured at 540 nm. The protein amount was quantified using standard graph generated from BSA.
6. Methylation-assisted RLuc signal was normalized with respective FLuc signal and the protein concentration of respective sample (RLuc-photons/FLuc photon/total protein).
7. Specificity of spit-reporter sensor is assessed with RLuc signal variation between H3K9 and H3L9 sensor (*see* Fig. 4a).
8. Similarly the sensor signal in response to the treatment of methyltransferase inhibitors at various concentrations and demethylase inhibitor (JIB-04) at various concentrations, were assessed by comparing to the normalized signals measured from the controls (*see* Fig. 4b).

3.2.2 Optical CCD Camera Imaging

1. Optical CCD camera imaging was performed in intact cells plated in 12- or 24-well culture plates.
2. Plating the cells and treatment conditions are similar what we have used for luminometer assay.
3. The optical-CCD camera (IVIS®-optical imaging system) was initialized 10 min before the start of the experiment.
4. After required treatment condition the culture medium was carefully removed and washed once with 1 mL PBS.
5. Added 400 μL of CTZ (10 μg/mL in PBS) in PBS and immediately placed in the dark box and acquired signal for 3 min.
6. To acquire FLuc signal for normalization, another set of cells at similar treatment condition was added with 400 μL of d-Luciferin (120 μg/mL in PBS) and acquired signal for 1 min after 10 min of pre-incubation time (*see* **Note 5**).
7. For each condition we used triplicate wells for imaging.
8. RLuc and FLuc signals were measured by drawing ROI above the respective wells using Living image software and normalized RLuc-complementation signal with normalizing FLuc signal. Since the cell numbers are the same we didn't do any normalization for total protein.

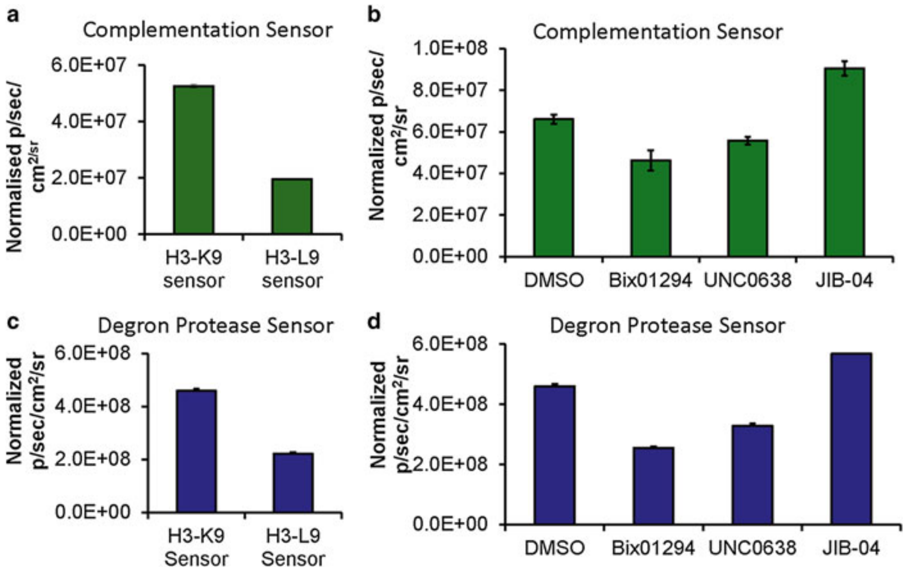

Fig. 4 In vitro imaging with split-RLuc complementation and Degron protease blockade sensors in HEK293T cells. Graph shows normalized RLuc signals recorded from (**a**) HEK293T cells transfected with plasmid vector expressing H3K9 and H3L9 split-RLuc complementation sensors, and (**b**) HEK293T cells expressing H3K9 sensor treated with Bix01294 (1 μM), UNC0638 (1 μM), and JIB-04 (0.5 μM). Graph shows normalized FLuc signals recorded from (**c**) HEK293T cells transfected with H3K9 and H3L9 degron protease blockade sensors, and (**d**) HEK293T cells expressing H3K9 degron protease blockade sensor treated with Bix01294 (1 μM), UNC0638 (1 μM) and JIB-04 (0.5 μM)

3.3 *In Vivo* Imaging in Nude Mice Model by Optical CCD Camera

1. Nude mice handling should be performed following Institutional Animal Care and Use Committee guidelines.
2. We used stable cells coexpressing split-reporter imaging sensor and FLuc-EGFP normalizing protein for the study.
3. To start with, HEK293T stable cells was trypsinized and collected in PBS on day 1.
4. Cell number in PBS suspension was evaluated using hemocytometer.
5. Stable cell suspension in PBS was adjusted to a concentration of 5×10^6 cells/50 μL.
6. Stable cell preparation in PBS must be implanted within 2 h after trypsinization.
7. To implant the stable cells, nude mice with an age group of 4–5 weeks was anesthetized with 2% isofluorane with oxygen flow of 0.8–1 L/min.
8. Stable cell suspension (5×10^6 cells/50 μL) was mixed with 50 μL of growth factor reduced matrigel just before implantation.
9. Cell suspension mix was injected on either side of the lower flank region (5×10^6 cells/xenograft) using 0.5 mL insulin syringe.

10. Tumor growth must be monitored periodically until it grows to a volume of approximately 50–60 mm^3. It may take 3–4 weeks.
11. After tumor growth, animals were randomly divided into three groups and labeled with ear tag.
12. Animals were optically imaged to capture RLuc and FLuc signals on the day of methyltransferase and demethylase inhibitors treatment but before administration. To capture RLuc signal, CTZ (200 μg in 100 μL of PBS; 5 mg/mL stock in 100% ethanol) was injected intravenously 5 s before imaging, whereas to capture FLuc signals, d-Luciferin (3 mg in 100 μL PBS) was injected intraperitoneally 5 min before capturing images.
13. To image RLuc signal animals were acquired for 5 min immediately after CTZ injection whereas for FLuc imaging the animals were imaged for 30 min with 1 min acquisition to identify peak signal window.
14. Control group animals were injected with vehicle control, whereas second and third groups were treated with Bix01294 (20 mg/kg body weight) and JIB-04 (20 mg/kg body weight) respectively. Bix01294 and JIB-04 was administered intraperitoneally with a maximum volume of 250 μL in sterile physiological saline and 10% PEG400.
15. After Bix01294 and JIB-04 administration, image capturing was done every day for a period of 10 days using optical-CCD camera. RLuc and FLuc signals were captured with an interval of minimum 6 h. Alternatively, normalization reporters, such as EGFP (FLuc-EGFP) can be used to capture signals simultaneously in the same session.
16. Images were analyzed with Living Image analysis software. For analysis, regions of interest (ROI) was drawn over the area of signal acquired around the xenografts, and the signal was defined as maximum photons per second per square centimeter per steradian (p/s/cm^2/sr) (*see* Fig. 5a, b).

3.4 Generation of HEK293T Cells Stably Coexpressing Degron-Blockade Histone Methylation (H3K9) or Mutant (H3L9) Sensors with RLuc-mRFP Normalizing Vector (See Note 6)

1. Plasmids (5 μg each) expressing fusion proteins of H3K9 degron (pcPur-FLuc2-Suv39H1-$(G_4S)_3$-H3K9-Degron) or H3L9 degron (pcPur-FLuc2-Suv39H1-$(G_4S)_3$-H3L9-Degron) sensors and normalizing RLuc-mRFP plasmid were cotransfected in HEK293T cells in 10 cm plate plated at 70% confluence 24 h before transfection by using lipofectamine 2000 transfection agent using manufacturer-suggested protocol. The cells were incubated at 37 °C with 5% CO_2 for 24 h.
2. Rest of the selection methods are similar to what we have used in Subheading 3.1. Optimal clones express equal level of sensor fusion protein were used for in vitro and in vivo evaluation of histone methylation using degron protease blockade sensors.

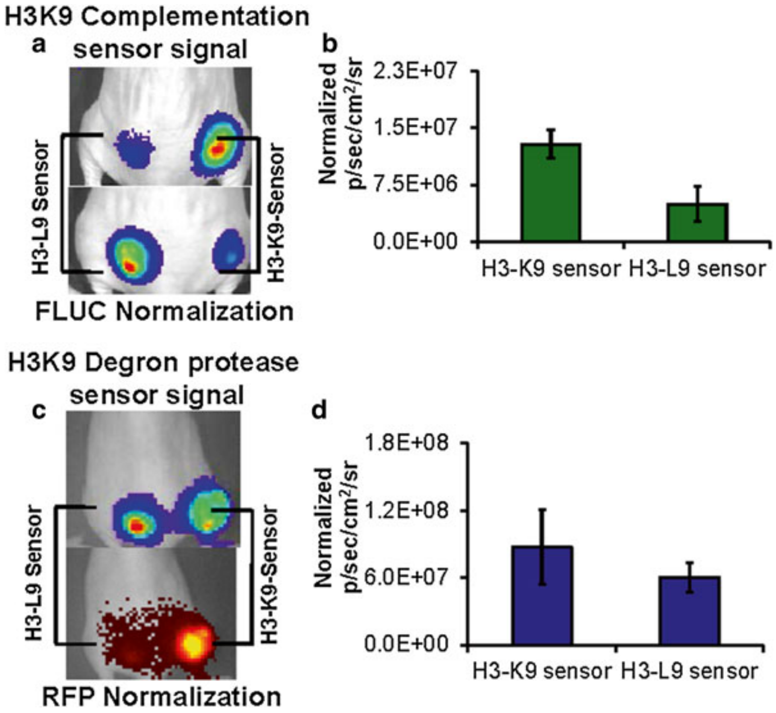

Fig. 5 In vivo imaging with split-RLuc complementation and Degron protease blockade sensor. (**a**) Optical bioluminescence images showing RLuc and FLuc signals recorded from HEK293T xenografts expressing wild-type (H3K9) and mutant (H3L9) split-RLuc complementation sensors and a normalization FLuc reporter. (**b**) Graph shows normalized RLuc signals quantified from figure "a". (**c**) Optical bioluminescence images showing FLuc and RFP signals recorded from HEK293T xenografts expressing wild-type (H3K9) and mutant (H3L9) degron protease blockade sensors. (**d**) Graph shows normalized FLuc signal quantified from figure "c"

3.5 *In Vitro* Evaluation of Degron-Blockade Sensor by Luminometer and Optical CCD Camera Imaging (In Response to Histone Methyltransferase and Demethylase Inhibitors)

1. Plated HEK293T cells (1.5×10^5 cells/well) stably expressing the histone methylation imaging sensors (H3K9-degron-RLuc-mRFP and H3L9-degron-RLuc-mRFP) were plated in 12-well plates in DMEM with 10% FBS on day 1 and incubated at 37 °C with 5% CO_2 for the cells to attach and attain normal morphology.
2. 24 h later the medium was changed to DMEM with 2% FBS and the cells (triplicate for each condition) were treated with different concentrations of Bix01294 (0, 0.5, 1, 2, 3, and 4 μM), UNC0638 (0, 1, 2, 3, 5, and 8 μM) and JIB-04 (0, 0.1, 0.2, 0.3, 0.4, 0.5, and 0.6 μM) for 24 h and used for assessing luciferase activity by luminometer after lysing the cells, and by using CCD camera imaging in intact cells. The cells treated with DMSO were used as vehicle control.

3.5.1 Luminometer Assay

Luminometer assay was exactly what we have used in Subheading 3.2.1 (*see* Fig. 4c, d).

3.5.2 Optical CCD Camera Imaging

1. Optical CCD camera imaging with degron-blockade sensor was followed as described in Subheading 3.2.2 using plasmid vectors expressing Degron-protease blockade sensors.

3.6 In Vivo Imaging in Nude Mice Model

1. For In vivo imaging, same protocol described in Subheading 3.3 was followed using stable HEK293T cells expressing degron-protease blockade sensors (*see* Fig. 5c, d and **Note 6**).

4 Notes

1. Methylation in histone tails plays crucial role in regulating gene expression in cells through the recruitment of a specific group of proteins with structural domains (chromodomain, bromodomain, and CHD domains) called royal family of proteins to these targets. The chromodomains of each royal family of proteins are unique, and they are specifically recruited to a particular methylation mark when methylation occurs to these marks. The chromodomain from each protein maintains its high affinity binding for a specific type of histone methylation mark (H3K4, H3K9, H3K27, H3K36, H3K79, and H4K20). While the recruitment of specific chromodomain proteins to methylation marks, such as H3K9, H3K27, and H4K20, maintain transcriptionally inactive constitutive heterochromatin, the other methylation marks, such as H3K4, K3K36, and H3K79 provide structural integrity to transcriptionally active facultative heterochromatin. Hence this process is highly complex, and in this study we constructed histone methylation imaging sensors for a few specific marks and evaluated the sensitivity and specificity as a proof of principle studies in cells and in living animals. We explored the recruitment of chromodomains of specific royal family protein to respective methylation mark upon methylation by methyltransferase as a principle to design our methylation sensors.
2. Split-reporter protein complementation for various optical reporters (Firefly, *Renilla* and *Gaussia* Luciferases; Green and Red Fluorescent proteins) have been developed by us and used for studying protein–protein interactions and protein folding. We have extensively studied the use of split reporters for imaging protein–protein interactions and protein folding for several cellular proteins [13–19]. Briefly, in this strategy N- and C-terminal portion of reporter proteins complement each other and restore enzymatic activity only when they come close to each other through the interaction of interlinked study proteins or due to conformational changes occur within the study protein. We adopted this strategy to design our histone methylation imaging

sensor, in which chromodomain of Suv39H1 (or PC2, or HP1, etc.) royal family protein binds to a small substrate peptide derived from histone (H3: amino acids 1–13 for H3K4 and H3K9; amino acids 15–30 for H3K27; amino acids 25–42 for H3K36; amino acids 73–87 for H3K79, and amino acids 8–25 of H4 for H4K20) protein upon methylation in specific methylation mark recruit respective chromodomain cloned within the fusion protein, and this interaction causes conformational changes to assist the complementation of N- and C-terminal portion of split-*Renilla* luciferase (RLuc) protein resulting in the recovery of luciferase activity that can be measured as an indirect indicator for methylation occurred to specific mark used in the sensor (*see* Fig. 1).

3. Degrons are the proteasomal recognition sequences present in either N- (N-degron) or C- (C-degron) terminal end of many eukaryotic proteins. Protein to which the degron sequences are appended will be degraded by the endogenous proteasomal degradation mechanisms. Here, we designed a degron-blockade histone methylation-imaging sensor comprising full-length codon optimized firefly luciferase (FLuc2), chromodomain of Suv39H1, $(G_4S)_3$ linker, 13 amino acid H3K9 substrate domain from H3 protein, and C-terminal degron sequence of mouse ornithine decarboxylase enzyme at the end. This sensor fusion protein is degraded by cellular proteasome when it is not methylated. But when methylated, it creates a conformational lock through the recruitment of inbuilt chromodomain, which then lead to the blockage of sensor fusion protein from proteasomal degradation. Therefore the measured FLuc signal is directly proportional to the level of methylation in H3K9 methylation mark (*see* Fig. 2).
4. To generate mutant plasmid vectors expressing split-RLuc complementation (H3L9) and degron-blockade sensors (H3L9 degron), codon encodes lysine at H3K9 methylation mark was replaced with leucine codon (K9L).
5. Pre-incubation is important for the substrate to enter the cells and saturate the expressed luciferase proteins.
6. In degron-protease blockade imaging sensors, we used FLuc to provide methylation signal while RLuc-mRFP was used to acquire normalizing signal. RFP signal was captured with a excitation wave length at 540 nm and emission at 600 nm.

Acknowledgement

The funding support by National Institutes of Health (NIH grant R01 CA161091 and R21 CA185805 to R.P) and Department of Radiology, Stanford University is gratefully acknowledged. We also thank Dr. Sanjiv Sam Gambhir, Chairman, Department of

Radiology, Stanford University, for his constant support. We gratefully acknowledge the use of the SCi^3 Core Facility and Canary Center, Stanford University.

References

1. Kouzarides T (2007) SnapShot: histone-modifying enzymes. Cell 128:802
2. Kouzarides T (2007) Chromatin modifications and their function. Cell 128:693–705
3. Guenther MG, Levine SS, Boyer LA, Jaenisch R, Young RA (2007) A chromatin landmark and transcription initiation at most promoters in human cells. Cell 130:77–88
4. Rivera C, Gurard-Levin ZA, Almouzni G, Loyola A (2014) Histone lysine methylation and chromatin replication. Biochim Biophys Acta 1839:1433–1439
5. Holm K, Grabau D, Lovgren K, Aradottir S, Gruvberger-Saal S, Howlin J, Saal LH, Ethier SP, Bendahl PO, Stal O, Malmstrom P, Ferno M, Ryden L, Hegardt C, Borg A, Ringner M (2012) Global H3K27 trimethylation and EZH2 abundance in breast tumor subtypes. Mol Oncol 6:494–506
6. Seligson DB, Horvath S, McBrian MA, Mah V, Yu H, Tze S, Wang Q, Chia D, Goodglick L, Kurdistani SK (2009) Global levels of histone modifications predict prognosis in different cancers. Am J Pathol 174:1619–1628
7. Seligson DB, Horvath S, Shi T, Yu H, Tze S, Grunstein M, Kurdistani SK (2005) Global histone modification patterns predict risk of prostate cancer recurrence. Nature 435:1262–1266
8. Shinkai Y, Tachibana M (2011) H3K9 methyltransferase G9a and the related molecule GLP. Genes Dev 25:781–788
9. Vedadi M, Barsyte-Lovejoy D, Liu F, Rival-Gervier S, Allali-Hassani A, Labrie V, Wigle TJ, Dimaggio PA, Wasney GA, Siarheyeva A, Dong A, Tempel W, Wang SC, Chen X, Chau I, Mangano TJ, Huang XP, Simpson CD, Pattenden SG, Norris JL, Kireev DB, Tripathy A, Edwards A, Roth BL, Janzen WP, Garcia BA, Petronis A, Ellis J, Brown PJ, Frye SV, Arrowsmith CH, Jin J (2011) A chemical probe selectively inhibits G9a and GLP methyltransferase activity in cells. Nat Chem Biol 7:566–574
10. Wang L, Chang J, Varghese D, Dellinger M, Kumar S, Best AM, Ruiz J, Bruick R, Pena-Llopis S, Xu J, Babinski DJ, Frantz DE, Brekken RA, Quinn AM, Simeonov A, Easmon J, Martinez ED (2013) A small molecule modulates Jumonji histone demethylase activity and selectively inhibits cancer growth. Nat Commun 4:2035
11. Sekar TV, Foygel K, Devulapally R, Paulmurugan R (2015) Degron protease blockade sensor to image epigenetic histone protein methylation in cells and living animals. ACS Chem Biol 10:165–174
12. Sekar TV, Foygel K, Gelovani JG, Paulmurugan R (2015) Genetically encoded molecular biosensors to image histone methylation in living animals. Anal Chem 87:892–899
13. Paulmurugan R, Gambhir SS (2003) Monitoring protein-protein interactions using split synthetic *Renilla* luciferase protein-fragment-assisted complementation. Anal Chem 75:1584–1589
14. Paulmurugan R, Gambhir SS (2005) Firefly luciferase enzyme fragment complementation for imaging in cells and living animals. Anal Chem 77:1295–1302
15. Paulmurugan R, Gambhir SS (2006) An intramolecular folding sensor for imaging estrogen receptor-ligand interactions. Proc Natl Acad Sci U S A 103:15883–15888
16. Paulmurugan R, Gambhir SS (2007) Combinatorial library screening for developing an improved split-firefly luciferase fragment-assisted complementation system for studying protein-protein interactions. Anal Chem 79:2346–2353
17. Paulmurugan R, Ray P, De A, Chan CT, Gambhir SS (2006) Split luciferase complementation assay for studying interaction of proteins x and y in cells. CSH Protoc 2006; doi:10.1101/pdb.prot4596
18. Paulmurugan R, Ray P, De A, Chan CT, Gambhir SS (2006) Split luciferase complementation assay for studying interaction of proteins X and Y in living mice. CSH Protoc 2006; doi:10.1101/pdb.prot4595
19. Paulmurugan R, Tamrazi A, Massoud TF, Katzenellenbogen JA, Gambhir SS (2011) *In vitro* and *in vivo* molecular imaging of estrogen receptor α and β homo- and heterodimerization: exploration of new modes of receptor regulation. Mol Endocrinol 26:2029–2040

Chapter 18

Preparation and Assay of Simple *Light off* Biosensor Based on Immobilized Bioluminescent Bacteria for General Toxicity Assays

G.V.M. Gabriel and V.R. Viviani

Abstract

We describe a simple *light off* bioluminescent biosensor for general environmental toxicity assays based on immobilized bioluminescent bacteria engineered with beetle luciferases.

Key words Bioluminescent biosensor, Toxicity biosensor, pH-sensitive firefly luciferase

1 Introduction

Biosensors, analytical devices that combine the recognition of a biological substance of interest and the transduction of the response in a measurable signal, are widely used for environmental applications, allowing a quantitative and specific analysis [1–4]. They are useful due to their easy preparation and storage, minimum quantity of sample required, relatively low cost, good reproducibility, selectivity and sensitivity, fast response time, and, in addition they are useful to analyze bioavailability [1, 3].

Among the different kinds of biosensors, bioluminescent biosensors are very fast and sensitive and are gaining in popularity, because they rely on luciferases or photoproteins (enzymes that require oxygen to oxidize luciferin, producing light in a quantitative fashion). They can be divided into enzymatic and whole cell biosensors, in which the whole cell biosensor can be further divided into *light on* and *light off*. In the *light off* biosensors, the luminescence is inhibited by specific agents that affect the metabolism, reducing the intensity of the light signal, which can be monitored by photodetecting devices such as photometers, luminometers, and CCD cameras [5–7].

Sung-Bae Kim (ed.), *Bioluminescence: Methods and Protocols*, Methods in Molecular Biology, vol. 1461,
DOI 10.1007/978-1-4939-3813-1_18, © Springer Science+Business Media New York 2016

A *light off* biosensor is built by cell transformation with an expression vector containing the reporter gene expressing luciferase [8] and the cells can be used in liquid cultures or immobilized to detect the toxicity of liquid samples and chemicals based on the decrease of bioluminescence intensity upon contact with toxic factors [9], such as heavy metals [5, 6, 10–12]. Here we describe the preparation and use of a simple *light off* biosensor to measure general toxicity of water samples and bioprospection of extracts, based on the transformation of *E. coli* with two beetle luciferases (*Macrolampis* sp2 firefly and *Pyrearinus termitilluminans* click beetle) [13]. Each luciferase has its own peculiarities, allowing their use for specific applications.

2 Materials

2.1 Buffers and Solutions

1. 0.1 mg/mL Ampicillin.
2. 40 mM ATP in 80 mM $MgSO_4$.
3. 10 mM d-Luciferin.
4. 10 mM d-Luciferin in 50 mM sodium citrate buffer pH 5.0.
5. 1 M dithiothreitol (DTT).
6. 1 M isopropyl-β-d-1-thiogalactopyranoside (IPTG).
7. 100 mM Tris–HCl pH 5.0 and pH 8.0.
8. 1.0 mg/mL 2,3,5-triphenyl tetrazolium chloride (TTC).

2.2 Media

1. Luria-Bertani (LB) Miller medium.
2. Agar pH 7.5: 10.0 g/L Casein enzymic hydrolysate, 5.0 g/L Yeast extract, 10.0 g/L Sodium chloride, 15.0 g/L Agar.
3. Broth pH 7.5: 10.0 g/L Casein enzymic hydrolysate, 5.0 g/L Yeast extract, 10.0 g/L Sodium chloride.
4. Top agar: LB broth with 0.7% (w/v) agarose.

2.3 Vectors and Bacterial Strains

1. *Escherichia coli* BL21 (DE3).
2. pPro vector (plasmid: Invitrogen).

2.4 Beetle Luciferases cDNA

1. *Macrolampis* sp2 firefly.
2. *Pyrearinus termitilluminans* larval click beetle.

2.5 Metal Solutions at 5.0 μg/mL

1. 0.0294 mM $AgNO_3$.
2. 0.02 mM $CuSO_4$.
3. 0.0184 mM $HgCl_2$.
4. 0.019 mM $NiSO_4$.

5. 0.0174 mM $PbCl_2$.
6. 0.0173 mM $ZnSO_4$.

2.6 Disinfectant and Sanitizing Reagents

1. 0.0831 mM 1-Propanol.
2. 3 % Boric acid.
3. 70 % Ethanol.
4. 1 % Phenol.
5. 3 % Hydrogen peroxide.
6. 2 % Iodine.
7. 0.0471 mM Sodium carbonate.

2.7 Equipments

1. Charge-coupled device (CCD) camera Light Capture II (ATTO, Japan).
2. Centrifuge 5810 R (Eppendorf).
3. Ice water bath.
4. Incubator (37 °C) (EletroLab, Brazil).
5. Luminometer AB-2200 (ATTO, Japan).
6. Sonicator Ultrassonic Processor XL (Misonix, USA).
7. Spectrofluorometer F-4500 (Hitachi, Japan).
8. Water bath preset at 42 °C (Stern 6, Sieger, LojaLab, Brazil).

3 Methods

This method consists in preparing immobilized bioluminescent *E. coli*, by transformation of *E. coli* with pPro-Mac or pPro-Pte luciferase plasmids, followed by IPTG induction, immobilization in agarose matrix and, finally, assaying the in vivo luminescence in the absence (control) and presence of toxicants. Inhibition of bacterial luminescence intensity in relation to the respective controls is taken as evidence of general toxicity due to inhibition of ATP production in the cells. The luminescence assay can be performed using liquid cultures, or more conveniently using immobilized bacteria.

3.1 Bacterial Transformation

E. coli are transformed with recombinant plasmids pPro-Mac and pPro-Pte, containing *Macrolampis* sp2 firefly and *Pyrearinus termitilluminans* click beetle luciferase genes, respectively.

1. Add 1 μL of the luciferase plasmids (~10–50 ng) to 50 μL of competent *E. coli* cells. Gently swirl the microtubes several times to mix their contents. Place the tubes on ice for 30 min.
2. Immediately incubate the microtubes in a preheated water bath at 42 °C during 45 s. Do not shake the tubes.

3. Rapidly transfer the microtubes to ice. Allow the cells to cool down for 2 min.
4. Add 200 μL of LB broth medium to each microtube. Incubate the microtubes in a shaking incubator at 37 °C at 225 cycles/min during 1 h to allow the bacteria to recover and express the antibiotic resistance marker encoded by the plasmid.
5. Transfer 100 μL of the transformed cells into LB agar medium Petri dishes containing the appropriate antibiotic (in our case we use ampicillin) and spread with the aid of the handle Drigalski spatula.
6. Invert the plates and incubate them at 37 °C O/N. After 12–16 h the transformed colonies should appear in the plates.

3.2 Induction of Heterologous Luciferase Expression in Bacteria

1. Select one transformed colony with the aid of the Henle loop and inoculate it in Falcon tube filled with 5 mL of LB broth and the appropriate antibiotic (in our case we use ampicillin). Transfer the Falcon tubes to a shaking incubator at 37 °C at 225 cycles/min to grow up the cells overnight or until $Abs_{600} \sim 1.0$.
2. Transfer 1 mL of the cultured cells to a sterile Erlenmeyer containing 100 mL of LB broth, and place it in a shaking incubator at 37 °C at 225 cycles/min, monitoring the cell growth until $Abs_{600} = 0.40$.
3. Discontinue the growth by transferring the Erlenmeyer to a refrigerator for approximately 10–15 min.
4. Add 40 μL of 1 M IPTG to the cultured cells in the Erlenmeyer and induce protein expression by incubating in a shaking incubator at 20 °C at 225 cycles/min until $Abs_{600} = 1.5$.
5. After induction verify the luciferase expression by in vivo bioluminescence activity (*see* **Note 1**) using a luminometer (*see* **Note 2**).

3.3 In Vivo Luminometric Assay of Bioluminescence in Liquid Cultures

The induced bacteria in liquid cultures can be directly incubated with toxic agents as follows (*see* **Note 3**):

1. Mix 500 μL of the liquid cultures (of the **step 5** in Subheading 3.2) with 50 μL of toxic samples in water (metals at the concentration of 5.0 μg/mL or sanitizers). Incubate the treated cultures during 1 h at room temperature (~22 °C).
2. Mix 90 μL of the treated suspension with 10 μL of 10 mM d-Luciferin at pH 5.0 in a luminometer tube and measure luminescence intensity in *cps* in the luminometer.

3.4 Luminescence Assay Using Immobilized Bacteria and CCD Imaging

In order to assay several samples at the same time, an 96-well plate with immobilized bioluminescent bacteria can be prepared and used to simultaneously screen several samples in a more convenient, fast, and sensitive format.

3.4.1 Preparation of Immobilized Bacteria

The immobilized bacteria are prepared as follows:

1. Mix in 9 mL of melted Top Agar cooled down to ~40 °C in a water bath with 1 mL of the induced liquid cultures (of the **step 5** in Subheading 3.2), 10 μL of 1 M IPTG and 10 μL of the appropriate antibiotic (in our case we use ampicillin).
2. With the aid of a micropipette, quickly transfer 50–100 μL of this mixture in each well of the 96-well microplate.
3. Allow the bacterial/agarose medium to solidify during 1 h, and leave the immobilized bacteria during 12 h at room temperature (~22 °C).
4. After that, store the Elisa plate at 4 °C for up to 30 days (*see* **Note 4**).
5. Whenever the immobilized bacteria are to be used, remove the Elisa from the refrigerator, allow to warm up at room temperature (~22 °C) for at least 2 h, and use them for the toxicity assays.

3.4.2 Luminescence Assay of Immobilized Bacteria Using CCD Imaging

When the immobilized bacteria are ready to be used, proceed as follows to do the luminescence assay using CCD imaging:

1. Add 10 μL of toxicant sample to each well of the Elisa plate (*see* **Note 5**).
2. Allow the toxicant sample to penetrate the immobilized bacteria in each well by incubation at room temperature (~22 °C) during 2 h.
3. As a control use water or the solvent were the samples are diluted.
4. Add 10 μL of 10 mM d-Luciferin pH 5.0 to each well. Allow luciferin to penetrate the agarose gel during 30 min at room temperature.
5. Analyze the bioluminescence using a CCD photodetection system or in a plate reader.
6. The luminescence intensity of the samples and controls can be quantified by densitometry using the proper algorithm provided by the instrument maker (*see* Fig. 1).

3.5 Tetrazolium Colorimetric Assay of Cell Viability

In order to check for cell viability after treatment of the bacterial cultures, the tetrazolium salt colorimetric assay is employed as follows:

1. Mix 90 μL of the liquid or immobilized cultures with 10 μL of toxic samples (for example, metals at 5.0 μg/mL or sanitizers) and 10 μL of 2, 3, 5-triphenyltetrazolium chloride (TTC) at 1 mg/mL. Incubate at 37 °C for 1 h and check for the appearance of red color as an indication of reducing bioactivity (*see* **Note 6** and Fig. 2).

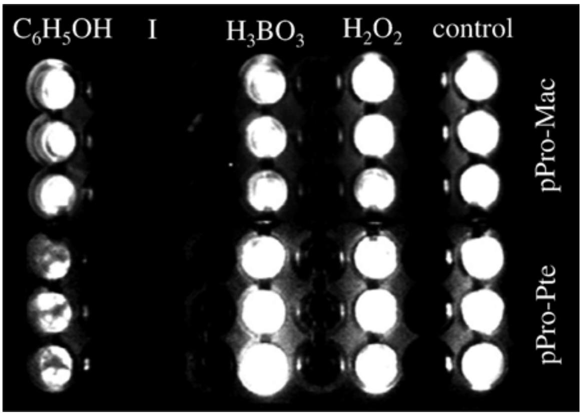

Fig. 1 CCD bioluminescence imaging of bioluminescent *E. coli* transformed with pPro-Mac and pPro-Pte after exposure to sanitizing agents 1 % phenol (C_6H_5OH), 2 % iodine (I), and 3 % boric acid (H_3BO_3) for 1 h at 4 °C (Adapted from Gabriel et al. [13])

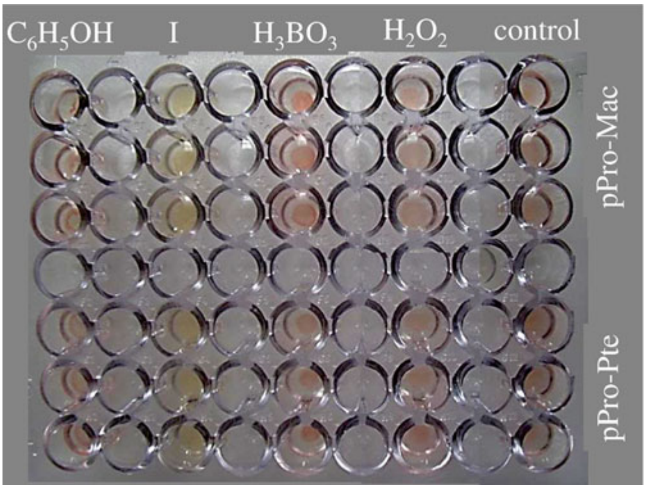

Fig. 2 Tetrazolium colorimetric assay of *E. coli* transformed with pPro-Mac and pPro-Pte after exposure to sanitizing agents 1 % phenol (C_6H_5OH), 2 % iodine (I), and 3 % boric acid (H_3BO_3) and incubation for 1 h at 4 °C (Adapted from Gabriel et al. [13])

4 Notes

1. The bioluminescent activity depends on the enzyme utilized. In our assay, *Macrolampis* sp2 luciferase can be used for fast assays using a more sensitive detection system, due to the rapid flash-like kinetics, whereas *Pyrearinus termitilluminans* click beetle luciferase can be used in cases where a less sensitive detection system is used due to its higher activity and slower kinetics, allowing integration for longer time. For *Macrolampis* sp2 the expected luciferase activity is around 15×10^7 cps/mL

and for *P. termitilluminans* the expected luciferase activity is around 20×10^7 cps/mL [13].

2. Use the induced cells of the liquid culture to do the in vivo assays (*see* Subheading 3.2) and to prepare immobilized the bacteria in Top Agar (*see* Subheading 3.4.1).
3. It must be emphasized that this cell biosensor assay, does not give any clue about the specific compound or group of toxic compounds present in the assayed sample, it just gives a fast and general information about the toxicity of the sample.
4. The plate can be stored at 4 °C until 3 weeks with high luminescence activity.
5. This *light off* biosensor can be adapted to be used for bioprospection of antibiotics and other bactericidal samples.
6. The tetrazolium reagent has no color. When reduced it gives a bright red color, indicating the presence of reducing power of live bacteria.

References

1. Gomes SASS, Rebelo MJF (2003) A new laccase biossensor for polyphenols determination. Sensors 3:166–175
2. Chien-Yuan C, Karube I (1992) Biosensors and flow injection analysis. Curr Opin Biotechnol 3:31–39
3. Buonasera K, Pezzotti G, Pezzotti I, Cano JB, Giardi MT (2011) Biosensors: new frontiers for environmental analysis. Rev Politécnica 13:93–100
4. Belkin S (2003) Microbial whole-cell sensing systems of environmental pollutants. Curr Opin Microbiol 6:206–212
5. Tauriainen S, Karp M, Chang W, Virta M (1997) Recombinant luminescent bacteria for measuring bioavailable arsenite and antimonite. Appl Environ Microbiol 63:4456–4461
6. Tauriainen S, Karp M, Chang W, Virta M (1998) Luminescent bacterial sensor for cadmium and lead. Biosens Bioelectron 13:931–938
7. Thouand G, Horry H, Durand MJ, Picart P, Bendriaa L, Daniel P, DuBow MS (2003) Development of a biosensor for on-line detection of tributyltin with a recombinant bioluminescent *Escherichia coli* strain. Appl Microbiol Biotechnol 62:218–225
8. Mirasoli M, Feliciano-Cardona JS, Michelini E, Roda A, Daunert S (2002) Development and characterization of a fluorescent whole-cell biosensor for L-arabiose with internal response correcting using two GFP mutants. In: Stanley PE, Kricka LJ (eds) Bioluminescence and chemiluminescence: progress and current applications, 1st edn. World Scientific, Hackensack, NJ, pp 331–334
9. Choi SH, Gu MB (2002) A portable toxicity biosensor using freeze-dried recombinant bioluminescent bacteria. Biosens Bioelectron 17:433–440
10. Abd-El-Halleem D, Ripp S, Scott C, Sayler GS (2002) A luxCDABE-based bioluminescent bioreporter for the detection of phenol. J Ind Microbiol Biotechnol 29:233–237
11. Abd-El-Halleem D, Zaki S, Abulhamd A, Elbery H, Abu-Elreesh G (2006) Acinetobacter bioreporter assessing heavy metals toxicity. J Basic Microbiol 46:339–347
12. Eltzov E, Marks RS (2011) Whole-cell aquatic biosensors. Anal Bioanal Chem 400:895–913
13. Gabriel GVM, Lopes PS, Viviani VR (2014) Suitability of *Macrolampis* firefly and *Pyrearinus* click beetle luciferases for bacterial light off toxicity biosensor. Anal Biochem 445:72–78

Part III

Applications to Living Subjects and Instrumentations

Chapter 19

In Vivo Bioluminescent Imaging of ATP-Binding Cassette Transporter-Mediated Efflux at the Blood–Brain Barrier

Joshua Bakhsheshian, Bih-Rong Wei, Matthew D. Hall, R. Mark Simpson, and Michael M. Gottesman

Abstract

We provide a detailed protocol for imaging ATP-binding cassette subfamily G member 2 (ABCG2) function at the blood–brain barrier (BBB) of transgenic mice. D-Luciferin is specifically transported by ABCG2 found on the apical side of endothelial cells at the BBB. The luciferase–luciferin enzymatic reaction produces bioluminescence, which allows a direct measurement of ABCG2 function at the BBB. Therefore bioluminescence imaging (BLI) correlates with ABCG2 function at the BBB and this can be measured by administering luciferin in a mouse model that expresses luciferase in the brain parenchyma. BLI allows for a relatively low-cost alternative for studying transporter function in vivo compared to other strategies such as positron emission tomography. This method for imaging ABCG2 function at the BBB can be used to investigate pharmacokinetic inhibition of the transporter.

Key words D-Luciferin, BCRP, ABCG2, Optical imaging, Neuroimaging

1 Introduction

The blood–brain barrier (BBB) plays a vital role in protecting the central nervous system by preventing a variety of molecules from entering the brain. This protective barrier is mediated in part by ATP-binding cassette transporters, primarily P-glycoprotein and ABCG2, located on the apical membrane of capillary endothelial cells [1]. While protecting the brain, these transporters also restrict the delivery of potentially therapeutic molecules aimed at the management of neurologic disorders. As therapeutic molecules do not reach the brain parenchyma in clinically relevant concentrations, the BBB is a major obstacle to drug delivery to the brain.

Mouse models have been used to investigate ABCG2 function at the BBB, and the findings can be extrapolated to provide clinical relevance [2, 3]. The mouse ortholog of ABCG2 has 81 % protein sequence homology with human ABCG2 [4] and the substrate and inhibitor specificity of human and mouse ABCG2 is very

Sung-Bae Kim (ed.), *Bioluminescence: Methods and Protocols*, Methods in Molecular Biology, vol. 1461,
DOI 10.1007/978-1-4939-3813-1_19, © Springer Science+Business Media New York 2016

similar [5]. Amino acid mutations have been shown to alter the substrate and antagonist specificity in both species [6]. The overlapping substrate and inhibitor specificity of human and mouse ABCG2 supports utilization of mouse models in understanding the functional roles of ABCG2.

This protocol describes a noninvasive imaging modality using D-Luciferin in transgenic mice. We have previously shown that D-Luciferin is a specific substrate of ABCG2 (and not other ABC transporters expressed at the BBB). Therefore, D-Luciferin can be used to study ABCG2 function at the BBB [7]. Real-time function at the BBB is often studied using positron emission tomography (PET) [8], but D-Luciferin is not amenable for radiotracer labeling. As such, we decided to take advantage of the fact that D-Luciferin is a substrate for the enzyme firefly luciferase (FLuc). In the presence of FLuc, ATP, and O_2, D-Luciferin generates a photon of light (bioluminescence), and this can be detected with commercially available charge-coupled device detectors. To study the BBB function of ABCG2, we utilized a GFAP-FLuc transgenic mouse model [2], in which the expression of FLuc is controlled by the glial fibriliary acid protein (GFAP) promoter. GFAP is predominately expressed in astrocytes in the parenchyma of the brain [9] and is found behind the BBB. As luciferin is enzymatically converted to oxyluciferin, the production of bioluminescence can allow one to measure the amount of D-Luciferin in the brain parenchyma.

In this model, when D-Luciferin is injected into GFAP-FLuc transgenic mice, bioluminescent signal from the brain is low due to the efflux of D-Luciferin by Abcg2 at the BBB (*see* Fig. 1). However,

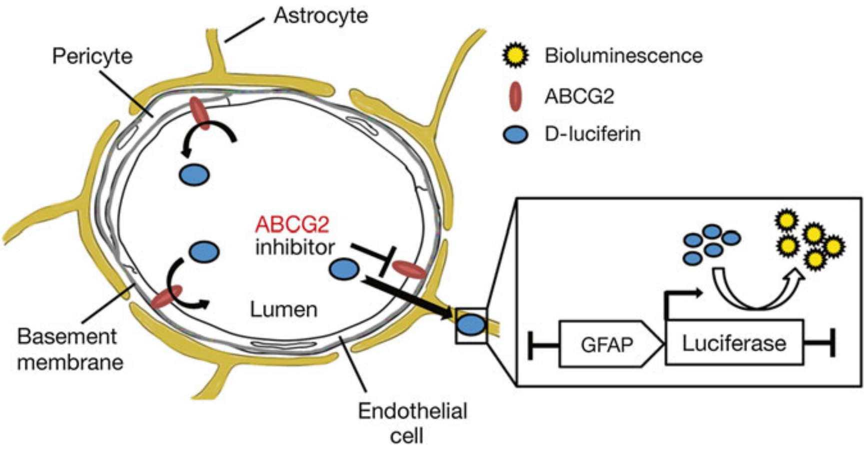

Fig. 1 Scheme depicting the basis of the imaging protocol. ABCG2 transporters normally prevent D-Luciferin from crossing brain endothelial cells, by pumping it back from the apical membrane into the luminal space. However, when ABCG2 is inhibited, luciferin can cross the endothelial cells (BBB) and enter the parenchymal space. In astrocytes, firefly luciferase expressed under the GFAP promoter uses luciferin as a substrate, producing bioluminescence. The light generated can be captured by a sensitive optical camera and act as a surrogate indicator of luciferin uptake into the brain

in the presence of a pharmacologic blocker of ABCG2 (or some other mechanism for interfering with ABCG2 expression or function), D-Luciferin can cross the BBB and enter astrocytes in the brain, where FLuc is expressed. This results in an elevated bioluminescent signal. Previously, we have shown that a dose-dependent increase in bioluminescence from the brain can be observed with ABCG2 inhibitors of interest. These data can be used to calculate the effective dose of ABCG2 inhibition at the BBB in vivo. Therefore, bioluminescence imaging (BLI) of mice expressing the luciferase enzyme in the brain can be used to monitor ABCG2 function at the BBB. Here, we provide a detailed protocol for this assay of BBB function.

2 Materials

2.1 Chemicals

1. The substrate, D-Luciferin (PerkinElmer (Waltham, MA)) (*see* **Note 1**).
2. There are several ABCG2 inhibitors that are commercially available. The potency and efficacy varies for each inhibitor (*see* **Note 2**).
   (a) Ko-143 (Tocris Bioscience (Minneapolis, MN)).
   (b) Nilotinib and gefitinib (Cayman Chemical (Ann Arbor, MI)).
   (c) Elacridar and tariquidar (MedKoo Biosciences (Chapel Hill, NC)).

2.2 In Vivo Studies

1. D-Luciferin solution is prepared by dissolving in saline to obtain 30 mg/mL stock solutions and stored at -20 °C protected from light (*see* **Note 1**).
2. As indicated by solubility profiles, candidate inhibitors of ABCG2 can be dissolved in appropriate stock solutions. For example, lipophilic molecules such as tariquidar and elacridar can be dissolved in vehicle containing 2:2:1 dimethyl sulfoxide, propylene glycol, and water (5 % Dextrose) (*see* **Notes 2–6**). Molecules that are more water-soluble can be prepared in normal saline solution and filtered as described for D-Luciferin above.

2.3 Anesthesia

1. The mice are administered isoflurane at 2–5 %. Procedures conducted with anesthesia can be done under low-pressure high flow ventilation hoods to collect excess isoflurane.

2.4 Animal Model

1. The FVB/N-Tg(GFAP-FLuc)-Xen mouse (Taconic Farms (Germantown, NY)). This is a transgenic mouse line that carries the firefly luciferase (FLuc) gene under the transcriptional control of the mouse GFAP promoter [2]. Expression of the reporter is observed primarily in the brain (*see* **Note 7**).

2. For mouse identification, two methods can be employed. For both methods, the identification is susceptible to loss of the identification marker over time, by falling or being torn out. Both can be purchased from Kent Scientific Corporation (Torrington, CT).
   (a) Ear tags—a metal ID can be placed on the pinna of the ear with an applicator.
   (b) Ear punch—ear notches or holes are placed with an ear punch device, following universal mouse numbering systems [10].
3. Prior to experiments, the weight of each mouse should be recorded.

2.5 Bioluminescence Imaging Unit

1. An IVIS spectrum and charged-coupled device (CCD) optical imaging system, Living Image Software (PerkinElmer, Waltham, Massachusetts) can be used for spatiotemporal detection and analysis of the luciferase - luciferin reaction in multiple mice.

3 Methods

3.1 Bioluminescence Imaging

1. Four to five mice should be used for each condition to reach statistical significance. Depending on the bioluminescence imaging unit housing, up to five mice can be simultaneously imaged. In addition, for each experimental run there should be at least one sham mouse receiving only luciferin and vehicle (*see* Fig. 2 and **Notes 8** and **9**).
2. Anesthesia is induced in a chamber with 2–5 % isoflurane in O_2. Anesthesia is maintained with 2 % isoflurane via a nosecone, for the duration of the procedure.
3. Responses to anesthesia can be monitored by changes in physiological parameters including: respiratory rate, evidence of sensation, and reflex.
4. Body temperature of the animal can be maintained by use of a heated circulating water pad, heated air, heat lamp, or heated platform.
5. Measure baseline bioluminescence from the brain of each mouse (without co-injected inhibitor or vehicle).
6. Specify the appropriate acquisition settings (Exposure time, Binning, F/stop) (*see* **Note 10**).
7. Administer 18 mg/kg of D-Luciferin via intraperitoneal (i.p.) injections using a 25-gauge needle (*see* Table 1 and **Notes 11** and **12**).

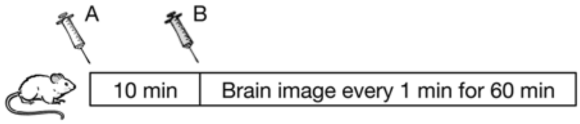

Mouse	A	B
Experimental	i.v. ABCG2 inhibitor	i.p. luciferin
Control A	i.v. vehicle	i.p. luciferin
Control B	Nothing	i.p. luciferin
Control C	i.v. control inhibitor	i.p. luciferin

Fig. 2 Scheme demonstrating experimental and control setup with dosages. Either the vehicle or nothing is injected for option A and mice are injected with luciferin for all experimental conditions

8. Immediately place mice in the IVIS100 optical imaging system (PerkinElmer, Waltham, Massachusetts), in a supine position (i.e., lying on the back) and record bioluminescent signal for 60 min with sequential acquisitions at 1 min intervals (*see* **Notes 12–14**).
9. At least 24 h following **step 2**, animals are again anesthetized (*see* **step 1**), temporarily placed under a heating lamp to dilate the lateral tail veins and to facilitate ease of i.v. injections (*see* **Notes 15–17**). Inhibitors are administered by tail vein injections using a 30½-gauge needle (*see* **Notes 17–19**).
10. Exactly 10 min following **step 3**, the inhibitor injections are followed by i.p. injections of D-Luciferin, (100 μL for 18 mg/kg) using a 25-gauge needle (*see* **Note 20**).
11. The mice are then immediately placed in the optical imaging system in a supine position. While anesthesia is maintained in the imaging unit with 2 % isoflurane with nose cones, bioluminescent signals are recorded in 60-min sequential acquisitions with 1-min intervals using IVIS100 (PerkinElmer) (*see* **Note 21**).
12. After the imaging procedure (60 min), the mice are removed from the imaging system, placed in animal cages, and monitored to ensure they are not displaying any signs of distress.

3.2 Analysis of BLI Data

1. To quantify the light output from the mouse brain region, define a consistent region of interest (ROI) over the cranium and examine all bioluminescence values in the same ROI in sequential images using LivingImage software (PerkinElmer, Waltham, Massachusetts) (*see* **Notes 21** and **22**).
2. Each data point is corrected for the respective mouse's baseline signal level (without inhibitor) generated in **step 2**, and background autoluminescence (*see* **Notes 23–25**).

Table 1
Luciferin injection calculations for mice of varying weights. Required luciferin stock for injection is supplemented with saline, making up a total 100 μL injection volume

Desired dose (mg/kg)	Luciferin stock solution (mg/mL)	Mouse weight (g)	Luciferin needed (mg)	Volume of luciferin stock (μL)	Saline (μL)	Total injection volume (μL)
18	10	35	0.63	63	37	100
18	10	34	0.61	61.2	38.8	100
18	10	33	0.59	59.4	40.6	100
18	10	32	0.58	57.6	42.4	100
18	10	31	0.56	55.8	44.2	100
18	10	30	0.54	54	46	100
18	10	29	0.52	52.2	47.8	100
18	10	28	0.50	50.4	49.6	100
18	10	27	0.49	48.6	51.4	100
18	10	26	0.47	46.8	53.2	100
18	10	25	0.45	45	55	100

3. Time-activity curves can be created for each mouse by plotting the total flux (photon/s) versus time (min).
4. The area under the time-activity-curve (AUC, p/s · min) can be calculated by the trapezoidal method using Prism 6.0 (GraphPad software).
5. If varying doses of the inhibitor are tested, the effective concentration where 50% (EC_{50}) of maximal bioluminescence is achieved can be calculated. The area under the time-activity-curve is plotted against the concentration of inhibitor used, and the EC_{50} can be calculated with Prism 6.0 (GraphPad software).
6. After the data are tested for homogeneity of variance, differences in mean AUC (p/s · min) can be compared using a one-way analysis of variance followed by the Bonferroni post-*t* test for multiple comparisons ($\alpha = 0.05$).

4 Notes

1. Luciferin absorbs light maximally at a wavelength of 350 nm [11], which can result in photodegradation from natural light exposure. In a laboratory setting, wrapping the solution vessel in aluminum foil, or using a brown glass vial, ensures protection from incident light.

2. Ko-143 is a potent ABCG2 inhibitor [12]. Gefitinib, nilotinib [13], tariquidar [14] and elacridar [15] are dual ABCG2 and P-gp inhibitors. Ko-143, gefitinib, and nilotinib were shown to inhibit ABCG2 at the BBB, indicated by increased bioluminescent signal in the GFAP-FLuc animal model [5]. Elevated bioluminescence was not observed with tariquidar or elacridar (they are shown to be more efficacious inhibitors of P-gp than ABCG2). In our original study, DCPQ, a specific P-gp inhibitor, was used as a negative control, in addition to administering vehicle-only. As DCPQ is not commercially available, an alternate specific high-affinity P-gp inhibitor may be utilized such as zosuquidar, cyclosporin A, or verapamil [16]. It is critical to confirm that P-gp inhibitors intended to be used as negative controls do not interfere with ABCG2 function in vitro.
3. Prepare stock solutions of the inhibitors that will allow you to inject 100 μL volumes by direct tail vein injections of 4, 6, 8, 16, and 32 mg/kg. To achieve this, first prepare stock solutions of 25 mg/mL inhibitor in 1:1 dimethyl sulfoxide and propylene glycol. These can be stored at −20 °C. To prepare injectable solutions, dilute with additional 2:2:1 dimethyl sulfoxide, propylene glycol, and water (5% Dextrose) (*see* Table 2 for sample calculations for preparing inhibitor solutions for an average 30 g mouse). Saline is not used in preparation of the stock solution to avoid precipitation and hydrolysis of inhibitors, but is used for dilution of stock solution and for preparation of injectable inhibitor solution. The numbers displayed in Table 2 can be scaled based on the total number of mice to be injected for each condition. The injection volume is kept at 100 μL to limit the volume of vehicle administration and to keep the total volume of solution administration (including inhibitor and luciferin substrate) below 200 μL (maximum amount allowed for injection).
4. It is important to use an agent that does not physically disrupt the BBB, which may confound the results by providing an alternate route for luciferin to bypass the BBB. If necessary, to evaluate BBB disruption one may use Evans blue (*see* **Note 5**) or sodium fluorescein (*see* **Note 6**) to determine increased brain penetration following injection of a test agent [17, 18].
5. Evans blue is a marker that binds albumin avidly in blood plasma. Albumin has a 60 kDa molecular weight, and does not cross the BBB. A detailed protocol is provided in [17]. Briefly, 2 mL/kg of a 2% (w/v) solution of Evans blue in saline is administered i.v. with a 25-gauge needle. Evans blue is allowed to circulate for 30 min before mice are euthanized and the brain extracted. An analog scale-based evaluation of the intensity and distribution of the bluish coloration is used to evaluate the degree of the BBB permeabilization.

Table 2
Sample calculations for preparation of injectable solutions of ABCG2 inhibitors

Inhibitor stock solution				Injectable solution				
Desired dose (mg/kg)	Mouse weight (g)	Inhibitor needed (mg)	Inhibitor stock solution (mg/mL)	Stock solution to use (μL)	DMSO (μL)	PEG (μL)	Saline (μL)	Total injection volume (μL)
32	30	0.96	25	38.4	20.8	20.8	20	100
16	30	0.48	20	24	28	28	20	100
8	30	0.24	10	24	28	28	20	100
4	30	0.12	5	24	28	28	20	100

The numbers displayed can be scaled based on the total number of mice to be injected for each condition. Stock solutions of inhibitor are prepared in a 1:1 dimethyl sulfoxide and propylene glycol solution for storage, and prepared for injection immediately prior to the experiment

6. A spectrophotofluorimetric sodium flourescein uptake measurement (excitation at 440 nm and emission at 525 nm) enables detection of subtle alterations in BBB permeability. A detailed protocol is provided in ref. 18. It is suggested that changes in BBB permeability to sodium fluorescein may be the earliest and the most sensitive indicator of BBB disruption and therefore in many instances. Briefly, 2 mL/kg of a 2 % [wt: vol] solution in saline can be administered at a dose of 5 mL/kg body weight of animal i.p. with a 25-gauge needle. Sodium fluorescein is allowed to circulate for 30 min before mice are euthanized.
7. This model was generated for the study of transcriptional regulation of the GFAP gene [9], for example, to observe changes in expression associated with kainic acid-induced astrogliosis [2]. In the protocol reported here, we use the same mouse strain to indicate the ability of D-Luciferin to cross the BBB using baseline expression, and do not require induction of expression by inflammatory processes such as kainic acid.
8. D-Luciferin i.p only (control B in Fig. 2) can serve as a control for bioluminescent variations that may be caused by experimental error in the amount of luciferin injected, or other causes.
9. Administering luciferin via i.p. injection is the standard route of administration in in vivo studies. Intravenous injections of D-Luciferin are possible, but introduce a more technically demanding protocol, including more injections, tail catheter line placements, and catheter or needle ‘clogging’ due to precipitation of solutions. Another disadvantage of i.v. injections is the fast kinetics/clearance with the lack of a plateau phase,

which may not provide sufficient time to saturate luciferin at the site of interest (brain), impeding reproducible measurements and leading to additional error [19].

10. The acquisition setting is adjusted to produce a signal above the noise/background, but less than the detection limit (60 K counts) of the camera. A higher binning increases the pixel size at the loss of spatial resolution. 'F/stop' sets the size of the camera aperture and the amount of light that is collected. Therefore, a larger lens opening (f/1) will maximize sensitivity.
11. Instead of the 150 mg/kg of D-Luciferin used in a standard BLI protocol [19], 18 mg/kg of D-Luciferin is used, as it produces a low baseline signal from the brain region [7]. This lower dose is used to avoid saturating ABCG2 transporters at the BBB while increasing the sensitivity to detect changes in bioluminescent signal produced by inhibiting ABCG2 function. Prior to performing functional studies, an experiment can be performed with mice injected with a range of luciferin doses (for example, 150, 80, 40, 20, 10, and 5 mg/kg D-Luciferin) to ensure a dose is utilized that produces a low baseline signal with the instrument and settings being used.
12. It is important to measure baseline bioluminescence under identical conditions, since anesthesia induces changes in the blood flow of the animal, and may alter the pharmacokinetics of D-Luciferin and subsequent bioluminescence production.
13. The photon emission in living brain tissue is limited substantially by anatomical layers. BLI signal from the ventral brain is higher [20] and signal does arise from the cochlear spiral ganglion [21]; therefore mice are imaged in the supine position (i.e., on their back).
14. The body of the mice can be covered with black construction paper, exposing only the head region. This reduces any bioluminescence signal that may be produced from the periphery. The GFAP-FLuc mouse model produces a low-level signal from the exposed skin regions (tail and foot pads).
15. Tail vein injections are technically demanding and require practice and accuracy to correctly perform them. This technique can be performed after anesthesia induction; however, it can also be performed without anesthesia when using proper restraining devices.
16. To help locate the lateral veins, a heated stage or heat lamp may be utilized to dilate the vasculature. Hold the tail so that the lateral vein is uppermost and insert the needle. Draw back on the syringe slightly to make sure the needle is inserted in the blood vessel, indicated by blood being drawn. In the event that the injected agent is not introduced to the vein, the surrounding tissue will blanch.

17. It is advised to use a small volume syringe with attached needles (Becton, Dickinson and Company), as the 'dead space' volume is lower, increasing accuracy of injections and minimizing wastage of injectable solutions. Care should be taken to remove air bubbles in the syringe.
18. Alternatively, a tail vein catheter with minimal dead space may be used for rapid near-simultaneous injection to multiple mice. However, the catheters need to be coated with heparin to avoid clogging of the catheter. One should be cautious with coating the catheters with heparin in a saline solution, because this may cause precipitation of the lipophilic inhibitor agent during the injection process.
19. To help administer the inhibitor to multiple mice within a short time interval, the "snipped glove" technique may be employed. A glove is snugly placed around the anesthesia tubing and taped securely in place. The finger tips of the glove are then snipped, and each finger opening acts as a different outlet or nose cone to be fitted loosely around the muzzle of each mouse for anesthesia maintenance on the benchtop.
20. The time delay between inhibitor injection, luciferin injection, and acquisition is recorded during each BLI experiment and can be used for time-line correction (acquisition time = 60 min), enabling precise data evaluation.
21. The optical signal intensity is expressed as photon flux (photon count/s). Each image can be displayed as a pseudo-colored photon-count image superimposed onto a grayscale anatomic image of the same animal (*see* Fig. 3).
22. While outside the scope of the protocol described here, an ex vivo confirmation that the signal from the ROI can be performed. **Steps 1–6** are completed as described, except mice are imaged for 20–25 min only. This is the time period where maximal bioluminescence has been shown [7, 19]. The mice are immediately sacrificed; brains are removed and placed in the imaging unit for BLI. Mice with similar baseline bioluminescent signals and weight should be utilized. Four to five mice are needed for each group. The ratio between in vivo and ex vivo imaging of mice receiving luciferin only and luciferin + inhibitor should be similar. In addition, a statistical difference in bioluminescence between luciferin only and luciferin + inhibitor can be captured ex vivo.
23. Each animal serves as its own control. For example, the production of bioluminescence with luciferin only by animal A is X, and the production of bioluminescence with luciferin + inhibitor by animal A is Y; the fold signal change (Y/X) can be calculated for each animal and then averaged across multiple animals receiving the same inhibitor.

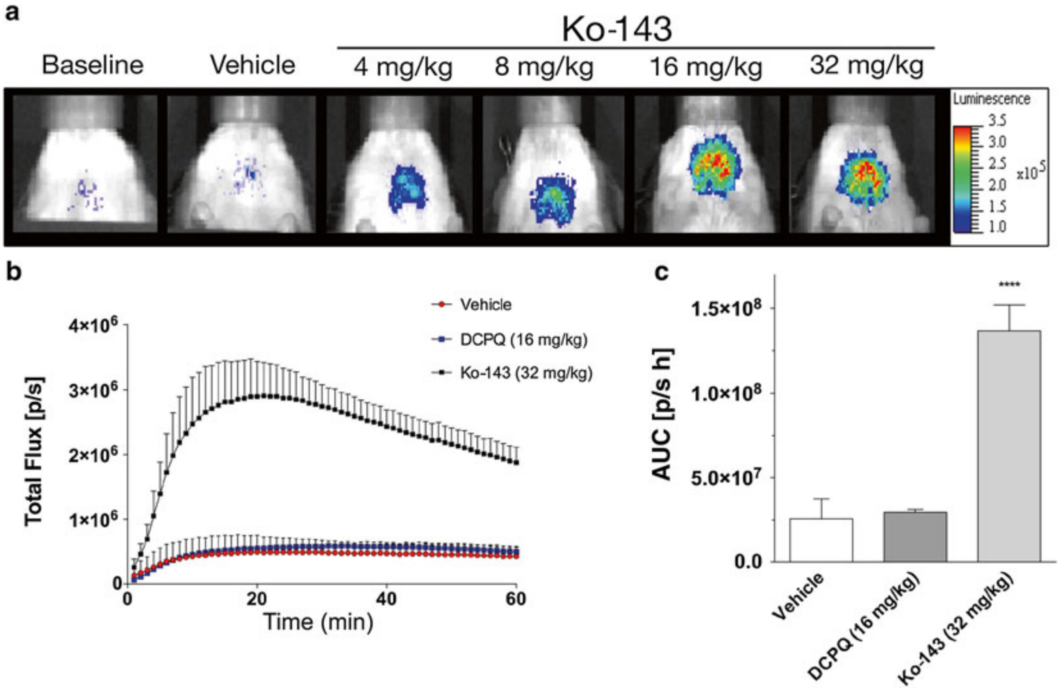

Fig. 3 Ko-143 produces a dose-dependent increase in bioluminescence in vivo. Mice were measured at baseline (receiving luciferin only), and then measured again with vehicle-only or different Ko-143 concentrations prior to receiving luciferin. (**a**) Representative pseudo-colored photon-count images of bioluminescence measurements from the same region of interest (ROI) and animal under different experimental conditions. (**b**) Analyses of the dynamic total flux (photons/s), also referred to as the time-activity curve, from the ROI (brain region) measured at 1-min intervals for 60 min after D-Luciferin administration. Mice were administered either vehicle, DCPQ (P-gp inhibitor) or Ko-143 before D-Luciferin. Data represent means ± SD of four experiments ($n = 4$). The area under the curve (AUC) can be calculated from the time-activity-curve. (**c**) Calculated AUC (photon/s h) for each of the conditions are displayed. Data represent means ± SD of four experiments (****$P < 0.0001$)

24. Further, a control animal (luciferin without inhibitor) should be utilized in each experimental protocol to act as an indicator of potential confounding factors. For example, on Day 1 the production of bioluminescence with luciferin only is X by animal B, on Day 2 this is repeated and the production of bioluminescence is Z by animal B. The standard variation in signals with luciferin injection is Z/X (<1.1 fold change is ideal), and should be taken into consideration for each run.
25. All datasets should be corrected for background autoluminescence. To accomplish this, a separate region of interest can be drawn outside the targeted region of interest to calculate fluctuations in the background signal. This measurement can be subtracted from the readings during that run.

Acknowledgments

We thank Mr. George Leiman for editorial assistance. This research was supported by the Intramural Research Program of the National Institutes of Health (NIH), National Cancer Institute. Joshua Bakhsheshian is a NIH Medical Research Scholar. The Medical Research Scholars Program is a public–private partnership supported jointly by the NIH and contributions to the Foundation for the NIH from Pfizer, the Leona M. and Harry B. Helmsley Charitable Trust, the Howard Hughes Medical Institute, as well as other private donors (listed at www.fnih.org/work/programs-development/medicalresearch-scholars-program).

References

1. Hartz AM, Bauer B (2010) Regulation of ABC transporters at the blood-brain barrier: new targets for CNS therapy. Mol Interv 10:293–304
2. Zhu L, Ramboz S, Hewitt D, Boring L, Grass DS, Purchio AF (2004) Non-invasive imaging of GFAP expression after neuronal damage in mice. Neurosci Lett 367:210–212
3. Vlaming ML, Lagas JS, Schinkel AH (2009) Physiological and pharmacological roles of ABCG2 (BCRP): recent findings in Abcg2 knockout mice. Adv Drug Deliv Rev 61:14–25
4. Allen JD, Brinkhuis RF, Wijnholds J, Schinkel AH (1999) The mouse Bcrp1/Mxr/Abcp gene: amplification and overexpression in cell lines selected for resistance to topotecan, mitoxantrone, or doxorubicin. Cancer Res 59:4237–4241
5. Bakhsheshian J, Hall MD, Robey RW, Herrmann MA, Chen JQ, Bates SE, Gottesman MM (2013) Overlapping substrate and inhibitor specificity of human and murine ABCG2. Drug Metab Dispos 41:1805–1812
6. Robey RW, Honjo Y, Morisaki K, Nadjem TA, Runge S, Risbood M, Poruchynsly MS, Bates SE (2003) Mutations at amino-acid 482 in the ABCG2 gene affect substrate and antagonist specificity. Br J Cancer 89:1971–1978
7. Bakhsheshian J, Wei BR, Chang KE, Shukla S, Ambudkar SV, Simpson RM, Gottesman MM, Hall MD (2013) Bioluminescent imaging of drug efflux at the blood-brain barrier mediated by the transporter ABCG2. Proc Natl Acad Sci U S A 110:20801–20806
8. Kannan P, John C, Zoghbi SS, Halldin C, Gottesman MM, Innis RB, Hall MD (2009) Imaging the function of P-glycoprotein with radiotracers: pharmacokinetics and in vivo applications. Clin Pharmacol Ther 86:368–377
9. Bignami A, Eng LF, Dahl D, Uyeda CT (1972) Localization of the glial fibrillary acidic protein in astrocytes by immunofluorescence. Brain Res 43:429–435
10. Dickie M (1975) Keeping records in biology of the laboratory Mouse. Dover Publications, New York, NY
11. Bowie LJ (1978) Synthesis of firefly luciferin and structural analogs. Methods Enzymol 57:15–28
12. Allen JD, van Loevezijn A, Lakhai JM, van der Valk M, van Tellingen O, Reid G, Schellens JH, Koomen GJ, Schinkel AH (2002) Potent and specific inhibition of the breast cancer resistance protein multidrug transporter in vitro and in mouse intestine by a novel analogue of fumitremorgin C. Mol Cancer Ther 1:417–425
13. Ozvegy-Laczka C, Hegedus T, Varady G, Ujhelly O, Schuetz JD, Varadi A, Kéri G, Orfi L, Német K, Sarkadi B (2004) High-affinity interaction of tyrosine kinase inhibitors with the ABCG2 multidrug transporter. Mol Pharmacol 65:1485–1495
14. Kannan P, Telu S, Shukla S, Ambudkar SV, Pike VW, Halldin C, Gottesman MM, Innis RB, Hall MD (2011) The "specific" P-glycoprotein inhibitor Tariquidar is also a substrate and an inhibitor for breast cancer resistance protein (BCRP/ABCG2). ACS Chem Neurosci 2:82–89
15. Agarwal S, Sane R, Gallardo JL, Ohlfest JR, Elmquist WF (2010) Distribution of gefitinib to the brain is limited by P-glycoprotein (ABCB1) and breast cancer resistance protein (ABCG2)-mediated active efflux. J Pharmacol Exp Ther 334:147–155

16. Shepard RL, Cao J, Starling JJ, Dantzig AH (2003) Modulation of P-glycoprotein but not MRP1- or BCRP-mediated drug resistance by LY335979. Int J Cancer 103:121–125
17. Manaenko A, Chen H, Kammer J, Zhang JH, Tang J (2011) Comparison Evans Blue injection routes: intravenous versus intraperitoneal, for measurement of blood-brain barrier in a mice hemorrhage model. J Neurosci Methods 195:206–210
18. Morrey JD, Olsen AL, Siddharthan V, Motter NE, Wang H, Taro BS, Chen D, Ruffner D, Hall JO (2008) Increased blood-brain barrier permeability is not a primary determinant for lethality of West Nile virus infection in rodents. J Gen Virol 89:467–473
19. Aswendt M, Adamczak J, Couillard-Despres S, Hoehn M (2013) Boosting bioluminescence neuroimaging: an optimized protocol for brain studies. PLoS One 8:e55662
20. Kadurugamuwa JL, Modi K, Coquoz O, Rice B, Smith S, Contag PR, Purchio T (2005) Reduction of astrogliosis by early treatment of pneumococcal meningitis measured by simultaneous imaging, in vivo, of the pathogen and host response. Infect Immun 73:7836–7843
21. Kanzaki S, Fujioka M, Yasuda A, Shibata S, Nakamura M, Okano HJ, Ogawa K, Okano H (2012) Novel in vivo imaging analysis of an inner ear drug delivery system in mice: comparison of inner ear drug concentrations over time after transtympanic and systemic injections. PLoS One 7:e48480

Chapter 20

Theranostic Imaging of Cancer Gene Therapy

Thillai V. Sekar and Ramasamy Paulmurugan

Abstract

Gene-directed enzyme prodrug therapy (GDEPT) is a promising therapeutic approach for treating cancers of various phenotypes. This strategy is independent of various other chemotherapeutic drugs used for treating cancers where the drugs are mainly designed to target endogenous cellular mechanisms, which are different in various cancer subtypes. In GDEPT an external enzyme, which is different from the cellular proteins, is expressed to convert the injected prodrug in to a toxic metabolite, that normally kill cancer cells express this protein. Theranostic imaging is an approach used to directly monitor the expression of these gene therapy enzymes while evaluating therapeutic effect. We recently developed a dual-GDEPT system where we combined mutant human herpes simplex thymidine kinase (HSV1sr39TK) and *E. coli* nitroreductase (NTR) enzyme, to improve therapeutic efficiency of cancer gene therapy by simultaneously injecting two prodrugs at a lower dose. In this approach we use two different prodrugs such as ganciclovir (GCV) and CB1954 to target two different cellular mechanisms to kill cancer cells. The developed dual GDEPT system was highly efficacious than that of either of the system used independently. In this chapter, we describe the complete protocol involved for in vitro and in vivo imaging of therapeutic cancer gene therapy evaluation.

Key words Bioluminescence, Gene-directed enzyme prodrug therapy, Herpes simplex thymidine kinase, In vivo imaging, Firefly luciferase

1 Introduction

Gene-directed enzyme prodrug therapy (GDEPT) is a promising therapeutic strategy, in which enzyme-coding genes are introduced into cancer cells to convert nontoxic prodrugs into active cytotoxic compounds. HSV1-TK/GCV and NTR/CB1954 are two different GDEPT systems currently in different stages of clinical trials [1]. Active GCV compound of HSV1-TK/GCV GDEPT strategy inhibits DNA synthesis in actively dividing cancer cells, whereas, active compound of CB1954 in NTR/CB1954 GDEPT systems exerts cytotoxicity to cells with all stages of cell cycle. Further, these two GDEPT strategies have potential bystander effect and therefore extend the cytotoxicity to the adjacent cells, which are not expressing the GDEPT system and ensure the complete removal of

Sung-Bae Kim (ed.), *Bioluminescence: Methods and Protocols*, Methods in Molecular Biology, vol. 1461,
DOI 10.1007/978-1-4939-3813-1_20, © Springer Science+Business Media New York 2016

tumor. But the limitation is the need of higher level of expression GDEPT enzymes to achieve therapeutic conversion of prodrugs in to active metabolites. Most of the gene therapy systems suffer from poor gene delivery efficiency. Hence to improve therapeutic efficiency with minimum level of gene expression we combined two different therapeutic genes target two different cellular mechanisms to kill cancer cells. The combination of these two GDEPT systems seems highly potential in terms of enhanced therapy and reduction in the amount of prodrugs needed for treatment. We showed the enhanced therapeutic effect of HSV1-TK-NTR fusion dual-GDEPT system in triple negative breast cancer cells such as SUM159 and MDA-MB-231 [2]. Additionally, it was highly efficient against metastatic tumor in mice model [3]. In this chapter we describe the protocol details by which the fusion HSV1-TK-NTR clone was generated and how it was evaluated for cancer gene therapy in cells and human xenograft models in mice. Further, we provide different methods to image and evaluate the expression of this fusion protein in living animals by theranostic imaging.

Theranostic imaging combines treatment of specific disease and evaluating the therapeutic efficacy of particular drug simultaneously [4]. In conventional approach, separate set of agents will be administered for treatment, and thereafter imaging agents or contrasting substances will be given just before diagnostic imaging of particular disease. In GDEPT, therapeutic genes used for treating cancer can be tracked by designing imaging substrates, which monitor therapeutic gene expression while injected prodrugs can treat cancer. Further, when two genes are fused, multiple modality imaging could be used to evaluate the therapeutic efficiency of either of the gene separately or in combination (*see* Fig. 1). Theranostic imaging applications facilitates saving time by evaluating therapeutic efficacy of any therapeutic systems while measuring the expression level of delivered therapeutic genes, as it combines both diagnosis and therapy together. Additionally, personalized therapy in cancer has been widely accepted as a promising treatment strategy. By applying theranostic imaging, personalized therapy could be adopted as it reveals the aftermath of therapy right away. Theranostic imaging also helps to understand the problems of innate immunity while therapeutic evaluation are attempted.

A wide spectrum of therapeutic reporter genes are investigated for the past two decades, and many of them reached clinical trials. Herpes simplex virus 1-thymidine kinase (HSV1-TK), *E. coli* Nitroreductase (NTR), and cytosine deaminase (CD) are the major GDEPT therapeutic reporters investigated in details. Additionally, for the first time we developed a fusion form of two therapeutic genes which hold the potentials of reporter genes and studied them to reveal the enhanced therapeutic efficacy by imaging [3]. Other than these enzyme-based reporters, many transporters and receptors, such as sodium iodide symporter (NIS), somatostatin receptor type 2 has also been investigated as therapeutic reporters [5]. Imaging

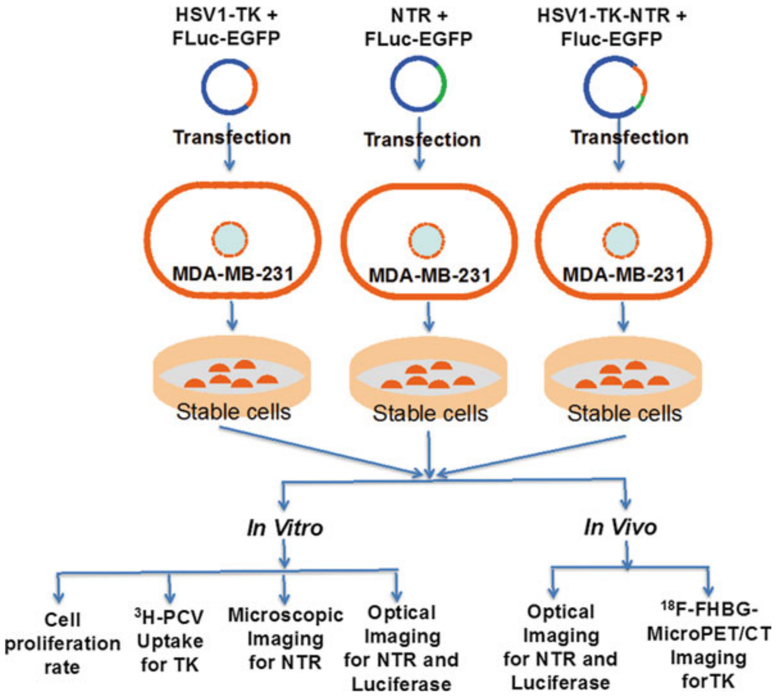
HSV1-TK +
FLuc-EGFP
NTR +
FLuc-EGFP
HSV1-TK-NTR +
Fluc-EGFP
Transfection
Transfection
Transfection
MDA-MB-231
MDA-MB-231
MDA-MB-231
Stable cells
Stable cells
Stable cells
In Vitro
In Vivo
Cell proliferation rate
3H-PCV Uptake for TK
Microscopic Imaging for NTR
Optical Imaging for NTR and Luciferase
Optical Imaging for NTR and Luciferase
18F-FHBG-MicroPET/CT Imaging forTK

Fig. 1 Schematic representation outlines the in vitro and in vivo therapeutic evaluation of HSV1-TK-NTR fusion theranostic gene therapy system evaluated in MDA-MB-231 triple negative breast cancer model

modalities such as PET, MRI, and optical imaging are generally applied to monitor the therapeutic efficacy of gene therapy vectors. HSV1-TK has been thoroughly evaluated using PET imaging. [^{18}F]-Fluoro-3-hydroxymethyl butyl guanine ([^{18}F]-FHBG) and [^{18}F]-fluoro-5-ethyl-1-beta-d-arabinofuranosyluracil ([^{18}F]-FEAU) labeled with fluorine-18 and fluoro-5-iodo-1-beta-d-arabinofuranosyluracil (FIAU) labeled with Iodine-124 are mainly used to image the therapeutic value of HSV1-TK using PET imaging [6]. Alternatively, MRI imaging agents like 5-methyl-5,6-dihydrothymidine (5-MDHT) have been developed and investigated to evaluate HSV1-TK therapeutic gene [7]. Additionally, to evaluate the extent of gene delivery, fusion genes such as GFP-HSV1-TK and FLuc-HSV1-TK has been used to image through optical imaging modalities [8]. Activity NTR could be imaged through fluorescence microscopy by applying CytoCy5S dye, which fluoresce when reduced by NTR enzyme [9]. Altogether, imaging modalities are chosen based on the type of reporter genes to be investigated.

Delivery vehicles are the important component in the successful execution of gene therapy. Plasmid vectors, viral vectors, synthetic liposomes, and nanoparticles have so far been used as vehicles of choice in gene therapy. All of these vehicles have advantages and limitations depending on the gene of interest and target organs involved. Plasmid vectors along with liposome complexes were initially employed for successful execution of gene delivery, but they were not efficient delivery vehicles to deliver genes in animal models. However, plasmid vehicles in assistance with other delivery vehicles such as super paramagnetic iron oxide nanoparticles and functionalized silica nanoparticles have shown promising delivery of nucleic acids and siRNAs [10]. Viral vectors have revolutionized the field of gene therapy by enabling the selective delivery of therapeutic genes in small animals and humans. Viruses specifically attack their host by introducing and stably maintaining their genomes by using the replication machineries of host cells. Manipulations of viral genomes allowed them to be efficiently introduced and stably integrated into host genome without causing any pathogenicity. Many types of viral vectors are developed from viruses' derived different families. Adenovirus, Adeno-associated virus (AAV), and Lentivirus are most common viruses adopted to develop viral vectors. Viral vectors differ with each other in terms of infectivity, efficiency in gene transfer, and maintenance in host cells [11]. Host immunity-associated restriction of viral vectors lead to reduction in the efficiency of gene therapy [12]. Adenoviral vectors are developed from adenoviruses that have nonenveloped double-stranded DNA, not stably integrating into human genomes and will not multiply with host cells. However, efficient gene transfer, high titer production of vectors, and capacity of transducing transgenes of more than 30 kb made them one of the most commonly used viral vectors in gene therapy [13]. Adenoviral vector usage has been put in hold after the death of a man in 1999. Since it caused upper respiratory infections, many patients already have antibodies against adenovirus that limits the usage of adenoviral vectors for gene therapy and vaccination. Further, rapid clearance of adenovirus from blood also hampered the use of adenoviral vectors in gene therapy [14]. Nevertheless recent developments in improving the targeting efficiency and sustained release of viral vectors appear to be promising for novel cancer gene therapy [15]. Adeno-associated viral (AAV) vectors are developed from AAV belongs to *parvoviridae* family. AAV can package and deliver a linear single-stranded DNA genome with the help of a helper virus such as adenovirus and herpesvirus. AAV can infect on both dividing and nondividing host cells, develop minimal host immune response, maintain long-term transgene expressions, and it is nonpathogenic in nature. All these properties made this vector suitable for gene delivery in small animal models and humans [12]. Since the first application of AAVvector to introduce cystic fibrosis transmembrane regulator (CFTR) gene to treat cystic fibrosis in humans [16], many attempts were taken to treat several other diseases. In cancer, AAV mediated delivery of HSV1-TK showed high level of anti-tumor activity [17]. Although a few successful clinical trials are reported, investigations are on to improve the potentiality of AAV for efficient gene delivery.

Lentiviral vectors are other gene delivery vehicles under investigation for gene therapy applications. Lentiviral vectors are developed from single-stranded RNA viruses belong to retroviridae family. Murine leukemia viruses (MLV)-based vectors are the most commonly used lentiviral vectors. Lentiviral vectors are designed by replacing gag, pol, and env genes of MLV genomes with expression cassette containing specific promoter and gene to be transferred and expressed. Therapeutic genes are stably integrated in dividing and quiescent cells with lentiviral vectors. Lentiviral particles are produced by co-transfecting three different vectors such as packaging vector, transfer, and envelope-encoding vectors in HEK293FT cells. Third generation lentiviral vectors are further improved with more safety features in which they replaced tat-independent constitutive promoter in transfer vector [18]. Modern lentiviral vectors are developed further to yield insignificant insertional mutagenesis that was a major setback in γ-retroviral vectors previously used for gene therapy. Lentiviral vectors are used to treat many immune-associated diseases such as X-SCID and melanoma. In cancer immunotherapy, it has been used to induce anti-tumor immune response. With the desirable outcomes it generated in clinics, lentiviral vectors seem a potential delivery vehicle for the successful treatment of major diseases including cancer. Adenovirus, lentivirus, and adeno-associated viral vectors are the important vectors that are used for the gene therapy in clinical trials associated with major diseases. Poxvirus, herpes virus, and alpha viruses are also investigated to introduce alternative gene delivery vectors. Because of side effects they caused, other viral vector may take several years to actively take part in the mainstream gene therapy missions.

2 Materials

2.1 Expression of NTR, HSV1-TK, and HSV1-TK-NTR Fusion

1. Plasmid vectors pcPur-NTR, pcPur-HSV1-TK, and pcPur-HSV1-TK-NTR (*see* Fig. 2 and **Note 1**).
2. MDA-MB-231 cells (ATCC®, Manassas, VA).
3. Dulbecco's modified Eagle's medium (DMEM) with 10% fetal bovine serum and 1% penicillin and streptomycin solution (GIBCO BRL, Frederick, MD).
4. Lipofectamine 2000 and serum free OptiMEM medium (Life Technologies, Grand Island, NY).
5. 37 °C Incubator with 5% CO_2 (Thermo scientific, Sunnyvale, CA).

2.2 Evaluation of NTR Gene Expression

1. CytoCy5S dye (a quenched substrate of NTR enzyme fluoresce upon reduction by NTR enzyme).
2. Fluorescent microscope with Cy5 and/or TxRed filters (Leica Microsystems, Buffalo Grove, IL).

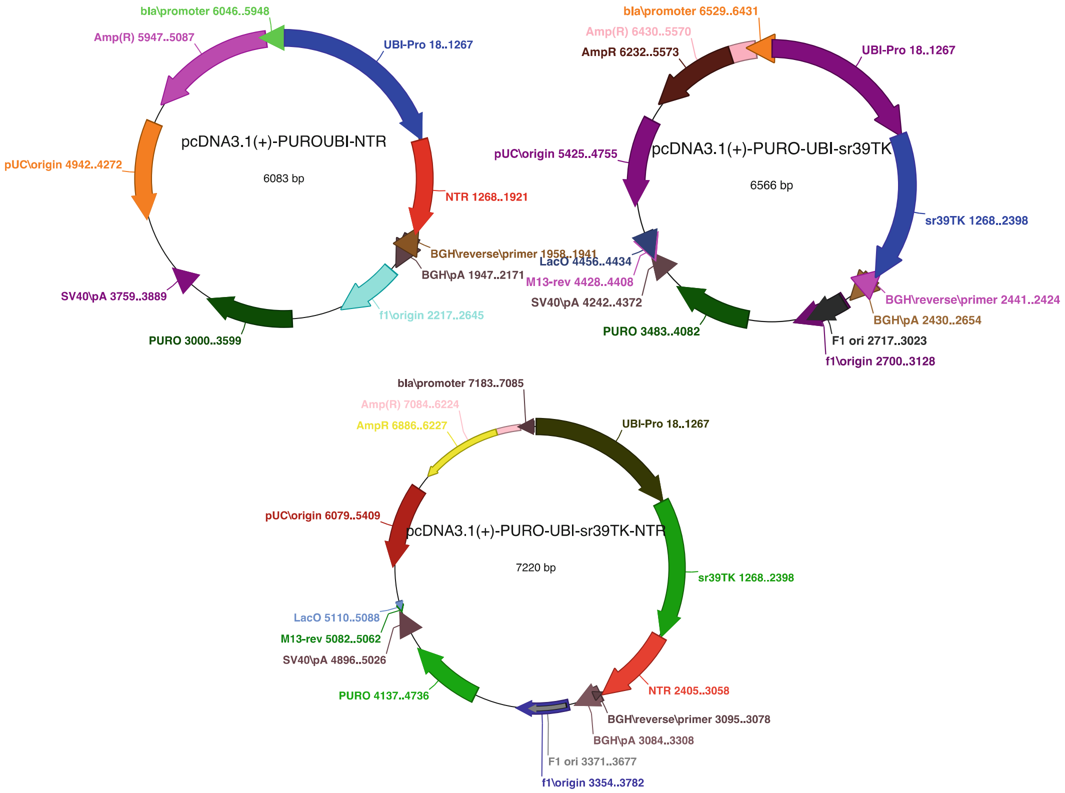
bla\promoter 6046..5948
Amp(R) 5947..5087
UBI-Pro 18..1267
pcDNA3.1(+)-PUROUBI-NTR
6083 bp
pUC\origin 4942..4272
NTR 1268..1921
BGH\reverse\primer 1958..1941
BGH\pA 1947..2171
SV40\pA 3759..3889
f1\origin 2217..2645
PURO 3000..3599
bla\promoter 6529..6431
Amp(R) 6430..5570
AmpR 6232..5573
UBI-Pro 18..1267
pUC\origin 5425..4755
pcDNA3.1(+)-PURO-UBI-sr39TK
6566 bp
sr39TK 1268..2398
LacO 4456..4434
M13-rev 4428..4408
SV40\pA 4242..4372
BGH\reverse\primer 2441..2424
BGH\pA 2430..2654
PURO 3483..4082
F1 ori 2717..3023
f1\origin 2700..3128
bla\promoter 7183..7085
Amp(R) 7084..6224
AmpR 6886..6227
UBI-Pro 18..1267
pUC\origin 6079..5409
pcDNA3.1(+)-PURO-UBI-sr39TK-NTR
7220 bp
sr39TK 1268..2398
LacO 5110..5088
M13-rev 5082..5062
SV40\pA 4896..5026
PURO 4137..4736
NTR 2405..3058
BGH\reverse\primer 3095..3078
BGH\pA 3084..3308
F1 ori 3371..3677
f1\origin 3354..3782

Fig. 2 Plasmid vector maps of NTR, HSV1-TK, and HSV1-TK-NTR fusion theranostic reporter genes express under a constitutive ubiquitin promoter

3. Fluorescent assisted cell sorter (FACS) (BD Biosciences, San Jose, CA).

2.3 ^{3}H-Penciclovir (^{3}H-PCV) Uptake

1. ^{3}H-PCV (specific activity 14.9 Ci/mmol) (Moravek Biochemicals, La Brea, CA, USA).
2. Scintillation fluid (Cytoscint).
3. Scintillation counter (Beckman Coulter, Brea, CA).
4. 0.1 N NaOH.
5. Ice cold PBS (GIBCO BRL, Frederick, MD).
6. MDA-MB-231 cells (ATCC, Manassas, VA).
7. DMEM Medium, FBS, Penicillin, and streptomycin for cell culture (GIBCO BRL, Frederick, MD).
8. Bio-Rad protein assay kit (Bio-Rad, Hercules, CA).

2.4 Therapeutic Evaluation in Cells

1. MDA-MB-231 cells stably expressing NTR or HSV1-TK or HSV1-TK-NTR fusion.
2. Ganciclovir (GCV) and CB1954 (Sigma, St. Louis, MO).

3. A colorimetric assay reagent for cell activity, 3-(4,5-dimethylthiczol-2-yl)-2,5-diphenyltetrazolium bromide (MTT).
4. Infinite-1000 (Tecan-Safire) spectrofluorometer.
5. Nanodrop (Thermo scientific, Sunnyvale, CA).

2.5 Therapeutic Evaluation in Small Animal Model

1. MDA-MB-231 cells stably coexpressing HSV1-TK, NTR, and HSV1-TK-NTR fusion proteins along with firefly luciferase-EGFP (FLuc-EGFP).
2. d-Luciferin (Biosynth, Itasca, IL).
3. Nude mice (nu/nu) (Charles River, San Diego, CA).
4. MicroPET/CT (Inveon, Siemens, Malvern, PA, USA).
5. Optical imaging instrument with cooled CCD camera and living image in vivo imaging software (Perkin Elmer, Waltham, MA).

3 Methods

3.1 Generation of Stable Cells Coexpressing NTR or HSV1-TK or HSV1-TK-NTR Fusion with FLuc-EGFP

1. Plasmids (5 μg each) expressing fusion proteins of NTR or HSV1-TK or HSV1-TK-NTR, and FLuc-EGFP fusion proteins were co-transfected in MDA-MB-231 cells in 10 cm plate plated at 70% confluence 24 h before transfection by using lipofectamine 2000 transfection agent using manufacturer suggested protocol. The cells were incubated at 37 °C with 5% CO_2 for 24 h.
2. 24 h after transfection, cells were trypsinized and plated to a 1:3 subculture ratio in 10 cm plates and puromycin (Life Technologies, Grand Island, NY) was added to a final concentration of 500 ng/mL.
3. The cells were further incubated for 48 h. The dead cells were washed and added fresh medium with 500 ng/mL of puromycin. At this stage more than 80% of cells died. The steps were repeated till no further cell death was observed. The cells were FACS sorted for EGFP expression and CytoCy5S reduction, and plated at low dilution (2000 cells/10 cm plate in 10 mL medium with 500 ng/mL puromycin).
4. The cells were incubated further for 2 weeks with medium change once in every 3 days.
5. At this stage colonies of 2–3 mm in diameter were formed from individual cells.
6. Single colony of transfected cells were selected and expanded by plating first in 12-well plate followed by 10 cm plate.
7. The cells expanded from several colonies that express NTR or HSV1-TK or HSV1-TK-NTR with FLuc-EGFP fusion proteins were tested for the identification of clones that express

equal level of sensor fusion proteins by immunoblot analysis using HSV1-TK antibody and mRNA expression by real time qRT-PCR (*see* **Note 2**).

8. The identified stable clones of cells were used for further in vitro and in vivo therapeutic evaluations.

3.2 Expression and Functional Analysis of NTR Using CytoCy5S Dye

1. CytoCy5S is a quenched substrate of NTR enzyme. When this dye is reduced by the catalytic action of NTR enzyme, the resulting reduced fluorescent product is retained inside the cells.
2. CytoCy5S dye was used to check the expression of NTR in MDA-MB-231 cells stably expressing NTR, and HSV1-TK-NTR proteins.
3. To check the function of NTR, MDA-MB-231 stable cells expressing NTR, and HSV1-TK-NTR were plated in 12 well culture and treated with CytoCy5S dye (1 μg/mL) 24 h after initial plating and incubated further at 37 °C for 2 h.
4. The cells were washed with PBS before viewed in fluorescent microscope under Cy5 or TxRed filter (*see* Fig. 3 and **Note 3**).
5. Alternatively, MDA-MB-231 cells after CytoCy5S treatment can be analyzed with standard FACS analysis in live cell suspension to confirm the expression of NTR in NTR and HSV1-TK-NTR fusion.

3.3 Functional Analysis of HSV1-TK Expression by ^{3}H-PCV Uptake

1. HSV1-TK phosphorylates ^{3}H-PCV and retains phosphorylated ^{3}H-PCV inside the cells; therefore the level of ^{3}H-PCV uptakes by cells indicates the amount of functional HSV1-TK present in cells.
2. ^{3}H-PCV-uptake assay was done to confirm the functionality of HSV1-TK in MDA-MB-231 cells stably expressing HSV1-TK and HSV1-TK-NTR fusion protein.

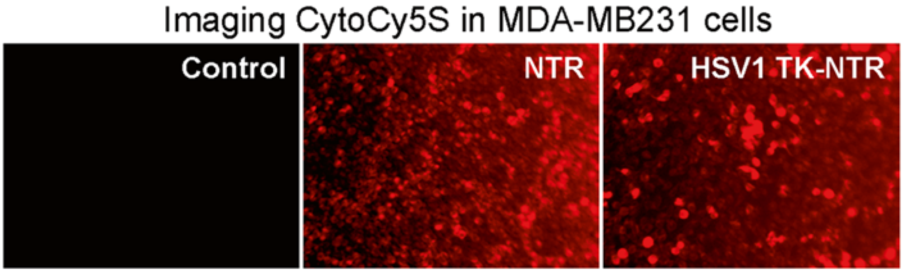

Fig. 3 Microscopic images of MDA-MB-231 stable cells expressing NTR, and HSV1-TK-NTR fusion protein showing the accumulation of reduced CytoCy5S substrate of NTR protein

3. Stable MDA-MB-231 cells expressing HSV1-TK and HSV1-TK-NTR fusion protein were plated to 70–80% confluence in 12-well culture plate.
4. After 24 h incubation at 37 °C and 5% CO_2, ^{3}H-PCV (0.5 µCi/well) was added to each well and incubated further at 37 °C for 3 h.
5. ^{3}H-PCV treated MDA-MB-231 cells were washed twice with PBS after aspirating the medium (The standard protocols described to handle radio-active compounds should be followed).
6. To each well, 1 mL of 0.05 N NaOH was added and kept at RT for 10 min for complete cell lysis.
7. Protein amount from every well was measured using Bio-Rad protein assay kit.
8. Cell lysate from each well was added with 10 mL scintillation fluid (Cytoscint) and the radioactivity was recorded in scintillation counter.
9. The functionality of HSV1-TK was assessed using the percentage conversion of ^{3}H-PCV/mg protein/total count.
10. Appropriate negative control (untransfected cells) should be used to subtract the background activity from endogenous thymidine kinase.

3.4 Therapeutic Evaluation of NTR, HSV1-TK, and HSV1-TK-NTR Fusion in Cells

1. To evaluate the therapeutic efficiency of NTR, HSV1-TK, and HSV1-TK-NTR fusion, MDA-MB-231 stable cells expressing NTR, HSV1-TK, and HSV1-TK-NTR along with FLuc-EGFP fusion protein were used.
2. Stable cells were seeded in 12-well culture plate to a confluence of 60–70% (1.0×10^5 cells/well in 12 well plate and 0.5×10^5 cells/well in 24 well plates).
3. The cells were treated with GCV (1 µg/mL) and CB1954 (10 µM) individually or in combinations 24 h after initial plating of the cells. The medium was changed to 2% FBS at the time of treatment.
4. The cells were analyzed for induced apoptotic cells by PI-staining-based FACS analysis [3], trypan blue exclusion assay and MTT assay [19]. The analysis was performed once in every 24 h for up to 4 days.
5. The ratios of apoptotic cells measured from different assays were compared with controls (untreated stable cells and cell without therapeutic gene and treated with drug combinations) to estimate therapeutic evaluation of different gene therapy vectors.

3.5 Therapeutic Evaluation of NTR, HSV1-TK, and HSV1-TK-NTR Fusion in Subcutaneous and Metastatic Tumor Xenografts in Nude Mice by Optical (Bioluminescence and Fluorescence) and microPET Imaging

3.5.1 Therapeutic Optical Bioluminescence Imaging of NTR, HSV1-TK, and HSV1-TK-NTR Fusion in Nude Mice Model

1. Nude mice handling was done following Institutional Animal Care and Use Committee guidelines.
2. Generated MDA-MB-231 stable cells coexpressing NTR or HSV1-TK or HSV1-TK-NTR with FLuc-EGFP fusion proteins were used for the study.
3. MDA-MB-231 stable cells expressing NTR or HSV1-TK or HSV1-TK-NTR and FLuc-EGFP fusion proteins were trypsinized and collected in PBS on day 1.
4. Cell numbers in PBS suspension were evaluated using hemocytometer.
5. Stable cell suspension in PBS was adjusted to a concentration of 5 millions/50 μL.
6. Stable cell preparation in PBS must be implanted within 2 h after trypsinization (*see* **Note 4**).
7. To implant the stable cells, nude mice with an age group of 4–5 weeks was anesthetized with 2% isofluorane with oxygen flow of 0.8–1 L/min (*see* **Note 5**).
8. Stable cell suspension (5 millions/50 μL) was mixed with 50 μL of growth factor reduced matrigel just before implantation.
9. Cell suspension mix was injected on either side of the lower flank and shoulder regions (five million cells per xenograft) for subcutaneous xenograft model. For metastatic model 0.5×10^5 cells in 200 μL PBS was tail vein injected slowly over 1 min time.
10. Tumor growth was monitored periodically until it grows a volume of approximately 50–60 mm^3 for subcutaneous xenograft model and by bioluminescence imaging for metastatic model. It may take 3–4 weeks for the tumor to grow.
11. After tumor growth, animals were administered with d-Luciferin substrate (3 mg in 100 μL PBS) and optical images were captured with CCD camera 5 min after substrate injection. The same day animals were imaged with microPET/CT system using [^{18}F]-FHBG injection (radioactive substrate for HSV1-TK).
12. After imaging, animals were treated with GCV (40 mg/kg body weight) and CB1954 (40 mg/kg body weight) independently or in combinations to different groups animals for therapeutic evaluation. The animals were treated two times with an interval of 5 days. Prodrugs were treated intraperitoneally with a maximum volume of 250 μL in sterile physiological saline and 10% PEG400 [3].
13. Animals must be optically imaged every day through out the experimental period for the expressed FLuc-EGFP bioluminescence by injecting d-Luciferin (3 mg/animal).
14. Images can be analyzed with Living Image analysis software. For analysis, regions of interest (ROI) were drawn over the area of signal acquired around the xenografts, and the signals

must be defined as maximum photons per second per square centimeter per steradian (p/s/cm^2/sr) (*see* Fig. 4a).

15. FLuc signal indicates the volume of tumor, and therefore reduced FLuc signal in due course of time indicates the enhanced therapeutic efficiency of HSV1-TK-NTR fusion protein.
16. Therapeutic evaluation was compared by the amount of FLuc signal captured in nude mice xenograft model expressing HSV1-TK-NTR fusion with nude mice xenograft model expressing NTR or HSV1-TK alone.

3.5.2 Therapeutic Evaluation of NTR, and HSV1-TK-NTR Fusion by Optical Fluorescence Imaging in Nude Mice Model

1. For fluorescence imaging, same procedure described in Subheading 3.5.2 was followed except the CytoCy5S treatment for monitoring NTR instead of FLuc-EGFP for bioluminescence imaging.
2. MDA-MB-231 stable cells expressing NTR and HSV1-TK-NTR fusion protein pretreated with CytoCy5S dye before implantation to monitor therapeutic effect of tumor implants before they develop in to tumor or post tumor growth by injecting 25 μg of CytoCy5S/animal in 200 μL of PBS by tail 4 h before fluorescence imaging.
3. Nude mice model with implanted cells were subjected to fluorescence imaging immediately after injected with cells.
4. Animals were treated with GCV (40 mg/kg body weight) and CB1954 (40 mg/kg body weight) the same day after imaging.
5. Fluorescence images were captured every day throughout the experimental period.
6. Images were analyzed as described earlier.
7. CytoCy5S fluorescent signal is an indication of NTR enzyme expression at the time of imaging, hence any reduction in CytoCy5S signal is an indication of down-regulation of NTR expression due to cell death (*see* Fig. 4b and **Note 6**).

3.5.3 Therapeutic Evaluation of NTR, and HSV1-TK-NTR Fusion by microPET Imaging in Nude Mice Model

1. Positron Emission Tomography/Computed tomography (PET/CT) imaging was done to evaluate therapeutic potential of HSV1-TK using [^{18}F]-FHBG.
2. MDA-MB-231 stable cells are implanted in nude mice as described above.
3. PET/CT imaging was done before and 9 days after prodrug treatment.
4. Nude mice bearing metastatic xenografts of MDA-MB-231 stable cells were anesthetized with isoflurane, and injected intravenously with 7.4–8.9 MBq of [^{18}F]-FHBG in 200 μL volume.
5. After 3 h, PET images were captured with 5 min static PET scans.

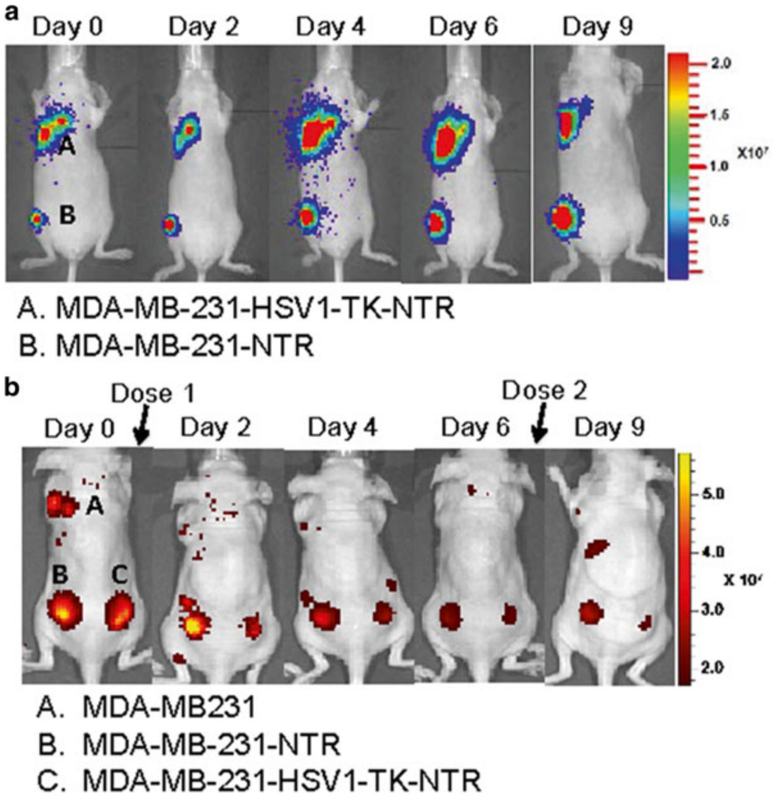
a
Day 0
Day 2
Day 4
Day 6
Day 9
2.0
1.5
X10^{7}
1.0
0.5
A
B
A. MDA-MB-231-HSV1-TK-NTR
B. MDA-MB-231-NTR
b
Dose 1
Dose 2
Day 0
Day 2
Day 4
Day 6
Day 9
5.0
4.0
X 10^{4}
3.0
2.0
A
B
C
A. MDA-MB231
B. MDA-MB-231-NTR
C. MDA-MB-231-HSV1-TK-NTR

Fig. 4 Optical imaging of nude mice models bearing MDA-MB-231 tumor xenograft expressing NTR, and HSV1-TK-NTR fusion protein. (**a**) Optical images of nude mice bearing MDA-MB-231 tumor xenograft model captured in CCD camera after injecting with d-luciferin substrate for the coexpressed FLuc-EGFP over time to monitor tumor growth. (**b**) Fluorescent images acquired from nude mice model pretreated with CytoCy5S dye (NTR substrate) and followed over time after co-treated with GCV (40 mg/kg body weight) and CB1954 (40 mg/kg body weight) combination twice at a interval of 5 days

6. CT scan also was done for anatomic localization.
7. Image analysis was done with IRW software (Siemens).
8. Data was corrected for partial volume effect and spillover using calibration factors obtained from scanning a cylinder containing phantoms of different sizes, and is presented as %ID/g.
9. MicroPET/CT imaging is useful for monitoring metastatic tumor growth in the internal organs with tomographic information while showing therapeutic gene expression (HSV1-TK) by substrate accumulation.
10. We used both bioluminescence and microPET/CT imaging to monitor therapeutic gene expression while monitoring tumor growth (*see* Fig. 5).

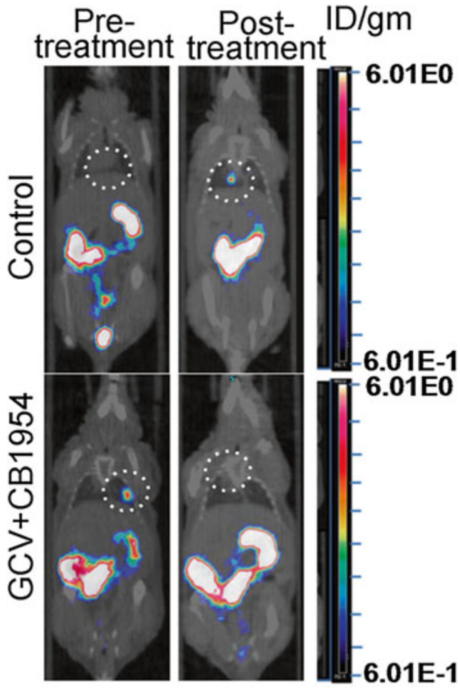

Fig. 5 Micro-PET/CT fusion images of nude mice bearing MDA-MB-231 metastatic xenograft in the lungs. *Top panel* showing images of nude mice before and after treated with vehicle control. The *bottom panel* showing images of animals before and after treated with two doses of GCV and CB1954 combination. Reproduced in part from Sekar et al. with permission from Theranostics, Ivyspring International Publisher Pty Ltd. [1]

4 Notes

1. pcPur vector is a modified version of pcDNA3.1+ vector that express puromycin resistant gene instead of Neomycin.
2. MDA-MB-231 stable cells expressing NTR, HSV1-TK, and HSV1-TK-NTR fusion should be periodically checked with CytoCy5S dye and/or ^{3}H-PCV uptake assays to confirm the maintenance of transgenes expression.
3. Reduced CytoCy5S (a Cy5-labeled quenched substrate) fluoresces at ‘red-shifted’ wavelengths at 638 nm.
4. MDA-MB-231 stable cells should be implanted within 2 h from the time of trypsinization.
5. Nude mice animals should be preferably 4–6 weeks old during the time of tumor implantation.
6. Control tumors also yield autofluorescence signal at early time point due to low threshold of the target signal and it disappears over time.

Acknowledgement

We thank the Department of Radiology and Canary Center at Stanford for their facilities and support. The funding support by National Institutes of Health (NIH grant R01 CA161091 and R21 CA185805 to R.P) is gratefully acknowledged. We also thank Dr. Sanjiv Sam Gambhir, Chairman, Department of Radiology, Stanford University, for his constant support. We gratefully acknowledge the use of the SCi^3 Core Facility, Stanford University.

References

1. Duarte S, Carle G, Faneca H, de Lima MC, Pierrefite-Carle V (2012) Suicide gene therapy in cancer: where do we stand now? Cancer Lett 324:160–170
2. Sekar TV, Foygel K, Willmann JK, Paulmurugan R (2013) Dual-therapeutic reporter genes fusion for enhanced cancer gene therapy and imaging. Gene Ther 20:529–537
3. Sekar TV, Foygel K, Ilovich O, Paulmurugan R (2014) Noninvasive theranostic imaging of HSV1-sr39TK-NTR/GCV-CB1954 dual-prodrug therapy in metastatic lung lesions of MDA-MB-231 triple negative breast cancer in mice. Theranostics 4:460–474
4. Kelkar SS, Reineke TM (2011) Theranostics: combining imaging and therapy. Bioconjug Chem 22:1879–1903
5. Penheiter AR, Russell SJ, Carlson SK (2012) The sodium iodide symporter (NIS) as an imaging reporter for gene, viral, and cell-based therapies. Curr Gene Ther 12:33–47
6. Buursma AR, Rutgers V, Hospers GA, Mulder NH, Vaalburg W, de Vries EF (2006) 18F-FEAU as a radiotracer for herpes simplex virus thymidine kinase gene expression: in-vitro comparison with other PET tracers. Nucl Med Commun 27:25–30
7. Bar-Shir A, Liu G, Greenberg MM, Bulte JW, Gilad AA (2013) Synthesis of a probe for monitoring HSV1-tk reporter gene expression using chemical exchange saturation transfer MRI. Nat Protoc 8:2380–2391
8. Ponomarev V, Doubrovin M, Serganova I, Vider J, Shavrin A, Beresten T, Ivanova A, Ageyeva L, Tourkova V, Balatoni J, Bornmann W, Blasberg R, Gelovani Tjuvajev J (2004) A novel triple-modality reporter gene for whole-body fluorescent, bioluminescent, and nuclear noninvasive imaging. Eur J Nucl Med Mol Imaging 31:740–751
9. Bhaumik S, Sekar TV, Depuy J, Klimash J, Paulmurugan R (2012) Noninvasive optical imaging of nitroreductase gene-directed enzyme prodrug therapy system in living animals. Gene Ther 19:295–302
10. Jin S, Leach JC, Ye K (2009) Nanoparticle-mediated gene delivery. Methods Mol Biol 544:547–557
11. Howarth JL, Lee YB, Uney JB (2010) Using viral vectors as gene transfer tools (Cell Biology and Toxicology Special Issue: ETCS-UK 1 day meeting on genetic manipulation of cells). Cell Biol Toxicol 26:1–20
12. Daya S, Berns KI (2008) Gene therapy using adeno-associated virus vectors. Clin Microbiol Rev 21:583–593
13. Volpers C, Kochanek S (2004) Adenoviral vectors for gene transfer and therapy. J Gene Med 6:S164–S171
14. Green NK, Seymour LW (2002) Adenoviral vectors: systemic delivery and tumor targeting. Cancer Gene Ther 9:1036–1042
15. Kasala D, Choi JW, Kim SW, Yun CO (2014) Utilizing adenovirus vectors for gene delivery in cancer. Expert Opin Drug Deliv 11:379–392
16. Flotte T, Carter B, Conrad C, Guggino W, Reynolds T, Rosenstein B, Taylor G, Walden S, Wetzel R (1996) A phase I study of an adeno-associated virus-CFTR gene vector in adult CF patients with mild lung disease. Human Gene Ther 7:1145–1159
17. Pan JG, Zhou X, Luo R, Han RF (2012) The adeno-associated virus-mediated HSV-TK/GCV suicide system: a potential strategy for the treatment of bladder carcinoma. Med Oncol 29:1938–1947
18. Escors D, Breckpot K (2010) Lentiviral vectors in gene therapy: their current status and future potential. Arch Immunol Ther Exp (Warsz) 58:107–119
19. Devulapally R, Sekar NM, Sekar TV, Foygel K, Massoud TF, Willmann JK, Paulmurugan R (2015) Polymer nanoparticles mediated codelivery of antimiR-10b and antimiR-21 for achieving triple negative breast cancer therapy. ACS Nano 9:2290–2302

Chapter 21

Development of a Multicolor Bioluminescence Imaging Platform to Simultaneously Investigate Transcription Factor NF-κB Signaling and Apoptosis

Vicky T. Knol-Blankevoort, Laura Mezzanotte, Martijn J.W.E. Rabelink, Clemens W.G.M. Löwik, and Eric L. Kaijzel

Abstract

Here we describe a novel multicolor bioluminescent imaging platform that enables us to simultaneously investigate transcription factor nuclear factor-κB (NF-κB) signalling and apoptosis. We genetically modified the human breast cancer cell line MDA-MB-231 to express green, red, and blue light-emitting luciferases to monitor cell number and viability, NF-κB promoter activity, and to enable specific cell sorting and detection, respectively. Z-DEVD-animoluciferin, the pro-luciferin substrate, was used to determine apoptotic caspase 3/7 activity. We used this multicolored cell line for the in vitro evaluation of natural compounds and in vivo optical imaging of tumor necrosis factor (TNFα)-induced NF-κB activation (Mezzanotte et al., PLoS One 9:e85550, 2014).

Key words Multicolor, Bioluminescence, TNFα, NF-κB, Apoptosis, Breast cancer, *Gaussia*

1 Introduction

In the last decades bioluminescent reporters have been employed extensively for the development of cell-based assays and in vivo imaging [1–10]. Multicolor bioluminescence systems allow high detectability in in vitro as well as in in vivo settings. In particular, the combined use of d-Luciferin-dependent luciferases with different peak emission wavelengths ('multicolored' luciferases) [11], expanded the potential of cell-based assays and in vivo imaging.

New imaging tools will help in understanding the molecular mechanisms that lead to cancer progression and metastasis as well as resistance to chemotherapy.

The Nuclear Factor-κB (NF-κB) signal transduction pathway has been identified as a key pathway in inflammation-associated cancer, in cell transformation and tumor growth and in cell invasion and metastasis, especially in breast cancer [12–14].

Sung-Bae Kim (ed.), *Bioluminescence: Methods and Protocols*, Methods in Molecular Biology, vol. 1461,
DOI 10.1007/978-1-4939-3813-1_21, © Springer Science+Business Media New York 2016

NF-κB inhibitors can be used as adjuvants along with chemo- and radiotherapy or for cancer prevention. Different natural compounds have been discovered that directly or indirectly suppress NF-κB activity and they have been examined for chemoprevention, chemosensitization, or adjuvants [15–20].

Here we show how we develop and validate a new triple-colored cancer cell system. This system is generated by lentiviral transduction of the human breast cancer cell line MDA-MB-231 with different bioluminescent reporters. We used the click beetle green 99 (CBG99) luciferase to monitor cell vitality and the red mutant of firefly luciferase (PpyRE9) to monitor NF-κB promoter activity. The blue extGLuc, a transmembrane form of *Gaussia* luciferase, (GLuc), was used as a reporter for in vitro cell sorting and ex vivo analysis. In addition, noninvasive imaging of apoptosis in luciferase expressing cells, both in vitro and in vivo was possible by using the luciferase pro-substrate ZDEVD-aminoluciferin, containing the DEVD tetrapeptide sequence recognized by caspase 3 and 7 [21].

2 Materials

2.1 Cell Culture

1. MDA-MB-231 human breast cancer cells (ATCC number HTB-26TM) grown at 37 °C in a 5% CO_2 humidified incubator.
2. Dulbecco's modified Eagle's medium (Invitrogen, Grand Island, USA) supplemented with 10% fetal bovine serum (Sigma, St. Louis, USA), 100 U/mL penicillin (Sigma) and 0.1 mg/mL streptomycin (Sigma).
3. Human recombinant TNFα (Sigma, St. Louis, USA).

2.2 Lentiviral Vectors Construction

1. pGL3-CBG99 (Promega, Madison, WI, USA).
2. pGL4.32 [luc2P/ NF-κB -RE/Hygro] (Promega, Madison, WI, USA).
3. restriction enzymes *Nhe*I, *Xba*I, *Kpn*I, and *Nco*I (New England Biolabs inc, MA, USA).
4. NEBuffer 2.1 and NEBuffer 1.1 (New England Biolabs inc, MA, USA).
5. T4 DNA Polymerase (New England Biolabs inc, MA, USA).
6. Taq polymerase (Promega, Madison, WI, USA).
7. pRRL-PGK (gift from Prof. R. Hoeben [22]).
8. pGex-6p-2-PpyRE9 (gift from Prof. B. Branchini [7, 23]).
9. pNFAT vector (gift from Prof. M.R. Van de Brink [24]).
10. Forward primer with a *Nco*I restriction site 5′-GGCGGCCATGGAAGACGCCAAAAACATAAAG-3′.
11. Reverse primer with *Xba*I restriction site 5′-GTCTAGATTAGATTTTCCGCCCTTCTTGGCCTT-3′.

2.3 Cell Transduction/Selection

1. HEK293T cells (ATCC® CRL-1573).
2. T-175 flask (Sigma, St. Louis, USA).
3. Dulbecco's modified Eagle's medium (Life Technologies) high glucose (4.5 g/L) supplemented with 10% fetal bovine serum (Sigma, St. Louis, USA).
4. Polyethyleneimine (PEI; 1 mg/mL, pH 7.4) (Polysciences, Eppelheim, Germany).
5. 1 M HCl.
6. 0.22-μm cellulose acetate filter (Sigma, St. Louis, USA).
7. pCMV-VSVG vector.
8. pMDLg-RRE (gag/pol) vector.
9. pRSV-REV vector.
10. Opti-MEM (Life Technologies).
11. 37 °C/5% CO_2 incubator.
12. Sterile low-protein binding 0.45-μm filter (VWR international B.V., Amsterdam, Netherlands).
13. p24 Elisa 2.0 kit (ZeptoMetrix Corporation, New York, USA).

2.4 Fluorescence Activated Cell Sorting (FACS)

1. Polyclonal anti-GLuc antibody (Nanolight tech., Pinetop, AZ, USA).
2. Secondary antibody fluorescent labelled: Alexa 488 (Invitrogen, Grand Island, USA).
3. FACS buffer: PBS + 0, 5% BSA.

2.5 MTS Assay

1. 96-well plates (Greiner bio-one, Alphen a/d Rijn, Netherlands).
2. Puromycin (Invitrogen, Grand Island, USA).
3. CellTiter 96H AQueous One Solution Cell Proliferation Assay (Promega, Madison, WI, USA).
4. ELISA microplate reader (VersaMax Molecular Devices, Sunnyvale, CA, USA).

2.6 Luciferase Assay

1. 96-well dark plates (Greiner bio-one, Alphen a/d Rijn, Netherlands).
2. Puromycin (Invitrogen, Grand Island, USA).
3. Phosphate buffered saline (PBS) pH 7, 4.
4. Reporter lysis buffer (Promega, Madison, WI, USA).
5. SpectraMax L luminescence microplate reader (Molecular Devices, Sunnyvale, CA, USA).

2.7 Reporter Gene Activity Assay

1. 96-well dark plates (Greiner, bio-one, Alphen a/d Rijn, Netherlands).
2. Tumor necrosis factor α (TNFα) 10 ng/mL (Sigma, St. Louis, USA).

3. Compounds to validate the cell line.
4. D-Luciferin (Synchem, Elk Grove Village, IL USA) final concentration of 0, 5 mM.
5. IVIS® Spectrum/Living Image Software 4.0 (Caliper, Alameda, CA, USA).
6. Coelenterazine (Nanolight tech., Pinetop, AZ, USA) final concentration of 20 mM.

2.8 Western Blot Analysis

1. Blotbuffer: prepared from 10× concentrated solution Bio-Rad 100 mL blotbuffer 10× + 200 mL MeOH + 700 mL aquadest.
2. PBS pH 7, 4.
3. PBST: PBS + 0.1 % Tween 20.
4. Elk milk powder (Campina).
5. Blockbuffer: 2 % (w/v) protifar in PBST (20 mL PBST + 400 mg protifar).
6. SuperSignal chemiluminescent substrate (Pierce, Bleiswijk, Netherlands).
7. Nuclear and Cytoplasmic extraction reagents (Thermo Scientific, Rockford, USA).
8. Pierce BCA protein assay kit (Thermo Scientific, Rockford, USA).
9. Nitrocellulose membrane (Sigma, St. Louis, USA).
10. anti-P65 polyclonal antibody (Cell Signaling Technology, Danvers, USA).
11. GAPDH antibody (Cell Signaling Technology).
12. IVIS Spectrum/ Living Image Software 4.0 (Caliper, Alameda, CA, USA).

2.9 Caspase 3/7 Activity Assay

1. Triple-colored MDA-MB-231 cells.
2. 96-well dark plates (Greiner bio-one, Alphen a/d Rijn, Netherlands).
3. D-Luciferin (Synchem, Elk Grove Village, IL USA).
4. Caspase-Glo 3/7 Assay (Promega, Madison, WI, USA).

2.10 Xenograft Model

1. Triple-colored MDA-MB-231 cells.
2. female athymic (BALB/c nu/nu) mice (6 weeks old).
3. D-Luciferin (Synchem, Elk Grove Village, IL USA).

2.11 Induction of NF-kB

1. Triple-colored MDA-MB-231 xenograft model.
2. PBS pH 7, 4.
3. TNFα (20 mg/kg) (Sigma, St. Louis, USA).
4. Natural compound to validate the cell line.
5. Celastrol (Cayman, Michigan, USA).

2.12 Induction of Apoptosis

1. Triple-colored MDA-MB-231 xenograft model.
2. Natural compound to validate the cell line.
3. Z-DEVD aminoluciferin (50 mg/kg) Promega, Madison, WI, USA).

2.13 Immunohistochemistry

1. Triple-colored MDA-MB-231 xenograft tumors.
2. 4 % formaldehyde.
3. Ethanol (100, 96, 70 %).
4. Butanol.
5. Paraffin.
6. Starfrost glass slides (Knittel glass, Braunschweig, Germany).
7. Polyclonal rabbit anti-GLuc antibody (Nanolight tech., Pinetop, AZ, USA).
8. Anti-rabbit–FITC antibody (Santa Cruz, Dallas, Texas, USA).

3 Methods

3.1 Ethical Statement

1. Review and approval of the Bioethics Committee of Leiden University, The Netherlands for animal experiments.
2. All animals received human care in compliance with the "Code of Practice Use of Laboratory Animals in Cancer Research" (Inspectie W&V, July 1999).

3.2 Cell Culture

1. Maintain MDA-MB-231 human breast cancer cells in Dulbecco's modified Eagle's medium supplemented with 10 % fetal bovine serum, 100 U/mL penicillin and 0.1 mg/mL streptomycin.
2. Grow the cells at 37 °C in a 5 % CO_2 humidified incubator.

3.3 Lentiviral Vectors Construction

1. To create the pRRL-PGKCBG99: excise the click beetle green 99 (CBG99) luciferase gene with *Nhe*I and *Xba*I from pGL3-CBG99 and clone in the MCS of pRRL-PGK.
2. Construct the bicistronic pLM-NF-κB PpyRE9 vector by: amplifying the PpyRE9 luciferase gene from the vector pGex-6p-2-PpyRE9 using the following primers: forward primer with a *Nco*I restriction site 5′-GGCGGCCATGGAAGACGCCAAAAACATAAAG-3′ and reverse primer 5′-GTCTAGATTAGATTTTCCGCCCTTCT TGGCCTT-3′ with a *Xba*I restriction site.
3. Clone the PpyRE9 luciferase gene by replacing the luc gene in the pGL3 control vector to create the pGL3-PpyRE9 vector using the *Nco*I and *Xba*I restriction sites.

4. To create the pGL3-NF-κB PpyRE9 vector: Excise NF-κB promoter responsive elements from the vector pGL4.32 [*luc2*P/NF-κB-RE/Hygro] with *Kpn*I and *Nco*I and clone into the pGL3-PpyRE9 vector.
5. Excise the NF-κB PpyRE9 cassette with *Kpn*I and *Xba*I restriction enzymes, blunt and clone into the bicistronic bidirectional pNFAT vector in which the NFAT-CBRed cassette had been deleted.
6. Check the resulting bicistronic lentiviral vector (named pLM-NF-κB PpyRE9) for orientation. The new plasmid contains the original GLuc under the control of PGK promoter in one direction and the NF-κB PpyRE9 cassette in the other direction (*see* **Note 1**).

3.4 Cell Transduction and Selection

Produce self-inactivating lentiviruses:

Day –1: Plate cells

HEK293T cells are usually split in a ratio of 1:15 twice a week. Seed cells from one 10 cm^2 dish to one T-175 flask. The next day the confluency should be 60–70%.

Day 0: Co-transfection of HEK293T cells, PEI method

Refresh medium (20 mL/flask) prior to transfection. Perform transient transfection on HEK293T cells by overnight PEI method:

Tube 1

pCMV-VSVG	7.5 μg
pMDLg-RRE (gag/pol)	11.4 μg
pRSV-REV	5.4 μg
transfer vector plasmid	13.7 μg

- Mix DNA plasmids;
- Add Opti-MEM to a total volume of 1000 μL.

Tube 2

- 3 μL PEI (1 mg/mL)/μg DNA (*see* **Note 2**).
- Add Opti-MEM to a total volume of 1000 μL.

Slowly add tube 1 to tube 2, while mixing. After 10 min, this can be added to the medium of flasks containing HEK293T cells. Incubate overnight in 37 °C/5% CO_2 incubator.

Day 1: Refresh medium

Remove the old medium, add 16 mL of fresh medium to the cells in each T175 flask and put the cells back into the incubator (*see* **Note 3**).

Day 2: Harvest virus

48 h post transfection virus-containing supernatant can be harvested by collecting medium to a sterile 50-mL tube. To reduce blocking of the filter, spin down (5 min; ~700 × *g*; table centrifuge) cell debris from supernatant. Add 16 mL of fresh medium to the cells. This provides the possibility to do a second round of harvesting within 1 or 2 days, with almost the same viral yield as 48 h post transfection.

Day 3: Harvest virus, p24 ELISA

Harvest virus as described above. Filter the collected medium (48 and 72 h post transfection) with the lentivirus through a sterile low-protein binding 0.45-μm filter. After filtration, aliquot virus in tubes of 10 mL (or less) each, and store at −80 °C (*see* **Note 4**). Additionally store a small aliquot (volume 10 μL), to be used for titration with a p24 ELISA assay. The p24 ELISA assay is described in the manual of the kit: http://www.zeptometrix.com/docs/PI0801008.pdf. For the standard curve make eight concentrations: 256, 128, 64, 32, 16, 8, 4, and 2 pg/mL from HIV-1 p24 antigen standard (2.5 ng/mL). The dilution factor of the virus depends on the origin of the virus sample (*see* **Note 5**). For some experiments (high moi; serum free) it might be necessary to concentrate viral stocks (10–200 fold) by ultracentrifugation.

Day 4: Transduction cells.

Transduce MDA-MB-231 cells in sequential steps (see **Note 6**). Firstly, transduce MDA-MB-231 cell with a lentivirus expressing pRRL-PGKCBG99 and select by limiting dilution methods. Secondly, transduce the obtained CBG99 luciferase positive cell line with the pLM-NF-κB PpyRE9 lentivirus and FACS-sorted using a polyclonal anti-GLuc antibody. This leads to the production of a triple-colored MDA-MB-231 cell line as a tool for monitoring vitality and NF-κB promoter activity as depicted in Fig. 1.

3.5 In Vitro Assay MTS and Luciferase Assay

1. Seed triple-colored MDA-MB-231 cells in 96-well plates.
2. 24 h later, treat with different concentrations of puromycin (0.1–10 μg/mL), a known selective antibiotic toxic to eukaryotic cells.
3. After another 24 h of incubation, divide plates for the different analyses.
4. To assess cell viability: use an MTS colorimetric assay using CellTiter 96®AQ$_{\text{ueous}}$ One Solution Cell Proliferation Assay according to manufacturers' description. In brief, add MTS solution to the medium for 2 h after which the absorbance was measured at 490 nm with an ELISA microplate reader.
5. To measure the luciferase activity biochemically: wash cells with PBS, harvest in reporter lysis buffer and assay for luciferase activity with a luminometer.
6. Make the cell viability curve for both MTS -and luciferase assays.

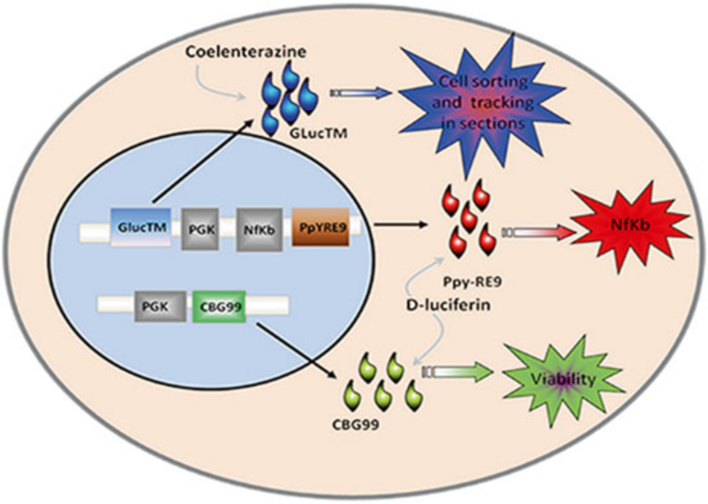

Fig. 1 Cartoon of the multicolor MDA-MB-231 cell line. Lentiviral constructs are integrated in the cell genome and lead to the expression of PpyRE9 luciferase upon activation of NF-κB promoter, the constitutive expression of GLuc and the constitutive expression of CBG99 luciferase that serves as availability control reporter

3.6 Reporter Gene Activity Assay

1. Seed triple-colored MDA-MB-231 cells in 96-well dark plates at a concentration of 5000 cells/well, 24 h prior treatment.
2. Validate the cell line for NF-κB responses by adding TNFα (10 ng/mL) for different time points of incubation (ranging from 2 to 72 h).
3. After establishing the optimal period of TNFα stimulation, investigate the effect of the plant-derived compounds on TNFα-induced NF-κB activation in the MDA-MB-231 cells.

   Treat cells with medium (negative control), TNFα (10 ng/mL, positive control), TNFα together with: celastrol (0.1–2.5 μM), followed by another 24 h of incubation.
4. Determine luciferase activity as follows:
   (a) Replace the medium in plate with PBS and add d-Luciferin at a final concentration of 0.5 mM (*see* **Note** 7).
   (b) Measure luciferase activity using an IVIS Spectrum. Keep the instrument stage at 37 °C and imaging set up is FOV C.
   (c) Measure light output using an open filter and a series of band pass filter (20 nm) ranging from 500 to 700 nm each for 5 s, 5 min after substrate addition to live cells.
   (d) Express all the data in photon-flux and analyze with Living Image Software 4.0.

(e) Apply a spectral unmixing algorithm to the images to separate the red and green luciferases. Select for the region of interest and apply the unmixing algorithm using the Living Image Software 4.0. Select for plate or mouse and indicate that two components need to be separated. In the option section, select a low pass (LP) filter at 560 nM for better separation of the red signal.

(f) Calculate data depicting multiple region of interests (ROIs) corresponding to the well areas of the 96-well black plates in the images corresponding to the unmixing results. CBG luciferase activity in the green spectrum (peak emission wavelength 540 nm) has been used as an indication of cell vitality and the PpyRE9 luciferase activity in the red spectrum (peak emission wavelength 620 nm) as an indication of promoter activity.

(g) Carry out the measurement of extGLuc expression using native coelenterazine at a final concentration of 20 μM.

Celastrol was shown to have an inhibitory effect on TNFα-induced NF-κB signaling in MDA-MB-231 cells (*see* Fig. 2).

3.7 Western Blot Analysis of P65 in Nuclear Extracts

1. To confirm the results of the reporter gene assays a western blot was done to analyse NF-κB activity in the nuclear extracts.
2. Seed MDA-MB-231 cells (1×10^6 cells/well) in 6-well plates for 24 h, and treat with medium (negative control), TNFα (10 ng/mL positive control), or TNFα (10 ng/mL) with celastrol (0.1, 0.5, and 1 μM) or betulinic acid (0.5, 1, 10, and 30 μM).
3. After 24 h of treatment, collect cells and make nuclear extracts using Nuclear and Cytoplasmic extraction reagents.
4. Determine total amount of protein of each sample by a Pierce BCA protein assay kit.
5. Apply 15 μg of nuclear extracts to a 10% SDS-PAGE and transfer onto a nitrocellulose membrane.
6. Block in 2% Protifar milk powder for 1 h at RT.
7. After washing, incubate the membrane with an anti-P65 polyclonal antibody in TPBS 1:1000 dilutions overnight at 4 °C. Use a GAPDH antibody to correct for the amount of total protein.
8. Wash the blots, expose to an HRP-conjugated secondary antibody for 1 h at RT, and detect using enhanced chemiluminescence (ECL) reagents.
9. Perform the detection of ECL signals with the IVIS Spectrum and quantification of bands using Living Image Software 4.0.

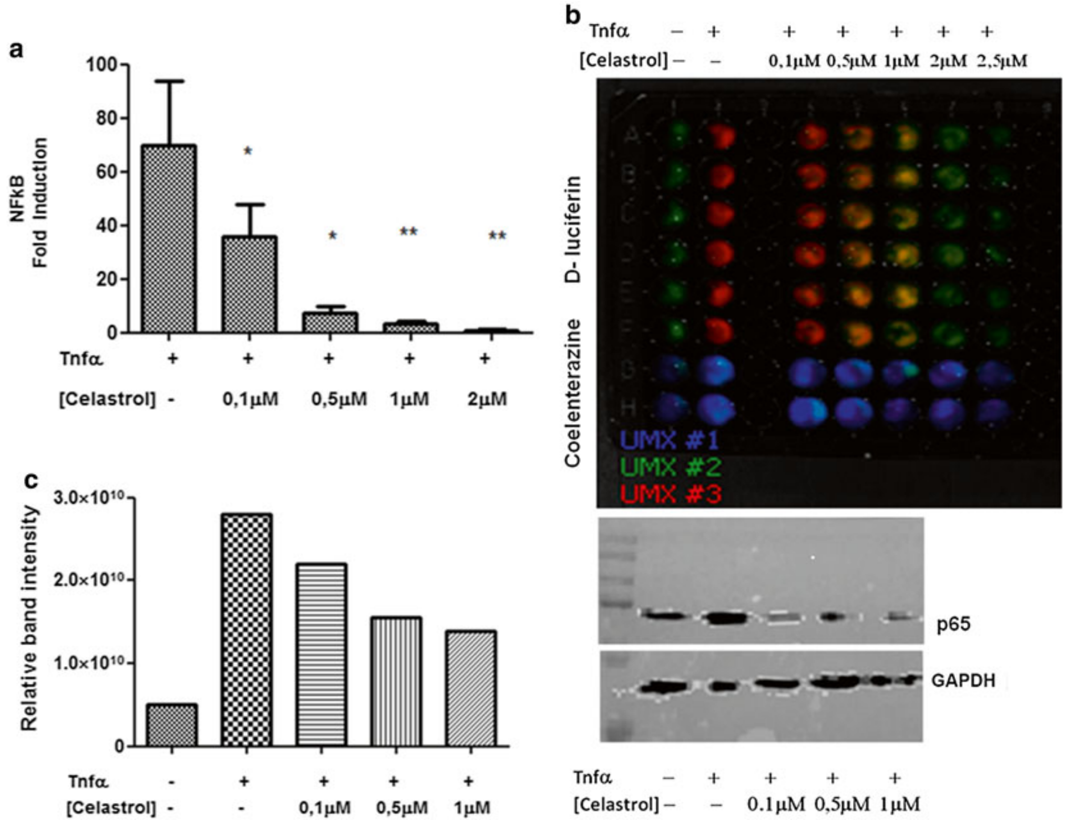

Fig. 2 (**a**) Graph representing the decrease in fold NF-κB induction in MDA-MB-231 cells using celastrol by the multicolor assay (**p* value < 0.05; ***p* value < 0.01). (**b**) Composite image of the unmixed spectrum of luciferases: *green signals* represent CBG99 emission, *red signals* represent PpyRE9 emission spectrum and blue signals represent ExtGluc expression in control cells (first column) and cells treated with TNFα in combination with increasing concentrations of celastrol (0.1–3 μM). (**c**) *Left*: graph reporting the relative band intensity of p65 protein from the nuclear extract of control sample and samples treated with TNFα (10 ng/mL) or TNFα + celastrol (0.1 μM; 0.5 and 1 μM). *Right*: p65 protein detection in nuclear extracts and GAPDH used as control protein (figure adapted from Mezzanotte L et al. [1])

3.8 Caspase 3/7 Activity Apoptosis Assay

1. Seed triple-colored MDA-MB-231 cells in a 96-well dark plate for 24 h to attach.
2. Treat the cells with medium (negative control), or chemopreventive natural compounds, followed by another 4 h or 24 h of incubation (*see* **Note 8**).
3. Divide the rows of cells to estimate the effect of the different compounds on cell viability and apoptosis.
4. Establish the cell viability by the addition of d-Luciferin to live cells.
5. Determine the caspase 3/7 activity by adding the luciferase prosubstrate, Z-DEVD-aminoluciferin of a Caspase-Glo 3/7 Assay.

6. Divide the bioluminescent signals generated by the addition of the Z-DEVD-aminoluciferin by the signals generated by the CBG99 luciferase upon addition of d-Luciferin in order to correct the data set for the amount of viable cells.

3.9 In Vivo Assays

3.9.1 Triple-Colored MDA-MB-231 Xenograft Model

1. Implant triple-colored MDA-MB-231 cells (2×10^6) in the mammary fat pads of female athymic (BALB/c nu/nu) mice (*see* **Note 9**).
2. Image Mice weekly. Tumors reached a palpable size (around 150 mm^3) after 2–3 weeks.
3. Inject d-Luciferin (150 mg/kg) intraperitoneally and image after 5 min using a FOV C and a 30 s acquisition time for both open filter and band pass filters acquisition (*see* **Note 10**).

3.9.2 Induction of NF-κB

1. When tumor growth reached an exponential increase in CBG luciferase signals, randomize mice in three groups.
2. A control group received an intratumoral injection of PBS and an intravenous injection of PBS.
3. The second and third group TNFα (20 μg/kg) was injected intravenously in the second and third group. Next, these mice were given an intratumoral injection of celastrol (2 mg/kg) or PBS. Mice were imaged after the injection and after 24 h with the same settings. Evaluation of NF-κB induction was performed by comparison of images before and 24 h after treatment.

Figure 3 shows the In vivo monitoring of NF-κB signaling by bioluminescence imaging.

3.9.3 Induction of Apoptosis

1. To measure induction of apoptosis, grow triple-colored MDA-MB-231 tumors as described above, intratumorally inject with celastrol and after 4 and 24 h inject Z-DEVD-aminoluciferin (50 mg/kg) intraperitoneally.
2. Measure the activation of caspase 3/7, 20 min after injection of substrate using an open filter and an exposure time of 30 s.

Effects of the chemopreventive natural compound celastrol on caspase 3/7-mediated apoptosis were demonstrated both in vitro and in vivo (*see* Fig. 4).

3.9.4 Immunohistochemistry

1. Remove tumors surgically, fix in 4% formaldehyde overnight and further process for paraffin embedment.
2. Make sections (5 μm) using a standard microtome and place on glass slides.
3. Use a polyclonal rabbit anti-GLuc antibody and an anti-rabbit-FITC antibody to reveal the presence of GLuc positive tumor cells.

3.9.5 Statistical Analysis

1. Perform each in vitro experiment in triplicate with six replicate samples per data point.
2. A Student's *t*-test has been applied to determine statistically significant differences in the promoter activity between positive controls and treated conditions. For in vivo experiments wherein more than two groups were compared, one-way ANOVA followed by Tukey's post-hoc test was used to determine significant differences among treated groups.

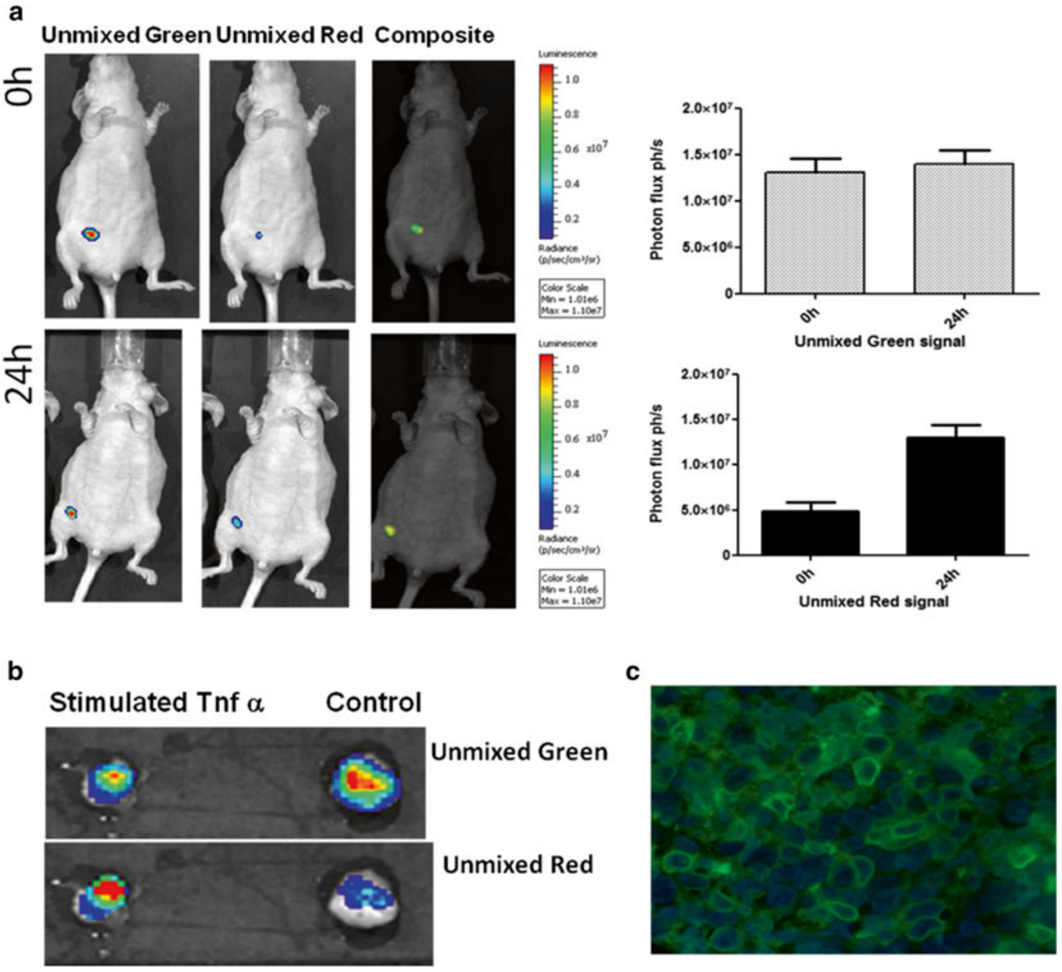
a
Unmixed Green
Unmixed Red
Composite
0h
24h
Luminescence
1.0
0.8
0.6 x10^7
0.4
0.2
Radiance (p/sec/cm²/sr)
Color Scale Min = 1.01e6 Max = 1.10e7
Photon flux ph/s
2.0×10⁷
1.5×10⁷
1.0×10⁷
5.0×10⁶
0
0h
24h
Unmixed Green signal
Unmixed Red signal
b
Stimulated Tnf α
Control
Unmixed Green
Unmixed Red
c

Fig. 3 (**a**) Representative picture of unmixed and composite images obtained with unmixing algorithm application at 0 and 24 h after TNFα injection in a mouse model of breast cancer. *On the left*, the images corresponding to the *green signal* (vitality) while in the *middle* the images corresponding to the *red signal* (NF-κB induction). The graphs represent the average unmixed *red* and *green signals* obtained 0 and 24 h after TNFα injection in three different mice. (**b**) Representative picture of unmixed images obtained with ex vivo analysis of tumors derived from mice challenged with or without TNFα. (**c**) Image showing GLuc expression on the membrane of cells derived from excised tumors and detected using a polyclonal anti-GLuc antibody and a FITC-conjugated secondary antibody (figure adapted from Mezzanotte L, et al. [1])

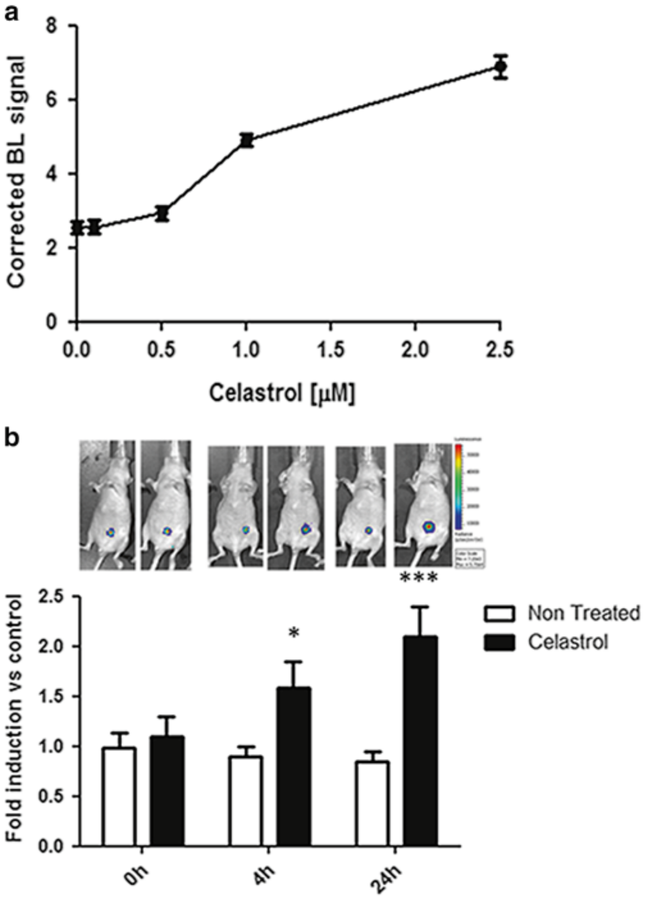

Fig. 4 (**a**) Graph representing effects of the chemopreventive natural compound celastrol on caspase 3/7-mediated apoptosis measured with the caspase 3/7 glo assay and corrected for cell vitality at 4 h after treatment. (**b**) Graph reporting celastrol-induced caspase 3/7-mediated apoptosis in vivo. Caspase 3/7 activity was measured using DEVD luciferin at 0, 4, and 24 h. **A single treatment of celastrol (2 mg/kg) significantly increased the fold induction of caspase 3/7 activity at 24 h compared to controls** (**p* value, 0.05; ****p* value, 0.001) (figure adapted from Mezzanotte L et al. [1])

4 Notes

1. In the process of designing and cloning the vectors for the production of the desired reporter cell line it is important to choose the right promoter-reporter couple. Green luciferase shows a total light emission that is higher than the red luciferase when using the same promoter. Therefore if inducible promoter is characterized by a strong induction, red luciferase is preferred and the green luciferase needs to be cloned with the constitutive promoter. This strategy will help to achieve better separation of signals.

2. Ideally the PEI solution should be frozen and thawed between 4 and 10 times to reach the highest possible transfection efficiency.
3. If your construct contains a GFP (or other fluorescent) marker gene, the transfection efficiency can be checked easily 24–48 h post transfection.
4. Multiple times freezing and thawing is not recommended as it may result in loss of functional titer. Viral stocks should be stable for a long time (at least 3 years) at −80 °C. For use after this period, retitering of the stock is advised.
5. Depending on the origin of the virus sample the dilution factor for p24 ELISA is as follows:
    - (a) Dilute medium at day 2 or 3 post transfection 1:2000 and 1:12,000 in assay diluent (virus production with a third-generation production system)
    - (b) Dilute medium at day 2 or 3 post transfection 1:12,000 and 1:72,000 in assay diluent (virus production with a second-generation production system)
    - (c) Dilute concentrated virus 1:40,000–1:1,500,000 in assay diluent. Dilution factor depends on concentrating factor and initial viral titer.
    - (d) No dilution of medium of transduced cells, which have been washed and trypsinized several times. This is done to test for the presence/absence of lentivirus in case cells have to be transferred to a lower level safety lab.
6. Sequential transduction using different lentivirus for the different promoter-reporter couple allows to select for a cell line with the desired expression of the green or red luciferase. This is important to achieve balanced expression of the reporters. Sometimes a too high expression of a reporter in respect to the other generates signals difficult to unmix.
7. Risk of oversaturation of your image. In our experiments a concentration of d-Luciferin of 0.5 mM resulted in a proper amount of signal. Depending on your condition d-Luciferin concentration may need to be adjusted in order to avoid saturation of pixels in the image and also time of acquisition need to be adjusted.
8. Consider possible toxicity of compounds when measuring caspase activity. Depending on the compounds, concentration and time of incubation should be adjusted in order to avoid excessive cytotoxicity that results in low luminescent signals from cells.
9. The protocol as used here has been optimized for triple-colored MDA-MB-231 cells. If different cells are used, the protocol may need to be adapted and optimized. To avoid an allergic reaction in the mice, it is important that the cells are washed with PBS and free of culture medium.

10. When imaging using the Living Image software, grayscale images are recorded first with dimmed light. Pseudo-color images are recorded and superimposed over the grayscale white light photo after photon emission is integrated. Pseudo-color maps can be adjusted by changing the scale and threshold values, this is purely graphic and has no effect on the actual measurement.

Acknowledgements

This work is supported in part by NanoNextNL, a micro and nanotechnology consortium of the Government of the Netherlands and 130 partners and by the FP7 European Union Marie Curie IAPP Program, BRAINPATH, under grant number 612360.

References

1. Mezzanotte L, An N, Mol IM, Lowik CW, Kaijzel EL (2014) A new multicolor bioluminescence imaging platform to investigate NF-κB activity and apoptosis in human breast cancer cells. PLoS One 9:e85550
2. Michelini E, Cevenini L, Mezzanotte L, Coppa A, Roda A (2010) Cell-based assays: fuelling drug discovery. Anal Bioanal Chem 398:227–238
3. Brasier AR, Ron D (1992) Luciferase reporter gene assay in mammalian cells. Methods Enzymol 216:386–397
4. Wood KV (1990) Luc genes: introduction of colour into bioluminescence assays. J Biolumin Chemilumin 5:107–114
5. Contag CH, Jenkins D, Contag PR, Negrin RS (2000) Use of reporter genes for optical measurements of neoplastic disease in vivo. Neoplasia 2:41–52
6. De A, Lewis XZ, Gambhir SS (2003) Noninvasive imaging of lentiviral-mediated reporter gene expression in living mice. Mol Ther 7:681–691
7. Branchini BR, Ablamsky DM, Murtiashaw MH, Uzasci L, Fraga H, Southworth TL (2007) Thermostable red and green light-producing firefly luciferase mutants for bioluminescent reporter applications. Anal Biochem 361:253–262
8. Nakajima Y, Kimura T, Sugata K, Enomoto T, Asakawa A, Kubota H, Ikeda M, Ohmiya Y (2005) Multicolor luciferase assay system: one-step monitoring of multiple gene expressions with a single substrate. Biotechniques 38: 891–894
9. Michelini E, Cevenini L, Mezzanotte L, Ablamsky D, Southworth T, Branchini B, Roda A (2008) Spectral-resolved gene technology for multiplexed bioluminescence and high-content screening. Anal Chem 80:260–267
10. Gammon ST, Leevy WM, Gross S, Gokel GW, Piwnica-Worms D (2006) Spectral unmixing of multicolored bioluminescence emitted from heterogeneous biological sources. Anal Chem 78:1520–1527
11. Mezzanotte L, Que I, Kaijzel E, Branchini B, Roda A, Lowik C (2011) Sensitive dual color in vivo bioluminescence imaging using a new red codon optimized firefly luciferase and a green click beetle luciferase. PLoS One 6:e19277
12. Liu M, Sakamaki T, Casimiro MC, Willmarth NE, Quong AA, Ju X, Ojeifo J, Jiao X, Yeow WS, Katiyar S, Shirley LA, Joyce D, Lisanti MP, Albanese C, Pestell RG (2010) The canonical NF-κB pathway governs mammary tumorigenesis in transgenic mice and tumor stem cell expansion. Cancer Res 70:10464–10473
13. Huber MA, Beug H, Wirth T (2004) Epithelial-mesenchymal transition: NF-κB takes center stage. Cell Cycle 3:1477–1480
14. Wurdinger T, Badr C, Pike L, de Kleine R, Weissleder R, Breakefield XO, Tannous BA (2008) A secreted luciferase for ex vivo monitoring of in vivo processes. Nat Methods 5:171–173
15. Lin Y, Bai L, Chen W, Xu S (2010) The NF-κB activation pathways, emerging molecular targets for cancer prevention and therapy. Expert Opin Ther Targets 14:45–55

16. Haefner B (2006) Targeting NF-κB in anticancer adjunctive chemotherapy. Cancer Treat Res 130:219–245
17. Katula KS, McCain JA, Radewicz AT (2005) Relative ability of dietary compounds to modulate nuclear factor-κB activity as assessed in a cell-based reporter system. J Med Food 8:269–274
18. Ralhan R, Pandey MK, Aggarwal BB (2009) Nuclear factor-κB links carcinogenic and chemopreventive agents. Front Biosci (Schol Ed) 1:45–60
19. Castillo-Pichardo L, Martinez-Montemayor MM, Martinez JE, Wall KM, Cubano LA, Dharmawardhane S (2009) Inhibition of mammary tumor growth and metastases to bone and liver by dietary grape polyphenols. Clin Exp Metastasis 26:505–516
20. Jeong WS, Kim IW, Hu R, Kong AN (2004) Modulatory properties of various natural chemopreventive agents on the activation of NF-κB signaling pathway. Pharm Res 21:661–670
21. Scabini M, Stellari F, Cappella P, Rizzitano S, Texido G, Pesenti E (2011) In vivo imaging of early stage apoptosis by measuring real-time caspase 3/7 activation. Apoptosis 16:198–207
22. Carlotti F, Bazuine M, Kekarainen T, Seppen J, Pognonec P, Maassen JA, Hoeben RC (2004) Lentiviral vectors efficiently transduce quiescent mature 3T3-L1 adipocytes. Mol Ther 9:209–217
23. Branchini BR, Ablamsky DM, Davis AL, Southworth TL, Butler B, Fan F, Jathoul AP, Pule MA (2010) Red-emitting luciferases for bioluminescence reporter and imaging applications. Anal Biochem 396:290–297
24. Na IK, Markley JC, Tsai JJ, Yim NL, Beattie BJ, Klose AD, Holland AM, Ghosh A, Rao UK, Stephan MT, Serganova I, Santos EB, Brentjens RJ, Blasberg RG, Sadelain M, van den Brink MR (2010) Concurrent visualization of trafficking, expansion, and activation of T lymphocytes and T-cell precursors in vivo. Blood 116:e18–e25

Chapter 22

A Multichannel Bioluminescence Determination Platform for Bioassays

Sung-Bae Kim and Ryuichi Naganawa

Abstract

The present protocol introduces a multichannel bioluminescence determination platform allowing a high sample throughput determination of weak bioluminescence with reduced standard deviations. The platform is designed to carry a multichannel conveyer, an optical filter, and a mirror cap. The platform enables us to near-simultaneously determine ligands in multiple samples without the replacement of the sample tubes. Furthermore, the optical filters beneath the multichannel conveyer are designed to easily discriminate colors during assays. This optical system provides excellent time- and labor-efficiency to users during bioassays.

Key words Cortisol, Steroid hormone, Bioluminescence, Assay device, Single-chain probe

1 Introduction

Bioluminescence-based assays are intrinsically very simple, sensitive, and do not require an external light source or other cofactors in contrast to fluorescence-based ones [1, 2]. The bioluminescence assay is adapted in miniaturized analytical devices such as microfluidic devices [3]. Although microfluidic devices are versatile, they are generally integrated in a small chip and thus sophisticated to operate.

An ideal optical platform for sensing bioluminescence is required (1) to be highly sensitive to samples emitting weak bioluminescence, (2) to provide simplified and user-friendly protocols upon sensing bioluminescence, (3) to allow a high sample throughput and miniaturization in size.

The present protocol introduces fabrication of a high-precision multichannel bioluminescence determination platform accommodating bioluminescent probes. The optical system was equipped with a variable slide holder carrying a multichannel microslide, an optical filter, and a mirror-like interior design for focusing the generated photons to the detector. The bottom of the platform is

Sung-Bae Kim (ed.), *Bioluminescence: Methods and Protocols*, Methods in Molecular Biology, vol. 1461,
DOI 10.1007/978-1-4939-3813-1_22, © Springer Science+Business Media New York 2016

designed to fit in the sample cell of conventional optical detectors (diameter = 3.5 cm), such as a luminometer (GloMax 20/20n, Promega) and a spectrophotometer (AB-1850, ATTO).

The practical advantage of the bioluminescence determination platform is demonstrated by determining (i) a stress hormone in human saliva and (ii) multicolor-imaging agonistic and antagonistic effects of estrogens with the assay system. The present platform may be broadly utilized in determining various hormones and chemicals in physiological and environmental samples with a simplified protocol, convenience, and high precision.

2 Materials

1. COS-7 cell derived from the previously established CV-1 African green monkey kidney line.
2. Human saliva collected from volunteers.
3. Saliva collection tube (SARSTEDT) carrying cotton.
4. Standard concentrations of cortisol as a control.
5. A lysis buffer in a *Renilla* luciferase assay kit (E291A, Promega).
6. 100× Native coelenterazine (nCTZ) in a *Renilla* luciferase assay kit (E2820, Promega).
7. High glucose Dulbecco's Modified Eagle Medium (DMEM) supplemented with 10% fetal bovine serum (FBS).
8. 10% Fetal bovine serum (FBS).
9. 17β-estradiol (E_2), a endogenous estrogen.
10. 4-hydroxytamoxifen (OHT), a synthetic antiestrogen.
11. polychlorinated biphenyls (PCB), a synthetic chemical mimicking estrogen.
12. *o,p′*-dichlordiphenyltrichloroethane (*o,p′*-DDT), a pesticide mimicking estrogen.
13. 1× phosphate-buffered saline (PBS; Sigma).
14. A bioluminescence assay kit, Bright-Glo (E2820, Promega).
15. pcDNA 3.1(+) vector encoding "Simer-R2", designed for illuminating antagonistic activities of estrogens in the authors' previous paper [4].
16. pcDNA 3.1(+) vector encoding "Simer-G4", designed for illuminating agonistic activities of estrogens in the authors' previous paper [4].
17. pCS2+ vector encoding "cSimer7" for the probe expression in mammalian and Xenopus cell lines in the authors' previous paper [5].

3 Methods

The bioluminescence determination platform is fabricated and utilized for the following experiments: (1) the determination of stress hormones in human saliva using the bioluminescence determination platform and a single-chain bioluminescent probe carrying the ligand binding domain of glucocorticoid receptor (GR LBD) (*see* **Note 1**) in the luminometer (GloMax 20/20n, Promega) and (2) simultaneous determination of agonistic and antagonistic activities of woman sex hormones with multicolor imaging.

3.1 Fabrication of Bioluminescence Determination System

1. On the basis of the blueprint (*see* Fig. 1a), manufacture the parts 1–7 of the prototypical bioluminescence determination platform, which is designed to accommodate a disposable 6-channel microslide (2.5 × 7.5 cm, μ-slide VI$^{0.4}$; ibidi) growing mammalian cells (*see* **Note 2**).
2. Assemble the above parts by an order including the disposable 6-channel microslide, the mirror cap with honeycomb-like

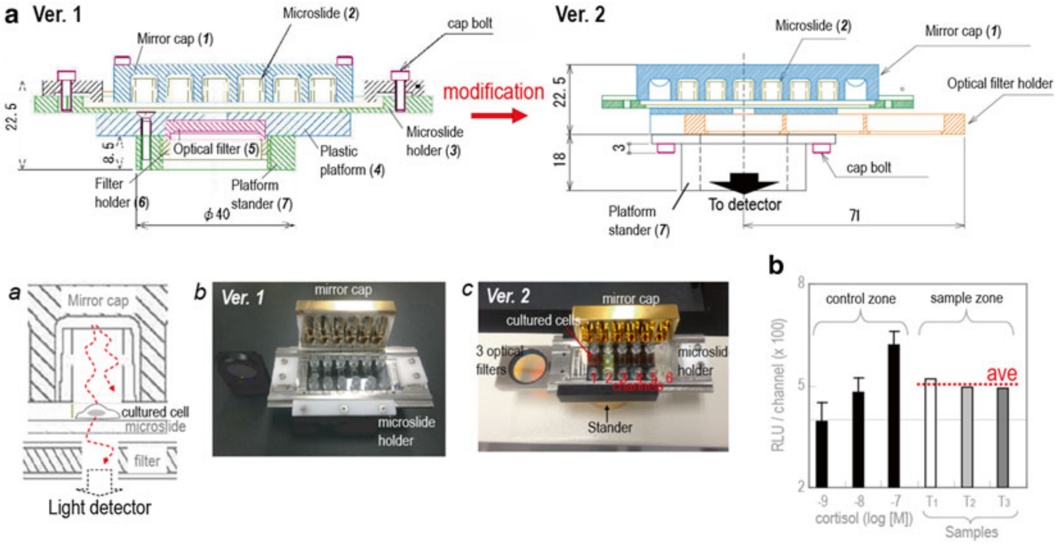
a
Ver. 1
Mirror cap (1)
Microslide (2)
cap bolt
22.5
8.5
Optical filter (5)
Plastic platform (4)
Microslide holder (3)
Filter holder (6)
Platform stander (7)
ϕ 40
modification
Ver. 2
Microslide (2)
Mirror cap (1)
Optical filter holder
22.5
18
3
cap bolt
Platform stander (7)
To detector
71
a
Mirror cap
cultured cell
microslide
filter
Light detector
b
Ver. 1
mirror cap
microslide holder
c
Ver. 2
mirror cap
cultured cells
3 optical filters
microslid holder
1 2 3 4 5 6
channels
Stander
b
control zone
sample zone
ave
RLU / channel (x 100)
8
5
2
-9
-8
-7
cortisol (log [M])
T1
T2
T3
Samples

Fig. 1 Construction of a bioluminescent determination platform for determining steroid hormone levels in physiological samples. (**a**) An illustration of the platforms ver. 1 and 2. The microslide is placed on a microslide holder (3), which is designed to slide on to the plastic platform (4) like a conveyer belt. The microslide is fixed by bolts and covered by a mirror cap (1). *Numbers in the parenthesis* represents part numbers. *Inset a* highlights a channel of the microslide. The bioluminescence (*dotted line*) is reflected by the mirror cap and focused on the detector side at the bottom. The *insets b* and *c* show the practical pictures of the platforms ver. 1 and 2. (**b**) Determination of a stress hormone levels in human saliva. COS-7 cells stably expressing cSimgr7 were exposed to saliva samples, and the developed bioluminescence reflects the cortisol levels in the saliva samples ($n = 3$). The T_1, T_2, and T_3 in the X-axis represent tested saliva samples which develop the optical intensities in the channels of the microslide (ibidi). Reproduced in part from Kim et al. with permission from Chem. Pharm. Bull. [5]

internal barriers (*see* **Notes 3** and **4**), the microslide holder (**part 3**) (*see* **Note 5**), and the optical filter (ver. 1) (*see* **Note 6**).

3. For multicolor determination of bioluminescence, a filter holder may be applied to carry three different optical filters (ver. 2), i.e., blue (470-nm bandpass), green (520-nm bandpass), and red (600-nm long-pass) (*see* **Note** 7).

3.2 Determination of Stress Hormones in Saliva with the Bioluminescence Determination Platform

Cortisol levels as a stress marker in human saliva may be determined using the bioluminescence determination platform as follows:

1. Establish a COS-7 cell line stably expressing "cSimgr7" growing the cells in a culture medium containing G418 after transient transfection of pcSimgr7 [5] (*see* **Note 8**) and subculture into 6-channel microslides (ibidi), where the three left channels are allotted to standards of cortisol, whereas the other three channels are assigned for the determination of cortisol in the saliva samples.

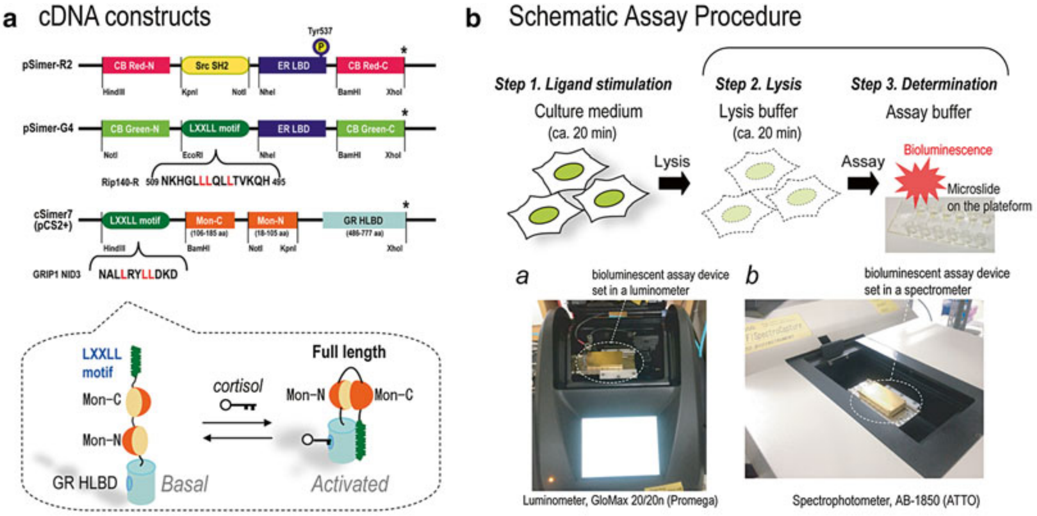
a
cDNA constructs
pSimer-R2
CB Red-N
Src SH2
ER LBD
CB Red-C
Tyr537
P
HindIII
KpnI
NotI
NheI
BamHI
XhoI
pSimer-G4
CB Green-N
LXXLL motif
ER LBD
CB Green-C
NotI
EcoRI
NheI
BamHI
XhoI
Rip140-R 509 NKHGLLLQLLTVKQH 495
cSimer7 (pCS2+)
LXXLL motif
Mon-C (106-185 aa)
Mon-N (18-105 aa)
GR HLBD (486-777 aa)
HindIII
BamHI
NotI
KpnI
XhoI
GRIP1 NID3
NALLRYLLDKD
LXXLL motif
Mon-C
Mon-N
GR HLBD
Basal
cortisol
Full length
Mon-N
Mon-C
Activated
b
Schematic Assay Procedure
Step 1. Ligand stimulation
Culture medium
(ca. 20 min)
Lysis
Step 2. Lysis
Lysis buffer
(ca. 20 min)
Assay
Step 3. Determination
Assay buffer
Bioluminescence
Microslide on the plateform
a
bioluminescent assay device set in a luminometer
Luminometer, GloMax 20/20n (Promega)
b
bioluminescent assay device set in a spectrometer
Spectrophotometer, AB-1850 (ATTO)

Fig. 2 (**a**) Constructs of single-chain probes and the working mechanism. Abbreviations: *GR HLBD* the hinge and ligand-binding domain of human glucocorticoid receptor, *ER LBD* the ligand-binding domain of human estrogen receptor, *Mon-N and -C* the N- and C-terminal domain of Monsta, *CB Red-N and -C* the N- and C-terminal domain of click beetle luciferase red, *Src SH2* the SH2 domain of *v*-Src, *LXXLL motif* a conserved motif of coactivators interacting glucocorticoid receptor, where "L" means leucine and "X" means any amino acid. (**b**) A protocol for developing bioluminescence with mammalian cells, cultured in a microslide. The cultured mammalian cells were exposed to hormones or chemicals beforehand. In response to the hormones, the conformation of the single-chain probe is changed, where an intracellular protein complementation occurs. The cells were lysed and exposed to an assay buffer comprising the substrate for light development. The *insets a* and *b* shows pictures showing the platform is placed in a conventional luminometer (GloMax 20/20n, Promega) or a spectrophotometer (AB-1850, ATTO). The platform is designed to set in the chamber of the luminometer and spectrophotometer. Reproduced in part from Kim et al. with permission from Chem. Pharm. Bull. [5]

2. Separately, collect the salivary samples from volunteers using a specific saliva collection tube (SARSTEDT) carrying cotton. Centrifuge the tube and stock the saliva in a 4 °C refrigerator before use (*see* **Note 9**).
3. Stimulate the cells for 20 min with 60 μL of saliva samples or standard cortisol concentrations (10^{-7}, 10^{-8}, or 10^{-9} M) dissolved in culture media in a CO_2 incubator (Sanyo) (*see* **Notes 10** and **11**).
4. After washing out the solutions in the slide with a PBS buffer, lyse the cells on the microslides with 40 μL of a lysis buffer (Promega) for 20 min (*see* **Note 12**).
5. Set the microslide on the bioluminescence determination platform (*see* Fig. 2b) in a luminometer (GloMax 20/20n; Promega).
6. Determine the optical intensities from each channel of the microslides in order, immediately after injection of an assay buffer dissolving nCTZ (Promega) to the channels ($n=3$) with a multichannel pipet. The result is shown in Fig. 1a (*see* **Note 13**).

3.3 Multicolor Imaging of Agonistic and Antagonistic Effects of Woman Sex Hormones Using the Multichannel Bioluminescence Determination Platform

The agonistic and antagonistic effects of estrogen are determined in green and red colors using the multichannel bioluminescence determination platform (*see* Fig. 3).

1. Grow COS-7 cells in a 6-channel microslide (μ-slide VI$^{0.4}$, ibidi) using DMEM supplemented with 10% FBS.
2. Transiently cotransfect the COS-7 cells with pSimer-R2 and pSimer-G4 (*see* Fig. 2a), and incubate for 24 h in a cell incubator (Sanyo).
3. Stimulate the cells in each channel of the microslide with 10^{-5} M of 17β-estradiol (E_2), 4-hydroxytamoxifen (OHT), polychlorinated biphenyls (PCB), or *o,p′*-dichlordiphenyltrichloroethane (*o,p′*-DDT) for 20 min.
4. Wash the channels in the microslide once with 1× PBS (Sigma) and fill with 50 μL of Bright-Glo assay solution carrying d-Luciferin as the substrate (Promega) (*see* **Note 14**).
5. Three minutes after further incubation in the cell incubator, estimate the optical intensities from each channel near-simultaneously by conveying the filter holder and microslide holder of the optical platform ver. 2 set in the luminometer (GloMax 20/20n, Promega) (*see* **Note 15**).
6. Determine the optical intensities of the five hormone samples first under a blue filter.
7. After switching the filter to green or red, estimate bioluminescence intensities from the same samples again for fidelity.

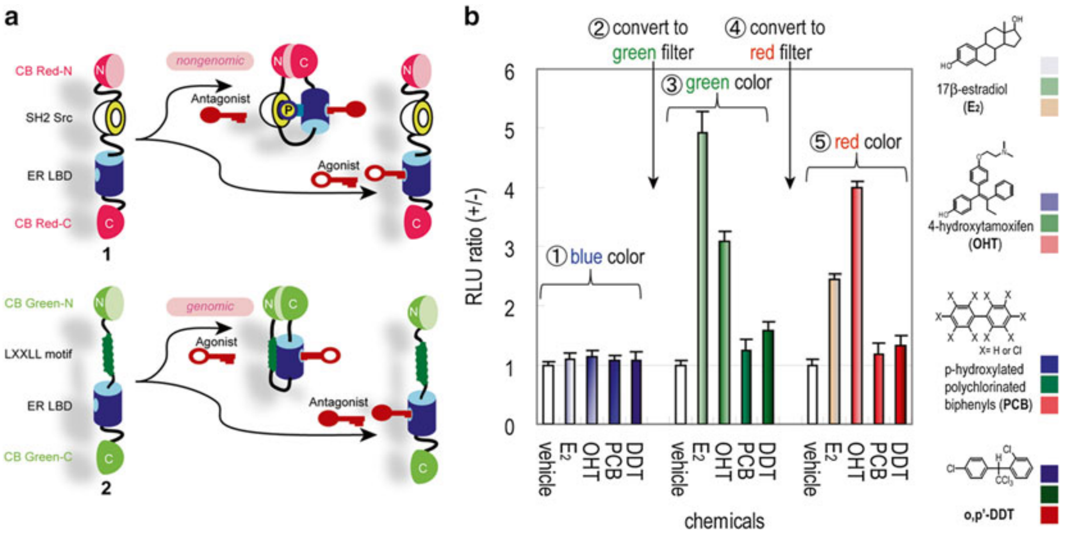

Fig. 3 Multicolor imaging of agonistic and antagonistic effects of 17β-estradiol (E_2) and chemicals using the bioluminescence determination platform. (**a**) Schematic drawing of the ligand recognition steps of pSimer-R2 and pSimer-G4. In response to antagonist, the ligand-binding domain of estrogen receptor (ER LBD) interacts with the SH2 domain of *v*-Src. This interaction induces reconstitution of the fragmented click beetle luciferase red (CB Red). Similarly, in response to agonist, ER LBD binds a common LXXLL motif of coactivators. This binding restores the green bioluminescence through the intramolecular interactions between the N- and C-terminal fragments of CB green. (**b**) Relative optical intensities of blue, green, and red bioluminescence, shown in signal-to-background ratios. The *numbers* indicates the experimental sequence including the timing of the filter switching. The *left*, *middle*, and *right bars* in groups demonstrate *blue*, *green*, and *red* color intensities, respectively. Reproduced in part from Kim et al. with permission from Chem. Pharm. Bull. [5]

4 Notes

1. Glucocorticoid receptor (GR) is responsible for many metabolic actions including stress responses. Cortisol-activated GRs are dimerized and recruit coactivators. Because all the coactivators have a common α-helical peptide, called an LXXLL motif, the binding between GR LBD and the LXXLL motif was utilized for cortisol sensing in the present single-chain probes (*see* Fig. 2a).
2. The bioluminescence determination platform consists of a mirror cap for focusing bioluminescence on the detector and blockading outer interferences (**part 1**; *see* Fig. 1a), a 6-channel microslide (ibidi) for raising cells (**part 2**), a variable microslide holder for carrying the microslide (**part 3**), a plastic conveyer platform for supporting the microslide holder (**part 4**), a set of optical filters (**part 5**), a variable filter holder carrying 1–3 optical filters (**part 6**), and an inner-holed platform stander for

supporting the platform and passing the generated bioluminescence to the bottom (**part 7**).

3. The mirror cap is beneficial and useful for a weak light determination rather than a strong light. Another role of the cap is to fix the microslide on the deck and thus allows a precise determination of the samples in the platform.
4. The honeycomb-like internal barriers of the mirror cap (**part 1**) efficiently blockades interference light from the other channels. As highlighted with dotted lines in Fig. 1a, bioluminescence emitted from each channel is reflected by the mirror cap to the bottom slit (7 × 24 mm). The bioluminescent signal passes the optical filter beneath the slit and finally reaches the detector at the bottom.
5. The microslide holder (**part 3**) may be modified according to experimental preference. A side of this microslide holder is designed like a saw tooth to fit each channel of the microslide on the bottom slit.
6. The optical filters in the tray are placed beneath the bottom slit to be assembled according to experimental preference.
7. The variable optical filter holder is embedded into the surface-plated device stand for a better reflection of the photons to the detector.
8. "cSimgr7" is a single-chain bioluminescent probe that was previously developed for illuminating cortisol, a stress hormone [5].
9. The saliva is supposed to be collected at the same time and to use up in 24 h after collection.
10. Although some cortisol is bound to globulin in saliva, majority of the cortisol is free in saliva and extracted into the live cells carrying cSimgr7 for emitting bioluminescence.
11. The known clinical range of salivary cortisol ranging from 0.2 to 2.8×10^{-8} M.
12. After injection of a lysis buffer into the slide, gently homogenize the slide on a shaker.
13. The excellent selectivity of the probe to cortisol reflects the stress sensitivity of our body via a glucocorticoid receptor.
14. Since Simer-G2 and Simer-R4 are made of split-click beetle luciferases green and red, any reagent kit comprising d-Luciferin, ATP, and Mg^{2+} is acceptable for the bioluminescence development.
15. The overall standard deviations (SDs) with the platform were significantly decreased, where the averaged SDs in blue, green, and red region were 0.10, 0.19, and 0.13 in RLU ratios, respectively. These values are one-fourth smaller than those without the device-aid.

Acknowledgements

This work was supported by grants from Japan Society for the Promotion of Science (JSPS), grants number 26288088, 16K14051, and 15KK0029.

References

1. Fan F, Wood KV (2007) Bioluminescent assays for high-throughput screening. Assay Drug Dev Technol 5:127–136
2. Kim SB (2012) Labor-effective manipulation of marine and beetle luciferases for bioassays. Protein Eng Des Sel 25:261–269
3. Roda A, Guardigli M, Michelini E, Mirasoli M (2009) Bioluminescence in analytical chemistry and in vivo imaging. Trends Anal Chem 28:307–322
4. Kim SB, Umezawa Y, Kanno KA, Tao H (2008) An integrated-molecule-format multicolor probe for monitoring multiple activities of a bioactive small molecule. ACS Chem Biol 3:359–372
5. Kim SB, Suzuki T, Kimura A (2013) A bioluminescent assay system for whole-cell determination of hormones. Chem Pharm Bull 61:706–713

Chapter 23

A Bioluminescence Assay System for Imaging Metal Cationic Activities in Urban Aerosols

Sung-Bae Kim, Ryuichi Naganawa, Shingo Murata, Takayoshi Nakayama, Simon Miller, and Toshiya Senda

Abstract

A bioluminescence-based assay system was fabricated for an efficient determination of the activities of air pollutants. The following four components were integrated into this assay system: (1) an 8-channel assay platform uniquely designed for simultaneously sensing multiple optical samples, (2) single-chain probes illuminating toxic chemicals or heavy metal cations from air pollutants, (3) a microfluidic system for circulating medium mimicking the human body, and (4) the software manimulating the above system. In the protocol, we briefly introduce how to integrate the components into the system and the application to the illumination of the metal cationic activities in air pollutants.

Key words Air pollutant, Particulate matter 2.5 (PM2.5), Bioluminescence, Assay system, Luciferase, Toxicity

1 Introduction

Bioluminescence-based assays are intrinsically very simple, sensitive, and do not require an external light source, optical filters, or cofactors for light emission, unlike fluorescence-based ones [1, 2].

Because of the merits, bioluminescence-based assays can be adapted into miniaturized analytical devices such as microfluidic devices [3]. As the authors have separately developed three key components, artificial luciferases (ALuc®), single-chain bioluminescent probes [4, 5], and a bioluminescence determination platform [6], we introduce a new bioluminescence assay system for illuminating the activities of chemicals from air pollutants.

A series of single-chain bioluminescent probes carrying engineered fragments of luciferases was expressed in mammalian cell lines, which were grown in a multichannnel microslide. The microslide is set on a bioluminescence determination platform in

Sung-Bae Kim (ed.), *Bioluminescence: Methods and Protocols*, Methods in Molecular Biology, vol. 1461,
DOI 10.1007/978-1-4939-3813-1_23, © Springer Science+Business Media New York 2016

a bioluminescence assay system. The chemical-contaminated medium is circulated in the microslide and stimulates the single-chain bioluminescent probes in the mammalian cells. The bioluminescence emitted from the single-chain probes is simultaneously determined by arrayed photon multipliers in the bottom of the bioluminescence determination platform. The present protocol briefly introduces the fabrication process of the bioluminescence assay system and the application to the determination of the metal cationic activities in air pollutants.

2 Materials

1. Glasgow Modified Minimum Essential Medium (GMEM).
2. A certified reference material of urban aerosols (CRM14028, National Institute for Environmental Studies (NIES)), soluble in GMEM (*see* **Note 1**).
3. A supernatant of the GMEM-diluted urban aerosol sample: 10 mg of the urban aerosol is diluted in 2 mL GMEM and overnight-incubated with a stirrer (final conc: 5 mg/mL). The mixture was filtered by a 0.2 μm syringe-driven filter unit (Millipore) and made the supernatant.
4. A disposable 6-channel microslide (2.5 × 7.5 cm, μ-slide VI$^{0.4}$; ibidi).
5. A single-channel photomultiplier (PMT; Hamamatsu).
6. A single-pass medium circulation pump.
7. A pOPTHM vector, which is a prokaryotic cell expression vector encoding ALuc16 for *Escherichia coli* (*E. coli*).
8. Isopropyl β-d-1-thiogalactopyranoside (IPTG).
9. A hen egg-white lysozyme (HEWL).
10. An ethylenediaminetetraacetic acid (EDTA).
11. African green monkey kidney fibroblast-derived COS-7 cells.
12. TransIT-LT1 (Mirus), a lipofection reagent.
13. pcDNA 3.1 (+) vector, a mammalian expression plasmid.
14. A heavy metal cation-free Tris–HCl buffer (0.05 M, pH 8.2) (*see* **Note 2**).
15. A stabilized standard light source for PMTs (L11494-525, Hamamatsu).

3 Methods

3.1 Construction of a Bioluminescence Assay System Mounting a Multichannel Bioluminescence Determination Platform

The present bioluminescence assay system is fabricated from the multichannel bioluminescence determination platform of Chapter 22 as follow.

1. Manufacture a mirror cap with slantingly bored holes at the side (Part #1), where the distance between the holes should be fit to the channel distance of the disposable microslide (Part #2), which grows mammalian cells (*see* **Notes 3** and **4**).
2. Array eight of single-channel photomultipliers (PMT) (Part #3) in front of the circuit board inside the black container (*see* **Notes 5** and **6**).
3. Cap the light-sensing site of the PMT with a shutter unit (Part #4) (*see* **Note** 7), and link it to the terminal of the sample stage (Part #5) via a plastic light-conduction path (Part #6) (*see* **Note 8**).
4. Connect the PMT to the circuit units of a photon counter (Part #7) and a controller (Part #8). The mechanical fan (Part #9) cools down the circuit temperature by air.
5. Connect the USB slot (Part #10) to a USB port of a personal computer for the power supply and the system control.
6. Optionally, a single-pass medium circulation pump (Part #11) can be mounted at a side of the sample stage (*see* **Note 9**).
7. For controlling the 8-arrayed PMTs in the system, the following specification of software needs to be custom-made (*see* **Note 10**):
   (a) The software should consist of functions of the power supply to PMT and PMT signal acquisition.
   (b) A function to turn on and off individual PMT.
   (c) Signal acquisition time range: 0.5–600 s.
   (d) Signal acquisition interval: 0.5–100 s.
   (e) Signal display format: photon count in relative luminescence unit (RLU).
   (f) File format for data saving: binary or comma-separated values (CSV) format.
   (g) Operation system:Windows.
8. Finely adjust the light paths and shutter units for normalizing the photon counts from the eight-different PMTs using the stabilized standard light source.

3.2 Simultaneous Determination of Metal Cation-Driven Bioluminescence of ALuc®

A heavy metal cation-free sample of an artificial luciferase (ALuc®) should be prepared beforehand. We exemplify the ALuc purification protocol with ALuc16, a variant of ALuc®, as follow:

1. Generate a cDNA construct of ALuc16 carrying a Strep-II tag at the C-terminal end via a polymerase chain reaction (PCR).

2. Subclone the construct into a pOPTHM vector (providing a cleavable N-terminal His$_6$-MBP tag).
3. Express the vector in the bacterial strain SHuffle T7 Express *lysS* (New England Biolabs) with 0.3 mM IPTG induction and overnight incubation in 37 °C.
4. Harvest the bacterial cells by centrifuge. Resuspend and sonicate the pellet in an ice-cold lysis buffer (50 mM Tris–HCl pH 8.0, 500 mM KCl, 5 mM imidazole, 0.2 mg/mL HEWL, and 1 EDTA-free Protease Inhibitor Cocktail tablet (Roche Diagnostics)).
5. Centrifuge the lysate at 22,000 rpm for 40 min, and pass the subsequent supernatant over a 5 mL HisTrap HP column (GE Healthcare).
6. Wash and elute the ALuc16 fusion protein using an ÄKTA Purifier system (GE Healthcare) as follows:
   (a) Wash the column with 100 mL of a wash buffer (20 mM Tris–HCl pH 8.0, 50 mM potassium phosphate pH 8.0, 100 mM NaCl, and 15 mM imidazole pH 8.0)
   (b) Elute ALuc16 in an imidazole gradient (15–300 mM) over 80 mL.
   (c) Dialyze the eluted sample to a heavy metal cation-free Tris–HCl buffer (0.05 M, pH 8.2) at 4 °C for 24 h, and finally adjust the concentration to 1 mg/mL by dilution (*see* **Note 11**).
7. Further dilute the stock 5000-fold to 0.2 μg/mL with the heavy metal cation-free Tris–HCl buffer (0.05 M, pH 8.2) before experiments.
8. Stand an 8-well PCR tube (200 μL) by fitting it into the bored holes of the mirror cap (Part #1).
9. Mix 20 μL of the diluted ALuc16 (0.2 μg/mL) with 20 μL of a metal cation (Mn(II), Cu(II), Zn(II), Cd(II)), or a supernatant of GMEM-diluted urban aerosols in each tube of a 8-well PCR tube (200 μL) (*Solution A*).
10. Separately prepare the corresponding substrate solution carrying native coelenterazine (nCTZ) by diluting the stock nCTZ solution (Promega) 100 fold with the heavy metal cation-free Tris–HCl buffer (*Solution B*).
11. Simultaneously inject 10 μL of Solution B into the Solution A (40 μL) in the 8-well PCR tube with a multichannel micropipette (Gilson).
12. Immediately mount the PCR tube on the sample stage (Part #5) of the bioluminescence assay system equipped with a PMT array (*see* Fig. 1).
13. Measure the optical intensities from the 8-well PCR tube with the assay system controlled by the specific software in a personal

computer (*see* **Note 12**). Figure 2a shows the typical results representing the metal cation-driven bioluminescence intensities (*see* **Note 13**). Optionally, the measured photon counts (RLUs) may be normalized according to the relative photon sensitivities of the PMTs to the stabilized standard light source (*see* **Note 14**).

14. Ensure the optical intensities from the 8-well PCR tube with an image analyzer (LAS-4000, FujiFilm) equipped with a cooled CCD camera (*see* Fig. 2b).

3.3 Determination of Activities of Metal Cations Extracted into Mammalian Cells

1. Grow COS-7 cells in a 6-channel microslide and transiently transfect with a mammalian expression plasmid, pcDNA 3.1(+), encoding ALuc16 using a lipofection reagent, TransIT-LT1 (Mirus).
2. Further incubate the cells in a CO_2 cell incubator (Sanyo, Japan) for 16 h.

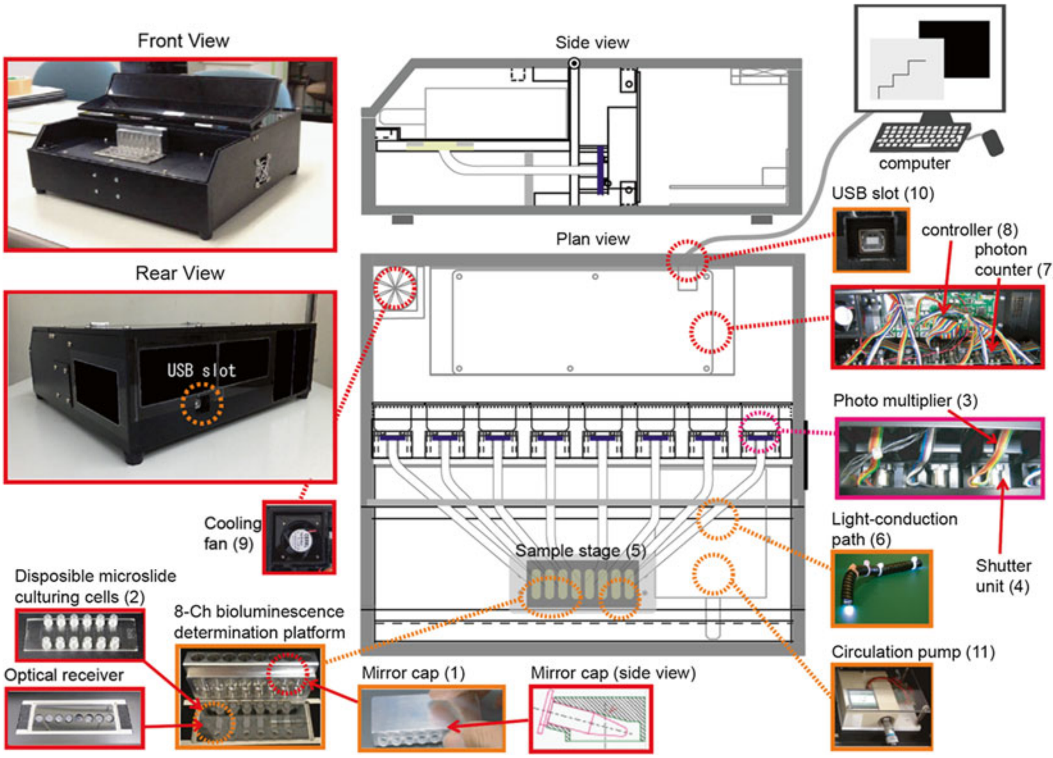
Front View
Side view
computer
USB slot (10)
controller (8)
photon counter (7)
Plan view
Rear View
USB slot
Photo multiplier (3)
Light-conduction path (6)
Shutter unit (4)
Cooling fan (9)
Sample stage (5)
Disposible microslide culturing cells (2)
8-Ch bioluminescence determination platform
Optical receiver
Mirror cap (1)
Mirror cap (side view)
Circulation pump (11)

Fig. 1 Instrumental construction of an 8-channel assay platform uniquely designed for simultaneously sensing multiple optical samples. Multiple samples are designed to set in a mirror cap (Part #1). Alternatively, bioluminescent cells can grow in a disposable 6-channel microslide (Part #2) and placed directly on the sample stage (Part #5). Eight photomultipliers (Part #3) are arrayed and connected to the sample stage via shutter units (Part #4) and plastic light-conduction path units (Part #6). The array of photomultipliers is connected to the corresponding photon counter (Part #7) and controller circuit (Part #8). The platform is air-cooled by a mechanical fan (Part #9) and connected to a personal computer via a USB slot (Part #10). Optionally, the medium in the microslide can be circulated by the single-pass medium circulation pump (Part #11). The part numbers shows in the *parentheses*

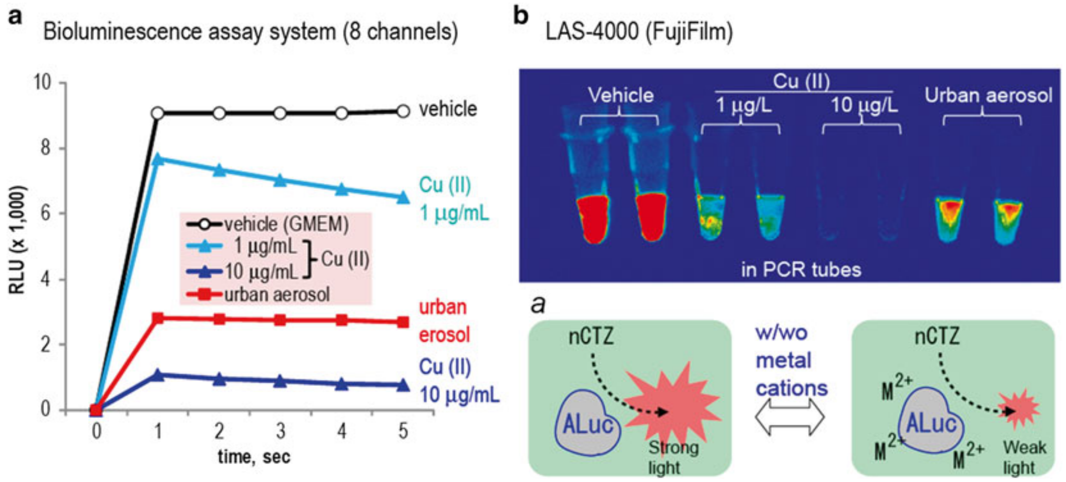

Fig. 2 Heavy metal cation-driven optical intensities of artificial luciferases (ALucs). (**a**) The time course of the optical intensities from 8-well PCR tube, where ALuc16 is mixed with vehicle (GMEM), Cu(II), or the supernatant of urban aerosol. The graphs shows average values of two independent measurement ($n = 2$). (**b**) The corresponding optical image of the 8-well PCR tube. The vehicle emits the strongest optical intensities, whereas the supernatant of urban aerosol allows bioluminescence intensity between those of vehicle and 10 µg/L Cu(II). The *inset a* shows the working mechanism of the cation-driven bioluminescence reaction in the PCR tube ($n = 2$). In metal cation circumstance, ALuc® exerts reduced optical intensities. Abbreviations: *GMEM* Glasgow modified minimum essential medium, *ALuc* artificial luciferase, *Cu(II)* divalent copper, *PCR tube* polymerase chain reaction tube (200 µL)

3. Remove the culture medium in the 6-channels of microslides growing COS-7 cells with a micropipette and wash once with the heavy metal cation-free PBS buffer.
4. Fill the channels of the microslide with (1) 60 µL of a vehicle solution (GMEM alone), (2) a heavy metal solution (Zn^{2+} or Mn^{2+}), and (3) the supernatant of the air pollutant solution cocktail, respectively.
5. Incubate the microslide in a CO_2 incubator for 30 min (*see* **Note 15**).
6. Remove the solutions and wash the channels of the microslide 3 times with the heavy metal cation-free Tris–HCl buffer.
7. Simultaneously inject 50 µL of Solution B into the vacant channels of the microslide with a multichannel micropipette (Gilson) and mount the microslide on the sample stage (Part #5) of the bioluminescence assay system equipped with a PMT array.
8. Measure the optical intensities from the microslide with the assay system using the custom-made software. Fig. 3 shows the typical results showing the metal cation-driven bioluminescence intensities from living mammalian cells in the microslide.

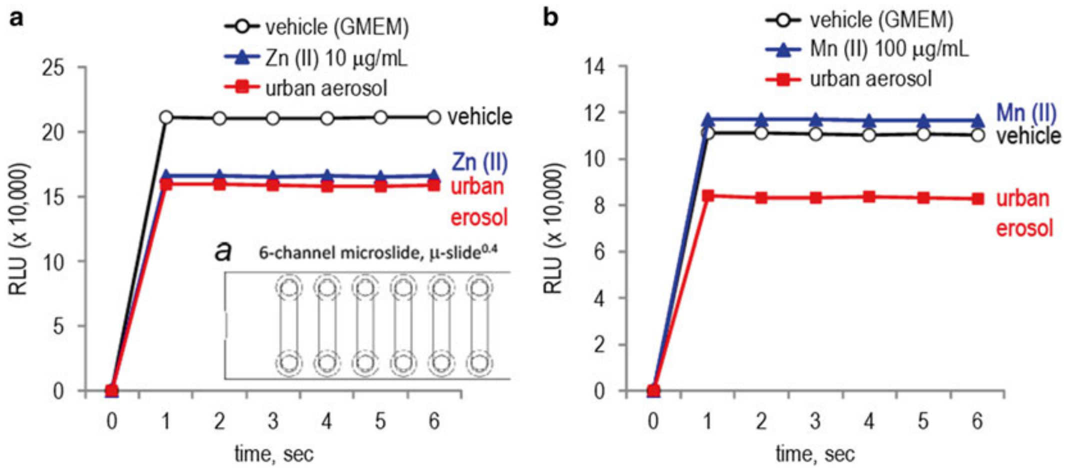

Fig. 3 Heavy metal cation-driven bioluminescence intensities of living COS-7 cells expressing ALuc16 in microslides. (**a**) The time course of the optical intensities from a 6-channel microslide, where ALuc16 is sequestered in the endoplasmic reticulum (ER). The cells are stimulated with vehicle (GMEM), 10 μg/mL Zn(II), or the supernatant of urban aerosol. The graphs shows average values of two independent measurement ($n = 2$). *Inset a* shows a plan view of the 6-channel microslide growing COS-7 cells. (**b**) The time course of the optical intensities from a 6-channel microslide, growing COS-7 cells expressing ALuc16. The cells are stimulated with vehicle (GMEM), 100 μg/mL Mn(II), or the supernatant of urban aerosol. The graphs shows average values of two independent measurement ($n = 2$)

4 Notes

1. The certified reference material of urban aerosols (CRM14028) is originally collected in Beijing city, China, and now commercially available from National Institute for Environmental Studies (NIES), Japan.
2. The heavy metal cation-free Tris–HCl buffer was previously certificated with an instrumental analysis using an inductively coupled plasma mass spectrometry (ICP-MS) in the authors' precedent paper [7].
3. The mirror cap is beneficial for both grip of the sample tubes (or microslide) and focusing of weak bioluminescence. Fixation of the microslide on the deck allows a precise determination of the samples in the system. The internal surface of the mirror cap is grinded to reflect bioluminescence.
4. The mirror cap comprises honeycomb-like internal barriers (Part #1), which efficiently blockade interference light from the other channels. Bioluminescence emitted from each channel is reflected by the interior surface of the mirror cap and reach to the terminal of the light-conduction path.
5. The PMT works by USB3.0 bus power and generates photon counts (relative luminescence unit, RLU) in response to lights.

6. It is useful to choose CMTs reporting a similar photon count in response to a stabilized standard light source (L11494-525, Hamamatsu).
7. An optical shutter is attached at the light-receiving area of the PMT to protect the PMT from strong current.
8. Because the assay system consists of eight single-channel PMTs, the photon counts between PMTs needs to be adjusted: e.g., every PMT should display a same photon count to a same light source. The shutter units (Part #4) enable us to adjust the photon counts between PMTs.
9. The medium circulation pump is useful for determining temporal elevation (time course) of bioluminescence from cells on each channel of the microslide, where the cells are stimulated by chemicals or urban aerosols.
10. This optical system allows simultaneous determination of bioluminescence from eight-different samples at once. This system significantly increases the sample throughput, compared to conventional luminometers including a 96-well plate reader, which measures every sample one-by-one.
11. The authors recommend that the purified ALuc16 in a high concentration (1 mg/mL) is dispensed in separate tubes and stocked in an 80 °C refrigerator for a long-time preservation. The stock may be diluted 5000-fold to 0.2 μg/mL with the heavy metal cation-free Tris–HCl buffer (0.05 M, pH 8.2) before experiments.
12. The present system allows to simultaneously monitor bioluminescence from eight kinds of samples without the replacement of the sample tube, in contrast to conventional instruments.
13. The optical intensities are dramatically decreased by divalent heavy metal cations. It is considered that the artificial luciferase, ALuc16, comprises a putative cation-binding site called “EF-hand”. Every heavy metal cation exerts unique activity to ALuc16. This feature was previously reported in the authors’ precedent study [7]. Because urban aerosols contain various heavy metal cations in a large quantity [8], they generally hamper the luciferase activity.
14. Every PMT in the assay system is supposed to report a same photon count in response to a same standard light source. However, the photon counts in RLUs between PMTs may be variable even by the climate. The RLU datasets on different scales can be adjusted by an appropriate formula and normalization.
15. Steroids are saturated in COS-7 cells within 20 min [9]. However, in case of hydrophilic metal cations, at least 30 min. of incubation time is required for the cell saturation by passive diffusion. A precedent study showed that 30 min is required until the majority of Mn^{2+} is uptaken into mammalian cells [10].

Acknowledgement

This work was partly supported by JSPS KAKENHI Grant Numbers 26288088, 15KK0029, and 16K14051.

References

1. Fan F, Wood KV (2007) Bioluminescent assays for high-throughput screening. Assay Drug Dev Technol 5:127–136
2. Kim SB (2012) Labor-effective manipulation of marine and beetle luciferases for bioassays. Protein Eng Des Sel 25:261–269
3. Roda A, Guardigli M, Michelini E, Mirasoli M (2009) Bioluminescence in analytical chemistry and in vivo imaging. Trends Anal Chem 28:307–322
4. Kim SB, Torimura M, Tao H (2013) Creation of artificial luciferases for bioassays. Bioconjug Chem 24:2067–2075
5. Kim SB, Izumi H (2014) Functional artificial luciferases as an optical readout for bioassays. Biochem Biophys Res Commun 448:418–423
6. Kim SB, Suzuki T, Kimura A (2013) A bioluminescent assay system for whole-cell determination of hormones. Chem Pharm Bull 61:706–713
7. Kim SB, Miller S, Suzuki N, Senda T, Nishihara R, Suzuki K (2015) Cation-driven optical properties of artificial luciferases. Anal Sci 31:955–960
8. Mitkus RJ, Powell JL, Zeisler R, Squibb KS (2013) Comparative physicochemical and biological characterization of NIST Interim Reference Material PM2.5 and SRM 1648 in human A549 and mouse RAW264.7 cells. Toxicol in Vitro 27:2289–2298
9. Kim SB, Sato M, Tao H (2008) Circularly permutated bioluminescent probes for illuminating ligand-activated protein dynamics. Bioconjugate Chem 19:2480–2486
10. Yanagiya T, Imura N, Enomoto S, Kondo Y, Himeno S (2000) Suppression of a high-affinity transport system for manganese in cadmium-resistant metallothionein-null cells. J Pharmacol Exp Ther 292:1080–1086

Chapter 24

Luminescence Imaging: (a) Multicolor Visualization of Ca^{2+} Dynamics in Different Cellular Compartments and (b) Video-Rate Tumor Detection in a Freely Moving Mouse

Kenta Saito, Masahiro Nakano, and Takeharu Nagai

Abstract

Luminescence exerts an ideal optical readout for imaging living subjects including no external light source, whereas the dim luminescence and poor color pallet should be addressed for the better utilities. To address the demerits and to prevail the advantages, we developed a bright luminescent protein, named yellow Nano-lantern, exhibiting about 10–20 times brighter than wild-type RLuc. In this chapter, we demonstrate two luminescence-based protocols in detail: i.e., (a) multicolor visualization of Ca^{2+} dynamics in different cellular compartments in a single cell using Ca^{2+} indicators based on cyan- and orange-Nano-lanterns and (b) video-rate tumor detection in a freely moving mouse using yellow Nano-lantern.

Key words Bioluminescence, Calcium dynamics, Tumor imaging, *Renilla* luciferase, Bioluminescence resonance energy transfer (BRET)

1 Introduction

Recent advances in fluorescence imaging techniques are revolutionizing the way of research in medicine, pharmacology, and biology. Fluorescence imaging is widely used for tracking, visualization, and quantification of cellular and molecular process in living cells as well as whole organisms. However external light illumination required for fluorescence excitation sometimes causes problems such as photodamage, autofluorescence, and photobleaching. On the other hand, as luminescence imaging does not require external light illumination, it can circumvent these potential problems in fluorescence imaging. Despite its advantages, luminescence imaging has remained underexploited because of the dim luminescence and poor color variants. To prevail the luminescence imaging technique, we developed a bright luminescent protein, yellow Nano-lantern [1]. It is a chimera protein of enhanced version of *Renilla* luciferase (RLuc) 8 [2] and yellow fluorescent protein Venus [3]

Sung-Bae Kim (ed.), *Bioluminescence: Methods and Protocols*, Methods in Molecular Biology, vol. 1461,
DOI 10.1007/978-1-4939-3813-1_24, © Springer Science+Business Media New York 2016

fused with high bioluminescence resonance energy transfer (BRET) efficiency, which yields bright yellow light emission. Moreover, we expanded the color pallets of Nano-lantern to cyan and orange colors [4] by replacing the Venus in yellow Nano-lantern to mTurquoise2 [5], and mKO2 [6], respectively. Nano-lanterns exhibited about 10–20 times brighter than wild-type RLuc. Owing to the brightness, they enabled visualization of fine subcellular structures such as actin and tubulin in living cells and simultaneous monitoring multiple gene expression or Ca^{2+} changes in different cellular compartments. Yellow Nano-lantern also enabled sensitive tumor detection at video-rate in a freely moving unshaved mouse [7].

In this chapter, we describe in detail the protocols for (a) multicolor visualization of Ca^{2+} dynamics in different cellular compartments in a single cell using Ca^{2+} indicators based on cyan- and orange-Nano-lanterns (CNL and ONL, respectively) and (b) video-rate tumor detection in a freely moving mouse using yellow Nano-lantern (YNL). In the section (a), we demonstrate how to not only utilize conventional inverted microscope system for luminescence imaging but also unmix the two colors for quantitative analysis. In the section (b), we mainly instruct how to set up homemade imaging system for obtaining alternate luminescence and bright-field images.

2 Materials

2.1 Reagents and Samples for Multicolor Visualization of Ca^{2+} Dynamics

Culturing medium for HeLa cells (Dulbecco's modification of Eagle's medium (SIGMA, cat. no. D6046) containing 10% fetal bovine serum (FBS, GIBCO, S1500-500)).

- Observation medium (DMEM/F12 (1:1) (1×) (GIBCO, 11039-021)).
- Histamine.
- Coelenterazine-h (CTZh) (Promega, cat. no. S2011 or Wako cat. no. 031-22993).
- Methanol (for dissolving CTZh).
- HeLa cells expressing both CNL-Ca^{2+} in mitochondria (mito-CNL (Ca^{2+})) and ONL-Ca^{2+} in nucleus (nuc-ONL (Ca^{2+})) attached to 35 mm glass bottom dish.
- HeLa cells expressing only mito-CNL (Ca^{2+}) or nuc-ONL (Ca^{2+}) attached to 35 mm glass bottom dish (reference sample of linear unmixing).

2.2 Reagents and Samples for Video-Rate Tumor Detection

1. RPMI1640 Medium "Nissui" 2 (Nissui) (for culturing colon26 cells).
2. Hank's Solution "Nissui" 2 (Nissui) (for transplantation of colon26 cells).

3. 1× PBS (for injection of CTZh).
4. Ethanol (for dissolving CTZh).
5. Pentobarbital Sodium Salt (Nacalai Tesque, Inc.).
6. Saline (Otsuka) (for dilution of pentobarbital).
7. CTZh (Promega).
8. YNL expressing colon26 cells.
9. 5-week-old male BALB/c mice.

2.3 Equipment for Multicolor Visualization of Ca^{2+} Dynamics

1. Micropipette (2, 100, and 1000 μL)
2. Pipette tips (2, 100, and 1000 μL)
3. Microcentrifuge tubes (1.5 mL)
4. Inverted microscope (*see* **Note 1**)
5. Objective lens (*see* Subheading 3.2)
6. Electron multiplying charge coupled device (EM-CCD) camera
7. Excitation light source (Nikon, Intensilight, for checking expression level of mito-CNL(Ca^{2+}) and nuc-ONL(Ca^{2+}) in cells)
8. Optical filter set for observing fluorescence of mTurquoise2 and mKO2 (for checking the expression level in cells)
    - An image splitting optics, W-VIEW GEMINI (Hamamatsu Photonics)
    - Dichroic mirror (Semrock, FF560-FDi01-25x36)
9. Black curtain (for covering microscopy system)
10. Imaging software
    - Personal computer

2.4 Equipment for Video-Rate Tumor Detection

1. Culture dish
2. Micropipette (2, 100, and 1000 μL)
3. Pipette tips (2, 100, and 1000 μL)
4. Needle (26G, 27G)
5. Disposable syringe (1 mL)
6. BD Lo-dose syringes 30G (BD)
7. Microcentrifuge tubes (1.5 mL)
8. Black curtain
9. Corrugated cardboard box (~60 cm × 60 cm × 60 cm)
10. C-mount lens (HF12.5SA-1) (Fujifilm)
11. Aluminum angle boxes (small: ~30 cm × 30 cm × 30 cm, large: ~100 cm × 100 cm × 100 cm)

12. Stainless box (~10 cm × 10 cm × 10 cm) (*see* **Note 2**)
13. Light source for bright-field illumination
14. Light diffuser
15. EM-CCD camera (*see* **Note 3**)
16. Multifunction wave generator (*see* **Note 4**)
17. Electrical shutter unit (*see* **Note 5**)
18. A couple of 50 Ω BNC (or SMA) cables
19. BNC branch connector
20. Oscilloscope (*see* **Note 6**)
21. Personal computer (PC) and imaging software for EM-CCD camera control and data analysis

3 Methods

3.1 Multicolor Visualization of Ca^{2+} Dynamics

3.1.1 Setting Microscopy System for Taking Luminescence Image

Although Nano-lanterns are about 20 times brighter than commercially available RLuc, emission signal of luminescent protein is still weaker than that from fluorescent protein. Therefore, to get the weaker luminescent signal by EM-CCD camera, we have to remove unexpected signal from external environment. For removing the signal, we carry out following processes.

1. Cover an inverted microscope with a black curtain.
2. Cover panels which emit light with a black curtain.
3. Turn off power of the electrical machine such as the microscope and filter wheel (if needed).
4. Take image with EM-CCD camera with opening camera shutter and check whether unexpected signal is entering to the camera or not.

3.1.2 Selecting Objective Lens

To get luminescence signal from Nano-lanterns as much as possible, we use higher numerical aperture (NA) and lower magnification objective lens. The combination of higher numerical aperture lens and intermediate low magnification lens is also useful to get the luminescence signal. For example, the combination of 40×, 1.3 NA, oil immersion objective lens and 0.5× intermediate magnification lens are effective.

3.1.3 Preparation of CTZh Solution

1. Dissolve 100 μg of CTZh in 40 μL of methanol (final concentration is 6 mM).
2. Keep the tube on ice until use (*see* **Note 7**).

3.1.4 Checking Expression Level of Nano-lanterns in Cells

1. Exchange culturing medium to observation medium in the glass bottom dish (*see* **Note 8**). We usually use 2 mL of observation medium in one dish.
2. Put the glass bottom dish on the microscope and focus the objective lens.
3. Find a good cell expressing mito-CNL (Ca^{2+}) and nuc-ONL (Ca^{2+}) in cells by checking fluorescence of mTurquoise2 and mKO2 (*see* **Note 9**).

3.1.5 Taking Luminescence Image of Nano-lanterns

1. Take 3.2 μL of CTZh in methanol into a new microcentrifuge tube.
2. Take 500 μL of the observation medium from the glass bottom dish and mix with the CTZh solution.
3. Add 500 μL of the solution in **step 2** to the glass bottom dish and mixed well by pipetting (final concentration of CTZh is 10 μM).
4. Focus the objective lens again by checking fluorescence of mTurquoise2 or mKO2.
5. Cover the inverted microscope with black curtain.
6. Taking luminescence image through an objective lens and W-VIEW GEMINI with EM-CCD camera.
7. Find best condition of EM-CCD camera by changing the exposure time and the EM-gain.
8. Start taking images with burst acquisition.
9. After a few minutes, histamine was added to the dish (final concentration of histamine is 10 μM) and continue taking images.
10. The signals from mito-CNL(Ca^{2+}) and nuc-ONL(Ca^{2+}) are separated by linear unmixing (*see* Fig. 1 and **Note 10**).

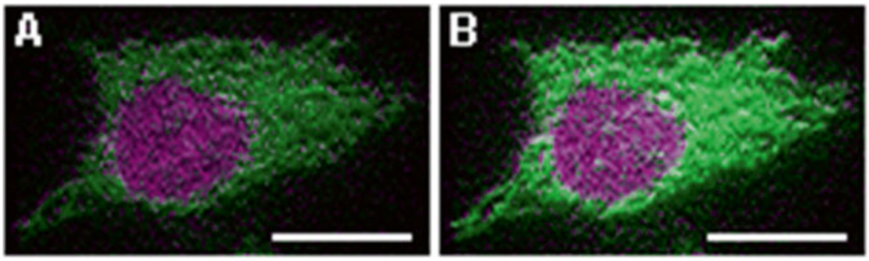

Fig. 1 Multicolor Ca^{2+} imaging in different cellular compartments using Ca^{2+} indicators based on CNL and ONL. Luminescence image of HeLa cell expressing mito-CNL(Ca^{2+}) and nuc-ONL(Ca^{2+}). (**a**) Merged image before histamine stimulation. (**b**) Merged image after histamine stimulation. *Green*; mito-CNL(Ca^{2+}), *Magenta*; nuc-ONL(Ca^{2+}). In this figure, we used 60×, 1.4 NA, oil immersion objective lens and iXon Ultra EM-CCD camera (Andor Technology). Exposure time of the camera was 2 s and the binning was 2. Scale bars represent 20 μm

3.2 Methods for Video-Rate Tumor Detection

3.2.1 Preparation of Tumor Bearing Mouse

1. Disperse colon26 cells stably expressing YNL (1.0×10^6 cells/mL) in Hank's solution.
2. 17 days before imaging, 100 μL of single cell suspension was subcutaneously transplanted on the back of anesthetized BALB/c male mouse using a BD Lo-dose syringe 30G with a 30G needle (*see* **Note 11**).
3. Maintain the mice on a 12 h dark/light cycle, with constant temperature and humidity until the imaging experiments.

3.2.2 Construction of Homemade Luminescence-Imaging System

1. Construct light-tight box from a large aluminum angle box and a black curtain as shown in Fig. 2a.
2. Attach a C-mount lens to the EM-CCD camera and put the EM-CCD camera with the lens in a small aluminum angle box. The aluminum angle box and the EM-CCD camera should be placed in a corrugated cardboard box to keep mice under the imaging system (*see* Fig. 2b).
3. The small aluminum angle box, the EM-CCD camera and a light source should be put in the light-tight box to block out the stray light from experiment room.
4. Place the stainless steel box under the EM-CCD camera (*see* **Note 12**).

3.2.3 Construction of an Alternating Shutter On/Off Control System

To detect tumor cells in a freely moving mouse, it is necessary to obtain both luminescence images of the tumor cells and bright-field images of the whole animals by synchronously controlling EM-CCD camera and electrical shutter unit. For example, iXon EM-CCD camera series (Andor Technology) give "FIRE output" signals at the timing of EM-CCD camera exposure. FIRE output can be used as external trigger signals for a multifunction wave generator. Then multifunction wave generator generates trigger signals for electrical shutter unit.

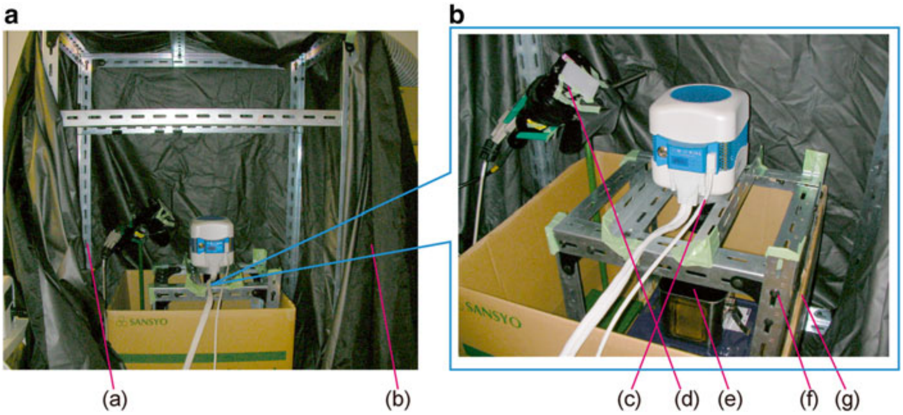

Fig. 2 Setup of homemade imaging system. Pictures of the light-tight box (**a**) and the detail inside (**b**). The light-tight box consists of (*a*) a large aluminum angle box, (*b*) a black curtain, (*c*) an EM-CCD camera with a C-mount lens, (*d*) an output end of light source with a light diffuser and an electrical shutter unit, (*e*) a stainless box, (*f*) a small aluminum angle box, and (*g*) a corrugated cardboard box

1. Set the EM-CCD camera parameters for video-rate imaging (30 frames/s at full-frame).
2. Connect the FIRE output from the EM-CCD camera to one of the oscilloscope's channels with a BNC cable and a BNC branch connector.
3. Connect the FIRE output from the BNC branch connector to the multifunction wave generator's trigger input.
4. Set parameters for the multifunction wave generator to generate the following signals: Function generation mode, burst; wave form, square; amplitude, 0–5 V; frequency, 15 Hz; cycle number, 1; phase, −1°; duty ratio, less than 50%.
5. To simultaneously monitor the FIRE output and multifunction wave generator's signal, connect the output signals of the multifunction wave generator to another channel of oscilloscope (*see* **Note 13**).
6. To simultaneously control the EM-CCD camera and the electrical shutter unit, connect the output signals of the multifunction generator to the external input for the shutter (*see* **Note 14**).

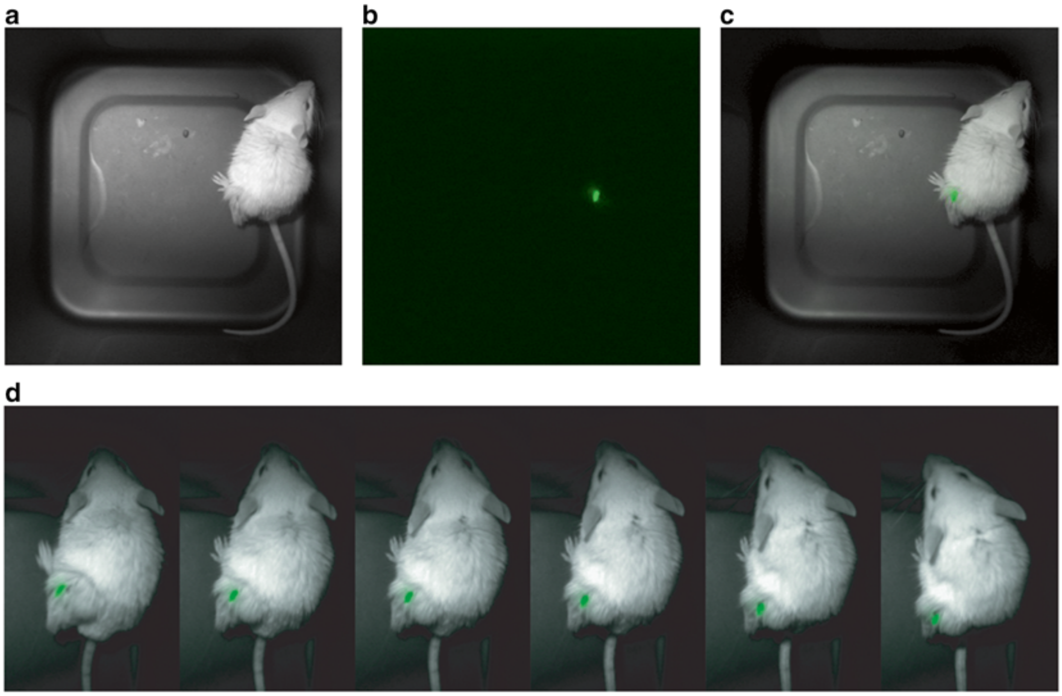

Fig. 3 Visualization of tumor cells in a freely moving unshaved mouse. Bright-field (**a**), luminescence (**b**), and merged images (**c**) of tumor cells stably expressing yellow Nano-lantern in a freely moving mouse. (**d**) Consecutive frames of video-rate images of the tumor cells in a freely moving mouse

3.2.4 Alternating Bright-Field and Luminescence Imaging of a Freely Moving Mouse

1. Dissolve 8 μg of CTZh in ethanol, and then dilute it in 1× PBS (*see* **Note 15**).
2. Inject CTZh solution intratumorally with a BD Low-dose syringe 30G.
3. Put the mouse onto the stainless steel box in the light-tight box, tightly close the black curtain and start video-rate imaging.
4. As shown in Fig. 3a, b, bright-field and luminescence images of a freely moving mouse can be obtained in an alternating sequence. Use imaging software to separate the odd numbered image sequence (bright-field images, *see* Fig. 3a) and the even numbered sequence (luminescence images, *see* Fig. 3b).
5. Make merged image sequence of the both sequences (*see* Fig. 3c), which allows us to determine the localization of tumor cells in a freely moving mouse (*see* Fig. 3d).

4 Notes

1. To avoid entering internal signal of microscope into EM-CCD camera, it is better to use manual microscope because LED is sometimes used in electrical microscope and this signal enters into the EM-CCD camera.
2. To prevent reflection of emitted light, inside of stainless box should be painted matte black.
3. To synchronously control electrical shutter unit with EM-CCD camera, EM-CCD camera should be equipped with TTL/CMOS output of exposure timing.
4. Multifunction generator should be equipped with external trigger input.
5. Electrical shutter unit should be equipped with external TTL trigger input.
6. Oscilloscope is needed to check timing of EM-CCD camera exposure time and shutter open time.
7. After dissolving CTZh with methanol, do not stock for a long time. We use the CTZh solution within 1 day.
8. We find that the luminescence intensity is decreased by adding fetal bovine serum to observation medium. Therefore, we use the medium without FBS for short-term observation within 1 h.
9. To avoid fluorescence photobleaching, we use weak excitation light intensity as much as possible.
10. When you take the reference luminesce image for linear unmixing, you should use the same condition of EM-CCD camera with the condition of **step 8** in Subheading 3.1.5.

11. Keep the cell suspension on ice. Before filling the syringe with cell suspension, it should be mixed well using a 1000 μL pipette tip with the pointed end cut off.
12. To allow soft illumination into the stainless steel box, reduce the light power (using ND filter or something similar), attach a light diffuser to spread the light, and turn the output end of the light source toward the roof of the black curtain.
13. The parameters generate "one pulse" signals in response to the FIRE output from the EM-CCD camera. Duty ratio changes the duration time of "turning on" during EM-CCD camera exposure. Adjustment of phase is sometimes required to avoid pulse generation during another exposure.
14. Because the shutter has both electrical and mechanical jitter (the delay time from ideal time signals), to prevent the light illumination from leaking into exposure for luminescence imaging, you may require precise adjustment of two parameters, phase and duty ratio.
15. The final concentration of ethanol should be less than 20%.

References

1. Saito K, Chang YF, Horikawa K, Hatsugai N, Higuchi Y, Hashida M, Yoshida Y, Matsuda T, Arai Y, Nagai T (2012) Luminescent proteins for high-speed single-cell and whole-body imaging. Nat Commun 3:1262
2. Loening AM, Fenn TD, Wu AM, Gambhir SS (2006) Consensus guided mutagenesis of *Renilla* luciferase yields enhanced stability and light output. Protein Eng Des Sel 19:391–400
3. Nagai T, Ibata K, Park ES, Kubota M, Mikoshiba K, Miyawaki A (2002) A variant of yellow fluorescent protein with fast and efficient maturation for cell-biological applications. Nat Biotechnol 20:87–90
4. Takai A, Nakano M, Saito K, Haruno R, Watanabe TM, Ohyanagi T, Jin T, Okada Y, Nagai T (2015) Expanded palette of Nano-lanterns for real-time multicolor luminescence imaging. Proc Natl Acad Sci U S A 112:4352–4356
5. Goedhart J, von Stetten D, Noirclerc-Savoye M, Leimousin M, Joosen L, Hink MA, van Weeren L, Gadella TW Jr, Royant A (2012) Structure-guided evolution of cyan fluorescent proteins towards a quantum yield of 93%. Nat Commun 3:751
6. Sakaue-Sawano A, Kurokawa H, Morimura T, Hanyu A, Osawa H, Kashiwagi S, Fukami K, Miyata T, Miyoshi H, Imamura T, Ogawa M, Masai H, Miyawaki A (2008) Visualizing spatiotemporal dynamics of multicellular cell-cycle progression. Cell 132:487–498
7. Saito K, Higuchi Y, Arai Y, Nagai T (2013) Video-rate imaging of luminescent tumour cells in freely moving unshaved mice. Protoc Exchange. doi:10.1038/protex.2013.024

Chapter 25

Photon Counting System for High-Sensitivity Detection of Bioluminescence at Optical Fiber End

Masataka Iinuma, Yutaka Kadoya, and Akio Kuroda

Abstract

The technique of photon counting is widely used for various fields and also applicable to a high-sensitivity detection of luminescence. Thanks to recent development of single photon detectors with avalanche photodiodes (APDs), the photon counting system with an optical fiber has become powerful for a detection of bioluminescence at an optical fiber end, because it allows us to fully use the merits of compactness, simple operation, highly quantum efficiency of the APD detectors. This optical fiber-based system also has a possibility of improving the sensitivity to a local detection of Adenosine triphosphate (ATP) by high-sensitivity detection of the bioluminescence. In this chapter, we are introducing a basic concept of the optical fiber-based system and explaining how to construct and use this system.

Key words Photon counting, Optical fiber, Single photon detector, Avalanche photodiode (APD), High sensitivity, Adenosine triphosphate, Luciferase, Bioluminescence

1 Introduction

The luminescence from fluorescent proteins or luciferases has become widely used as an optical readout for monitoring a molecular event of interest in a cell. The luminescence detection with a single photon level can provide a high sensitivity to an occurrence of the molecular event even in a low concentration of sample solution. A direct detection of photons emitted from the sample solution in a test tube is simplest, but the photon detector with a wide photon-sensitive area typically becomes necessary. Hence, we are introducing an alternative method, where the luminescent biomolecules are immobilized at an optical fiber end and the bioluminescence is detected with a single photon detector optically coupled to the optical fiber. The schematic setup is shown in Fig. 1. A basic system of this method has been investigated for application to a local detection with a fiberoptic biosensor [1, 2].

The biggest merit of this method is that single photon detectors with a small photon-sensitive area are available, because a

Sung-Bae Kim (ed.), *Bioluminescence: Methods and Protocols*, Methods in Molecular Biology, vol. 1461,
DOI 10.1007/978-1-4939-3813-1_25, © Springer Science+Business Media New York 2016

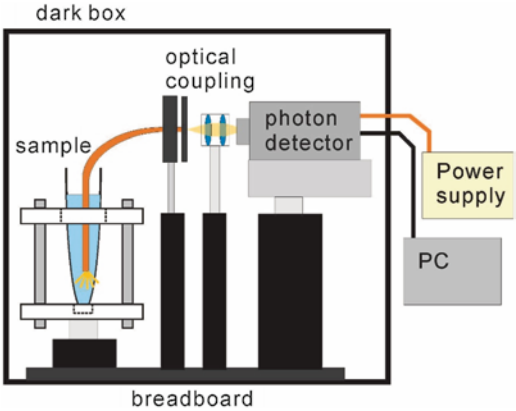

Fig. 1 Setup of optical fiber-based system. The luminescent biomolecules are immobilized at an optical fiber end and emit photons at the leading edge immersed in the sample solution. A part of the bioluminescence passes through the optical fiber and detected with a single photon detector optically coupled to another optical fiber end. The whole system is covered with the dark box to keep external light blocked out

photon-emission area is almost identical to the cross-section of a core in the optical fiber. Generally, single photon detectors with smaller photon-sensitive area have lower intrinsic noise. This feature is quite essential, because it gives the upper limit of the sensitivity of photon detection. Recently, single photon detectors with avalanche photo diodes (APDs) (*see* Fig. 2) [3] have become widely available with good performance, but their sensitive area is small and typically 0.1 mm. The optical fiber-based system allows us to fully use the merits of compactness, simple operation, high quantum efficiency, and low noise of these APD detectors.

As an application of this method, we have focused on high-sensitivity detection of Adenosine triphosphate (ATP), because ATP is a good indicator of biochemical reaction or life activity. Moreover, the ATP can be easily detected by using the luciferin–luciferase reaction involving the bioluminescence [4]. In this reaction, the oxidization of luciferin can be catalyzed by the enzyme luciferase and one photon is emitted via the oxidization process of one luciferin molecule bound into one luciferase molecule. The immobilization of luciferase molecules at the optical fiber end enables highly sensitive and local measurement of ATP.

Thus, we have constructed the optical fiber-based system with the APD detector for an ATP sensing [5]. Here, we show our optical coupling system designed for the use of the APD detector and how to construct the optical fiber-based system with our design parameters (*see* Fig. 3) [6]. The improvement of the current

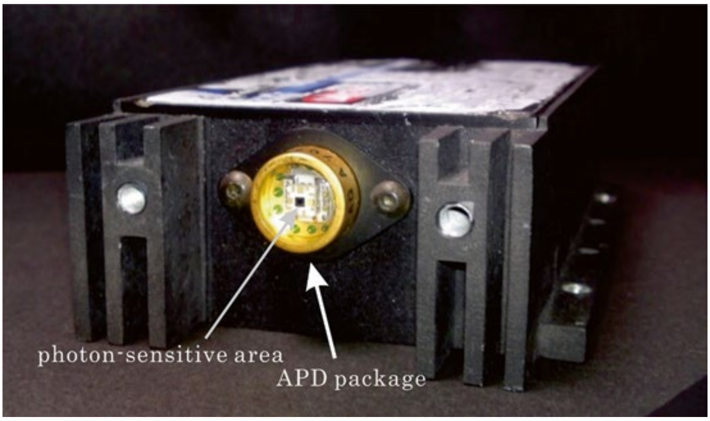

Fig. 2 APD photon counting module, SPCM-AQR14, provided by Perkin Elmer Inc. [3]. Recently, thanks to the development of semiconductor technologies, the single photon detectors with APDs have become widely available with good performance. Comparing to typical photo-multiplier tubes, they have the merits of compactness, simple operation, highly quantum efficiency, and low electric noise. A black piece located in the center of the APD package in the photo corresponds to the photon-sensitive area

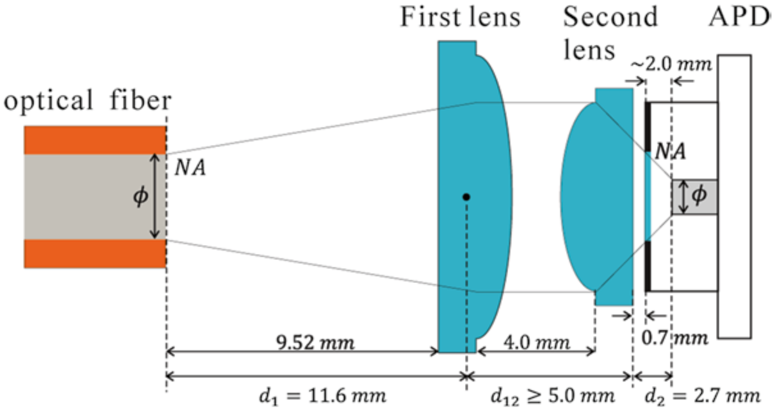

Fig. 3 Design of the optical coupling system between the optical fiber end and the APD detector. The procedure to determine the parameters is explained in ref. 4. Aspheric lens of 352240-B and 354330-B is used as a first lens and a second lens, respectively. Although d_2 is not exactly a distance between the flat surface and the sensitive area, we approximated it by $d_2 = 2.7$ mm

sensitivity is possible, if the optical coupling is re-designed for using a different photon detector with larger sensitive area and the optical fiber we used [7]. This method is generally applicable to the local detection of the luminescence emitted in the immediate vicinity of the optical fiber end in the sample solution.

2 Materials

Components for constructing the system include hand-made parts. The list is classified by three categories: biochemical, optical detection, and electronics and data acquisition parts.

2.1 Components for Immobilization and Sample

1. Tris-buffer for cleaning up the optical fiber end: 0.25 mM Tris–HCl with 0.15 M NaCl. Store at 3 °C. Here, we call it Tris-buffer A.
2. Solution of compound proteins containing a silica-binding protein molecule (SBP) and a luciferase molecule (SBP-luciferase) [8]. It is stored at −80 °C.
3. ATP standard in ATP Bioluminescence Assay Kit CLS II (Roche Co., Ltd). Store at 3 °C.
4. Tris-buffer for sample solution: 250 mM Tris–HCl mixed with 50 mM $MgCl_2$. Store at 3 °C. In the same manner, we call it Tris-buffer B here.

2.2 Components for Optical Detection

1. Commercial APD photon detector, SPCM-AQR14, provided by Perkin-Elmer Inc. [3]. Our design parameters are tuned for using this photon counting module (*see* **Note 1**).
2. DC power supply for the present APD detector, which has a capability of supplying the power of the voltage 5 V and the maximum current 1.5 A.
3. Two aspheric lenses, 352240-B and 354330-B, provided by Thorlabs Inc. The usage of this pair of lenses is based on the assumption of using the present APD detector.
4. Laser pointer of red light.
5. Several ND filters, but any filters are available if the red light can be reduced (*see* **Note 2**).
6. Dark box without a bottom plate and with a removable top plate. The small hole on the wall is necessary for passing both of signal and DC power cables (*see* **Note 3**).
7. Breadboard for constructing the optical detection system. The system constructed on the breadboard is covered with the dark box (*see* **Note 4**).
8. Hand-made holder for supporting a test tube as shown in Fig. 4 (*see* **Note 5**).
9. Commercial adapter for connecting the optical fiber cable with the FC connector and its holder (*see* **Note 6**).
10. Hand-made holder for mounting two aspheric lenses as shown in Fig. 5a and several setscrews with M1 size (*see* **Note 7**).

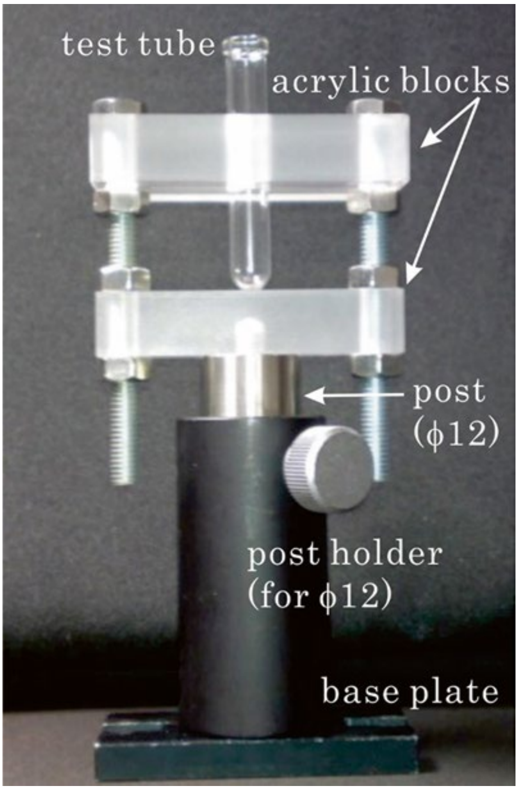

Fig. 4 Our hand-made holder for supporting the test tube. The dimensions of two acrylic blocks are 60 mm by 10 mm and 14 mm height. The size of the hole for putting the test tube in has been determined suitable for the actual diameter of the test tube we used. In our case, for example, the diameter is 8 mm. Two blocks are fixed with two bolts and eight nuts as shown in the photo. We used the post with the diameter of 12 mm, the post holder, and the base plate purchased from other optics companies (*see* **Note 5**)

11. Aluminum plate for mounting the APD photon counting module (*see* **Note 8**).
12. Several commercial opto-mechanical components, pillar posts, post holders, post cramping arms, and two translation stages (*see* **Note 9**).
13. Multimode optical fiber with a core diameter of 0.6 mm and a numerical aperture of 0.37. One end of the fiber has a FC connecter and the other end does not (*see* **Note 10**).
14. Several blackout cloths.
15. Coaxial cable for using as a signal cable.

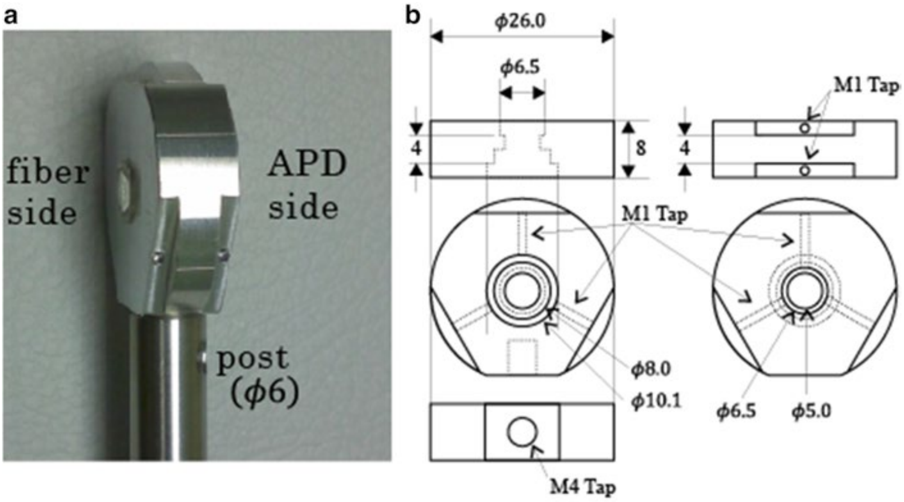

photo from side view   schematic drawing

Fig. 5 (**a**) Photo of our hand-made holder for mounting two aspherical lenses provided by Thorlabs Inc. The left-hand side of the holder is the fiber side and the right-hand side is the APD side. The thickness of the holder is 8 mm and cut out from the aluminum plate. The post of ϕ6 is attached to the bottom of the holder for being fixed on the breadboard. (**b**) Schematic drawing of our holder. On the face drawn in the left-hand side, the first lens 352240-B is set in the hole of ϕ10.1. The second lens 354330-B is mounted in the hole of ϕ6.5 on the face in the right-hand side, which is directed onto the APD side

2.3 Electronics and Data Acquisition

1. Commercial pulse counter for the TTL logic pulse (*see* **Note 11**).
2. Software for controlling the pulse counter and taking the number of counts as data (*see* **Note 12**).
3. Personal computer for data acquisition.
4. Connect the pulse counter to the PC and check a basic operation of data acquisition, which allows us to take a series of numbers of counts by a certain time interval as a data-set (*see* **Note 13**).

3 Methods

Once the optical fiber-based system is established, the procedure is composed only of two steps: preparation and actual measurement. After preparing the sensing part to the ATP, you should start taking data as soon as possible.

3.1 Construction of the Optical Fiber-Based System

1. Mount the first lens of 352240-B and the second lens of 354330-B into the lens holder with three setscrews for each (*see* Fig. 5a). Subsequently, align the position of two lenses roughly to overlap the center of two lenses with the central axis of the lens holder (*see* Fig. 3) (*see* **Note 14**).
2. Mount the APD photon detector, SPCM-AQR14, on the aluminum plate with normal screws. Subsequently, mount the adapter for the optical fiber end to its holder and connect the optical fiber end with the FC connector to the adapter.
3. Arrange the location of all components on the breadboard, which are the supporting holder, the fiber holder, the lens holder, and the plate of the photon detector with pillar posts, post holders, post cramping arms, and two translation stages (*see* Fig. 1). Make a rough alignment of optical components and subsequently fix them by tightening screws to the breadboard (*see* Fig. 3) (*see* **Note 15**).
4. Connect the signal cable from the APD detector to the pulse counter and also connect the DC power cable from the APD detector to the DC power supply, respectively (*see* **Note 16**).
5. Set the laser pointer and the optical fiber end without the FC connector and fix them with scotch tapes. Adjust the position and the angle of the laser pointer to make the red light enter into this end and secure it robustly. Confirm the outgoing red light from the other end of the optical fiber. After that, block the red light in front of the incident optical fiber end with a white paper.
6. Repeat the rough alignment of the optical fiber end, two lenses, and the APD detector, with the outgoing red light from the optical fiber end, which is turned on by removing the white paper. In this stage, adjust two distances between the optical fiber end and the first lens and between the second lens and the APD detector (*see* Fig. 3) (*see* **Note 17**).
7. Set the dark box to cover the all optical setup. Furthermore, overlay the whole dark box with blackout cloths to block out an external light from all optical components in the dark box. After extremely reducing the power of the red light with several ND filters, turn on the DC power supply for the APD detector and monitor the number of counts in the PC screen (*see* **Note 18**).
8. Open the top plate slightly and put your hands inside of the dark box to carefully keep the external light blocked out. In the following, make fine alignments by turning around adjustment knobs of the fiber holder, setscrews of the lens holder, and adjustment knobs of two translation stages to maximize the counting rate of the APD detector. This is the most important and difficult process. If the photon counting is completely

lost, try again from the rough alignment introduced in the **step 6** (*see* **Note 19**).

9. Turn off the DC power supply for the APD detector. Open the top plate of the dark box and remove the optical fiber by disconnecting the fiber end from the holder and releasing the other end.

3.2 Preparation

1. Cut the optical fiber end without the FC connector with a cutter knife and clean the cut surface with ethanol and Tris-buffer A. After cleaning up, immerse the cut surface in a solution of SBP-luciferase and leave it at temperature of 3–6 °C for a period of about 2 h. After that, take the fiber end from the solution and let it immerse in the Tris-buffer B until beginning measurements (*see* **Note 20**).
2. Make a 1:4:4:31 mixture of 20 mM d-luciferin solution, Tris-buffer B, ATP solution, and distilled water. To study the sensitivity of the ATP detection, prepare a series of sample solutions with different ATP concentration by diluting the original sample solutions. Furthermore, prepare an additional solution without ATP by mixing distilled water instead of the ATP solution.

3.3 Photon Counting

1. First, check and record the number of counts by using the solution without ATP as a reference. Open the top plate of the dark box and set the test tube containing the reference solution in the supporting holder.
2. Connect one optical fiber end with the FC connector to the holder and immerse the other end in the sample solution. Close the top plate of the dark box and cover it with the blackout cloths immediately, and then turn on the DC power supply. After the elapse of a certain period of time from immersing the fiber end, start the operation of the data acquisition (*see* **Note 21**).
3. Stop the data acquisition after a certain time. Turn off the power supply and open the top plate of the dark box for exchanging the other test tube. This is a reference data.
4. Restart the data acquisition after setting other test tube of the sample solution containing ATP. Confirm the excess of the number of counts in comparison with the reference data (*see* **Note 22**).
5. After the confirmation, continue the measurements with the sample solution of different ATP concentration. You can obtain data-sets at various ATP concentrations. Our results are shown in Fig. 6. From the data-set, we have successfully confirmed that this system has the sensitivity to the lower limit of 10^{-10} M of the ATP concentration [6] (*see* **Note 23**).

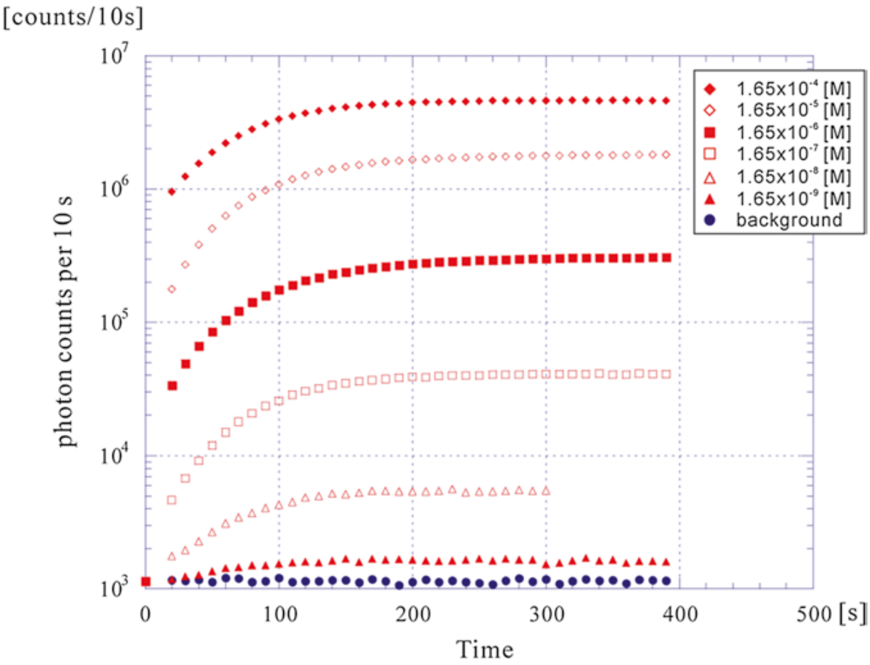

Fig. 6 Photon counts per 10 s as a function of time at various ATP concentrations. (© 2012 Masataka Iinuma, et al. Originally published in ref. 6 under CC BY 3.0 license. Available from:10.5772/1379). The build-up time was about 30 times longer than that in a solution containing only nonlocalized homogeneously dispersed SBP-luciferase, but the reason is open question. There are experimental results claiming the decrease in activity of immobilized luciferase molecules [9, 10]. From the data-set, we have successfully confirmed that this system has the sensitivity to the lower limit of 10^{-10} M of the ATP concentration [6]

4 Notes

1. If you use other photon detector with larger sensitive area as a cooled photo-multiplier tube, for example, higher sensitivity is possible. But the optical coupling system has to be designed again [7].
2. The huge reduction of a power of the red light to single photon level is necessary. In the case of using a typical laser pointer, for example, it is required to reduce 10^{-6} ~ 10^{-8} times lower power than the initial power.
3. Our dark box is made of five aluminum plates with the thickness of 3 mm and its dimension is about 40 cm by 40 cm and 40 cm height. The cardboard box is also available. The inner surfaces of the box should be painted all black.
4. Although it is recommended to purchase a breadboard from some optics companies, Thorlabs Inc., for example, it is also possible to make a hand-made type out of aluminum plate. If an optical anti-vibration table is available, it is easier to construct on the table instead of the breadboard.

5. Our hand-made holder is shown in Fig. 4. It consists of two blocks cut from thick acrylic board, two M6 bolts, and eight M6 nuts. The upper block has a hole for inserting the test tube and the lower block has a M6 tap for connecting a pillar post.
6. Two components are quite general and offered by some optics companies. You can buy the commercial components, FC fiber adapter plate (S1FC) and Mount (KM1CE), provided by Thorlabs Inc.
7. Photo and drawing of our hand-made lens holder are shown in Fig. 5a and b, respectively. This holder is made of aluminum plate with 8 mm thickness. Two lenses are fixed with three setscrews with M1 size for each.
8. The aluminum plate with 8 mm thickness is cut with 90 mm width and 150 mm length.
9. These mechanical components are quite general and offered by some optics companies. But it is much easier to get all at once from one optics company, Thorlabs Inc., for example.
10. It is easier to cut the optical fiber cable (BFL37-600, 1 m length, Thorlabs Inc.) at the center position with a normal cutter knife.
11. A PC-card type is convenient. We used CNT32-4MT(CM), CONTEC Co., Ltd.
12. The sample software is almost attached together with the product for user's convenience. It is easier to directly use the sample software. In most cases, taking the numbers of counts per a certain time is one of basic operations of the sample software.
13. The test of data acquisition is so important. It is recommended to check the performance with an additional pulse generator. The confirmation is possible by comparing the counts expected from the repetition rate of output pulses with actual counting data.
14. Don't touch two surfaces of lenses directly. If done accidentally, you should clean up the surface of lens by using a lens wiper with ethanol. Don't use the Kimwipes.
15. It is preferable to leave all components including the test tube and the optical fiber on the breadboard without fixing them. The location of the supporting holder is determined for not giving unnatural stress to the optical fiber. In addition, it is much better to use two translation stages as bases of the post holders of the FC fiber adapter and the plate of the ATP detector. These translation stages are useful for adjustment of d_1 and d_2 in Fig. 3. In the following, the height of the optical fiber end, the center of two lenses, and the center of the sensitive area of the APD detector should be adjusted for making the same level with a ruler. After that, they are roughly aligned as shown in Fig. 3, where the line of holes on the breadboard is useful as a mark of the straight line.

16. In this stage, it is better to pass three cables, the signal cable, the DC power cable, and the optical fiber through the small hole of the dark box.
17. It is easier to fix the location of the lens holder as a reference and to adjust the distances d_1 and d_2 with the translation stage.
18. Before turning on the DC power supply for the APD detector, it is better to darken whole experiment room. If not, you have to overlay the optical fiber end used as the entrance of the red light with blackout cloths at least. Confirm that the voltage of the power supply is firstly set to be zero for a safety operation and then turn on the DC power supply. After turning on, increase the voltage slowly and achieve to 5 V. If the counting rate is over 10^6 counts per second, reduce the power of the red light to an appropriate level by using additional ND filters, because it is highly probable that the APD detector is saturated in this case.
19. The tips of fine alignments are presented as follows. First, repeat two adjustments of the optical fiber end and of the second lens alternatively to get the maximum of the counting rate. It is recommended to adjust the fiber holder with adjustment knobs after slightly turning one of setscrews of the lens holder toward one direction for getting the highest counting rate and to repeat these operations for maximizing the counting rate. In this alignment, it may be better to adjust the only second lens leaving the first lens fixed. In the following, make the adjustments of d_1 and d_2 with the translation stages to get the maximum counts. After that, adjust the first lens with three setscrews and the optical fiber end alternatively as the similar way. Repeat the above sequential operations until the counting rate is saturated. The significant points in this procedure are to keep the external light blocked out and to spend enough time for the alignment.
20. Although the standard cleaving technique for cutting the optical fiber allows us to make a flat surface on the fiber end, the sensitivity with the flat surface is about 10 times lower than that with scabrous surface of the fiber end, which is created with the normal cutter knife. For improving the sensitivity, cutting without the cleaving technique is better [6]. After cutting it, immediately clean up the fiber end with ethanol and sequentially dry it with a dry air. It is better to use an air-gun for blowing a nitrogen gas, which is connected to a nitrogen gas tank. First, clean it with ethanol twice and then with Tris-buffer A once. Just before immobilizing the luciferase molecule, re-clean the fiber end with the ethanol and the Tris-buffer A and rinse it with new Tris-buffer A.
21. In taking data with the reference solution, it is a nice idea to measure operation-elapsed time until completing the preparation after immersing the fiber end in the reference solution.

22. If the excess of the number of counts is not confirmed, it is necessary to check the whole system carefully. There are roughly two possible reasons. One is on the sensing part, which is immersed to the solution of the SBP-luciferase, and it is significant to check the whole preparation process about the sensing part. The other is a possibility of making the misalignment in the optical coupling system during the operation such as connecting or disconnecting the optical fiber to the holder, giving an additional force to the optical fiber in opening or closing the top plate, and touching the lens holder accidentally, etc. In this case, you should check the number of counts with the red light of the laser pointer entering into one optical fiber end again.
23. It is better to start the ATP measurement from the sample solution with lower concentration. In exchanging other sample solution, you should clean up the sensing part by immersing it into Tris-buffer B.

Acknowledgement

This work has been partially supported by the International Project Center for Integration Research on Quantum, Information, and Life Sciences of Hiroshima University and the Grant-in-Aid for Scientific Research (C) (19560046) of Japanese Society for the Promotion of Science, JSPS.

References

1. Arnold MA (1991) Fluorophore- and chromophore-based fiberoptic biosensors. In: Blum LJ, Coulet PR (eds) Biosensor principles and applications. Marcel Dekker, New York, pp 195–211
2. Blum LJ, Gautier SM (1991) Bioluminescence- and chemiluminescence-based fiberoptic sensors. In: Blum LJ, Coulet PR (eds) Biosensor principles and applications. Marcel Dekker, New York, pp 213–247
3. Perkin Elmer Inc. (2012) Datasheet of SPCM-AQR-14. At present, Excelitas Technologies Corp provides the same APD detector. http://www.excelitas.com/Pages/Index.aspx
4. Fraga H (2008) Firefly luminescence: a historical perspective and recent developments. Photochem Photobiol Sci 7:146–158
5. Iinuma M, Ushio Y, Kuroda A, Kadoya Y (2009) High sensitivity detection of ATP using bioluminescence at an optical fiber end. Electron Commun Jpn 92:53–59
6. Iinuma M, Ushio Y, Kuroda A, Kadoya Y (2012) High-sensitivity detection of bioluminescence at an optical fiber end for an ATP Sensor. In: Yasin M, Harum SW, Arof H (eds) Fiber optic sensor. InTech, Rijeka, pp 459–474
7. Iinuma M, Tanaka R, Takahama E, Ikeda T, Kadoya Y, Kuroda A (2013) Investigation of bioluminescence at an optical fiber end for a high-sensitive ATP detection system. In: Harum SW, Arof H (eds) Current developments in optical fiber technology. InTech, Rijeka, pp 293–317
8. Taniguchi K, Nomura K, Hata Y, Nishimura Y, Asami Y, Kuroda A (2007) The Si-tag for immobilizing proteins on a silica surface. Biotechnol Bioeng 96:1023–1029
9. Nishiyama K, Watanabe T, Hoshina T, Ohdomari I (2008) The main factor of the decrease in activity of luciferase on the Si surface. Chem Phys Lett 453:279–282
10. Tanaka R, Takahama E, Iinuma M, Ikeda T, Kadoya Y, Kuroda A (2011) Bioluminescent reaction by immobilized luciferase. IEEE Trans EIS 131:23–28

INDEX

A

ABCG2. *See* ATP-binding cassette sub-family G member 2 (ABCG2)
Adeno-associated virus (AAV)....244
Adenosine triphosphate (ATP)....3, 19, 56–59, 92–94, 102–104, 111, 112, 131, 134, 138, 140, 141, 218, 219, 228, 277, 300, 302, 306, 308, 310
Air pollutant....279, 280, 284
Aminopeptidase N....91–98
Androgen....143–151
  receptor....143–147
Androgenicity....143–151, 168–169
Anti-GPR35 antibody....6, 15
Anti-His-tag antibody....45, 50
APD. *See* Avalanche photo diodes (APDs)
Apoptosis....45, 48, 104, 255, 256, 259, 264–265, 267
Artificial luciferases....43–53, 183, 279, 281, 284
Assay device....271
Assay system....45, 51, 84, 87, 107, 185, 272, 279–286
ATP. *See* Adenosine triphosphate (ATP)
ATP-binding cassette sub-family G member 2 (ABCG2)....227–229, 233–235
ATP-binding cassette transporter....227–237
Avalanche photo diodes (APDs)....300–303, 305, 306, 309

B

BBB. *See* Blood-brain barrier (BBB)
β-arrestin....4, 6, 13–14, 196–200
17β-estradiol....159, 166, 170, 177, 178, 272, 275, 276
Bestatin....92–97
Bifacial activity....153–163
Bioluminescence
  adenosine triphosphate (ATP)....300
  assays
    kit....44, 45, 51, 272, 302
    system....279–286
  in an ATP-independent manner....65
  capacity....19
  from cells....286
  cofactor-free....19
  CTZ analogs....19, 20
  determination platform....271–277, 279, 281
  emitted by molecular tension probes....19
  firefly luciferase....91, 102–114, 247, 256
  FLuc-EGFP....250
  green or red....275
  imaging platform....255
  in nude mice model....250–251
  intensities....28, 29, 148–150
  in vivo....91–98, 237
  with an IVIS Kinetic imaging system....92
  kinetic profiles....28
  in label-free cell....4
  measurement....55–60, 67, 70–71, 93–94
  metal cation-driven....281–283, 285
  for metastatic model....250
  and microPET imaging....250–253
  multicolor....255
  multiplexed....255
  of NanoLuc reporter....65, 66
  peak....108, 109
  pseudocolor image....46
  quantum yield....55–60
  rapamycin-dependent....135, 190
  reaction....55–60
  reporter....3
  from the single-chain probes....280
  spectra....28–29, 178–179, 184
  tension probe (TP)....184
  unmixing....263
  using split luciferase complementation....196
Bioluminescence resonance energy transfer (BRET)....28, 102–114, 118, 121–129, 175, 183, 290
  yellow fluorescent protein Venus....289
Bioluminescent bacteria....217–223
Bioluminescent biosensors....217
Bioluminescent capsules....48–49, 52
Bioluminescent imaging (BLI)....91, 95, 180, 189, 227–237
Bioluminescent probe....4, 156, 175, 184, 189, 271, 273, 277, 279, 280
Blood-brain barrier (BBB)....227–237
Breast cancer....144, 148, 149, 242, 243, 255, 256, 259, 266

C

Caged luciferin....91
Calcium dynamics....290–294
Caspase 3....49, 104, 106–107, 109–113, 256

Sung-Bae Kim (ed.), *Bioluminescence: Methods and Protocols*, Methods in Molecular Biology, vol. 1461,
DOI 10.1007/978-1-4939-3813-1, © Springer Science+Business Media New York 2016

Chemiluminescence............................20, 27–28, 30, 45, 263
Circular permutation (CP) 165–173
probe...165–173
Cirularly permutated luciferase 166, 167, 172
Click beetle (CB)...................................154, 156, 157, 159, 161, 162, 166, 167, 170, 196, 218, 219, 222, 256, 259, 274, 276, 277
green luciferase 256
luciferase............................154, 159, 161, 166, 167, 170, 219, 222, 274, 276, 277
Coelenterazine....................................19–30, 33, 45, 46, 48, 120, 122, 171, 177, 179, 185, 187, 191, 206, 258, 263, 272, 282, 290
Combinational probe.......................................184, 188–189
Complementary technology.......................................197, 201
Consensus amino acids...............................43, 44, 46, 51, 53
Copepod
crustaceans..33, 190
luciferase....................33, 34, 38, 39, 44, 51, 53, 190, 191
Cortisol...272–277
Crosstalk...153
Cyan-Nano-lantern (CNL)............................. 290, 291, 293

D

DeepBlueC™...20, 28, 29
Degron 205–207, 210–214
D-luciferin.................................3–15, 56–59, 131, 132, 144, 161, 197, 199, 201, 206, 209, 211, 218, 220, 221, 228–231, 234, 235, 237, 247, 250, 252, 255, 258, 262, 264, 265, 268, 275, 277, 306
in transgenic mice..228
Dynamic mass redistribution assay..................... 4, 6, 7, 9, 14

E

Electron-multiplying charge-coupled device (EM-CCD) camera.....................196–199, 201, 291–294, 296
Endoproteases 108
Enhanced green fluorescent protein (EGFP).............207–208, 210, 211, 247–252
Estrogen receptor (ER) 154, 156, 159, 165–173, 176, 274, 276

F

Factor Xa... 104, 106–107, 109–113
Firefly luciferase (FLuc)
EGFP.........................206–208, 210, 211, 247–250, 252
in N- and C-terminal fragments 144, 146, 147, 151, 153, 156, 157, 161, 162, 166, 196, 204, 276
pH-sensitive 117
splitted the two major catalytic steps.................131, 132
Firefly luciferin-luciferase reaction 59
Firefly luminescent intermediate-based protein–protein interaction assay (FlimPIA)..................131–133, 139–141
FK506-binding protein 12 (FKBP12).................135, 140, 191
FKBP-rapamycin-associated protein (FRB) 135, 136, 139, 140, 172, 184, 185, 189, 191
Fluorescence resonance energy transfer (FRET)..............14, 102–114, 133, 183
Fragment 198

G

Ganciclovir (GCV) 241, 246, 249–253
Gaussia luciferase (GLuc) 39, 47, 48, 65, 118, 256, 257, 259–262, 265, 266
Gene-directed enzyme prodrug therapy (GDEPT)...241, 242
Glucocorticoid receptor (GR) 273, 274, 276, 277
G protein-coupled receptor (GPCR) 4, 195–201
G protein-coupled receptor-35 (GPR35).......................3–15

H

Hank's balanced salt solution (HBSS)............................6, 8, 9, 21, 28, 44, 49, 51, 167, 171, 177, 180, 185, 190, 197, 199
buffer 6
Herpes simplex thymidine kinase....................................242
High-throughput screening (HTS)................... 91, 195–201
Histone lysine methylation.....................................203–205
Histone methylation
in vivo imaging 206, 210–213
optical imaging sensor 206, 209
Horseradish peroxidase (HRP)...................... 45, 49–51, 263
Human colorectal adenocarcinoma HT29 cell line 4
4-hydroxytamoxifen (OHT).......................... 154, 166, 177, 178, 272, 275

I

Imidazopyrazinone 19
In vivo imaging.......................65, 91–98, 197, 206, 210–211, 213, 247, 255
Insulin-like peptide 3 (INSL3)....................... 66–68, 71–74, 76, 82, 83, 85–87
Integrating sphere..56–60

L

Leukemia inhibitory factor (LIF).................66, 77–82, 88, 89
Ligand 7–9, 14, 143–148, 151, 153, 157–163, 165–171, 173, 176–180, 184, 188
Ligand binding domain (LBD)............143, 146, 159, 170, 176
Ligand–receptor binding assays...................................65–89
Light off biosensor 217–223
Living animal imageing..................................... 92, 203–214
Luciferase
activity 95, 208, 212, 214, 262, 263
antibody.. 257, 259, 265
artificial..................................43–53, 183, 279, 281, 284

- assay 146, 185, 257, 261
- beetle 55, 176, 191, 218, 274, 276
- from bioluminescent copepod crustaceans 34
- CBG99 259, 261, 262, 265
- cDNAs 34, 39
- circularly permutated 166
- click beetle 154, 159, 161, 166, 167, 170, 219, 222, 274, 276, 277
- complementation 196, 204
- copepod 33–40
- EGFP 247
- engineered fragments 279
- expression 220
- fragment 196–198
- *Gaussia princeps* 33, 47
- genes 3, 219, 259
- green 159
- immobilization at the optical fiber end 300
- in living animals 213, 242
- marine 19, 20, 44, 45, 47, 52, 176
- *Metridia longa* 33
- *Metridia pacifica* 36, 47
- molecule 300, 302, 307, 309
- monomeric 183
- *Photinus pyralis* 56, 102
- plasmids 219
- PpyRE9 256, 259, 262, 263
- probes 166, 196, 197
- prosubstrate 264
- *Pyrearinus termitilluminance* 55
- quantitation 205
- reaction 59, 300
- red 159, 274, 276
- *Renilla reniformis* 47, 176, 183
- reporter system 3
- sandwiched between two proteins 176
- secreted from marine planktonic copepods 33–40
- split 206, 214
- thermostable 102, 104

Luciferin
- acting at the GPR35 4
- adenylation 131
- in the brain parenchyma 227, 228
- caged 91
- efflux 228
- firefly 19, 59, 102, 104
- at a fixed dose 9, 10
- at the GPR35 4
- injections 232, 236, 237
- luciferase system 102
- in a mouse model 227, 228, 266
- with the pamoic acid solution 9
- partial agonism 9
- as a partial agonist 4, 13
- sodium salt 56, 57, 92
- solution 9, 58, 229, 306
- a weak partial agonist 13

Luciferyl adenylate 132
Luminescence 48, 55, 56, 59, 60, 70, 75, 81, 84, 106, 110–112, 117–130, 132, 133, 141, 148–150, 158–161, 169–171, 173, 178, 188, 196, 199–201, 217, 219–221, 223, 257, 281, 285, 289–297, 299
Luminometer 28, 56, 58–60, 114, 135, 139, 141, 149, 162, 169, 179, 206, 208–209, 212, 213, 219, 220, 261, 272–275, 286
LXXLL-like peptide 143
LXXLL motif 155, 157, 161, 162, 274, 276

M

Marine luciferase 19, 20, 44, 45, 47, 52, 176
Metal sensor 218
Metridia longa luciferase (MLuc) 33, 39
Metridia pacifica luciferase (MpLuc) 39, 47
mKate 104–108
Molecular strain probes 175–181
Molecular tension 175–180, 183–192
- probe 175–180, 183–192

Multichannel bioluminescence determination platform 271–277, 281
Multicolor 255, 262, 264, 273–276
- imaging 153–163, 272, 275, 276

N

Nano-lanterns 289, 290, 292–295
NanoLuc 65–73, 76–86, 88, 89, 118
National radiometry standard 56, 59
Neuroimaging 227
Nongenomic signaling pathways 154
N-terminal domain (NTD) 46, 132, 136, 143–145, 159
Nuclear factor-κB (NF-κB) 255
Nude mouse 95, 96

O

OHT. *See* 4-hydroxytamoxifen (OHT)
One-step agonism assay 4
One-step co-stimulation assay 4
Optical fiber 299–310
Optical imaging
- charged-coupled device (CCD) 206, 209, 230, 247
- IVIS100 231

Optical readout 299
Orange-Nano-lantern (ONL) 290, 291, 293
Oxyluciferin 131, 132, 228

P

Pamoic acid 6–10, 13
Particulate matter 2.5 (PM2.5) 286

PCA. *See* Protein-fragment complementation assay (PCA)
pHlash 118–128
Phosphorylation 161, 162, 165–173
Photomultiplier (PMT) 196, 280, 281, 283
Photon counting system 56, 299–310
pH sensor 117, 118
Plankton 33–40
Protease 4, 13, 102–114, 205, 207, 210–214, 282
Protein-fragment complementation assay (PCA) 133, 175, 183, 188
Protein-protein interaction (PPI)
  assay 131
  in biology and biotechnology 134
  combinational probe 184, 188–189
  of GPCR 185, 191
  of interest 166, 176
  optical imaging 183

Q

Quantum yield 55–60, 173

R

Ratiometric
  luminescence sensor 117–130
  luminescent probe 104
Reaction intermediate 132
Red fluorescent protein (RFP) 103, 104, 107, 108, 212–214
Renilla reniformis luciferase (RLuc) 176, 183
Renilla reniformis luciferase 8 (RLuc 8) 21, 28, 29, 47, 118, 128, 176, 177, 181, 183
Reporter-gene assay 33, 146
Reporter genes 3, 242, 243, 246
Resonance transfer 118, 175, 183
Resonant waveguide grating biosensor 4
RFP. *See* Red fluorescent protein (RFP)

S

Sequential BRET-FRET energy transfer 104
Sequential BRET-FRET process (SRET) 103, 104, 106, 108–110, 113, 114
The SH2 domain of Src 159, 166, 170
Single-chain multicolor probe with estrogen receptor (Simer) 154, 155
Single-chain probe
  carrying glucocorticoid receptor (GR) 273
  with circularly permutated split-luciferases 166
  emitting green or red bioluminescence 161, 276
  illuminating androgenicity 143–151
  for illuminating toxic chemicals 279
  multicolor 153
Single photon detector 299–301
SP05140 .... 6, 10
Split reporters 175, 205, 210, 213
SRET. *See* Sequential BRET-FRET process (SRET)
Steroid hormone 272–275
Substrate channeling 134, 139, 141

T

Tango™ U2OS-GPR35-*bla* cell line 4–7, 13
Therapeutic cancer gene therapy 241–253
Thrombin 104, 106–107, 109–113
TNFα. *See* Tumor necrosis factor α (TNFα)
Total photon flux 55, 56, 58–60, 92, 94, 97
Toxicity 118, 217–223, 268
  biosensor 217, 223
Tracer 70, 71, 73–82, 86–89
Tumor imaging 290–292, 294–296
Tumor necrosis factor α (TNFα) 256–258, 262–266
Two-step antagonism assay 4
Two-step desensitization assay 4

U

Urban aerosol 279–286

Y

YE210 6–8

Z

Zaprinast 6–8, 11–14
ZDEVD-aminoluciferin 256
Zooplankton 33, 36, 40, 190